DYNAMIC RESPONSE OF MULTISTORY BUILDINGS

Thesis by

Niels Norby Nielsen

In Partial Fulfillment of the Requirements

For the Degree of

Doctor of Philosophy

California Institute of Technology

Pasadena, California

1964

(Submitted May 25, 1964)

ACKNOWLEDGMENTS

The author's immediate advisors were Professors D. E.Hudson and G. W. Housner. Their guidance and many helpful suggestions in the preparation of this work is sincerely appreciated.

Professor T. K. Caughey gave freely of his time and was a constant source of encouragement.

The dynamic tests of the Olin Hall of Engineering on the campus of the University of Southern California were made possible through the active interest shown by Dean A. C. Ingersoll of the School of Engineering, The University of Southern California. The cooperation received from the firm of Brandow and Johnston, Structural Engineers, was very helpful to this investigation.

The dynamic tests of the nine-story Central Engineering Building of the Jet Propulsion Laboratory, the California Institute of Technology became possible through the efforts of Dr. W. H. Pickering and his staff. The cooperation received from the firm of Johnson, Nielsen and Steinbrugge, Structural Engineers is also appreciated.

A grant from the National Science Foundation helped defray some of the costs incurred in the dynamic tests.

The author is further indebted to the Ford Foundation for the Ford Foundation Faculty Fellowships received and to the California Institute of Technology for Institute scholarships and graduate teaching assistantships granted during the course of this investigation.

ABSTRACT

Two modern multistory buildings, one a five-story reinforced concrete building, the other a nine-story steel frame building, have been the subjects of an extensive series of dynamic tests. The vibrations of the buildings were induced by means of synchronized vibration exciters. The mathematical analysis needed in order to determine the stiffness and damping matrices from the experimentally determined modal properties of a structure has been developed.

Three translational and one torsional mode of vibration of the reinforced concrete building were investigated in considerable detail. The damping in each mode and the resonant frequency was determined under various levels of excitation. Complete mode shapes were determined as well. The measurements of the resonant frequencies show a well-defined nonlinearity that can be well explained from the hysteretic material properties. The values of damping were for all modes approximately 2% with a tendency for the value of damping to increase with increasing force levels.

A total of seven translational and three torsional modes of vibration of the nine-story steel frame building were investigated in detail. A mode in which the floor slabs vibrate horizontally as free-free beams was excited as well. The lowest translational modes in the two principal directions of the building had damping values of about 0.5%. The second lowest translational modes had damping values of approximately 1.0%. For both buildings the

damping values are considerably less than the values usually mentioned in the literature. Since most earlier tests used run-down tests rather than the steady-state tests used in the present work, comparison tests were run to explore possible differences in the test results. It was concluded that run-down tests could easily overestimate the values of damping by several hundred per cent. A new method for the measurements of natural periods of vibration of structures is proposed. The new method has several important advantages over wind-excited vibration tests which have been used extensively in the past to measure the natural periods of vibration of structures.

TABLE OF CONTENTS

CHAPTER I

INTRODUCTION

The transient response of a multistory building excited by an earthquake or an explosion is difficult to analyze in its full generality. Simplifying assumptions must be made concerning the force input as well as the dynamic characteristics of the structure. It would be desirable to have experimental results of the stresses and strains induced in actual buildings during strong-motion earthquakes or explosions in order to obtain information about the true interactions of the various elements of a multistory building. The response of the structure would depend upon many factors such as force input, size, shape, masses, stiffnesses of the various elements, degree and kind of foundation compliance, number and location of intentional and unintentional joints, energy dissipation characteristics, etc. Information of this kind is difficult to obtain since in any particular location, strong-motion earthquakes occur infrequently. Preliminary work in the determination of the dynamic properties of multistory buildings from measurements taken during earthquakes or nearby explosions has been carried out by Kobayashi,[1] Hudson,[2] Blume[3] and Hudson and Housner.[4]

Another method of obtaining information about the dynamic characteristics of multistory buildings is to somehow excite the buildings artificially into a vibrational motion. This would, of course, give no direct information about the effect an earthquake would have on the structure, but it would give information about the dynamic

characteristics of the structure such as its periods of vibration, mode shapes and energy absorption. Some of the earliest forced vibration tests are reported in ref. (5). Later tests have been carried out by a number of investigators; a description of the numerous ways of performing dynamic tests has been given by Hudson[6] whose paper contains an extensive bibliography listing most of the structural dynamics research carried out during the last 40 years.

Numerous laboratory tests on models and isolated building elements are reported in the literature. For example, Wilbur and Hansen[7] report static and dynamic tests of simply-supported reinforced concrete beams. Penzien[8] studied the damping characteristics of prestressed concrete beams. Pian, Hallowell and Bisplinghoff[9] investigated the damping capacity of built-up steel beams. While all of these studies are of value in extending our knowledge of the dynamic characteristics of the materials tested, it is very difficult to extend this knowledge to a description of the dynamic characteristics of any specific multistory building since, as already pointed out, the dynamic characteristics of a multistory building are affected by a large number of factors not necessarily governed by the characteristics of the materials of the structure.

The effect of foundation compliance on the dynamic response has been treated analytically by Lycan and Newmark, [10] an analog computer study was made by Merritt and Housner[11] and by Housner[12] who analyzed simultaneous recordings of acceleration of the basement of a building and of the ground some distance away from the building during an earthquake. The results indicated that

the effect of horizontal ground coupling was not appreciable for typical California soil conditions. It is of interest to note that in the dynamic tests described in Chapters III and IV, the motion of the ground floor in translation as well as in rotation was extremely small. On the other hand, in most of the dynamic tests of multistory buildings in Japan, as reported by Kawasumi and Kanai[13] and by Hisada and Nakagawa,[14] the results indicate that the ground motion accounts for most of the total response of the buildings. It is reasonable to assume then that in most of the Japanese tests a large portion of the energy dissipates into the ground rather than being dissipated in parts of the structure. In the present tests, as reported in Chapters III and IV, the reverse would be true. This points to the danger of comparing the results of dynamic tests without taking soil conditions into account.

The advent of modern high-speed computers has meant that many of the problems that are involved in analyzing the response of multistory buildings subjected to dynamic loads can now be treated in much more detail than was possible before. The analysis of nonlinear systems has been carried out by a number of investigators such as Penzien,[15] Veletsos and Newmark,[16] Berg[17] and Thomaides.[18] Computers have also made possible a closer look at some of the assumptions that are sometimes made in the analysis. Sekaran[18a] treated the effect of joint rotation. Rubenstein and Hurty[19] investigated the effects of joint rotation of a multistory steel frame building and Rubenstein[20] investigated the effect of axial deformation of the same building. The work presented here is no

exception; without the aid of a computer it would have been impossible to analyze in detail the data obtained from the forced vibration tests.

In the present work much attention has been given to the question of damping in structures. The question has been explored theoretically by Kimball,[21] White,[22] Den Hartog[23] and Jacobsen.[24] Values of damping determined from vibration tests are given by Kanai and Yoshizawa,[25] Dockstader, Swiger and Ireland,[26] Bleich and Teller[27] and Jacobsen.[28] The last reference includes abstracts of a large number of publications, most of them covering the damping as determined from Japanese vibration tests. The values of damping determined from the present tests are significantly smaller than the values usually mentioned in the literature. It was found that a very accurate speed control was needed to define precisely the response curve from a steady-state test. It was also found that run-down tests could lead to a determination of damping values that are up to 2.5 times as large as the damping determined from a steady-state test. Since most of the vibration tests of full-scale structures in the past have been in the form of run-down tests or, in a few cases, in the form of steady-state tests in which the speed of the exciter could not be controlled precisely, the values of damping as determined by earlier investigators should be treated with caution. These problems are discussed in detail in Chapter V.

The problem of determining the properties of a multistory building, when the force input as well as the response of the structure is known, has received very little attention. The most systematic treatment has been given by Berg.[29] Kanai[30] treated the special

problem of determining the stiffnesses of a multistory building when only information from one of the modes was available.

Contents of the Thesis

The aim of the work reported in this thesis has been to explore in considerable detail the dynamic characteristics of two modern multistory buildings.

In Chapter II the mathematical background of structural testing has been given. It is shown how the excitation of pure normal modes in general is an iterative process. The equations necessary to determine the stiffness and damping matrices from the experimentally determined modal properties have been developed. The determination of damping from the experimentally determined response curves has been treated in some detail. Some special problems encountered in the numerical analysis have been discussed in detail.

Chapter III discusses the experimental results obtained from dynamic tests of a five-story reinforced concrete building. Nonlinearities of the response are treated in detail. Four modes were excited in this structure; three of these were translational and one was a torsional mode.

Chapter IV concerns itself with the results of dynamic tests of a nine-story steel frame building. A total of eleven modes were determined experimentally, seven of these were translational, three were torsional and one was the mode in which the floor slabs vibrated horizontally as free-free beams. The natural periods of vibration were determined at 18 different stages of construction

covering a period of about 10 months.

In Chapter V the results of steady-state tests have been compared to those of run-down tests. In Chapter VI a new method for the measurement of the natural periods of structures is proposed.

Structural Vibration Exciters

A vibration exciter employing counter-rotating weights will apply inertia forces to the structure in one direction only, since the centrifugal forces from the rotating masses will be additive in one direction while their effects will cancel each other in the perpendicular direction. The forces applied to the structure are proportional to the square of the frequency and they vary sinusoidally with time. The four vibration exciters designed and developed at the California Institute of Technology for the California State Division of Architecture are of the above mentioned type in which two weights counter-rotate around a vertical axis. While the basic principle of creating sinusoidal forces by means of counter-rotating weights is the same as has been used in earlier vibration exciters, the present exciters are unique in two ways, (1) any number of the four can be run synchronized in phase of 180° out of phase, (2) the speed control of the exciters is extremely accurate, much more so than the speed controls of earlier vibration exciters. The speed can be controlled to an accuracy of about 0.1%, i.e., after running the exciters at a specific frequency, and recording the building response, it is possible to change the frequency of excitation to a new value that only differs 0.1% from the previous value.

The development of the exciters has been under the direction

of a special committee of the Earthquake Engineering Research Institute. The mechanical design of the vibration exciter and drive unit was carried out at Caltech under the direction of Professor D. A. Morelli. The electrical speed control and synchronization system was developed by Professor T. K. Caughey of Caltech. A description of the vibration exciters has been given by Hudson.[31]

Instrumentation

A total of six accelerometers were used simultaneously to record building response at different points in the building. The accelerometers were Statham strain gage accelerometers of ±2g range and 100 cps natural frequency. All accelerometers were mounted on a 6-3/4 lb steel block which made the assembly sufficiently heavy that friction could hold the block to the surface on which it was placed.

The signals from two of the accelerometers were amplified by a Brush carrier amplifier and were recorded on a direct inking Brush oscillograph. The signals from four of the accelerometers were amplified by two dual channel Sanborn carrier recorders and recorded by hot-wire writing arms on heat-sensitive recording charts. The two recorders were synchronized time-wise so that phase shifts in the responses of the four accelerometers could be investigated. The instrumentation set-up is shown in Fig. A-4 in the appendix. Typical response records from the Brush equipment are shown in Fig. 5-6 and from the Sanborn equipment in Figs. 5-2 and 5-4. A very complete description of instrumentation for structural vibrations has been given by Keightley.[32]

CHAPTER II

THEORY OF STRUCTURAL TESTING

The equation of motion of the multistory building of Fig. 2-1 is

$$[M]\{\ddot{x}\} + [C]\{\dot{x}\} + [K]\{x\} = \{f(t)\} \qquad (2.1)$$

In reducing the actual structure to the mathematical model of Eq. 2.1 and in the analysis that follows, the following assumptions are made:

1) The structure can be treated as a lumped-parameter system, i.e., the masses can be concentrated at the floor levels.
2) The system is linear.
3) Classical normal modes exist.
4) There is no base compliance.
5) The axial deformations of the columns are neglected.

The mass matrix $[M]$ is a diagonal matrix

$$[M] = \begin{bmatrix} m_1 & 0 & 0 \\ 0 & m_2 & 0 \\ 0 & 0 & m_n \end{bmatrix}$$

in which m_i is the mass of the i^{th} floor plus the contribution from the adjacent stories.

The stiffness matrix is

$$[K] = \begin{bmatrix} k_{11} & k_{12} & \cdots & k_{1n} \\ k_{21} & & & \\ k_{n1} & & \cdots & k_{nn} \end{bmatrix}$$

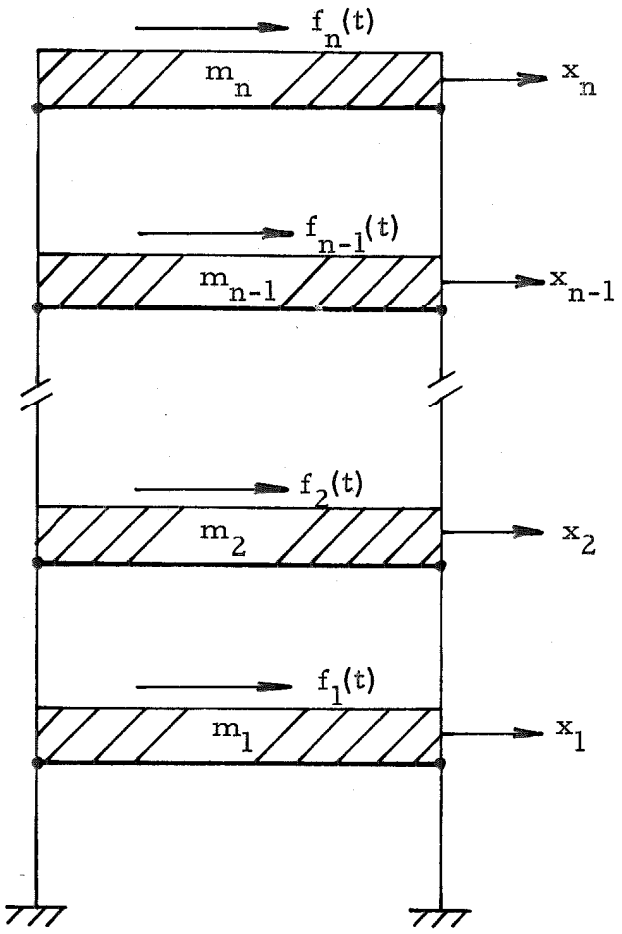

Fig. 2-1 BUILDING MODEL

in which k_{ij} is the force exerted on the i^{th} mass by the springs when the system has a configuration such that the i^{th} mass has a unit displacement and all other masses have zero displacement, i.e., $x_i=1$, $x_j=0$, $j \neq i$.

The damping matrix is

$$[C] = \begin{bmatrix} C_{11} & C_{12} \cdots\cdots C_{1n} \\ C_{21} & \\ C_{n1} \cdots\cdots\cdots\cdots C_{nn} \end{bmatrix}$$

in which C_{ij} is the force exerted on the i^{th} mass by the dashpots when the velocities of the masses are such that the i^{th} mass has a unit velocity and all other masses have zero velocity, i.e.,

$$\dot{x}_i=1, \qquad \dot{x}_j=0 , \qquad j \neq i$$

Let the displacement vector be

$$\{x\} = \begin{Bmatrix} x_1 \\ x_2 \\ \cdot \\ \cdot \\ \cdot \\ x_n \end{Bmatrix}$$

and the forcing vector be

$$\{f(t)\} = \begin{Bmatrix} f_1(t) \\ f_2(t) \\ \cdot \\ \cdot \\ \cdot \\ f_n(t) \end{Bmatrix}$$

$[M]$ is a diagonal matrix with positive diagonal elements. $[K]$ and

$[C]$ are symmetric.

The undamped natural frequencies and mode shapes are found from the homogeneous equation:

$$[M]\{\ddot{x}\} + [K]\{x\} = \{0\} \tag{2.2}$$

Let

$$\{x\} = [M]^{-1/2}\{\eta\} \tag{2.3}$$

Equation 2.2 then becomes

$$[M][M]^{-1/2}\{\ddot{\eta}\} + [K][M]^{-1/2}\{\eta\} = \{0\} \tag{2.4}$$

Premultiplying by $[M]^{-1/2}$:

$$[M]^{-1/2}[M][M]^{-1/2}\{\ddot{\eta}\} + [M]^{-1/2}[K][M]^{-1/2}\{\eta\} = \{0\} \tag{2.5}$$

or

$$[I]\{\ddot{\eta}\} + [\tilde{K}]\{\eta\} = 0 \tag{2.6}$$

$[K]$ is symmetric so $[\tilde{K}]$ is also symmetric since

$$[\tilde{K}]^T = \left([M]^{-1/2}[K][M]^{-1/2}\right)^T = [M]^{-1/2}[K]^T[M]^{-1/2} = [M]^{-1/2}[K][M]^{-1/2} = [\tilde{K}]$$

It is of interest to note that while $[\tilde{K}] = [M]^{-1/2}[K][M]^{-1/2}$ is a symmetric matrix, the matrix $[M]^{-1}[K]$ formed by premultiplying Eq. 2.2 by $[M]^{-1}$ is not in general symmetric. $[M]^{-1}[K]$ would only be a symmetric in the special case where all the masses in the system are identical.

A well known theorem in matrix algebra, see Perlis,[33] Hildebrand,[34] states that a symmetric matrix can be diagonalized by an orthogonal transformation. If it is assumed that the eigenvalues

are distinct and the orthogonal transformation matrix is normalized, then this transformation is unique. The elements of the diagonal matrix are equal to the eigenvalues. Let the transformation be

$$\{\eta\} = [\phi]\{\rho\} \tag{2.7}$$

such that

$$[\phi]^T [\phi] = [I] \tag{2.8}$$

Using the transformation given by Eq. 2.7 and premultiplying by $[\phi]^T$, Eq. 2.6 becomes

$$[\phi]^T[\phi]\{\ddot{\rho}\} + [\phi]^T[\tilde{K}][\phi]\{\rho\} = \{0\} \tag{2.9}$$

or

$$\{\ddot{\rho}\} + [\omega^2]\{\rho\} = \{0\} \tag{2.10}$$

The columns of $[\phi]$ are the eigenvectors of the system described by Eq. 2.6, so by the use of Eq. 2.3 the eigenvectors of the original system Eq. 2.2 are found to be:

$$[\psi] = [M]^{-1/2}[\phi] \tag{2.11}$$

The columns of $[\psi]$ are the normal modes of the original system. From Eq. 2.11 it follows that

$$[\phi] = [M]^{1/2}[\psi] \tag{2.12}$$

and

$$[\phi]^T = [\psi]^T [M]^{1/2} \tag{2.13}$$

Then from Eq. 2.8

$$[\phi]^T [\phi] = [\psi]^T [M]^{1/2} [M]^{1/2} [\psi] = [\psi]^T [M][\psi] = [I] \tag{2.14}$$

From the above equations it follows

$$[\phi]^T [\tilde{K}][\phi] = [\psi]^T [M]^{1/2} [\tilde{K}] [M]^{1/2} [\psi]$$

$$= [\psi]^T [M]^{1/2} [M]^{-1/2} [K] [M]^{-1/2} [M]^{1/2} [\psi] - [\psi]^T [K][\psi]$$

$$= \left[\omega^2 \right] \tag{2.15}$$

It would seem more direct to uncouple Eq. 2.2 by letting

$$\{x\} = [\psi]\{\rho\} \tag{2.16}$$

After premultiplying by $[\psi]^T$, Eq. 2.2 becomes

$$[\psi]^T [M] [\psi]\{\ddot{\rho}\} + [\psi]^T [K][\psi]\{\rho\} = \{0\} \tag{2.17}$$

or

$$[I]\{\ddot{\rho}\} + \left[\omega^2 \right] \{\rho\} = \{0\} \tag{2.18}$$

However, in some of the numerical analysis that follows it is more convenient to use the modal matrix in the form of Eq. 2.11

$$[\psi] = [M]^{-1/2} [\phi] \tag{2.11}$$

Expressed in this form one can take advantage of the fact that $[\phi]$ is a normalized orthogonal matrix.

In a passive system $[M]$ and $[K]$ are positive definite matrices and $[C]$ is a non negative matrix. This follows from the expressions for kinetic energy, potential energy and the dissipated energy, since

$$E_{kin.} = \frac{1}{2} \{\dot{x}\}^T [M]\{\dot{x}\} > 0 \qquad \text{for any } \{\dot{x}\} \neq \{0\} \tag{2.19}$$

$$E_{pot.} = \frac{1}{2} \{x\}^T [K]\{x\} > 0 \qquad \text{for any } \{x\} \neq \{0\} \tag{2.20}$$

$$E_{dis.} = \frac{1}{2} \{\dot{x}\}^T [C]\{\dot{x}\} \geq 0 \qquad \text{for any } \{\dot{x}\} \neq \{0\} \tag{2.21}$$

It is well known that since $[M]$ and $[K]$ are positive definite

matrices the eigenvalues ω^2 will be real and positive; also the eigenvectors $\{\psi\}$ will have real components. Including now the damping matrix Eq. 2.2 takes the form

$$[M]\{\ddot{x}\} + [C]\{\dot{x}\} + [K]\{x\} = \{0\} \tag{2.22}$$

As before let

$$\{x\} = [M]^{-1/2}\{\eta\} \tag{2.3}$$

After premultiplying by $[M]^{-1/2}$ Eq. 2.22 becomes

$$[I]\{\ddot{\eta}\} + [M]^{-1/2}[C][M]^{-1/2}\{\dot{\eta}\} + [M]^{-1/2}[K][M]^{-1/2}\{\eta\} = \{0\} \tag{2.23}$$

or

$$[I]\{\ddot{\eta}\} + [\tilde{C}]\{\dot{\eta}\} + [\tilde{K}]\{\eta\} = \{0\} \tag{2.24}$$

Since $[K]$ and $[C]$ are symmetric, $[\tilde{K}]$ and $[\tilde{C}]$ are also symmetric, let

$$\{\eta\} = [\phi]\{\rho\} \tag{2.7}$$

$[\phi]$ is the unique normalized orthogonal transformation matrix that uncoupled the undamped system. After premultiplying by $[\phi]^T$, Eq. 2.24 takes the form

$$[\phi]^T[\phi]\{\ddot{\rho}\} + [\phi]^T[\tilde{C}][\phi]\{\dot{\rho}\} + [\phi]^T[\tilde{K}][\phi]\{\rho\} = \{0\} \tag{2.25}$$

or

$$[I]\{\ddot{\rho}\} + [\phi]^T[\tilde{C}][\phi]\{\dot{\rho}\} + [\omega^2]\{\rho\} = \{0\} \tag{2.26}$$

Rayleigh[35] showed that if the damping matrix is a linear combination of the mass matrix and the stiffness matrix, the damped system will possess classical normal modes. The same transformation that led to uncoupled equations in the undamped case would also lead to uncoupled equations in the damped case. Let

$$[C] = a\,[M] + \gamma[K] \tag{2.27}$$

Then

$$[\phi]^T [\tilde{C}][\phi] = [\phi]^T [M]^{-1/2} [C][M]^{-1/2} [\phi]$$

$$= [\phi]^T [M]^{-1/2} \left(a\,[M] + \gamma[K] \right) [M]^{-1/2} [\phi]$$

$$= a\,[\phi]^T [M]^{-1/2} [M] [M]^{-1/2} [\phi] + \gamma [\phi]^T [M]^{-1/2} [K] [M]^{-1/2} [\phi]$$

$$= a\,[\phi]^T [\phi] + \gamma \left[\omega^2 \right] = a\,[I] + \gamma \left[\omega^2 \right] \tag{2.28}$$

Rayleigh's result is very useful since it attaches a physical description to the damping matrix. Since Eq. 2.27 is in terms of the uncoupled coordinate the i^{th} equation becomes

$$\ddot{\rho}_i + (a + \gamma \omega_i^2)\, \dot{\rho}_i + \omega_i^2 \rho_i = 0 \tag{2.29}$$

Expressing this equation in terms of the percentage of critical damping, Eq. 2.29 becomes

$$\ddot{\rho}_i + 2\beta_i \omega_i \dot{\rho}_i + \omega_i^2 \rho_i = 0 \tag{2.30}$$

In this equation

$$\beta_i = \frac{C}{C_{cr}} = \frac{a + \gamma \omega_i^2}{2\omega_i} \tag{2.31}$$

If $a = 0$ the damping matrix is proportional to the stiffness matrix and the damping mechanism can be represented as inter floor dashpots, i.e., relative damping. From Eq. 2.31 it follows that the percentage of critical damping is proportional to the natural frequency of the system. If $\gamma = 0$ the damping matrix is proportional to the mass matrix and the damping mechanism can be represented as dashpots connecting the masses to the base of the structure, i.e., absolute

damping. In this case it follows from Eq. 2. 31 that the percentage of critical damping is inversely proportional to the natural frequency.

As shown above the requirement that the damping matrix be a linear combination of the stiffness matrix and the mass matrix will lead to uncoupled equations of the type expressed in Eq. 2. 30. Furthermore, the same unique transformation that uncouples the system without damping will also uncouple the damped system, i. e., the mode shapes are the same in the two cases.

While Rayleigh's assumption is a sufficient condition, it is not a necessary condition. This was pointed out by Caughey[36] who went on to show that the necessary and sufficient condition for the existence of classical normal modes is that the same transformation that diagonalizes the damping matrix also uncouples the undamped system. In an undamped linear system the masses pass through their maximum and minimum positions at the same instant of time. If classical normal modes are to exist in a damped system the mode shapes must be the same as for the undamped system and the masses must pass through their maximum and minimum positions at the same instant of time.

Recently Caughey[37] showed that for linear systems with symmetric mass and stiffness matrices and for distinct eigenvalues a necessary and sufficient condition for the existence of classical normal modes could be expressed in the following form:

$$\left[M\right]^{-1/2}\left[C\right]\left[M\right]^{-1/2} = \sum_{\ell=0}^{n-1} a_\ell \left(\left[M\right]^{-1/2}\left[K\right]\left[M\right]^{-1/2}\right)^\ell \qquad (2.32)$$

In this equation n is the number of degrees of freedom of the system and ℓ takes on integer values. Equation 2.32 expresses a much wider class than Rayleigh's assumption. It can be seen that Eq. 2.32 leads to Rayleigh's assumption by letting $a_0=\alpha$, $a_1=\gamma$, $a_2=a_3=\ldots a_{n-1}=0$.

In the vibration tests on two multistory buildings described in Chapters III and IV, simultaneous measurements were recorded of the motion of several floors. The response records were synchronized timewise so it was possible to investigate whether the different floor masses passed through their maximum and minimum positions at the same instant of time when the system was excited into a pure natural mode. It was found that the masses did attain their maximum and minimum positions at the same instant of time.

This, however, does not prove that the damping matrix is truly of a form that would lead to classical normal modes in the situations investigated. It only shows that the damping matrix can be well approximated by a classical damping matrix, i.e., a matrix that is diagonalized by the same transformation that diagonalizes the mass and the stiffness matrices. O'Kelly[38] showed in performing perturbation analysis on a non-classically damped system that the first order approximation of the transformed damping matrix was the diagonal elements of this matrix. He went on to show in an analog computer study that for damping in each mode ranging up to 20% of critical damping that this approximation was well justified. Since the damping in the actual tests of structures was found to be less than 5%

of critical damping in all modes investigated, the assumption that classical normal modes exist seems well justified. In cases where classical normal modes do not exist the system can be analyzed by the more general method of Foss.[39]

The effect of damping on the natural frequencies of linear dynamic systems has been investigated by Caughey and O'Kelly[40] treating the case of classical normal modes as well as the case of nonclassical normal modes. It is of interest to note that if a system possesses classical normal modes the damped natural frequencies are always less than, or equal to, the corresponding undamped frequencies. In a system not possessing classical normal modes the damped natural frequency of the lowest mode may be higher than the corresponding undamped frequency. For damping values of the magnitude found in tests of multistory buildings, the differences between the damped natural frequencies and the undamped natural frequencies would be negligibly small.

Forced Excitation of Pure Normal Modes

The equation of motion of the damped system subjected to a forcing vector is:

$$[M]\{\ddot{x}\} + [C]\{\dot{x}\} + [K]\{x\} = \{f(t)\} \tag{2.1}$$

Let the system be uncoupled by the transformations used above, i.e.,

$$\{\ddot{\rho}\} + [2\omega_i\beta_i]\{\dot{\rho}\} + [\omega_i^2]\{\rho\} = [\phi]^T [M]^{-1/2}\{f(t)\} = \{g(t)\} \tag{2.33}$$

The i^{th} equation then becomes

$$\ddot{\rho}_i + 2\beta_i\omega_i\dot{\rho}_i + \omega_i^2\rho_i = g_i(t) \tag{2.34}$$

Assuming zero initial conditions, i.e., $\rho_i(0) = \dot{\rho}_i(0) = 0$ for all i then the r^{th} mode will be purely excited if

$$\begin{aligned} g_i(t) &= 0 \qquad \text{all } i \neq r \\ g_r(t) &\neq 0 \end{aligned} \tag{2.35}$$

or expressing the right hand side of Eq. 2.33

$$\left\{g_i(t)\right\} = \begin{Bmatrix} 0 \\ \vdots \\ 0 \\ g_r(t) \\ 0 \\ \vdots \\ 0 \end{Bmatrix} = \left[\phi\right]^T \left[M\right]^{-1/2} \left\{f(t)\right\} \tag{2.36}$$

Premultiply Eq. 2.36 by $\left(\left[\phi\right]^T\right)^{-1} = \left[\phi\right]$

$$\left[\phi\right] \begin{Bmatrix} 0 \\ \vdots \\ g_r(t) \\ \vdots \\ 0 \end{Bmatrix} = \left[M\right]^{-1/2} \left\{f(t)\right\} \tag{2.37}$$

Premultiply Eq. 2.37 by $\left[M\right]^{1/2}$

$$\left\{f(t)\right\} = \left[M\right]^{1/2}\left[\phi\right] \begin{Bmatrix} 0 \\ 0 \\ g_r(t) \\ 0 \\ 0 \end{Bmatrix} \tag{2.38}$$

Using

$$\left[\phi\right] = \left[M\right]^{1/2}\left[\psi\right] \tag{2.13}$$

Eq. 2.38 takes the form

$$\{f(t)\} = [M]^{1/2}[M]^{1/2}[\psi]\begin{Bmatrix} 0 \\ 0 \\ g_r(t) \\ 0 \\ 0 \end{Bmatrix} = [M][\psi]\begin{Bmatrix} 0 \\ 0 \\ g_r(t) \\ 0 \\ 0 \end{Bmatrix} = [M]\{\psi^{(r)}\}\, g_r(t) \qquad (2.39)$$

$g_r(t)$ may be any function of time. All that is required in order to excite the r^{th} mode of the system is that the force amplitudes be proportional to the mass at each station times the displacement coordinate of the r^{th} mode of that station. The largest response will of course be attained if the frequency of excitation is close to the natural frequency of the r^{th} mode.

Forced Excitation of Pure Normal Modes as an Iterative Process

In a complicated dynamic system the mode shapes may not be sufficiently well known to permit the use of the procedure explained above. An iterative process that converges on the excitation of a pure natural mode, say the r^{th} mode, might then be needed. Let all components of the initial forcing vector be sinusoidal with frequency ω but with arbitrary amplitudes. The equation of motion takes the form:

$$[M]\{\ddot{x}\} + [C]\{\dot{x}\} + [K]\{x\} = \{f(t)\} = \{P\}\sin\omega t \qquad (2.40)$$

As before let

$$\{x\} = [M]^{-1/2}\{\eta\} \qquad (2.3)$$

$$\{\eta\} = [\phi]\{\rho\} \qquad (2.7)$$

After performing the transformations of Eqs. 2.3 and 2.7 and after premultiplying by $[M]^{-1/2}$ and $[\phi]^T$, Eq. 2.40 takes the form:

$$\{\ddot{\rho}\} + \left[2\beta_i\omega_i\right]\{\dot{\rho}\} + \left[\omega_i^2\right]\{\rho\} = [\phi]^T [M]^{-1/2}\{P \sin\omega t\} = \{g(t)\} \tag{2.41}$$

The steady-state solution of Eq. 2.41 is known to be

$$\{\rho\} = \left[\frac{1}{z(\omega)}\right][\phi]^T [M]^{-1/2}\{P \sin(\omega t - \varphi)\} \tag{2.42}$$

where for simplicity

$$z_i(\omega) = \omega_i^2 \sqrt{\left[1-\left(\frac{\omega}{\omega_i}\right)^2\right]^2 + \left[2\beta_i \frac{\omega}{\omega_i}\right]^2} \tag{2.43}$$

Since

$$\{\eta\} = [\phi]\{\rho\} \tag{2.7}$$

and

$$\{x\} = [M]^{-1/2}\{\eta\} \tag{2.3}$$

Eq. 2.42 takes the form:

$$\{x\} = [M]^{-1/2}[\phi]\left[\frac{1}{z(\omega)}\right][\phi]^T [M]^{-1/2}\{P \sin(\omega t - \varphi)\} \tag{2.44}$$

and since the motion is steady state:

$$\{\ddot{x}\} = \omega^2 [M]^{-1/2}[\phi]\left[\frac{1}{z(\omega)}\right][\phi]^T [M]^{-1/2}\{P \sin(\omega t - \varphi)\} \tag{2.45}$$

Expressing Eq. 2.45 in terms of amplitudes of acceleration:

$$\{\ddot{x}\} = \begin{Bmatrix} |\ddot{x}_1| \\ |\ddot{x}_2| \\ |\ddot{x}_n| \end{Bmatrix} = \omega^2 [M]^{-1/2}[\phi]\left[\frac{1}{z(\omega)}\right][\phi]^T [M]^{-1/2}\{P\} \tag{2.46}$$

Let $\{P\}^{(1)}$ be any arbitrary distribution of force amplitudes and let $\omega \lesssim \omega_r$. Then it follows from Eq. 2.46:

$$\{\ddot{x}\}^{①} = \omega^2 [M]^{-1/2} [\phi] \left[\frac{1}{z(\omega)}\right] [\phi]^T [M]^{-1/2} \{P\}^{①} \tag{2.47}$$

Change the force distribution so that

$$\{P\}^{②} \underset{=}{\alpha} [M]\{\ddot{x}\}^{①} \tag{2.48}$$

and then from Eqs. 2.46, 2.47 and 2.48:

$$\{\ddot{x}\}^{②} \underset{=}{\alpha} \omega^2 [M]^{-1/2} [\phi] \left[\frac{1}{z(\omega)}\right] [\phi]^T [M]^{-1/2} [M] \omega^2 [M]^{-1/2} [\phi] \left[\frac{1}{z(\omega)}\right] [\phi]^T [M]^{-1/2} \{P\}^{①} \tag{2.49}$$

but

$$[M]^{-1/2} [M] [M]^{-1/2} = [I] \tag{2.8}$$

and

$$[\phi]^T [\phi] = [I] \tag{2.5}$$

so Eq. 2.49 becomes

$$\{\ddot{x}\}^{②} \underset{=}{\alpha} \omega^4 [M]^{-1/2} [\phi] \left[\frac{1}{z(\omega)}\right]^2 [\phi]^T [M]^{-1/2} \{P\}^{①} \tag{2.50}$$

After k iterations Eq. 2.50 takes the form:

$$\{\ddot{x}\}^{ⓚ} \underset{=}{\alpha} \omega^{2k} [M]^{-1/2} [\phi] \left[\frac{1}{z(\omega)}\right]^k [\phi]^T [M]^{-1/2} \{P\}^{①} \tag{2.51}$$

As $\omega \cong \omega_r$ and assuming distinct eigenvalues and small damping, say less than 10% of critical damping, the r^{th} element in the diagonal matrix $\left[\frac{1}{z(\omega)}\right]$ will be large compared to all other elements in the matrix, i.e.,

$$\frac{1}{z_r(\omega)} = \frac{1}{\omega_r^2\sqrt{\left[1-\left(\frac{\omega}{\omega_r}\right)^2\right]^2+\left[2\beta_r\frac{\omega}{\omega_r}\right]^2}} \gg \frac{1}{\omega_i^2\sqrt{\left[1-\left(\frac{\omega}{\omega_i}\right)^2\right]^2+\left[2\beta_i\frac{\omega}{\omega_i}\right]^2}}$$

$$= \frac{1}{z_i(\omega)} \qquad \text{for } r \neq i \tag{2.52}$$

As k becomes large

$$\left[\begin{array}{c} \\ \frac{1}{z(\omega)} \\ \\ \end{array}\right]^k \longrightarrow \begin{bmatrix} 0 & & \\ & 0 & \\ & & \left(\frac{1}{z_r(\omega)}\right)^k \\ & 0 & \\ & & 0 \end{bmatrix} \tag{2.53}$$

Let

$$[\phi]^T [M]^{-1/2} \{P\}^{(1)} = \{a\} \tag{2.54}$$

Then

$$\left[\begin{array}{c} \\ \frac{1}{z(\omega)} \\ \\ \end{array}\right]^k [\phi]^T [M]^{-1/2}\{P\}^{(1)} = \begin{bmatrix} 0 & & \\ & 0 & \\ & & \left(\frac{1}{z_r(\omega)}\right)^k \\ & 0 & \\ & & 0 \end{bmatrix}\{a\} = \begin{Bmatrix} 0 \\ 0 \\ a_r\left(\frac{1}{z(\omega)}\right)^k \\ 0 \\ 0 \end{Bmatrix}$$

$$= \begin{Bmatrix} 0 \\ 0 \\ b_r \\ 0 \\ 0 \end{Bmatrix} \tag{2.55}$$

Equation 2.51 then becomes

$$\begin{Bmatrix} x \\ \dot{x} \end{Bmatrix}^{(k)} \propto [M]^{-1/2}[\phi]\begin{Bmatrix} 0 \\ 0 \\ b_r \\ 0 \\ 0 \end{Bmatrix} \tag{2.56}$$

But since

$$\left[M\right]^{-1/2}\left[\phi\right] = \left[\psi\right] \tag{2.11}$$

Eq. 2.56 takes the form:

$$\left\{\ddot{x}\right\}^{(k)} \propto \left[\psi\right] \begin{Bmatrix} 0 \\ 0 \\ b_r \\ 0 \\ 0 \end{Bmatrix} = b_r \left\{\psi^{(r)}\right\} \tag{2.57}$$

For k sufficiently large the amplitudes of acceleration will be proportional to the r^{th} mode shape and since for steady state motion the acceleration is proportional to the displacement, the motion excited will be purely the r^{th} mode. It is obvious that the lower the damping in the structure and the better the separation of the natural frequencies, the fewer the number of iterations will be needed. Similarly, since the mode shapes are approximately known from an analysis of the structure, it is possible to cut down on the number of iterations needed by choosing an initial distribution of force amplitudes close to the masses multiplied by the components of the desired mode shape.

The iterative procedure has been found necessary in exciting the pure modes of aircraft structures for which the natural frequencies are usually close together. Lewis and Wrisley[41] report using 24 electrodynamic synchronized vibration exciters, the forces applied being variable in both frequency and magnitude in order to apply the iterative procedure in exciting pure natural modes. In most multistory buildings the natural modes are sufficiently well separated so that the natural modes of interest can be excited with only one or two vibration exciters placed in advantageous positions on one of the floors of the building.

Problems of mode interference usually do not exist for natural modes of the same type, for instance, if a multistory building behaves dynamically as a uniform shear beam, the lowest translational frequencies would be in the ratio of 1, 3, 5, 7 etc. However, the possibility exists that some torsional frequency might be close to one of the the translational frequencies. Similarly the natural frequency of the mode in which the floor slabs vibrate as free-free beams couldbe close to the natural frequency of one of the translational or torsional modes. These problems can, as will be shown later on, be solved by positioning two synchronized vibration exciters on one of the floors such that the undesired modes are subdued or eliminated entirely.

Forced Excitation of Pure Natural Modes, Synchronized Vibration Exciters Acting on Only One Mass

Let a sinusoidal force act on the k^{th} mass, i.e.,

$$\left\{f(t)\right\} = \begin{Bmatrix} 0 \\ \vdots \\ 0 \\ f_k(t) \\ 0 \\ \vdots \\ 0 \end{Bmatrix} = \begin{Bmatrix} 0 \\ \vdots \\ 0 \\ P_k \sin\omega t \\ 0 \\ \vdots \\ 0 \end{Bmatrix}$$

The equation of motion then becomes

$$\left[M\right]\left\{\ddot{x}\right\} + \left[C\right]\left\{\dot{x}\right\} + \left[K\right]\left\{x\right\} = \begin{Bmatrix} 0 \\ \vdots \\ 0 \\ P_k \sin\omega t \\ 0 \\ \vdots \\ 0 \end{Bmatrix} \qquad (2.58)$$

Performing the usual transformations leading to the uncoupled equations, Eq. 2.58 takes the form

$$\{\ddot{\rho}\} + \begin{bmatrix} \ddots & & \\ & 2\beta_i\omega_i & \\ & & \ddots \end{bmatrix} \{\dot{\rho}\} + \begin{bmatrix} \ddots & & \\ & \omega_i^2 & \\ & & \ddots \end{bmatrix} \{\rho\} = [\phi]^T [M]^{-1/2} \begin{Bmatrix} 0 \\ 0 \\ P_k \sin\omega t \\ 0 \\ 0 \end{Bmatrix}$$

$$= [\psi]^T \begin{Bmatrix} 0 \\ 0 \\ P_k \sin\omega t \\ 0 \\ 0 \end{Bmatrix} = \begin{Bmatrix} \psi_k^{(1)} \\ \psi_k^{(2)} \\ \vdots \\ \psi_k^{(n)} \end{Bmatrix} P_k \sin\omega t \qquad (2.59)$$

The steady state solution is equal to

$$\rho_i = \psi_k^{(i)} P_k \frac{1}{\omega_i^2 \sqrt{\left[1-\left(\frac{\omega}{\omega_i}\right)^2\right]^2 + \left[2\beta_i \frac{\omega}{\omega_i}\right]^2}} \sin(\omega t - \varphi_i) \qquad (2.60)$$

Assuming small damping, say less than 10% and for $\omega \cong \omega_r$ it is evident that if the natural frequencies of the system are well separated

$$\rho_i \cong 0 \qquad i \neq r$$

and

$$\rho_r = \psi_k^{(r)} P_k \frac{1}{\omega_r^2 \sqrt{\left[1-\left(\frac{\omega}{\omega_r}\right)^2\right]^2 + \left[2\beta_r \frac{\omega}{\omega_r}\right]^2}} \sin(\omega t - \varphi_r) \qquad (2.61)$$

Since

$$\{x\} = [M]^{-1/2} [\phi]\{\rho\} = [\psi]\{\rho\} \qquad (2.11)$$

then

$$\{x\} = \{\psi^{(r)}\} \psi_k^{(r)} P_k \frac{1}{\omega_r^2 \sqrt{\left[1-\left(\frac{\omega}{\omega_r}\right)^2\right]^2 + \left[2\beta_r \frac{\omega}{\omega_r}\right]^2}} \sin(\omega t - \varphi_r) \qquad (2.62)$$

From this equation it can be seen that the larger the k^{th} component in the r^{th} mode the larger the response. Also, if the k^{th} floor should be a node for the r^{th} mode, i.e., $\psi_k^{(r)}=0$, no motion will occur. So in order to eliminate the response of a specific mode the vibration exciters should be placed at one or more of the nodes for that particular mode.

Determination of the Stiffness and Damping Matrix From Experimentally Determined Modal Properties

Assuming again that classical normal modes exist, consider the equations:

$$[\psi]^T [M][\psi] = [I] \tag{2.14}$$

$$[\psi]^T [K][\psi] = \begin{bmatrix} \ddots & \\ & \omega_i^2 \\ & & \ddots \end{bmatrix} \tag{2.15}$$

$$[\psi]^T [C][\psi] = \begin{bmatrix} \ddots & \\ & 2\beta_i\omega_i \\ & & \ddots \end{bmatrix} \tag{2.63}$$

Premultiply Eq. 2.14 by $([\psi]^T)^{-1}$:

$$[M][\psi] = ([\psi]^T)^{-1} \tag{2.64}$$

Since the normal modes, i.e., the columns of $[\psi]$, are linearly independent, the modal vectors span the space and the existence of $([\psi]^T)^{-1}$ is guaranteed. Combining Eq. 2.64 with Eqs. 2.15 and 2.63 results in:

$$[K][\psi] = [M][\psi]\begin{bmatrix} \ddots & \\ & \omega_i^2 \\ & & \ddots \end{bmatrix} \tag{2.65}$$

$$[C][\psi] = [M][\psi]\begin{bmatrix} \ddots & \\ & 2\beta_i\omega_i \\ & & \ddots \end{bmatrix} \tag{2.66}$$

Expressing the equivalence of the r^{th} column of the left hand sides

and right hand sides of Eqs. 2.65 and 2.66:

$$[K]\{\psi^{(r)}\} = [M]\{\psi^{(r)}\}\,\omega_r^2 \tag{2.67}$$

$$[C]\{\psi^{(r)}\} = [M]\{\psi^{(r)}\}\,2\beta_r\omega_r \tag{2.68}$$

If the masses are known and $\{\psi^{(r)}\}$, ω_r and β_r have been determined from vibration tests of the structure, Eq. 2.67 expresses the unknown elements of the stiffness matrix in terms of known quantities. For each mode of an n degree-of-freedom system, Eq. 2.67 expresses n equations. If s modes have been determined experimentally, a total of s times n equations are available to determine the unknown elements in the stiffness matrix. Similarly s times n equations are available to determine the elements of the damping matrix, the equations being in the form of Eq. 2.68.

The number of unknown elements in the stiffness and damping matrix depends upon the coupling in the system. Three cases of practical interest will be considered here: I. Simply coupled system; II. Close coupled system; and III. Far coupled system.

I. Simply coupled system

Let the structure be represented by a mass-spring-dashpot system in which each mass is connected by springs and dashpots to adjacent masses only, and only one mass in the system is connected by a spring and a dashpot to the base. This type of a model would correspond to a "shear building" with infinitely rigid girders, i.e., with no rotation of the joints of the structure. In this case both the

stiffness and damping matrix will be tridiagonal; since in each row of the stiffness or damping matrix the elements in the matrix are interrelated there will be n unknown elements in the matrix. In order to solve Eqs. 2.67 and 2.68 the number of equations must be equal to or larger than the number of unknowns. Let the number of experimentally determined modes be s, then

$$sn \geq n \qquad \text{or} \qquad s \geq 1 \tag{2.69}$$

So, for the case of a simply coupled system only one mode is needed regardless of the number of degrees of freedom of the system. However, as will be shown, the equations resulting from only one known mode may be rather ill-conditioned.

For the sake of simplicity, the equations will be developed for a five-degree of freedom system. The extension to other systems will be obvious. Also, since Eqs. 2.67 and 2.68 are of the same form except for the difference in the column vector on the right hand sides, let the equations be developed only in terms of the elements of the stiffness matrix. Equation 2.67 can be expressed as

$$\begin{bmatrix} k_1+k_2 & -k_2 & 0 & 0 & 0 \\ -k_2 & k_2+k_3 & -k_3 & 0 & 0 \\ 0 & -k_3 & k_3+k_4 & -k_4 & 0 \\ 0 & 0 & -k_4 & k_4+k_5 & -k_5 \\ 0 & 0 & 0 & -k_5 & k_5 \end{bmatrix} \begin{Bmatrix} \psi_1^{(r)} \\ \psi_2^{(r)} \\ \psi_3^{(r)} \\ \psi_4^{(r)} \\ \psi_5^{(r)} \end{Bmatrix} = \begin{Bmatrix} m_1 \psi_1^{(r)} \omega_r^2 \\ m_2 \psi_2^{(r)} \omega_r^2 \\ m_3 \psi_3^{(r)} \omega_r^2 \\ m_4 \psi_4^{(r)} \omega_r^2 \\ m_5 \psi_5^{(r)} \omega_r^2 \end{Bmatrix} \tag{2.70}$$

For each mode determined experimentally, a set of equations in the

form of Eq. 2. 70 can be constructed. Equation 2. 70 can be expressed so that the unknown quantities appear as a column vector:

$$\begin{bmatrix} \varphi_1^{(r)} & \varphi_1^{(r)}-\varphi_2^{(r)} & 0 & 0 & 0 \\ 0 & \varphi_2^{(r)}-\varphi_1^{(r)} & \varphi_2^{(r)}-\varphi_3^{(r)} & 0 & 0 \\ 0 & 0 & \varphi_3^{(r)}-\varphi_2^{(r)} & \varphi_3^{(r)}-\varphi_4^{(r)} & 0 \\ 0 & 0 & 0 & \varphi_4^{(r)}-\varphi_3^{(r)} & \varphi_4^{(r)}-\varphi_5^{(r)} \\ 0 & 0 & 0 & 0 & \varphi_5^{(r)}-\varphi_4^{(r)} \end{bmatrix} \begin{Bmatrix} k_1 \\ k_2 \\ k_3 \\ k_4 \\ k_5 \end{Bmatrix} = \begin{Bmatrix} m_1\varphi_1^{(r)}\omega_r^2 \\ m_2\varphi_2^{(r)}\omega_r^2 \\ m_3\varphi_3^{(r)}\omega_r^2 \\ m_4\varphi_4^{(r)}\omega_r^2 \\ m_5\varphi_5^{(r)}\omega_r^2 \end{Bmatrix} \tag{2. 71}$$

Equation 2. 71 is in the form:

$$[A]\{y\} = \{b\} \tag{2. 72}$$

For an n degree of freedom system in which s modes have been determined experimentally $[A]$ will be a known (sn by n) matrix, $\{y\}$ will be an (n by 1) column vector containing the unknown quantities and $\{b\}$ will be an (sn by 1) column vector with known elements. If more than one mode has been determined experimentally the experimental errors will make the equations inconsistent. In this case a fitting procedure will be needed to make use of all the available data. The application of the method of "least squares" to this problem will be described later on.

If only one mode has been determined, Eqs. 2. 71 constitute a determinate set of equations. It can be seen from Eq. 2. 71 that the stiffness elements can be expressed in closed form as follows

$$k_s = \frac{\omega_r^2 \sum_{i=s}^{n} m_i \psi_i^{(r)}}{\psi_s^{(r)} - \psi_{s-1}^{(r)}} \qquad (2.73)$$

$$s=(1, 2, \ldots n)$$

In this equation k_s is the spring constant connecting the s^{th} mass to the $(s-1)^{th}$ mass. If the r^{th} mode shape should be such that both $\psi_s^{(r)}$ and $\psi_{s-1}^{(r)}$ are large and almost equal, the equation determining k_s could be very ill-conditioned. Figure 2-2 shows the experimentally determined mode shapes of the steel frame building described in Chapter IV. If only the first mode is used to determine the spring constants Eq. 2.73 could lead to relatively large errors in the determination of k_8 and k_7. If the modal coordinates shown in Fig. 2-2 were only accurate to within say ± 2% it is evident from Eq. 2.73 that the results for k_8 and k_7 could be in error by several hundred per cent. Similarly if only the second mode were used the results for k_3 and k_4 would be of doubtful value. In general, if only one mode is used in the determination of the stiffnesses, the use of Eq. 2.73 could lead to large errors in the determination of some of the k's.

From Eqs. 2.67 and 2.68 it is evident that the elements of the damping matrix can be determined in similar fashion leading to

$$C_s = \frac{2\beta_r \omega_r \sum_{i=s}^{n} m_i \psi_i^{(r)}}{\psi_s^{(r)} - \psi_{s-1}^{(r)}} \qquad (2.74)$$

It is interesting to note that the spring constants (or damping constants) that would be poorly determined by using the first mode only would be

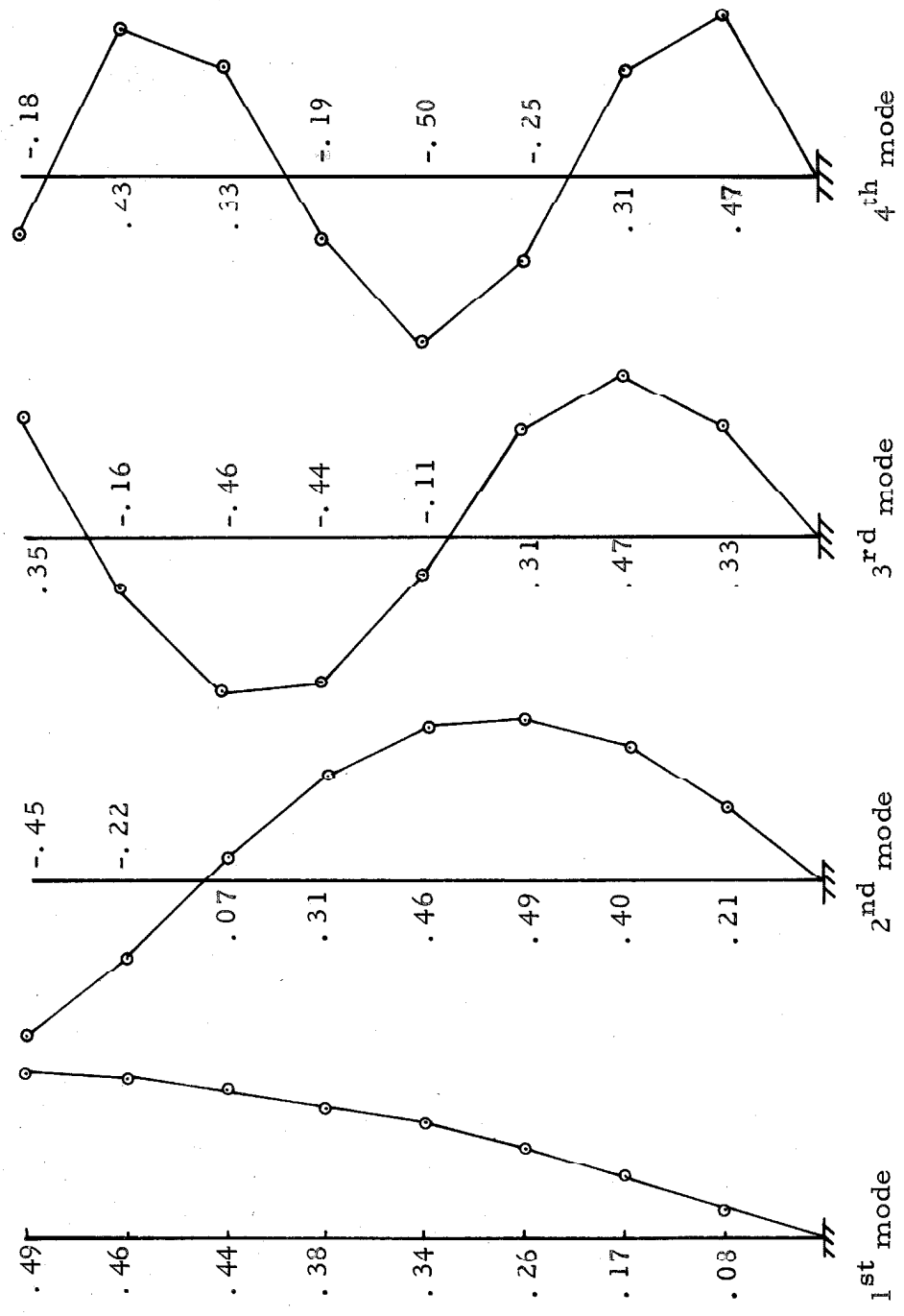

Fig. 2-2 EXPERIMENTALLY DETERMINED MODE SHAPES

well determined by using the second mode only and vice versa.

II. Close coupled system

Let each mass in the system be connected to adjacent masses by springs and dashpots and let each mass be connected by a spring and a dashpot to the base. If the damping matrix is a linear combination of the mass matrix and the stiffness matrix, i.e., the damping can be represented as a combination of relative and absolute damping, then the damping mechanism would be represented as a close coupled system. The stiffness and damping matrix would be tridiagonal but with no interrelation between the elements of each row or column. Each matrix would consist of 2n-1 unknown elements. For each mode experimentally determined, n equations of the type expressed in Eqs. 2.67 and 2.68 would be available. Let the number of experimentally determined modes be s, then in order to solve for the unknowns it is necessary that

$$sn \geq 2n-1$$

or

$$s \geq 2 - \frac{1}{n} \tag{2.75}$$

It is interesting to note that independent of the number of degrees of freedom in the system, two experimentally determined modes will suffice for the determination of the stiffness and damping elements in a close coupled system. Also, if two or more modes have been determined experimentally, the system of equations expressed by Eqs. 2.67 and 2.68 will always be overdetermined, i.e., the number of equations available will always exceed the number of unknowns.

Equation 2.67 states that:

$$\begin{bmatrix} k_{11} & k_{12} & 0 & 0 & 0 \\ k_{12} & k_{22} & k_{23} & 0 & 0 \\ 0 & k_{23} & k_{33} & k_{34} & 0 \\ 0 & 0 & k_{34} & k_{44} & k_{45} \\ 0 & 0 & 0 & k_{45} & k_{55} \end{bmatrix} \begin{Bmatrix} \psi_1^{(r)} \\ \psi_2^{(r)} \\ \psi_3^{(r)} \\ \psi_4^{(r)} \\ \psi_5^{(r)} \end{Bmatrix} = \begin{Bmatrix} m_1 \psi_1^{(r)} \omega_r^2 \\ m_2 \psi_2^{(r)} \omega_r^2 \\ m_3 \psi_3^{(r)} \omega_r^2 \\ m_4 \psi_4^{(r)} \omega_r^2 \\ m_5 \psi_5^{(r)} \omega_r^2 \end{Bmatrix} \tag{2.76}$$

Rewriting Eq. 2.76 so the unknown quantities appear as a column vector

$$\begin{bmatrix} \psi_1^{(r)} & \psi_2^{(r)} & 0 & 0 & 0 & 0 & 0 & 0 & 0 \\ 0 & \psi_1^{(r)} & \psi_2^{(r)} & \psi_3^{(r)} & 0 & 0 & 0 & 0 & 0 \\ 0 & 0 & 0 & \psi_2^{(r)} & \psi_3^{(r)} & \psi_4^{(r)} & 0 & 0 & 0 \\ 0 & 0 & 0 & 0 & 0 & \psi_3^{(r)} & \psi_4^{(r)} & \psi_5^{(r)} & 0 \\ 0 & 0 & 0 & 0 & 0 & 0 & 0 & \psi_4^{(r)} & \psi_5^{(r)} \end{bmatrix} \begin{Bmatrix} k_{11} \\ k_{12} \\ k_{22} \\ k_{23} \\ k_{33} \\ k_{34} \\ k_{44} \\ k_{45} \\ k_{55} \end{Bmatrix} = \begin{Bmatrix} m_1 \psi_1^{(r)} \omega_r^2 \\ m_2 \psi_2^{(r)} \omega_r^2 \\ m_3 \psi_3^{(r)} \omega_r^2 \\ m_4 \psi_4^{(r)} \omega_r^2 \\ m_5 \psi_5^{(r)} \omega_r^2 \end{Bmatrix} \tag{2.77}$$

Equation 2.77 is now in the form

$$[A]\{y\} = \{b\} \tag{2.72}$$

For an n degree of freedom system for which s modes have been determined experimentally $[A]$ is an (sn by 2n-1) matrix expressing the known mode shapes; $\{y\}$ is a (2n-1 by 1) column vector expressing the unknown spring constants and $\{b\}$ is an (sn by 1) column vector of experimentally determined elements. A similar analysis gives the

expression for the elements of the damping matrix as

$$\begin{bmatrix} \psi_1^{(r)} & \psi_2^{(r)} & 0 & 0 & 0 & 0 & 0 & 0 & 0 \\ 0 & \psi_1^{(r)} & \psi_2^{(r)} & \psi_3^{(r)} & 0 & 0 & 0 & 0 & 0 \\ 0 & 0 & 0 & \psi_2^{(r)} & \psi_3^{(r)} & \psi_4^{(r)} & 0 & 0 & 0 \\ 0 & 0 & 0 & 0 & 0 & \psi_3^{(r)} & \psi_4^{(r)} & \psi_5^{(r)} & 0 \\ 0 & 0 & 0 & 0 & 0 & 0 & 0 & \psi_4^{(r)} & \psi_5^{(r)} \end{bmatrix} \begin{Bmatrix} C_{11} \\ C_{12} \\ C_{22} \\ C_{23} \\ C_{33} \\ C_{34} \\ C_{44} \\ C_{45} \\ C_{55} \end{Bmatrix} = \begin{Bmatrix} 2m_1\beta_r \psi_1^{(r)} \omega_r \\ 2m_2\beta_r \psi_2^{(r)} \omega_r \\ 2m_3\beta_r \psi_2^{(r)} \omega_r \\ 2m_4\beta_r \psi_4^{(r)} \omega_r \\ 2m_5\beta_r \psi_5^{(r)} \omega_r \end{Bmatrix} \qquad (2.78)$$

III. Far coupled system

Let each mass in the system be connected to every other mass by springs and dashpots and let each mass be connected to the base by a spring and a dashpot. In the case of a multistory building, far coupling results when the girders are not infinitely rigid so that the joints in the structure rotate. For this case the stiffness and damping matrix are full. Each matrix will contain $n(n+1)/2$ unknown elements.

For each mode experimentally determined, n equations of the type expressed in Eqs. 2.67 and 2.68 are available. If s modes are determined experimentally in an n-degree of freedom system, then in order to solve for the unknowns, it is necessary that

$$sn \geq \frac{n(n+1)}{2} \qquad \text{or} \qquad s \geq \frac{n+1}{2} \qquad (2.79)$$

Equation 2.67 states that:

$$\begin{bmatrix} k_{11} & k_{12} & k_{13} & k_{14} & k_{15} \\ k_{12} & k_{22} & k_{23} & k_{24} & k_{25} \\ k_{13} & k_{23} & k_{33} & k_{34} & k_{35} \\ k_{14} & k_{24} & k_{34} & k_{44} & k_{45} \\ k_{15} & k_{25} & k_{35} & k_{45} & k_{55} \end{bmatrix} \begin{Bmatrix} \psi_1^{(r)} \\ \psi_2^{(r)} \\ \psi_3^{(r)} \\ \psi_4^{(r)} \\ \psi_5^{(r)} \end{Bmatrix} = \begin{Bmatrix} m_1 \psi_1^{(r)} \omega_r^2 \\ m_2 \psi_2^{(r)} \omega_r^2 \\ m_3 \psi_3^{(r)} \omega_r^2 \\ m_4 \psi_4^{(r)} \omega_r^2 \\ m_5 \psi_5^{(r)} \omega_r^2 \end{Bmatrix} \tag{2.80}$$

Rewriting Eq. 2.80 so that the unknown quantities are expressed as a column vector:

$$\begin{bmatrix} \psi_1 & \psi_2 & \psi_3 & \psi_4 & \psi_5 & 0 & 0 & 0 & 0 & 0 & 0 & 0 & 0 & 0 & 0 \\ 0 & \psi_1 & 0 & 0 & 0 & \psi_2 & \psi_3 & \psi_4 & \psi_5 & 0 & 0 & 0 & 0 & 0 & 0 \\ 0 & 0 & \psi_1 & 0 & 0 & 0 & \psi_2 & 0 & 0 & \psi_3 & \psi_4 & \psi_5 & 0 & 0 & 0 \\ 0 & 0 & 0 & \psi_1 & 0 & 0 & 0 & \psi_2 & 0 & 0 & \psi_3 & 0 & \psi_4 & \psi_5 & 0 \\ 0 & 0 & 0 & 0 & \psi_1 & 0 & 0 & 0 & \psi_2 & 0 & 0 & \psi_3 & 0 & \psi_4 & \psi_5 \end{bmatrix} \begin{Bmatrix} k_{11} \\ k_{12} \\ k_{13} \\ k_{14} \\ k_{15} \\ k_{22} \\ k_{23} \\ k_{24} \\ k_{25} \\ k_{33} \\ k_{34} \\ k_{35} \\ k_{44} \\ k_{45} \\ k_{55} \end{Bmatrix} = \begin{Bmatrix} m_1 \psi_1^{(r)} \omega_r^2 \\ m_2 \psi_2^{(r)} \omega_r^2 \\ m_3 \psi_3^{(r)} \omega_r^2 \\ m_4 \psi_4^{(r)} \omega_r^2 \\ m_5 \psi_5^{(r)} \omega_r^2 \end{Bmatrix} \tag{2.81}$$

Equation 2.81 is now in the form

$$[A]\{y\} = \{b\} \tag{2.72}$$

For an n degree of freedom system for which s modes have been determined experimentally $[A]$ is an (sn by n(n+1)/2) matrix expressing known mode shapes; $\{y\}$ is an (n(n+1)/2 by 1) column vector containing the unknown spring constants and $\{b\}$ is an (sn by 1) column vector of experimentally determined elements. A similar analysis gives the expression for the elements of the damping matrix:

$$\begin{bmatrix} \psi_1 & \psi_2 & \psi_3 & \psi_4 & \psi_5 & 0 & 0 & 0 & 0 & 0 & 0 & 0 & 0 & 0 & 0 \\ 0 & \psi_1 & 0 & 0 & 0 & \psi_2 & \psi_3 & \psi_4 & \psi_5 & 0 & 0 & 0 & 0 & 0 & 0 \\ 0 & 0 & \psi_1 & 0 & 0 & 0 & \psi_2 & 0 & 0 & \psi_3 & \psi_4 & \psi_5 & 0 & 0 & 0 \\ 0 & 0 & 0 & \psi_1 & 0 & 0 & 0 & \psi_2 & 0 & 0 & \psi_3 & 0 & \psi_4 & \psi_5 & 0 \\ 0 & 0 & 0 & 0 & \psi_1 & 0 & 0 & 0 & \psi_2 & 0 & 0 & \psi_3 & 0 & \psi_4 & \psi_5 \end{bmatrix} \begin{Bmatrix} C_{11} \\ C_{12} \\ C_{13} \\ C_{14} \\ C_{15} \\ C_{22} \\ C_{23} \\ C_{24} \\ C_{25} \\ C_{33} \\ C_{34} \\ C_{35} \\ C_{44} \\ C_{45} \\ C_{55} \end{Bmatrix} = \begin{Bmatrix} 2m_1\beta_r\omega_r\psi_1 \\ 2m_2\beta_r\omega_r\psi_2 \\ 2m_3\beta_r\omega_r\psi_3 \\ 2m_4\beta_r\omega_r\psi_4 \\ 2m_5\beta_r\omega_r\psi_5 \end{Bmatrix} \tag{2.83}$$

Solution of $[A]\{y\} = \{b\}$

Let $[A]$ be a (p by q) matrix with known elements; let $\{y\}$ be a (q by 1) column vector containing unknown elements and let $\{b\}$ be a (p by 1) column vector with known elements. If $q < p$ there are fewer independent equations than unknowns and no unique solution exists. If $q = p$ the number of independent equations is equal to the number of unknowns, $[A]$ is a square matrix and $\{y\} = [A]^{-1}\{b\}$ is the unique solution.

If $q > p$ there are more equations than unknowns and, in general, there will be no exact solution since inaccuracies in the experimental data will make the equations inconsistent. The Gauss-Markoff theorem[42] states that the least squares estimates are the "best" linear unbiased estimates, where "best" means minimum variance among the unbiased estimates.

Returning to

$$[A]\{y\} = \{b\} \tag{2.72}$$

and rewriting Eq. 2.72 in terms of the error vector $\{e\}$

$$[A]\{y\} - \{b\} = \{e\} \tag{2.84}$$

Squaring both sides of Eq. 2.84

$$\left([A]\{y\} - \{b\}\right)^T \left([A]\{y\} - \{b\}\right) = \{e\}^T \{e\} \tag{2.85}$$

or

$$\{y\}^T [A]^T [A]\{y\} - \{y\}^T [A]^T \{b\} - \{b\}^T [A]\{y\} + \{b\}^T \{b\} = \{e\}^T \{e\} \tag{2.86}$$

The minimal condition is determined by partial differentiation of Eq. 2.86 with respect to either $\{y\}^T$ or $\{y\}$:

$$2\left[A\right]^T\left[A\right]\{y\} - 2\left[A\right]^T\{b\} = \{0\} \tag{2.87}$$

$$\left[A\right]^T\left[A\right]\{y\} = \left[A\right]^T\{b\} \tag{2.88}$$

Equation 2.88 gives the "normal equations" and the simple expedient of premultiplying Eq. 2.72 by $\left[A\right]^T$ leads to Eq. 2.88 in which 1) the number of unknowns is equal to the number of equations 2) $\left[A\right]^T\left[A\right]$ is a symmetric matrix, and 3) the solution of Eq. 2.88 will be the "least squares" solution.

If some equations should be more reliable than others it would be necessary to minimize the weighted errors and Eq. 2.84 would then be of the form:

$$\left(\left[A\right]\{y\} - \{b\}\right)^T\left[W\right]\left(\left[A\right]\{y\} - \{b\}\right) = \{e\}^T\left[W\right]\{e\} \tag{2.89}$$

$\left[W\right]$ is a diagonal matrix in which W_i is the weight attached to the i^{th} equation. Again partial differentiation with respect to $\{y\}^T$ or $\{y\}$ leads to the equation:

$$\left[A\right]^T\left[W\right]\left[A\right]\{y\} = \left[A\right]^T\left[W\right]\{b\} \tag{2.90}$$

It should be noted that in a system of equations in which the number of equations exceeds the number of unknowns one is not free to multiply some equations by a constant and other equations by a different constant. This procedure would tend to weight some equations differently than other equations. An example will show this; let a system of equations be given, case I

$$
\begin{aligned}
2x-y &= 1 \\
3x + 5y &= 9 \\
10x + 12y &= 25
\end{aligned}
\tag{2.91}
$$

Solving the equations using the method of "least squares", Eq. 2.91 takes the form:

$$
\begin{bmatrix} 2 & 3 & 10 \\ -1 & 5 & 12 \end{bmatrix}
\begin{bmatrix} 2 & -1 \\ 3 & 5 \\ 10 & 12 \end{bmatrix}
\begin{Bmatrix} x \\ y \end{Bmatrix}
=
\begin{bmatrix} 2 & 3 & 10 \\ -1 & 5 & 12 \end{bmatrix}
\begin{Bmatrix} 1 \\ 9 \\ 25 \end{Bmatrix}
\tag{2.92}
$$

or

$$
\begin{bmatrix} 113 & 133 \\ 133 & 170 \end{bmatrix}
\begin{Bmatrix} x \\ y \end{Bmatrix}
=
\begin{Bmatrix} 279 \\ 344 \end{Bmatrix}
\tag{2.93}
$$

The solution of Eq. 2.93 is

$$
\begin{aligned}
x &= 1.10322 \\
y &= 1.16042
\end{aligned}
\tag{2.94}
$$

Let the same set of equations be given in the following form, case II

$$
\begin{aligned}
2x-y &= 1 \\
\frac{1}{3}x + \frac{5}{9}y &= 1 \\
\frac{10}{25}x + \frac{12}{25}y &= 1
\end{aligned}
\tag{2.95}
$$

The "least squares" solution now takes the form

$$
\begin{bmatrix} 2 & \frac{1}{3} & \frac{10}{25} \\ -1 & \frac{5}{9} & \frac{12}{25} \end{bmatrix}
\begin{bmatrix} 2 & -1 \\ \frac{1}{3} & \frac{5}{9} \\ \frac{10}{25} & \frac{12}{25} \end{bmatrix}
\begin{Bmatrix} x \\ y \end{Bmatrix}
=
\begin{bmatrix} 2 & \frac{1}{3} & \frac{10}{25} \\ -1 & \frac{5}{9} & \frac{12}{25} \end{bmatrix}
\begin{Bmatrix} 1 \\ 1 \\ 1 \end{Bmatrix}
\tag{2.96}
$$

The solution of Eq. 2.96 is

$$x = 1.08237$$
$$y = 1.16441 \qquad (2.97)$$

This example was constructed so that the right hand sides of Eq. 2.91 correspond to the measured values of the three lowest natural frequencies squared, i.e., ω_1^2, ω_2^2 and ω_3^2. After having found x and y from Eqs. 2.91 and 2.95 it is of interest to see how case I and case II would approximate the experimentally determined ω's. Using Eq. 2.94 the left hand sides of Eq. 2.91 have the values:

$$\begin{aligned} 2x-y &\equiv 1.046 \\ 3x+5y &\equiv 9.112 \\ 10x+12y &\equiv 24.957 \end{aligned} \qquad (2.98)$$

If one instead used Eq. 2.97 the left hand sides of Eq. 2.91 have the values:

$$\begin{aligned} 2x-y &\equiv 1.000 \\ 3x+5y &\equiv 9.069 \\ 10x+12y &\equiv 24.797 \end{aligned} \qquad (2.99$$

The right hand sides of Eqs. 2.98 and 2.99 are:

Case I	Case II
$\omega_1^2 = 1.046$	$\omega_1^2 = 1.000$
$\omega_2^2 = 9.112$	$\omega_2^2 = 9.069$
$\omega_3^2 = 24.957$	$\omega_3^2 = 24.797$

The measured values in this hypothetical example were $\omega_1^2=1$; $\omega_2^2=9$ and $\omega_3^2=25$. While case I tends to give the same absolute errors in the three equations, case II tends to give the same relative

errors when compared to the measured values ω_1^2, ω_2^2 and ω_3^2.

The above example was constructed so that it corresponds to the equations by means of which the stiffness matrix is determined from the experimentally measured natural frequencies and mode shapes.

If the three lowest modes were determined experimentally Eq. 2.67 could be written

$$\begin{aligned} \left[A^{(1)}\right]\{k\} &= [M]\{\psi^{(1)}\}\,\omega_1^2 \\ \left[A^{(2)}\right]\{k\} &= [M]\{\psi^{(2)}\}\,\omega_2^2 \\ \left[A^{(3)}\right]\{k\} &= [M]\{\psi^{(3)}\}\,\omega_3^3 \end{aligned} \tag{2.100}$$

in which $\left[A^{(1)}\right]$, $\left[A^{(2)}\right]$ and $\left[A^{(3)}\right]$ are constructed from the experimentally measured components of the first, second and third mode shapes. For an n degree of freedom system there would be 3n equations corresponding to Eq. 2.100. Equation 2.100 could have been written in the following form

$$\begin{aligned} \frac{1}{\omega_1^2}\left[A^{(1)}\right]\{k\} &= [M]\{\psi^{(1)}\} \\ \frac{1}{\omega_2^2}\left[A^{(2)}\right]\{k\} &= [M]\{\psi^{(2)}\} \\ \frac{1}{\omega_3^2}\left[A^{(3)}\right]\{k\} &= [M]\{\psi^{(3)}\} \end{aligned} \tag{2.101}$$

Referring to the numerical example above the solution of Eq. 2.100 would lead to a determination of the unknown $\{k\}$ such that the stiffness matrix would determine natural frequencies that would have about

the same absolute errors in ω_1^2, ω_2^2 and ω_3^2 when compared to the experimentally measured values. On the other hand Eq. 2.101 would give a stiffness matrix that would determine natural frequencies that would have approximately the same relative errors in ω_1^2, ω_2^2 and ω_3^2 when these values are compared to the experimentally measured values.

Finding the Natural Frequencies and Mode Shapes from Known System Properties

After having determined the system properties from the experimental measurements it is necessary to examine how well the mathematical model of the system really represents the actual structure. The equation of motion for undamped free vibrations is

$$[M]\{\ddot{x}\} + [K]\{x\} = \{0\} \qquad (2.2)$$

where $[K]$ is determined from the experimental results. A number of methods are available to solve the eigenvalue problem of Eq. 2.2. Some methods would be practical to use if only a few of the eigenvalues were needed. Other methods would be more practical to use if all the eigenvalues were needed. For example, Stodola's method (or matrix iteration) would be useful if only the dominant (or a few dominant) eigenvalues were needed. The first matrix iteration would yield the dominant eigenvalue and eigenvector. After using the orthogonality relationship the problem is "deflated" and the next matrix iteration yields the now dominant eigenvalue and eigenvector. However, round-off errors will give some inaccuracy in the determination of the

dominant eigenvalue and the process of "deflation" will lead to a further loss of accuracy in the determination of the second eigenvalue. The process involves "successive contamination" and would not be a practical method if all the eigenvalues and eigenvectors were needed. Holzer's method can be made to converge towards any eigenvalue with any degree of accuracy desired but the method is based on a simple recurrence relationship that only holds true in the special case of a simply connected system. In the present problem the system is not in general simply connected and it is of interest to determine all the eigenvalues and eigenvectors. Jacobi's method[43] requires the use of a computer but it leads to a determination of all the eigenvalues and eigenvectors to any desired degree of accuracy.

Let as before

$$\{x\} = [M]^{-1/2} \{\eta\} \tag{2.3}$$

After premultiplying by $[M]^{-1/2}$, Eq. 2.2 takes the form

$$[M]^{-1/2} [M] [M]^{-1/2} \{\ddot{\eta}\} + [M]^{-1/2} [K] [M]^{-1/2} \{\eta\} = 0 \tag{2.5}$$

or

$$\{\ddot{\eta}\} + [\tilde{K}] \{\eta\} = \{0\} \tag{2.6}$$

$[\tilde{K}]$ is a symmetric matrix and as shown before Eq. 2.6 can be reduced to the following form

$$[\phi]^T [\phi] \{\ddot{\rho}\} + [\phi]^T [\tilde{K}] [\phi] \{\rho\} = \{0\} \tag{2.9}$$

or

$$\{\ddot{\rho}\} + [\omega^2] \{\rho\} = \{0\} \tag{2.10}$$

If the $[\phi]$ can be found such that

$$[\phi]^T [\phi] = [I] \tag{2.8}$$

and

$$[\phi]^T [K][\phi] = [\omega^2] \tag{2.15}$$

the eigenvalues of the problem expressed in Eq. 2.2 will appear on the diagonal of the matrix in Eq. 2.15 and the eigenvectors of Eq. 2.2 will be

$$[\psi] = [M]^{-1/2} [\phi] \tag{2.12}$$

Without loss of generality, let the largest off-diagonal element of $[\tilde{K}]$ be $\tilde{k}_{12}$, and let $[\tilde{K}]$ be rotated as follows

$$[R_1]^T [\tilde{K}][R_1] \tag{2.102}$$

in which

$$[R_1] = \begin{bmatrix} c & -s & & \\ s & c & & \\ & & 1 & \\ & & & \ddots \\ & & & & 1 \end{bmatrix} \tag{2.103}$$

and

$$c = \frac{1}{\sqrt{1+t^2}} \quad ; \qquad s = \frac{t}{\sqrt{1+t^2}}$$

$$t = \frac{\tilde{k}_{22} - \tilde{k}_{11}}{2\tilde{k}_{12}} - \sqrt{\left(\frac{\tilde{k}_{22} - \tilde{k}_{11}}{2\tilde{k}_{12}}\right)^2 + 1} \tag{2.104}$$

Since $c^2 + s^2 = 1$ the rotation matrix $[R_1]$ is clearly an orthogonal matrix, i.e., $[R_1]^T [R_1] = [I]$. After performing the rotation of Eq. 2.102 the resulting matrix will be

$$\left[R_1\right]^T \left[\tilde{K}\right] \left[R_1\right] = \begin{bmatrix} b_{11} & 0 & b_{12} \cdots\cdots b_{1n} \\ 0 & b_{22} & b_{23} \cdots\cdots \\ b_{21} & b_{32} & b_{33} \cdots\cdots \\ \cdot & \cdot & \cdot \\ \cdot & \cdot & \cdot \\ \cdot & \cdot & \cdot \\ b_{n1} \cdots\cdots\cdots\cdots\cdots & & b_{n2} \end{bmatrix} = \left[b_1\right] \qquad (2.105)$$

Next make a new orthogonal rotation such that the largest off-diagonal element in $\left[b_1\right]$ is made zero, i.e.,

$$\left[R_2\right]^T \left[b_1\right]\left[R_2\right] = \left[R_2\right]^T \left[R_1\right]^T \left[\tilde{K}\right]\left[R_1\right]\left[R_2\right] = \left[b_2\right] \qquad (2.106)$$

Continuing this process $\left[\tilde{K}\right]$ will after k rotations be of the form

$$\left[R_k\right]^T \cdots \left[R_2\right]^T \left[R_1\right]^T \left[\tilde{K}\right]\left[R_1\right]\left[R_2\right] \cdots \left[R_k\right] = \begin{bmatrix} \omega^2 \end{bmatrix} \qquad (2.107)$$

It is not obvious that the rotation process will converge to the diagonal matrix expressed in Eq. 2.107 but it was shown by Newman[43] that by choosing k sufficiently large the sum of the squares of the off-diagonal elements of the rotated matrix can be made as small as desired. Thus by choosing k sufficiently large the matrix of Eq. 2.107 can be made to differ from a diagonal matrix by as little as desired. The eigenvalues are then found to any desired degree of accuracy from

$$\left[R_k\right]^T \cdots \left[R_1\right]^T \left[\tilde{K}\right]\left[R_1\right] \cdots \left[R_k\right] = \left[\phi\right]^T \left[\tilde{K}\right]\left[\phi\right] = \begin{bmatrix} \omega^2 \end{bmatrix} \qquad (2.108)$$

while the eigenvectors of the original problem of Eq. 2.2 are found as

$$\left[\psi\right] = \left[M\right]^{-1/2} \left[\phi\right] \qquad (2.12)$$

The above mentioned operations were programmed for the Burroughs 220 computer. Subroutines have later become available that more efficiently solve the eigenvalue problem by a tridiagonalization of the

matrix rather than the complete diagonalization procedure used above.

Determination of Damping from the Experimental Results

In the preceeding analysis the damping was treated as if it were purely viscous, i. e., damping forces proportional to velocities and independent of amplitudes. In an actual structure the damping forces are of course not truly viscous, but they can be treated as such by employing the principle of "equivalent viscous damping" as used by Jacobsen[24] to investigate the steady-state response of a single degree of freedom system with non-viscous damping. By using, instead of the actual damping force, the viscous damping force that would dissipate the same amount of energy per cycle it was possible to compare the steady-state response in the two cases. It is evident from Jacobsen's work that as long as the total damping in the structure is reasonably small, say less than 15% of critical damping, mixed damping can be treated satisfactorily by using the concept of equivalent viscous damping. The actual damping in a structure would probably be a combination of several kinds of damping, such as, viscous damping, Coulomb damping and quadratic velocity damping. It is not possible to detect from the shape of the resonance curve the type of damping that is present in a structure. Iwan[44] calculated theoretical steady-state response curves for a one degree of freedom system having a combination of hysteretic damping and viscous damping. The results

show clearly that the response curves are very similar to those of a system having viscous damping only. Several methods are available to determine the percentage of critical damping from an experimentally determined steady-state response curve.

Method I

It is well known that the damping in a linear single degree of freedom system can be evaluated from the width of the response curve measured at an amplitude of $\sqrt{2}/2$ times the resonant amplitude. The response curve is constructed as the displacement at constant force versus frequency. The damping is found as

$$\beta = \frac{c}{c_{cr}} = \frac{\Delta\omega}{2\omega_n} \tag{2.109}$$

where $\Delta\omega$ is the width of the response curve and ω_n is the natural frequency. In using this method of finding the damping it is assumed that the damping does not vary significantly over the amplitude range. Should the damping be strongly dependent upon amplitude level, it would be necessary to work out a scheme so that the forces applied by the vibration exciters could be regulated in such a way that the amplitude could be kept constant at all frequencies of excitation. This would require the eccentricity of the rotating weights to be changed as the frequency of excitation was changed.

Method II

Hudson[45] noticed a very simple approximate method of finding the equivalent viscous damping based directly on the acceleration response for a structure excited by an ω^2-excitation. Figure 2-3

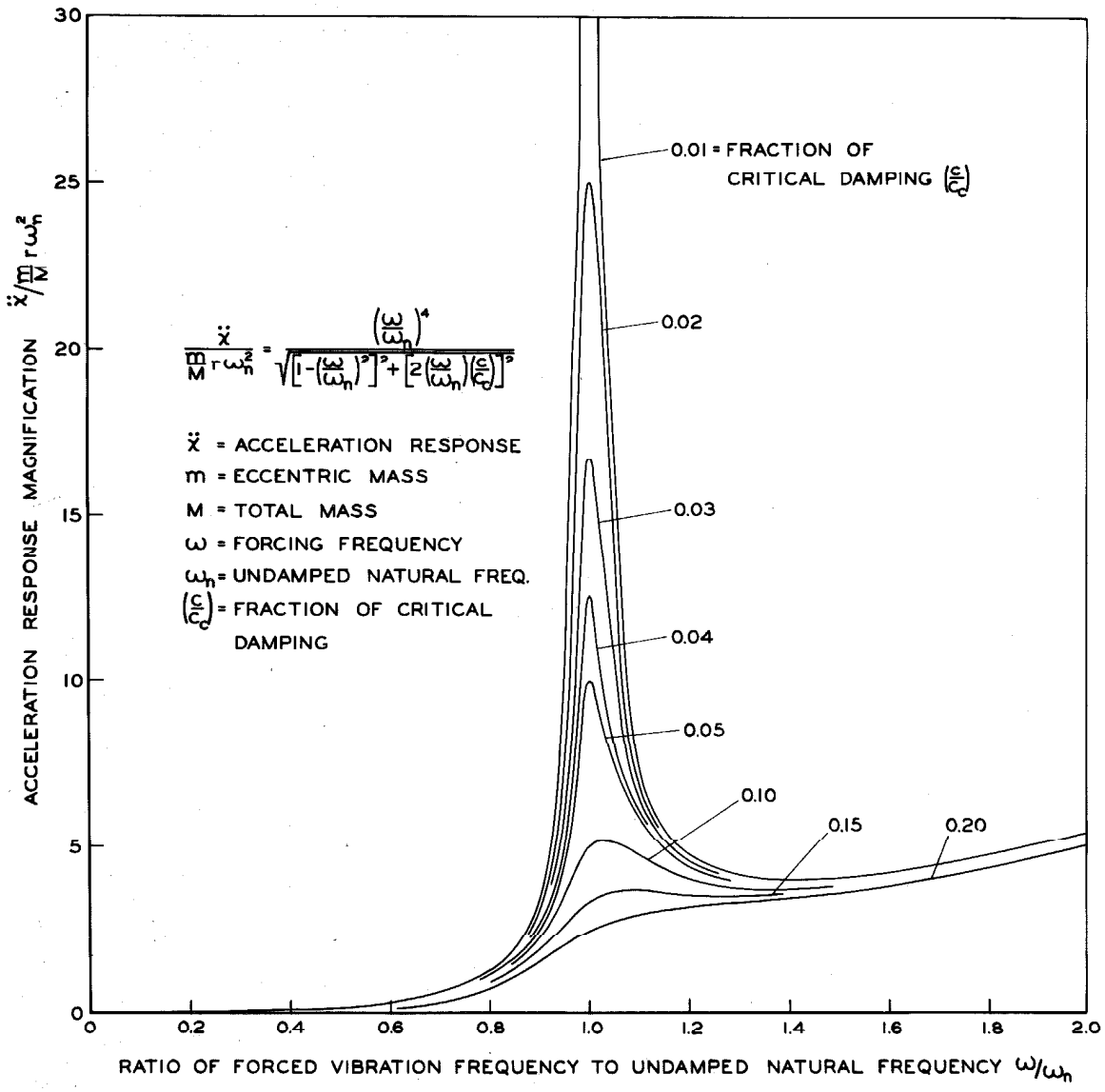

FIG. 2-3 COMPUTED ACCELERATION RESPONSE RESONANCE CURVES

shows the acceleration response of a single degree of freedom system for various values of damping. The acceleration is plotted versus frequency for an ω^2-excitation. It will be noted from the curves that for a frequency that lies above the resonant frequency the acceleration response curve will have a horizontal tangent and that at this point for moderate values of damping the acceleration will have approximately the same value regardless of the value of damping. On the other hand the values of acceleration at resonance will depend strongly on the damping value. Hudson calculated the ratios of the resonance peak amplitude to the amplitude of the curve where it has the horizontal tangent. Figure 2-4 shows these ratios as a function of damping. This method is very practical since if the acceleration is measured as the structure is excited by an ω^2-excitation, no data reduction is needed. For a multi degree of freedom system the question arises whether the response at the horizontal tangent to the response curve is influenced by the next higher mode. In order to investigate this from the experimentally determined response curve, it is of value to find an analytical expression that expresses the value of the frequency for which the response curve for the one degree of freedom system has its horizontal tangent. The expression for the acceleration of the single degree of freedom system is:

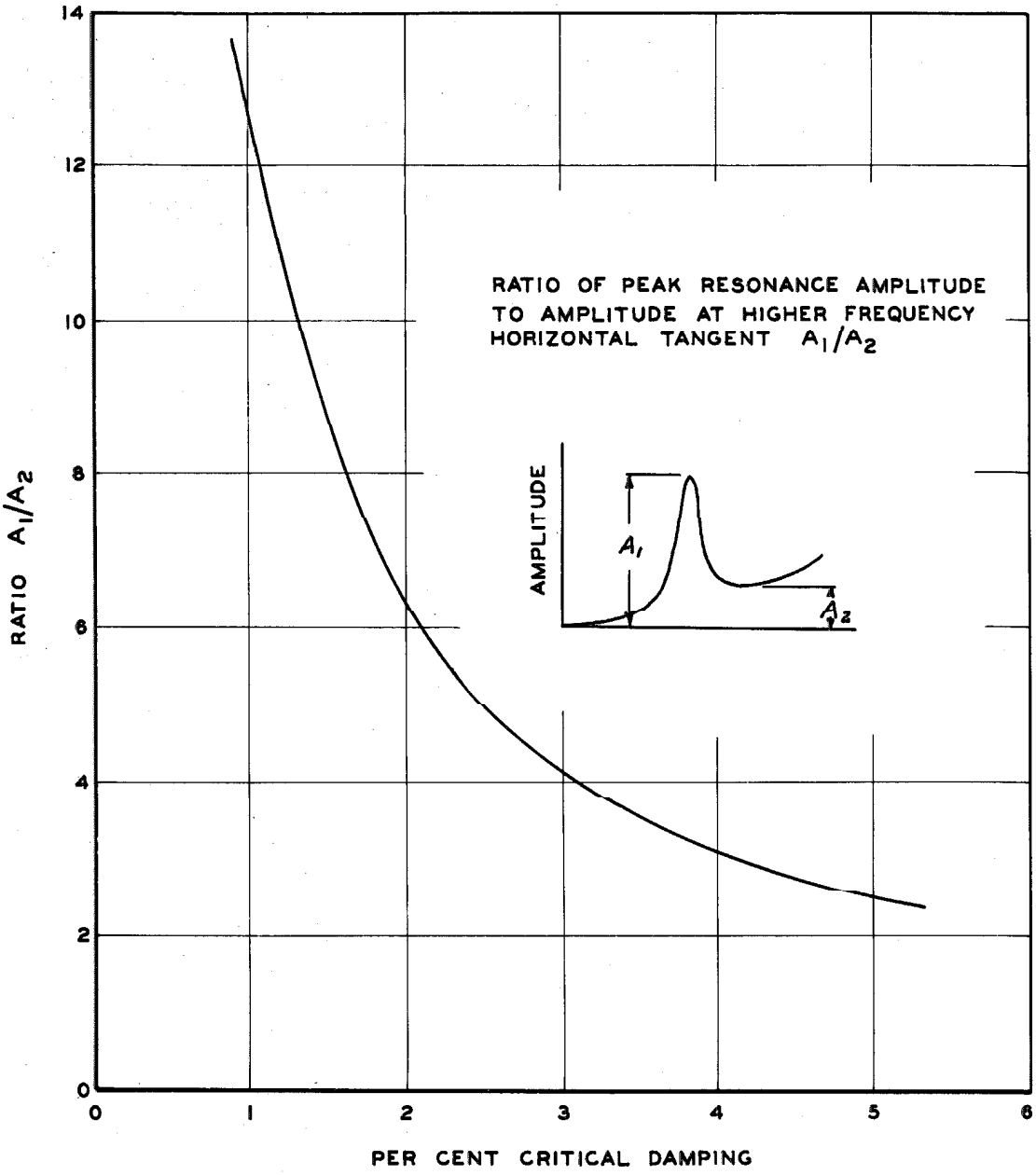

FIG. 2-4 RATIO OF PEAK AMPLITUDE TO HIGHER FREQUENCY HORIZONTAL SLOPE AMPLITUDE

$$\frac{\ddot{x}}{\frac{m}{M} r\omega_n^2} = \frac{\left(\frac{\omega}{\omega_n}\right)^4}{\sqrt{\left[1-\left(\frac{\omega}{\omega_n}\right)^2\right]^2 + \left[2\left(\frac{\omega}{\omega_n}\right)\left(\frac{c}{c_{cr}}\right)\right]^2}} \tag{2.110}$$

For simplicity let

$$\frac{\ddot{x}}{\frac{m}{M} r\omega_n^2} = z, \quad \frac{\omega}{\omega_n} = y \quad \text{and} \quad \frac{c}{c_{cr}} = \beta.$$

Equation 2.108 then becomes

$$z = \frac{y^4}{\sqrt{(1-y^2)^2 + (2\beta y)^2}} \tag{2.111}$$

The horizontal tangent to the response curve occurs at a value of $y = \omega/\omega_n$ such that $dz/dy = 0$. This condition gives:

$$y^4 - 3y^2 + 4\beta^2 y^2 + 2 = 0 \tag{2.112}$$

For small damping, say $\beta < 10\%$,

$$3y^2 >> 4\beta^2 y^2$$

and Eq. 2.112 can be written to a good approximation as

$$y^4 - 3y^2 + 2 = 0 \tag{2.113}$$

or

$$y = \frac{\omega}{\omega_n} = \begin{cases} \sqrt{2} \\ 1 \end{cases} \tag{2.114}$$

It is also possible to express the damping as a function of the ratio of peak acceleration amplitude to the acceleration amplitude at $\omega/\omega_n = \sqrt{2}$. At resonance $\omega/\omega_n = 1$ and Eq. 2.110 reduces to:

$$\frac{\ddot{x}}{\frac{m}{M} r\omega_n^2} = A_1 = \frac{1}{2\beta} \tag{2.115}$$

For $\omega/\omega_n = \sqrt{2}$, Eq. 2.110 reduces to:

$$\frac{\ddot{x}}{\frac{m}{M} r\omega_n^2} = A_2 = \frac{4}{\sqrt{1+8\beta^2}} \tag{2.116}$$

Combining Eqs. 2.115 and 2.116 gives

$$\frac{A_1}{A_2} = \frac{\sqrt{1+8\beta^2}}{8\beta} \tag{2.117}$$

For small values of damping, say $\beta < 10\%$ less than a 5% error in the determination of β will be made by expressing Eq. 2.115 in the following form

$$\frac{A_1}{A_2} = \frac{1}{8\beta} \tag{2.118}$$

It can be seen that Eq. 2.118 corresponds closely to Hudson's result expressed in Fig. 2-4.

Method III

The damping in any purely excited mode can also be found directly from the equations of motion of the structure. When synchronized sinusoidal forces act on all masses of the structure the equation of motion takes the form:

$$[M]\{\ddot{x}\} + [C]\{\dot{x}\} + [K]\{x\} = \{f(t)\} = \{F\} \sin \omega t \tag{2.1}$$

Performing the usual transformations given by

$$\{x\} = [\psi]\{\rho\} \tag{2.16}$$

normalized such that:

$$[\psi]^T [M][\psi] = [I] \tag{2.14}$$

After premultiplying by ψ^T, Eq. 2.1 becomes

$$\{\ddot{\rho}\} + \left[2\beta\omega\right]\{\dot{\rho}\} + \left[\omega^2\right]\{\rho\} = [\psi]^T\{F\}\sin\omega t \tag{2.119}$$

If the structure is excited in the i^{th} mode by letting $\omega \cong \omega_i$, the steady-state response will be

$$\rho_i = \{\psi^{(i)}\}^T\{F\}\frac{1}{\omega_i^2\sqrt{\left[1-\left(\frac{\omega}{\omega_i}\right)^2\right]^2 + \left[2\beta_i\frac{\omega}{\omega_i}\right]^2}}\sin(\omega t - \varphi_i) \tag{2.120}$$

As shown earlier for moderate damping and well separated modes, $\rho_j \cong 0$ for $j \neq i$ and

$$|\rho_i| = \{\psi^{(i)}\}^T\{F\}\frac{1}{\omega_i^2 2\beta_i} \tag{2.121}$$

Since

$$\{x\} = [\psi]\{\rho\} \tag{2.16}$$

Eq. 2.121 becomes

$$\{|x|\} = \{\psi^{(i)}\}\{\psi^{(i)}\}^T\{F\}\frac{1}{\omega_i^2 2\beta_i} \tag{2.122}$$

Then

$$\{|\dot{x}|\} = \{\psi^{(i)}\}\{\psi^{(i)}\}^T\{F\}\frac{1}{2\beta_i} \tag{2.123}$$

or

$$\{|\dot{x}|\} = \{\psi^{(i)}\}\left(\psi_1^{(i)}F_1 + \psi_2^{(i)}F_2 + \ldots + \psi_n^{(i)}F_n\right)\frac{1}{2\beta_i} \tag{2.124}$$

Knowing the force applied at each mass and determining the mode shape

and peak acceleration from a vibration test, Eq. 2.124 will allow a determination of the damping in the i^{th} mode. If only one vibration exciter is used say at the m^{th} floor and the acceleration at resonance is measured at the k^{th} floor, Eq. 2.124 becomes

$$\beta_i = \frac{\psi_k^{(i)} \psi_m^{(i)} F_m}{2 \left| \ddot{x}_k \right|} \tag{2.125}$$

It should be noted that the mode shape must be normalized so that

$$\sum_{j=1}^{n} m_j \left(\psi_j^{(i)} \right)^2 = 1 \tag{2.126}$$

Equation 2.125 in the case of a single degree of freedom system is reducible to the well known expression for the dynamic magnification factor as a function of damping.

Specific examples of the use of all three methods will be given in Chapters III and IV.

CHAPTER III

STEADY STATE VIBRATION TESTS OF A FIVE-STORY REINFORCED CONCRETE BUILDING

A five-story reinforced concrete building became available for dynamic testing during the period of construction of the building. The building is typical of the modern reinforced concrete frame buildings that are presently being constructed in the Southern California area. In order not to interfere with the construction, the tests had to be run Saturdays and Sundays. The tests were conducted in three weekends over a period of about two months. At the time of the initial tests, the building was completed except that partitions, false ceilings and windows were not yet in. The initial tests were chiefly exploratory in nature but the tests were also used to compare the results obtained from a run-down test with those obtained from a steady-state test. The results of the initial test are given in detail in Chapter V; this chapter also contains a description of the changes in dynamic characteristics of the building caused by the addition of partitions, false ceilings and windows. The vibration tests described in the present chapter were carried out when the building was in its finished state.

Description of Building

The building tested was a five-story reinforced concrete building, rectangular in plan, with no basement. The building was part of a complex of buildings; a service tower located at the northeast end of the building contained elevators and stair cases. This tower was not

connected to the building being tested. However, the basement under the tower did extend slightly under the north end of the building that was tested by means of one foot thick reinforced concrete walls. Overall dimensions of the building are shown in Fig. 3-1 and details of the building can be seen in Figs. A-1 through A-4 in the appendix. The total weight of the building was estimated from construction drawings to be 3810 kips.

The building was supported on a firm layer of sand with gravel encountered at a depth of about ten feet below the ground level by the use of drilled-and-belled caissons. The caissons on the sand and gravel were designed to carry a dead plus live load of 8,000 psf. The ground floor rested on compacted fill.

Specifications called for a minimum compressive strength of the concrete at 28 days to be 3,000 psi. The actual 28 day compressive strength of the concrete used varied between 3,100 psi and 3,900 psi as determined from standard cylinder tests.

The floor slabs were 4-1/2 inch reinforced concrete slabs, reinforced with No. 4 bars, 12 inch on center. Typical girders in the north-south direction had a depth of 3'-4" and a width at the base of 1'-2", top reinforcing consisted of two No. 10 bars, two No. 7 bars and three No. 9 bars, bottom reinforcing consisted of two No. 10 bars and two No. 11 bars. Typical beams in the north-south direction had a depth of 1'-6" and a width at the bottom of 1'-4", top reinforcing consisted of three No. 7 bars and bottom reinforcing consisted of three No. 8 bars. Typical joists in east-west direction had a depth

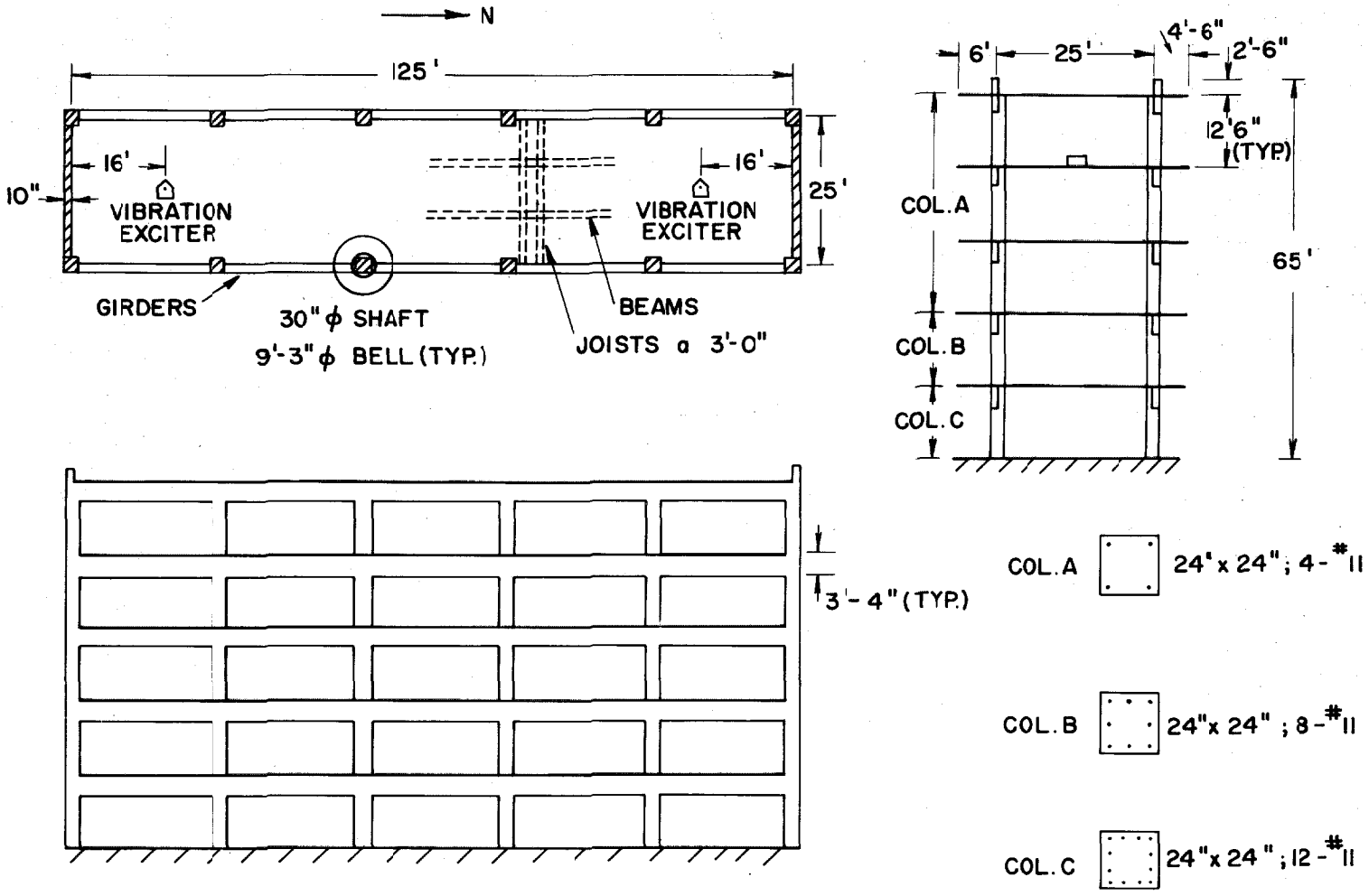

FIG. 3-1 FIVE-STORY R.C. BUILDING

of 1'-6" and a width at the bottom of 5-1/2", top reinforcing consisted of two No. 5 bars and bottom reinforcing consisted of two No. 7 bars. The end walls were 10" thick reinforced concrete walls reinforced with No. 4 bars, 10 inches on center each way.

Translational Motion in the Long North-South Direction

With the two vibration exciters located as shown in Fig. 3-1, the building was excited in translation in the long north-south direction by running the vibration exciters synchronized in phase. Figure 3-9 shows the recorded single amplitude acceleration of the third floor as a function of frequency. It can be seen that the first and second translational modes were excited. The modes are well separated. The lowest translational frequency is ω_1=2.31 cps and the second translational frequency is ω_2=7.26 cps. The ratio of the two frequencies is 3.14. This can be compared to a ratio of 3.0 for the vibration of a uniform shear beam. It can be seen from Fig. 3-10 that the first translational mode shape is close in appearance to that of a uniform shear beam.

It was possible to excite the first translational mode at several force levels. The second mode could only be excited at one force level without exceeding the load limit of the vibration exciters. Accelerometers were located on all floors at the geometrical center of the building and simultaneous readings were taken as the frequency of excitation was varied in steps of about .01 cps. Figures 3-2 and 3-3 show the response of all floors at and close to the lowest

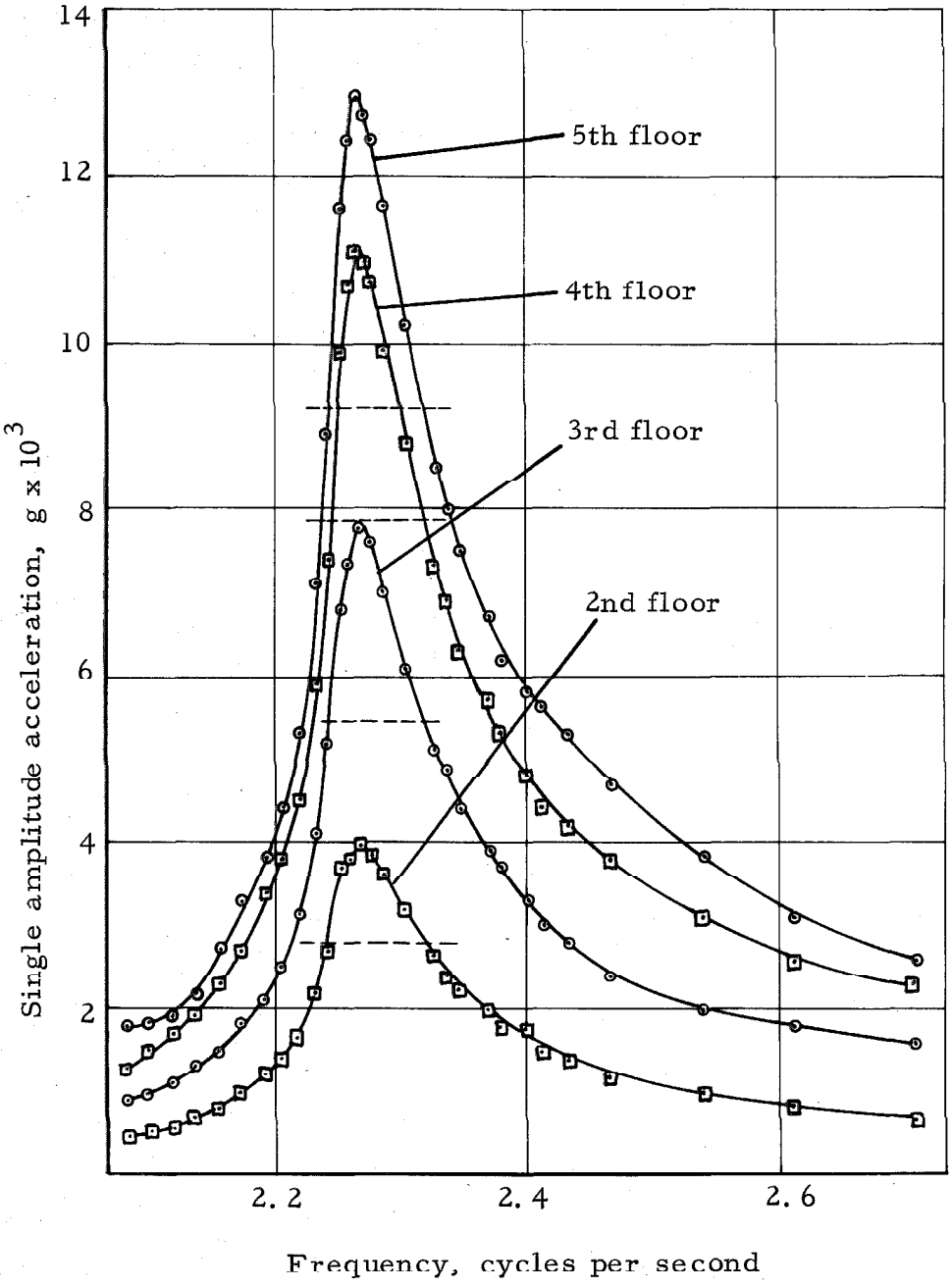

Fig. 3-2 RESPONSE CURVES, LOWEST TRANSLATIONAL MODE (N-S), TEST No. 2

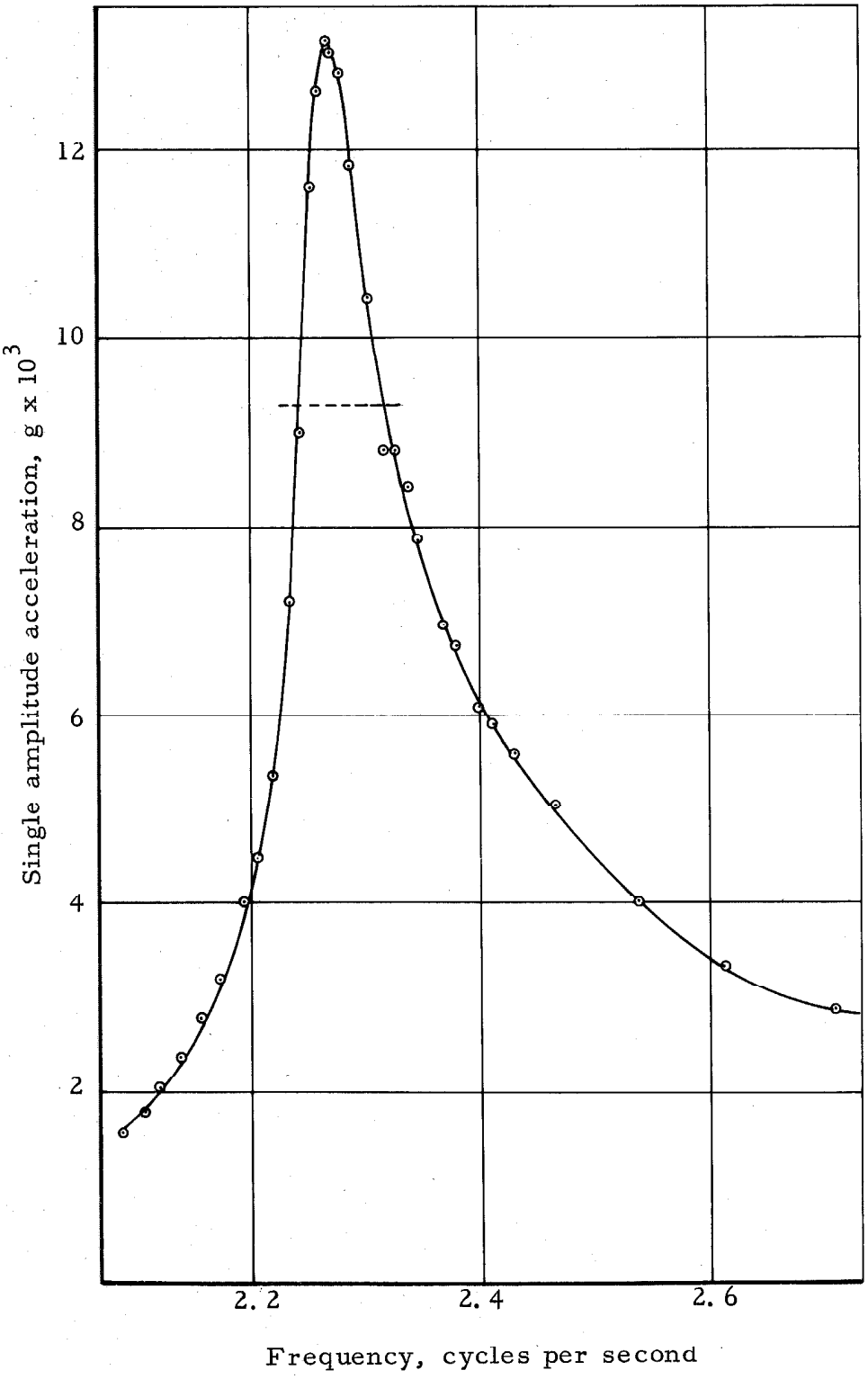

Fig. 3-3 RESPONSE OF ROOF, LOWEST TRANSLATIONAL MODE (N-S), TEST No. 2

translational frequency. It is evident from Figs. 3-2 and 3-3 that all floors experience their maximum response at the same frequency. The form of all the response curves is the same. For instance, it is found that measuring the width of the response curves at $\sqrt{2}/2$ times the peak response, the same value for the width is found regardless of which one of the response curves shown in Figs. 3-2 and 3-3 is used. It should be noted that all the response curves show single amplitude acceleration versus frequency, and the force output is proportional to the frequency squared. The width of the response curves at $\sqrt{2}/2$ times the peak acceleration amplitude cannot directly be used as an estimate of damping since this method is based on displacement amplitude at constant force excitation. However, the response curves are so narrow that the part of the curve pertinent to a determination of damping is very little affected by a reduction to displacement amplitude at constant force.

Table III-1 shows the peak response of all floors as the structure is excited at different force levels. It is seen that the mode shape stays constant regardless of level of force excitation. The resonant frequency of the first translational mode does change as the structure experiences higher stress levels. At the lowest stress level (test No. 1) the resonant frequency is 2.31 cps while at the highest stress level (test No. 3) the resonant frequency is 2.21 cps. It is interesting to note that test No. 4 corresponding to an intermediate stress level showed a resonant frequency of 2.21 cps. The sequence in which the tests are conducted is thus of importance in exploring the non-

TABLE III-1

Test number — Peak response values, N-S translational modes

mode

force at resonance

resonant frequency

		2nd fl.	3rd fl.	4th fl.	5th fl.	Roof
1 1st mode 567 lbs 2. 31 cps	single ampl. accel. $g \times 10^{-3}$	1. 59	3. 10	4. 36	5. 15	5. 55
	single ampl. displ. in. $\times 10^{-3}$	2. 91	5. 67	7. 99	9. 42	10. 18
	mode shape	. 17	. 33	. 46	. 55	. 59
1 2nd mode 5620 lbs 7. 26 cps	single ampl. accel. $g \times 10^{-3}$	9. 55	12. 80	8. 00	-3. 64	-13. 2
	single ampl. displ. in. $\times 10^{-3}$	1. 77	2. 36	1. 48	-. 67	-2. 42
	mode shape	. 42	. 57	. 36	-. 16	-. 59
2 1st mode 1422 lbs. 2. 27 cps	single ampl. accel. $g \times 10^{-3}$	3. 98	7. 65	10. 95	12. 90	13. 10
	single ampl. displ. in. $\times 10^{-3}$	7. 54	14. 5	20. 7	24. 4	24. 8
	mode shape	. 17	. 33	. 47	. 56	. 57
3 1st mode 2805 lbs 2. 21 cps	single ampl. accel. $g \times 10^{-3}$	8. 90	17. 1	24. 35	28. 45	28. 75
	single ampl. displ. in. $\times 10^{-3}$	17. 8	34. 2	48. 7	57. 0	57. 5
	mode shape	. 17	. 34	. 48	. 56	. 56
4 1st mode 1942 lbs 2. 21 cps	single ampl. accel. $g \times 10^{-3}$	6. 65	12. 5	18. 3	21. 3	21. 75
	single ampl. displ. in. $\times 10^{-3}$	13. 3	25. 0	36. 6	42. 6	43. 5
	mode shape	. 17	. 33	. 48	. 56	. 57

Values used in the determination of $[K]$ and $[C]$:

	2nd fl.	3rd fl.	4th fl.	5th fl.	Roof
$\omega_1 = 2.27$ cps; $\beta_1 = 2.0\%$	. 17	. 33	. 47	. 56	. 58
$\omega_2 = 7.26$ cps; $\beta_2 = 2.1\%$	. 42	. 57	. 36	-. 16	-. 59
masses (kips)	770	770	770	770	730

linearities in the response. This will be discussed at the end of this chapter in the section on non-linearities of the response. The change in resonant frequency from the lowest to highest stress level is about 4%; since the stiffness of the structure is proportional to the resonant frequency squared test No. 1 would lead to a determination of stiffnesses that would be about 8% higher than the stiffnesses determined from test No. 3. This non-linear behavior is also evident from Fig. 3-4, since the resonant frequency decreases with increasing stress levels; the behavior corresponds to that of a "softening spring".

In the following determination of the stiffness matrix the intermediate resonant frequency of ω_1=2.27 cps from test No. 2 has been used. The resonant frequencies and mode shapes as used in the determination of the stiffness matrix are listed in Table III-1 and also shown in Fig. 3-10.

Determination of $[K]$ Using 1st and 2nd Mode

As shown in Chapter II, the stiffness matrix $[K]$ can be determined from the following equation

$$[K] \{\psi^{(r)}\} = [M] \{\psi^{(r)}\} \omega_r^2 \qquad (2.67)$$

For each experimentally determined mode one equation of this form exists while Eq. 2.67 expresses as many equations as the system has degrees of freedom. In the present case two modes were determined experimentally in a five degree of freedom system, so 2 x 5 = 10 equations are available to determine the elements of the stiffness matrix. This allows for a determination of $[K]$ under two assump-

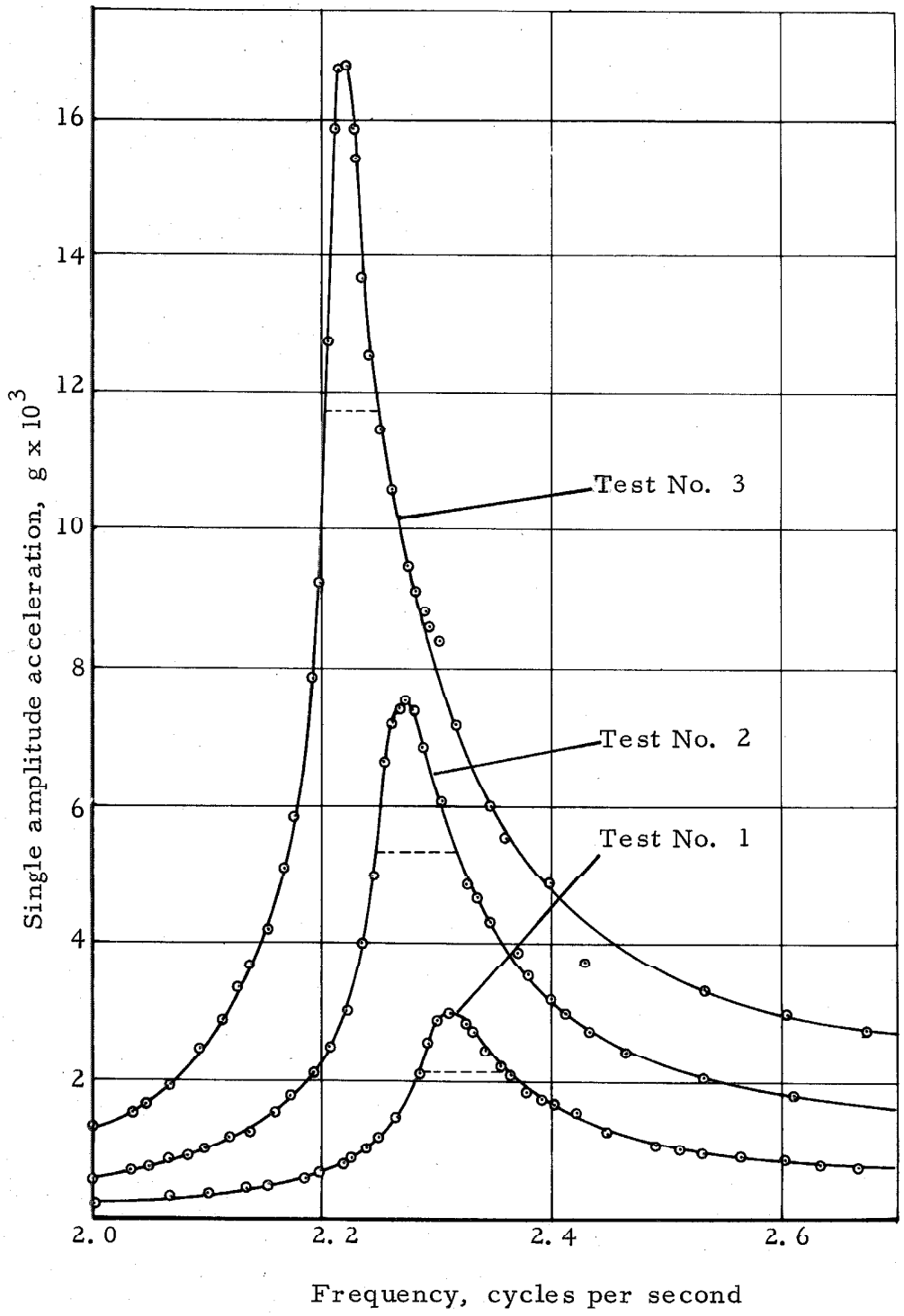

Fig. 3-4 3rd FLOOR RESPONSE, LOWEST TRANSLATIONAL MODE (N-S)

tions, since for a simply coupled system $[K]$ would have five unknown elements and for a close coupled system $[K]$ would have nine unknown elements.

Close coupled system

In a close coupled system the stiffness matrix $[K]$ is tridiagonal with no interrelation between the elements of each row (or column). There are (2n-1) unknown elements in $[K]$. Using the resonant frequencies, mode shapes and values of masses as listed in Table III-1, Eq. 2.77 takes the form

$$\begin{bmatrix} .17 & .33 & 0 & 0 & 0 & 0 & 0 & 0 & 0 \\ 0 & .17 & .33 & .47 & 0 & 0 & 0 & 0 & 0 \\ 0 & 0 & 0 & .33 & .47 & .56 & 0 & 0 & 0 \\ 0 & 0 & 0 & 0 & 0 & .47 & .56 & .58 & 0 \\ 0 & 0 & 0 & 0 & 0 & 0 & 0 & .56 & .58 \\ .42 & .57 & 0 & 0 & 0 & 0 & 0 & 0 & 0 \\ 0 & .42 & .57 & .36 & 0 & 0 & 0 & 0 & 0 \\ 0 & 0 & 0 & .57 & .36 & -.16 & 0 & 0 & 0 \\ 0 & 0 & 0 & 0 & 0 & .36 & -.16 & -.59 & 0 \\ 0 & 0 & 0 & 0 & 0 & 0 & 0 & -.16 & -.59 \end{bmatrix} \begin{Bmatrix} k_{11} \\ k_{12} \\ k_{22} \\ k_{23} \\ k_{33} \\ k_{34} \\ k_{44} \\ k_{45} \\ k_{55} \end{Bmatrix} = \begin{Bmatrix} 69.2 \\ 134.2 \\ 191.2 \\ 228.0 \\ 224.0 \\ 1742 \\ 2365 \\ 1494 \\ -665 \\ -2450 \end{Bmatrix}$$

These equations are now in the form of

$$[A]\{y\} = \{b\} \tag{2.72}$$

There are 10 equations and 9 unknowns to determine. Performing the least squares fit by premultiplying Eq. 2.72 by $[A]^T$:

$$[A]^T [A]\{y\} = [A]^T \{b\} \tag{2.88}$$

or

$$\begin{bmatrix} .205 & .296 & 0 & 0 & 0 & 0 & 0 & 0 & 0 \\ .296 & .639 & .296 & .231 & 0 & 0 & 0 & 0 & 0 \\ 0 & .296 & .434 & .360 & 0 & 0 & 0 & 0 & 0 \\ 0 & .231 & .360 & .784 & .360 & .094 & 0 & 0 & 0 \\ 0 & 0 & 0 & .360 & .351 & .206 & 0 & 0 & 0 \\ 0 & 0 & 0 & .094 & .206 & .690 & .206 & .060 & 0 \\ 0 & 0 & 0 & 0 & 0 & .206 & .339 & .419 & 0 \\ 0 & 0 & 0 & 0 & 0 & .060 & .419 & 1.024 & .419 \\ 0 & 0 & 0 & 0 & 0 & 0 & 0 & .419 & .685 \end{bmatrix} \begin{Bmatrix} k_{11} \\ k_{12} \\ k_{22} \\ k_{23} \\ k_{33} \\ k_{34} \\ k_{44} \\ k_{45} \\ k_{55} \end{Bmatrix} = \begin{Bmatrix} 743.4 \\ 2031.9 \\ 1392.3 \\ 1829.2 \\ 627.7 \\ -264.21 \\ 234.08 \\ 1042 \\ 1575 \end{Bmatrix}$$

k_{11} through k_{55} can now be determined. The results expressed in the form of $[K]$ are

$$[K] = \begin{bmatrix} 12911 & -6455 & 0 & 0 & 0 \\ -6455 & 13052 & -6556 & 0 & 0 \\ 0 & -6556 & 11951 & -5832 & 0 \\ 0 & 0 & -5832 & 10893 & -5395 \\ 0 & 0 & 0 & -5395 & 5606 \end{bmatrix} \quad \text{kips/in} \qquad (3.1)$$

Simply coupled system

In a simply coupled system, springs interconnect adjacent masses and only one mass is connected by a spring to the base. The stiffness matrix is tridiagonal but the elements in each row (or column) are interrelated. The number of unknown elements in the stiffness matrix is equal to the number of degrees of freedom of the system. Using the information from the two experimentally determined modes, Eq. 2.70 expresses 10 equations in the 5 unknowns k_1, k_2, k_3, k_4 and k_5. After expressing Eq. 2.70 in the form of Eq. 2.71, performing the least squares and solving Eq. 2.88, the results are

$$[K] = \begin{bmatrix} 13082 & -6573 & 0 & 0 & 0 \\ -6573 & 13015 & -6442 & 0 & 0 \\ 0 & -6442 & 12103 & -5662 & 0 \\ 0 & 0 & -5662 & 11176 & -5514 \\ 0 & 0 & 0 & -5514 & 5514 \end{bmatrix} \text{ kips/in} \qquad (3.2)$$

Comparing the stiffness matrices expressed in Eq. 3.1 and Eq. 3.2 it can be seen that they are almost identical. The stiffness matrix of Eq. 3.1 was found assuming springs between adjacent masses and also "absolute" springs connecting each mass to the base; since identical results are obtained for the stiffness matrix assuming only springs connecting the adjacent masses, it is concluded that there are no springs connecting each mass to the base. This, of course, is as would be expected. The result is of interest since, as will be shown later, a determination of the damping matrix will yield quite different results according to the two similar assumptions for the damping matrix indicating that the damping is best described by using not only "relative" dashpots but "absolute" dashpots as well. The fact that no "absolute" springs exist can also be seen from the stiffness matrix of Eq. 3.1; no assumption was here made as to any interrelation between the elements of each row (or column). Nevertheless, it can be seen from Eq. 3.1 that for each row the sum of the absolute values of the off diagonal terms is very close to the value of the diagonal term.

Determination of $[K]$ Using One Mode Only

The "best" determination of $[K]$ using the experimental results from both the first and the second translational modes was shown above. However, it is of interest to determine the stiffnesses as well by using in one case the first mode only and in another case the second mode only. For many structures the frequency limitations of the vibration exciters might allow a determination of one mode only so it is of interest to find how well the stiffnesses found from an experimental determination of just one mode compares with the results found by using two experimentally determined modes. As shown in Chapter II the stiffnesses can be expressed as

$$k_s = \frac{\omega_r^2 \sum_{i=s}^{n} m_i \psi_i^{(r)}}{\psi_s^{(r)} - \psi_{s-1}^{(r)}} \qquad s=(1, 2, \ldots, n) \tag{2.73}$$

The results are listed in Table III-2. In order to compare the results with those found by using both modes simultaneously in the calculations, the results expressed in Eq. 3.2 are also listed.

TABLE III-2

Spring Constants (N-S)

Experimental results used in calculations	1st and 2nd mode	1st mode only	2nd mode only
k_5 kips/in	5514	11200	5698
k_4 kips/in	5662	5022	5990
k_3 kips/in	6442	4594	7719
k_2 kips/in	6573	4859	4960
k_1 kips/in	6509	4980	5911

It is clear from Table III-2 that a determination of the stiffnesses in a building from only one experimentally determined mode can lead to quite erroneous results for some of the stiffnesses. From the above Eq. 2. 73 it is evident that the results most in error can be expected for springs connecting floors that in a particular mode have large and nearly equal displacements. Figure 3-10 shows the two experimentally determined mode shapes. It is evident that in using the first mode only that results very much in error could be expected for the determination of k_5. In using the second mode only results very much in error could be expected for k_2 and k_3. Table III-2 shows that these are the stiffnesses that are most in error when compared to the best determination accomplished by using the first and the second modal information simultaneously.

It is interesting to note from Table III-2 that if only one mode was determined experimentally the modal data from the second mode would lead to a better determination of the stiffnesses than would the modal data from the first mode only.

Natural Frequencies and Mode Shapes Determined from the Model of the Structure

After having determined the stiffness matrix from the available experimental results, it is of interest to see how the natural frequencies and mode shapes of the model compare to the experimental results. Since the determination of the stiffness matrix in general involves more equations than unknowns and a "least squares fit" was used in its determination, the natural frequencies and mode shapes

found from the model cannot be expected to show a complete agreement with the experimentally determined frequencies and mode shapes. Table III-3 shows the computed natural frequencies and mode shapes using the stiffnesses as determined above. In case a) the stiffness matrix is determined from the experimental results using the first and second mode. The stiffness matrix was found from 10 equations in 9 unknowns so little fitting of data was needed and one would expect the modal data for both the first and second mode to be very close to the experimental data. Table III-3 allows for a comparison between the calculated first and second mode and the experimentally determined modes. The agreement is seen to be very close. In case b) the frequencies and mode shapes were found using the stiffnesses as determined by using the experimental data from the first mode only. The stiffnesses were determined from a determinate system of 5 equations in 5 unknowns so no data fitting was necessary and the first mode as determined from the stiffnesses should of course be identical to the experimental results for the first mode. It is interesting to see in this case how well the second mode compares to the experimental results. The frequency of the second mode is found to be 6.94 cps versus the experimentally determined value of 7.26 cps. The mode shape of the second mode is distorted rather badly when compared to the experimentally determined mode shape. It is concluded that using the experimental data from the first mode only will not allow for extrapolation to give meaningful results for the higher modes.

Case c) corresponds to case b) but here only the experimental

TABLE III-3

Frequencies and mode shapes (N-S)

	Experimentally determined		a) using K from Eq. 3.1 using 1st and 2nd modes					b) using K from Table III-2 1st mode only				
cps frequency	2.27	7.26	2.27	7.33	11.50	14.61	17.06	2.27	6.94	11.23	14.31	18.42
mode	1	2	1	2	3	4	5	1	2	3	4	5
Roof	.58	-.59	.58	-.59	.48	-.33	.11	.58	-.44	.34	-.19	.60
5	.56	-.16	.56	-.17	-.38	.63	-.32	.56	-.30	.05	.07	-.76
4	.47	.36	.47	.35	-.48	-.34	.55	.47	.24	-.68	.44	.24
3	.33	.57	.33	.57	.23	-.32	-.64	.33	.63	-.01	-.69	-.07
2	.17	.42	.17	.42	.58	.52	.41	.17	.51	.65	.54	.02

TABLE III-3 (CONTINUED)

c) using

K from Table III-3
2nd mode only

cps frequency	2.48	7.26	11.56	14.25	17.38
mode	1	2	3	4	5
Roof	.59	-.59	.41	-.39	.13
5	.54	-.17	-.31	.64	-.40
4	.45	.35	-.45	-.09	.67
3	.36	.56	.05	-.47	-.57
2	.17	.42	.73	.46	.22

results from the second mode have been used. Again in this case the stiffnesses were found from 5 equations in 5 unknowns, no data fitting was needed, and the frequency and the mode shape for the second mode is in complete agreement with the experimental results. It can be seen that in this case the first modal data is very close to the experimentally determined data indicating that had only the second mode been known from experimental data it would still be possible from this data to establish quite well the modal properties of the first mode.

Table III-3 shows the frequencies and mode shapes for all the modes. It is, of course, conjecture to state anything about how well the higher modes would be in agreement with the actual higher modes of the structure. All that can be said f. i. in case a) is that the stiffness matrix as determined from the experimental results by exciting the structure in its two lowest modes leads to a model of the structure for which the two lowest modes are in exact agreement with the experimental results.

Experimentally Determined Stiffnesses Compared With Calculated Stiffnesses

From the known properties of the structure it is possible to calculate the stiffnesses of each story of the building. The stresses induced in the vibration tests are of such small magnitude that it is reasonable in calculating the moments of inertia for columns, walls and floor slabs to assume that concrete can resist tension as well as compression. In transforming the reinforcing steel into equivalent

concrete areas, a value of n equal to ten has been used. In calculating the stiffness of the girders, beams and floor slab, it is evident that the slab and the beams do not add fully to the stiffness as would be indicated by the elementary theory of bending. The slab was reduced in width using only the effective width as indicated by Timoshenko and Goodier.[46] Similarly, the effective stiffness of the beams was estimated at half of the otherwise indicated stiffness. It was found that the floor system had sufficient stiffness to make the effect of joint rotation negligible. The total stiffness of the individual stories can then be found from

$$k = \sum \frac{12EI}{L^3} \tag{3.3}$$

In Eq. 3.3 the summation extends over the stiffnesses for all the columns and the two end walls. The moments of inertia have been calculated assuming no cracks in the concrete and also assuming perfect bond between reinforcing steel and concrete. There is some doubt as to which value should be used for the dynamic modulus of elasticity for concrete and also which value should be used for the effective distance between floors. The static modulus of elasticity for concrete can be found as shown by Pauw[47] from the following equation

$$E_c = 33\, w^{3/2} \sqrt{f_c'} \tag{3.4}$$

In this equation w is the unit weight of concrete in pounds per cubic foot and f_c' is the concrete compressive strength in psi at 28 days. Equation 3.4 is based on laboratory tests of standard cylinders. It is

not at all evident that the dynamic modulus of elasticity of concrete as it affects the vibrational characteristics of a multistory building should be the same as that found from either static or dynamic tests of laboratory specimens. Even dynamic tests on models might not give an accurate indication of the true dynamic modulus of elasticity to be used as an average value extending throughout a multistory building. The value of E might not be a true materials constant; it might be affected by the geometry and dimensions of the structure, by the number and location of intentional and unintentional joints, by the quality of the workmanship, etc. Calculating the static modulus of elasticity for the type of concrete used in this building (150 pounds per cubic foot, 3000 psi at 28 days), Eq. 3.4 gives a value of $E_c = 3.4 \times 10^6$ psi.

Of even more importance in using Eq. 3.3 is the use of the effective story height. As seen in Fig. 3-1 the distance between finished floors is 150 inches, the girders in the long north-south direction have a depth of 40 inches, making the "free" height between floors equal to 110 inches. The dynamic modulus of elasticity of concrete can be calculated using the experimentally determined stiffnesses and Eq. 3.3, the E-value has been calculated using in one case a story height L equal to 150 inches and in the other case using L equal to 110 inches. The results are tabulated in Table III-4. The values of E found by using L = 150 inches are quite consistent from one story to the next; the values are generally slightly higher than the static modulus of elasticity of 3.4×10^6 psi. The values of E found by

TABLE III-4

Determination of E (N-S)

	Experimentally determined stiffnesses k kips/in	Each column I in^4	12 cols plus end walls I in^4	$E=\frac{kL^3}{12I}$ using L=150 inches E x 10^6 psi	$E=\frac{kL^3}{12I}$ using L=110 inches E x 10^6 psi
5th floor - Roof	5514	33, 840	456, 000	3.4	1.3
4th floor - 5th floor	5662	33, 840	456, 000	3.5	1.4
3rd floor - 4th floor	6442	33, 840	456, 000	4.0	1.6
2nd floor - 3rd floor	6573	36, 960	493, 000	3.7	1.5
1st floor - 2nd floor	6509	40, 080	530, 000	3.5	1.4

using the "free" story heights are on the other hand considerably lower than the expected values. Of course no definite conclusions as to the correct value of the dynamic modulus of elasticity of concrete can be reached from dynamic tests of just one reinforced concrete multistory building, but the fact that these tests, even with the simplifying assumptions that had to be used in the calculations, have shown lower than expected values points towards interesting future research.

Determination of the Damping in Each Mode From the Experimental Results

The value of damping expressed as the percentage of critical damping can be found from the response curves shown in Figs. 3-1 to 3-7 and from the peak responses as listed in Table III-1. In Chapter II three methods of determining the damping from the experimental results were listed:

I. Using the width of the response curve at $\sqrt{2}/2$ times the peak response after having reduced the response to displacement amplitude at constant force.

II. Using the relation between the peak acceleration response and the acceleration response at a frequency equal to $\sqrt{2}$ times the resonant frequency.

III. Using the expression

$$\beta_i = \frac{\psi_k^{(i)} \psi_m^{(i)} F_m}{2|\ddot{x}_k|} \qquad (2.125)$$

in which β_i is the percentage of critical damping in the i^{th} mode.

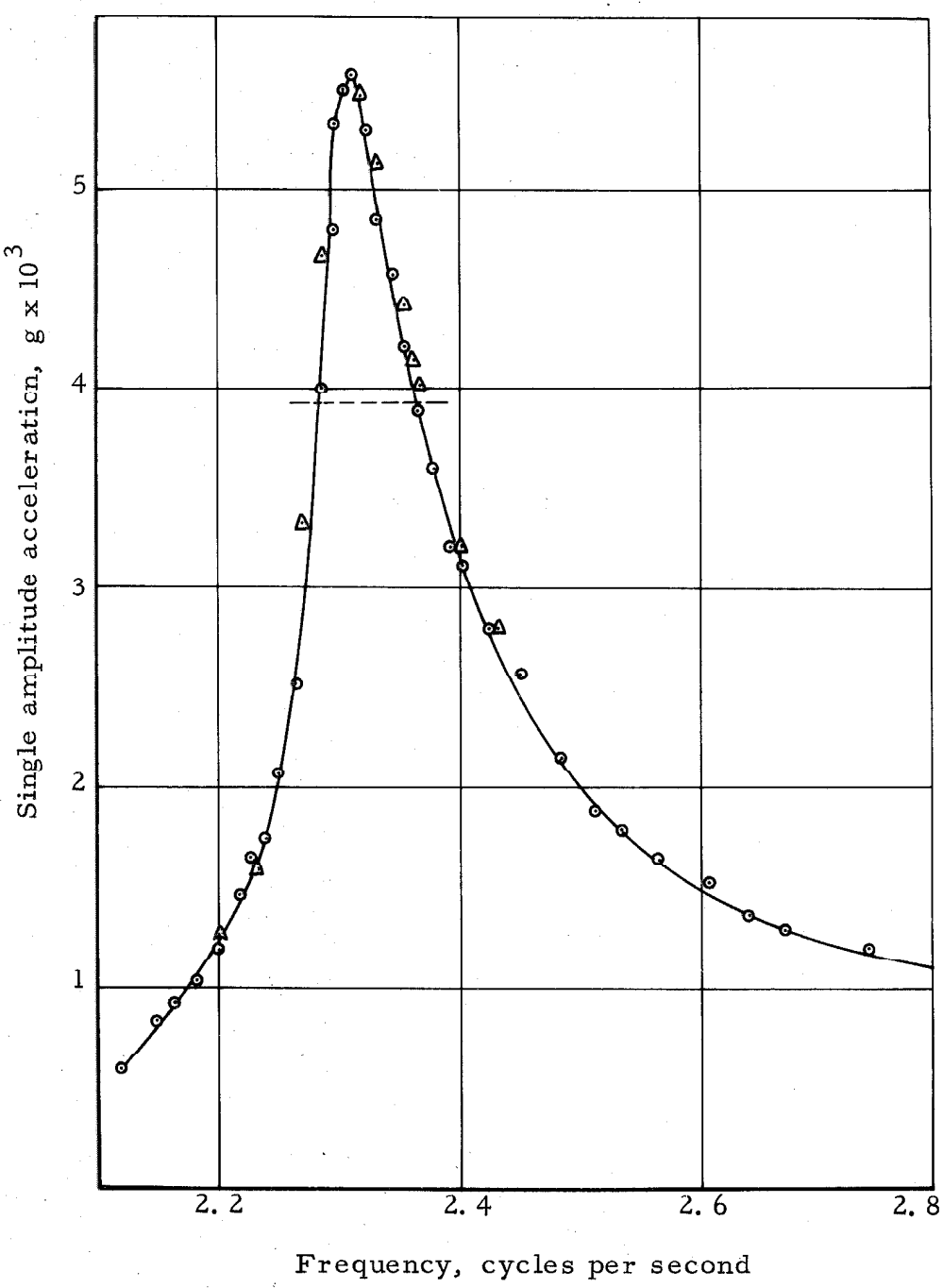

Fig. 3-5 RESPONSE OF ROOF, LOWEST TRANSLATIONAL MODE (N-S), TEST No. 1

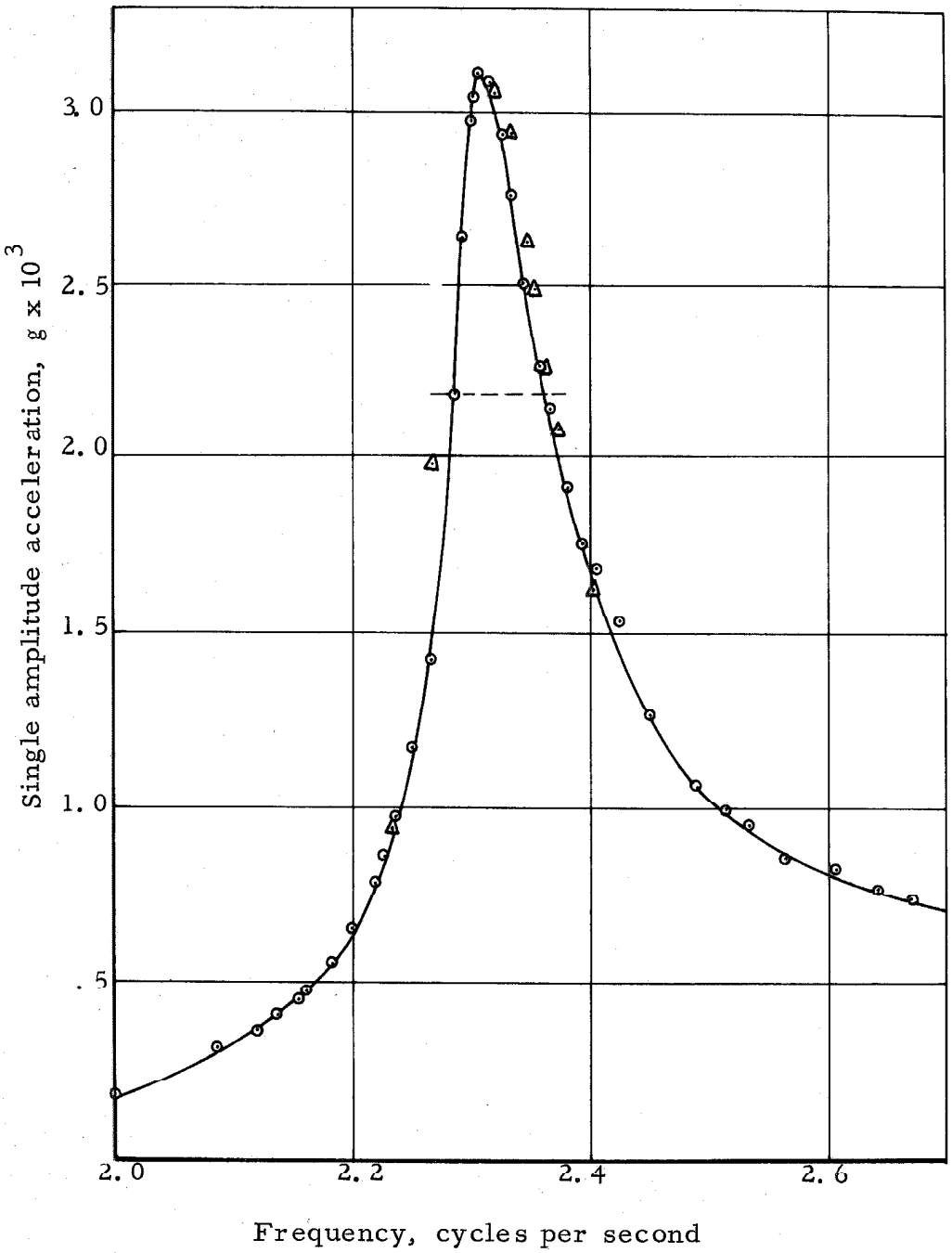

Fig. 3-6 3rd FLOOR RESPONSE, LOWEST TRANSLATIONAL MODE (N-S), TEST No. 1

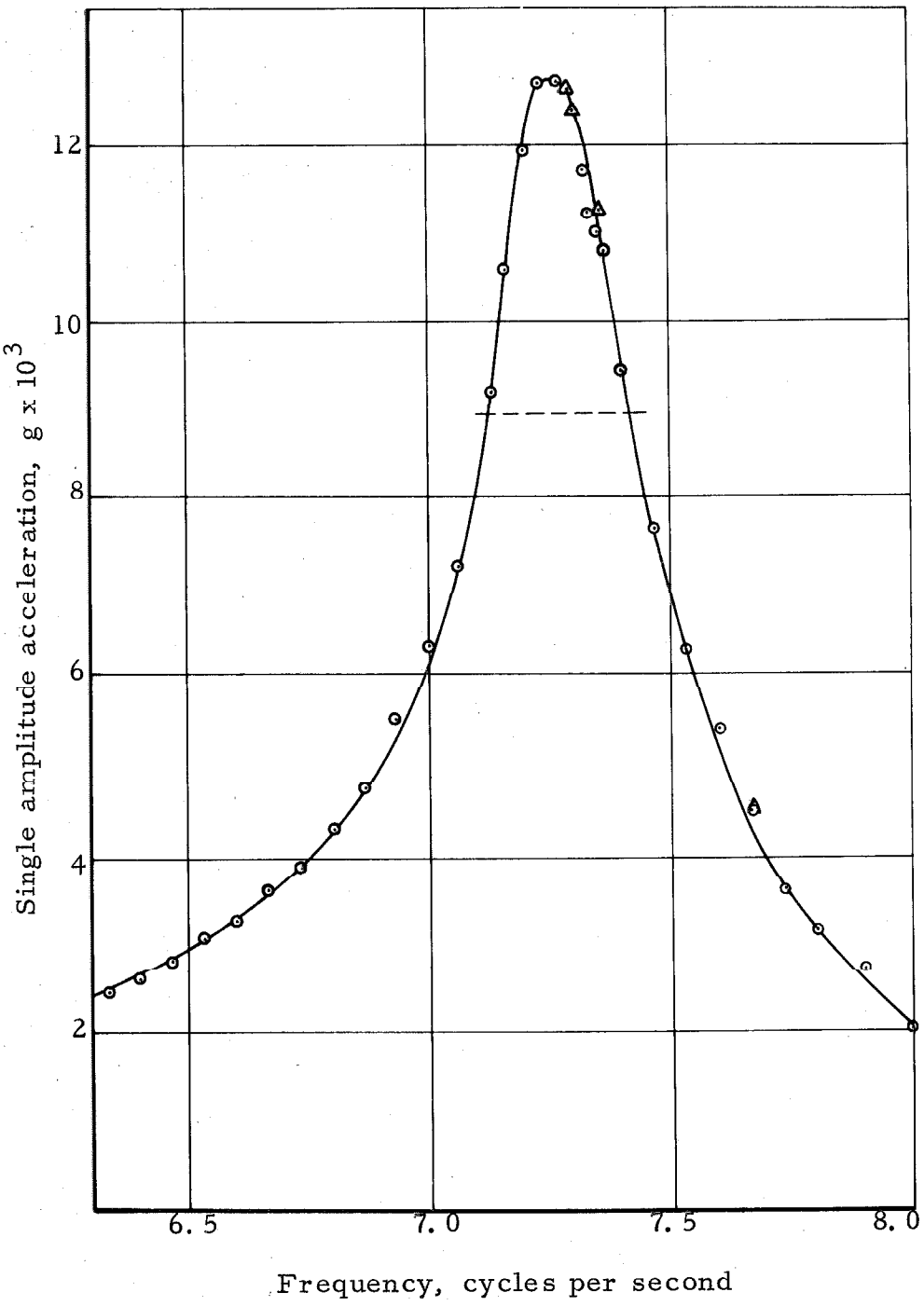

Fig. 3-7 3rd FLOOR RESPONSE, SECOND LOWEST TRANSLATIONAL MODE (N-S), TEST No. 1

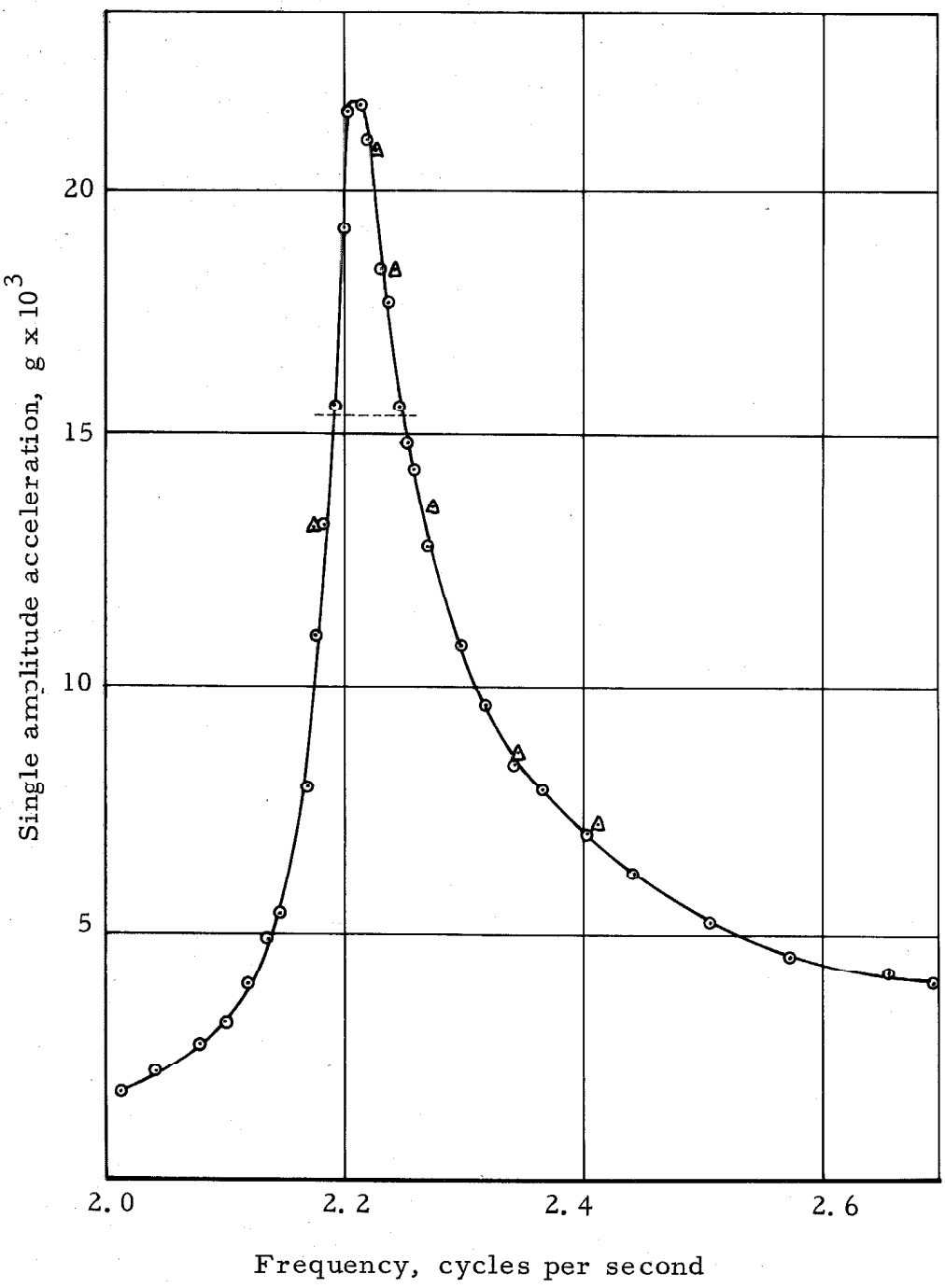

Fig. 3-8 RESPONSE OF ROOF, LOWEST TRANSLATIONAL MODE (N-S), TEST No. 4

$\psi_k^{(i)}$ and $\psi_m^{(i)}$ are the components of the i^{th} mode shape of the k^{th} mass and m^{th} mass, where the exciting force acts on the m^{th} mass and $|\ddot{x}_k|$ is the absolute value of the single amplitude acceleration of the k^{th} mass.

The damping as calculated by the use of all three methods is shown in Table III-5.

TABLE III-5
Determination of Damping (N-S)

Test No.	Resonant frequency cps	Force at resonance lbs	Mode	Method I	Method II	Method III
1	2.31	567	1	1.7%	2.0%	2.2%
1	7.26	5620	2	2.0%		2.1%
2	2.27	1422	1	1.7%	2.0%	2.2%
3	2.21	2805	1	1.1%	1.8%	1.9%
4	2.21	1942	1	1.3%	1.8%	1.8%

The width of the different response curves used in method I are shown on Figs. 3-2 to 3-8. It can be seen from Figs. 3-2 and 3-3 that the same value of damping is obtained regardless of which floor response is used for this determination. Method I gives lower values for the damping than the other two methods. There are several reasons why method I can be expected to give less accurate results than those obtained from either method II or III. First, as can be seen from Figs. 3-5, 3-6 and 3-8, the response as plotted by using decreasing frequencies of excitation tend to give a broader response

curve than that plotted by using increasing frequencies of excitation, indicating that the structure after having been excited at higher force levels has increased its damping capacity. The points enclosed by circles correspond to measurements taken as the frequency is being increased in steps of about .01 cps while the points enclosed by triangles correspond to measurements taken as the frequency of excitation is being decreased. All the response curves have been drawn using the results from tests using increasing frequencies of excitation.

Secondly, as shown by Caughey,[48] in structures with low damping, a region of instability might exist in the negative slope portion of the response curve above the resonant frequency. At the higher force levels of excitation, it was found that several minutes were needed for the vibration exciter to settle down to a steady frequency of vibration. Figure 3-4 shows clearly how at frequencies above the resonant frequency some of the points seem to depart from the otherwise smooth curves. Methods II and III on the other hand use information from the peak acceleration values and it was found in the vibration tests that not only was the response extremely steady when exciting the structure at the resonant frequency, but also, as is evident from the response curves shown, the exciting frequency could be changed in smaller steps close to the resonant frequency than at the steeper portions of the response curves.

Method II gave results that are very close to those of method III. In the present case the two modes are very well separated. In cases

of less separation between modes, method II cannot be expected to give reasonable results since the acceleration A_2 as determined at $\sqrt{2}$ times the resonant frequency would be influenced by the response of the next higher mode. All in all, method III seems to be the best method of determining the amount of damping from the experimentally determined peak response values.

It should be noted that all methods assume the structure to have a linear response; however, as shown in Fig. 3-4 the resonant frequency does change with force level, but the change in resonant frequency from the lowest to the highest force level is less than 5%. This change would have a negligible effect on the determination of the damping. Comparing the values of damping as determined by method III, it is evident that the damping of a purely viscous type that could be represented by dashpots connecting adjacent floors only, the amount of damping in the second mode would be expected to be about three times as much as the damping in the first mode. The damping in the first mode varies from 1.8% to 2.2%, showing a slight tendency for the damping to decrease with increasing stress levels.

Determination of the Damping Matrix $[C]$

As shown in Chapter II, the damping matrix can be determined from the following equation

$$[C]\left\{\psi^{(r)}\right\} = [M]\left\{\psi^{(r)}\right\} 2\beta_r\omega_r \qquad (2.68)$$

For each of the experimentally determined modes one equation of this form exists while each of these matrix equations consists of as

many equations as the system has degrees of freedom. Since two modes were determined experimentally, 2 x 5 = 10 equations are available to determine the unknown elements of $[C]$. This allows for a determination of $[C]$ under two assumptions since in a simply coupled system $[C]$ contains five unknown elements and in a close coupled system $[C]$ contains nine unknown elements. It has already been shown that the percentage of critical damping in the two modes is of approximately the same magnitude so the simply coupled system cannot be expected to give a good representation of the damping in the system. The simply coupled system is represented by dashpots connecting adjacent floors only, i.e., relative damping only, but for this system it has been shown that the percentage of critical damping will increase with increasing frequencies.

Close coupled system

The damping matrix is tridiagonal with no interrelation between the elements of each row (or column). Using the values for the natural frequencies and the mode shapes as listed in Table III-1 and damping values of β_1=2.0% and β_2=2.1%, the (2n-1) unknown elements of the damping matrix can be found from Eq. 2.68. This equation written in the form of Eq. 2.78 is of the type

$$[A]\{y\} = \{b\} \tag{2.72}$$

In the present case Eq. 2.72 represents ten equations in the nine unknown elements of the damping matrix. After performing the least squares fit by premultiplying Eq. 2.72 by $[A]^T$, the resulting set of equations can be solved. The results expressed in the form of $[C]$

are:

$$[C] = \begin{bmatrix} 10.09 & -4.59 & 0 & 0 & 0 \\ -4.59 & 10.20 & -4.68 & 0 & 0 \\ 0 & -4.68 & 9.40 & -4.17 & 0 \\ 0 & 0 & -4.17 & 8.56 & -3.79 \\ 0 & 0 & 0 & -3.79 & 4.72 \end{bmatrix} \quad \frac{\text{kips.-sec.}}{\text{in.}} \qquad (3.5)$$

It can be seen that for each row the diagonal element is larger than the absolute sum of the off-diagonal elements. This indicates that the mathematical model that represents the system will have not only "relative" dashpots but "absolute" dashpots as well. This of course was to be expected since the damping in the two modes is nearly equal. A system described by "relative" dashpots only would lead to values of damping that would increase proportionally with increasing frequencies. The second mode would thus have about three times as much damping as the first mode. The determination of $[C]$ involved a "least squares" fitting of data so it is necessary to investigate how well the damping matrix determines the percentage of critical damping in the two lowest modes for which the damping was found experimentally. In Chapter II it was shown that the damping matrix $[C]$ could be diagonalized by the following transformation:

$$[\psi]^T [C][\psi] = [2\beta_i\omega_i] \qquad (2.63)$$

Using the natural frequencies and mode shapes as shown in case a) of Table III-3 and normalizing the mode shapes so that

$$[\psi]^T [M][\psi] = [I] \qquad (2.8)$$

the following result is obtained by the use of $[C]$ as given in 3.5:

$$[\psi]^T [c][\psi] = \begin{bmatrix} .57 & .01 & 0 & 0 & 0 \\ .01 & 1.94 & .02 & -.01 & 0 \\ 0 & .02 & 4.14 & .03 & -.01 \\ 0 & -.01 & .03 & 6.42 & .01 \\ 0 & 0 & -.01 & .01 & 8.63 \end{bmatrix} \tag{3.6}$$

As can be seen from Eq. 3.6, the transformed matrix is well diagonalized, the elements on the diagonal are equal to $2\beta_i\omega_i$ where β_i is the percentage of critical damping in the i^{th} mode and ω_i is the natural frequency of the i^{th} mode in rad/sec. Using the natural frequencies of case a) of Table III-3, the following results for the damping in all modes are obtained:

$$\beta_1=2.0\%;\quad \beta_2=2.1\%;\quad \beta_3=2.9\%;\quad \beta_4=3.5\%;\quad \beta_5=4.0\%.$$

It can be seen that the damping in the two lowest modes is exactly equal to the damping used in the determination of the damping matrix $[C]$. This is not surprising in view of the fact that very little data fitting was necessary in the determination of $[C]$. Also, in the matrix-multiplication of Eq. 3.6, the determination of $2\beta_1\omega_1$ and $2\beta_2\omega_2$ involves only the use of the first and second mode and these as shown in Table III-3 deviate only slightly from the experimentally determined values.

It is questionable how well the values of damping in the higher modes represent the actual values of damping in the structure. To determine these values Eq. 3.6 involves the use of the mode shapes for the third, fourth and fifth mode and these were found from a knowledge of the modal properties of the first and the second mode

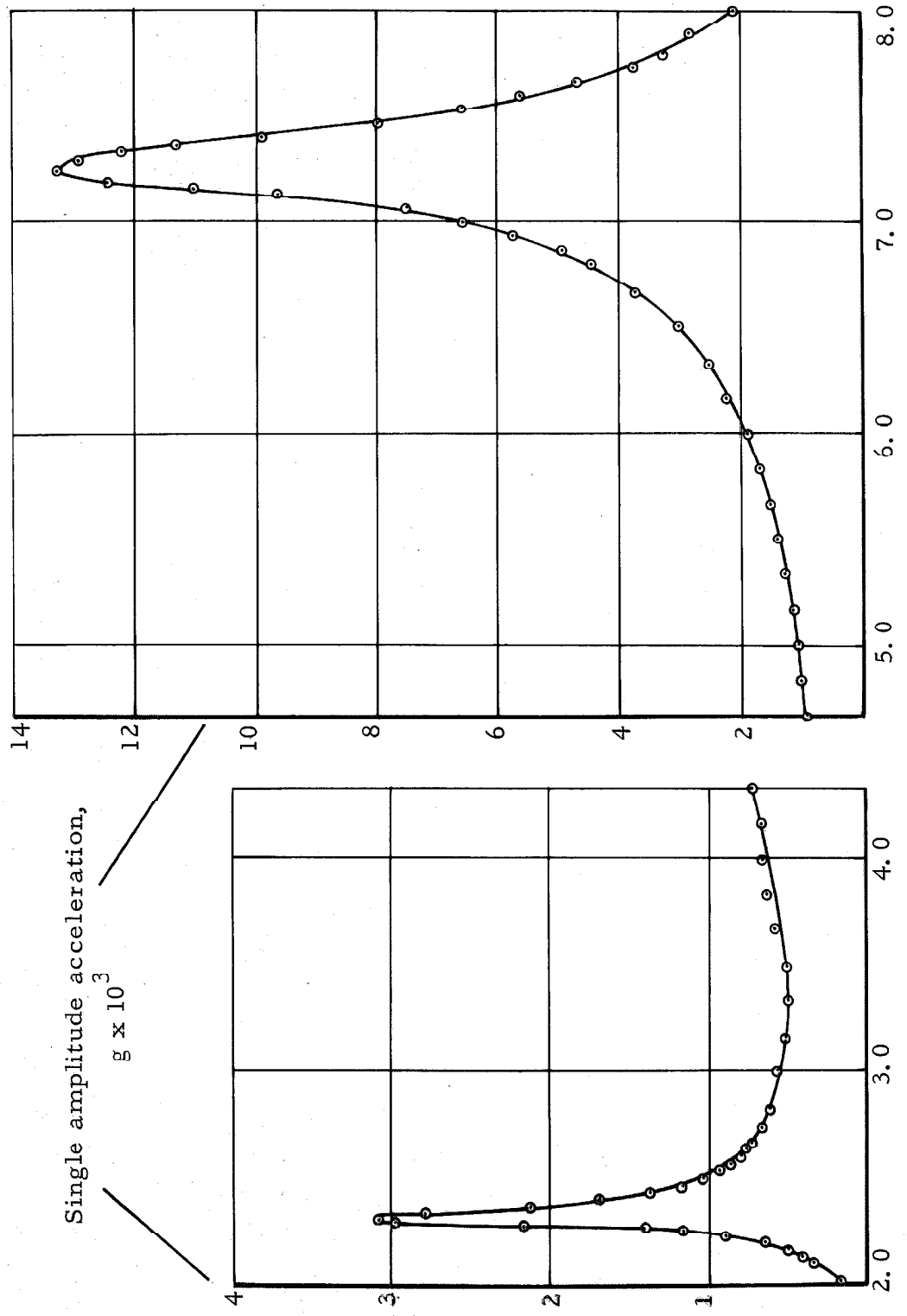

Fig. 3-9 3rd FLOOR RESPONSE, TEST NO. 1

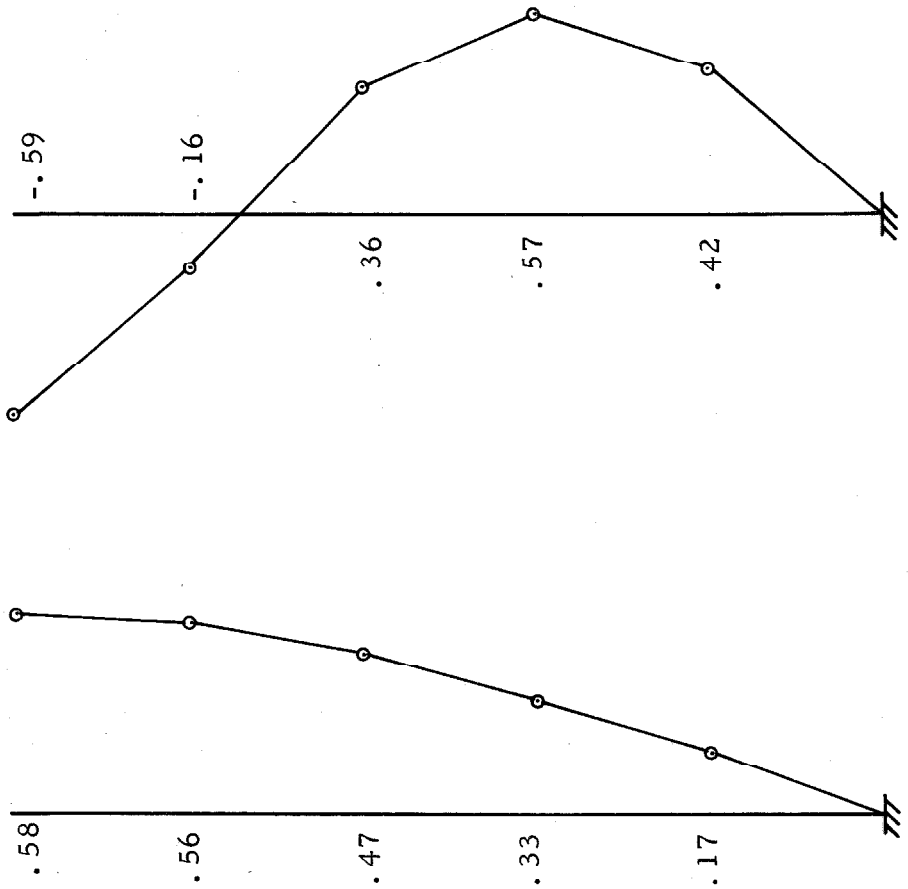

Fig. 3-10 MODE SHAPES (N-S)

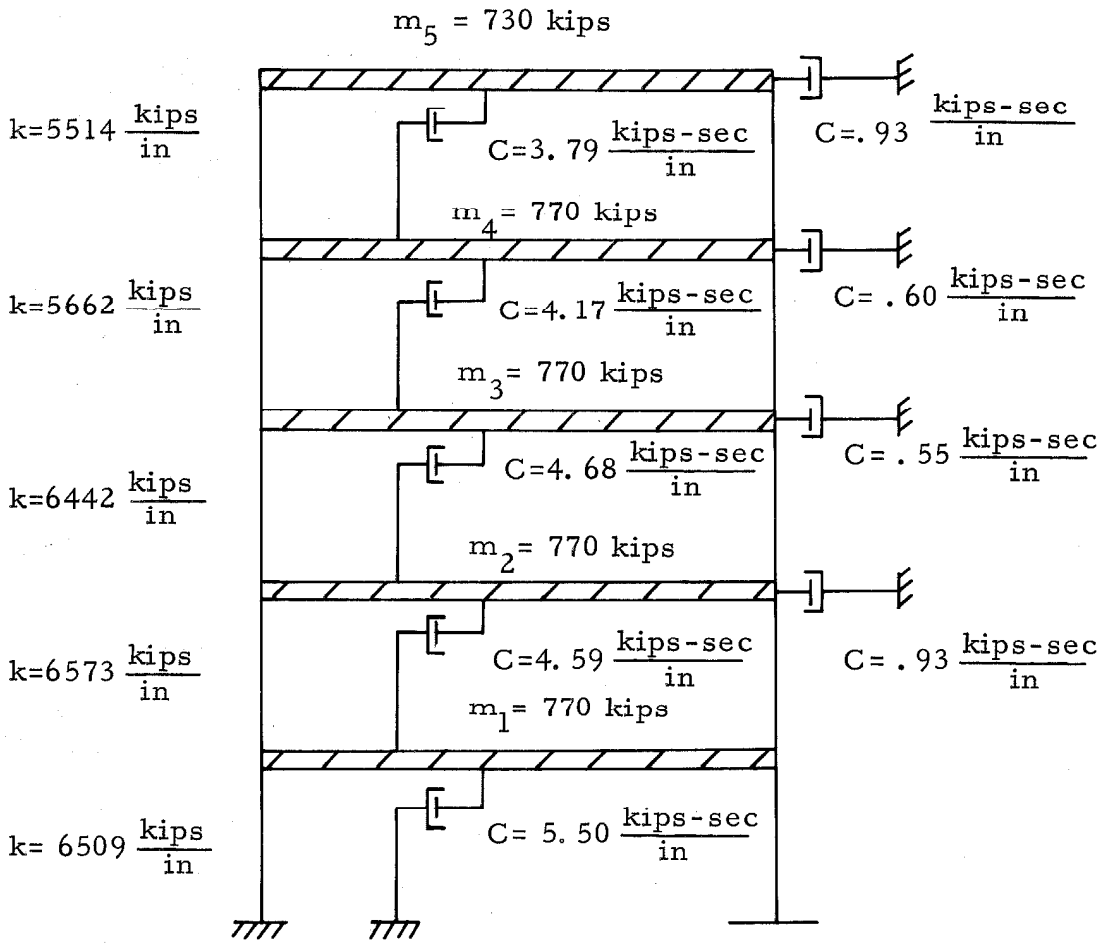

Fig. 3-11 EXPERIMENTALLY DETERMINED MODEL OF BUILDING (N-S)

only. So all that can be conservatively said is that the model of the structure shows the exact natural frequencies, mode shapes and values of damping in the first and second mode as the corresponding values found from the vibration tests of these two modes. Figure 6-11 shows the model of the structure or more precisely the "equivalent frame" representing the structure in the north-south direction. The "absolute damping" is much lower than the "relative" damping but it is still more than might be expected. Air damping would not be of a sufficient magnitude to account for the "absolute" dashpots. This has been shown by Merchant.[49]

But it should be noted that the representation of the damping by the use of equivalent dashpots is open to question. The "absolute" dashpots appear in the model due to the fact that the damping in the second mode is approximately equal to the damping in the first mode and this requires both "relative" and "absolute" dashpots.

If part of the damping were due to a Coulomb type damping, the damping would not be frequency dependent. It is possible that the "absolute" damping stems from movement of the foundation. This motion has been disregarded in the analysis above since very small motions of the base were recorded. A description follows in a subsequent section.

Translational Motion in the Short East-West Direction

With the same location of the two vibration exciters as described above, the structure was excited in translation in the short east-west direction by running the vibration exciters synchronized in

phase. In this direction it was only possible to excite the lowest translational mode, the exciters were run up to a maximum speed of about 8.5 cps and no indication of a second mode was evident from the recorded accelerations. Accelerometers were placed on all floors at the geometrical center of the floor slabs. Figure 3-12 shows the response of all floors at and close to the lowest translational frequency of 2.52 cps. It is evident from Fig. 3-12 that all floors experience their maximum response at the same frequency. Again in this case the form of all the response curves is the same and the percentage of critical damping as determined from the width of the response curve is found to give identical values regardless of which floor response is used in the determination of the value of damping.

Table III-6 shows the peak response of all floors as the structure is excited at different force levels. It is evident that the mode shape stays constant regardless of level of force excitation. The resonant frequency changes as the structure experiences higher stress levels. At the lowest stress level (test No. 5) the resonant frequency is 2.62 cps while at the highest stress level (test No. 10) the resonant frequency is 2.49 cps. Again in this case it is evident that the sequence in which the tests are conducted is of importance. Test No. 8 and test No. 11 correspond to approximately the same force level but the responses from the two tests are not identical. The fact that the structure experienced higher stress levels in tests No. 9 and 10 has changed the dynamic characteristics of the structure slightly, but enough so that these changes are evident from the response of the

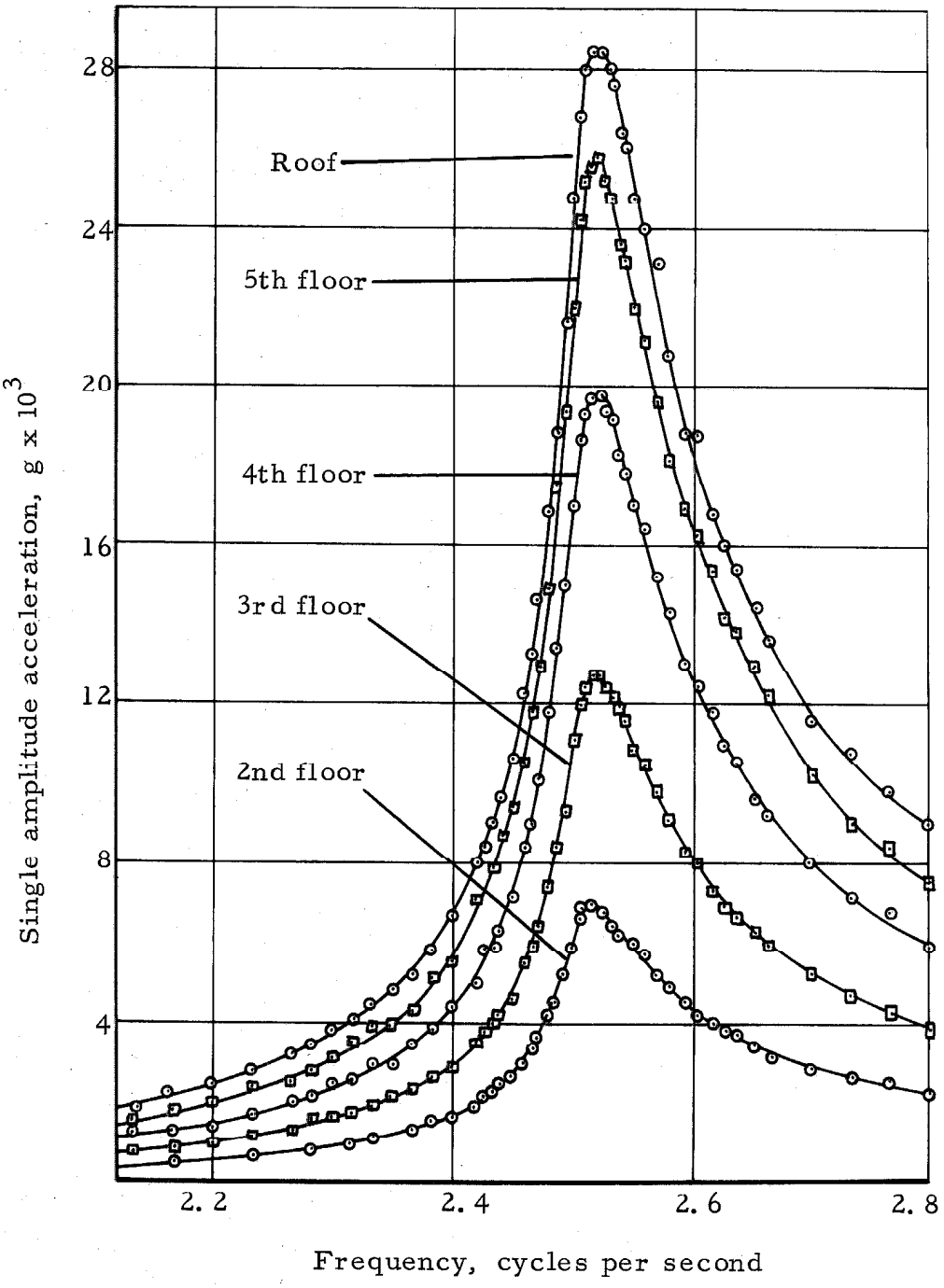

Fig. 3-12 LOWEST TRANSLATIONAL MODE (E-W), TEST No. 9

TABLE III-6

Peak response values, E-W translational mode

Test No. mode force at resonance resonant frequency		2nd fl.	3rd fl.	4th fl.	5th fl.	Roof
5 1st mode 729 lbs 2.62 cps	single ampl. accel. $g \times 10^{-3}$	2.00	3.54	5.47	7.05	7.92
	single ampl. displ. in. $\times 10^{-3}$	2.84	5.03	7.77	10.02	11.27
	mode shape	.16	.28	.43	.56	.63
6 1st mode 1302 lbs 2.59 cps	single ampl. accel. $g \times 10^{-3}$	3.33	5.85	9.10	11.8	13.55
	single ampl. displ. in. $\times 10^{-3}$	4.83	8.47	13.2	17.10	19.6
	mode shape	.16	.28	.43	.56	.65
7 1st mode 1818 lbs 2.57 cps	single ampl. accel. $g \times 10^{-3}$	4.43	7.87	12.42	16.2	18.9
	single ampl. displ. in. $\times 10^{-3}$	6.55	11.65	18.4	24.0	28.0
	mode shape	.15	.27	.43	.55	.65
8 1st mode 2380 lbs 2.54 cps	single ampl. accel. $g \times 10^{-3}$	5.50	10.2	15.65	20.3	22.5
	single ampl. displ. in. $\times 10^{-3}$	8.33	15.45	23.7	30.8	34.0
	mode shape	.15	.28	.43	.57	.63
9 1st mode 3085 lbs 2.52 cps	single ampl. accel. $g \times 10^{-3}$	6.92	12.65	19.7	25.8	28.5
	single ampl. displ. in. $\times 10^{-3}$	10.6	19.5	30.4	39.7	43.8
	mode shape	.15	.28	.43	.57	.63
10 1st mode 4110 lbs 2.49 cps	single ampl. accel. $g \times 10^{-3}$	8.50	15.8	24.6	32.5	35.5
	single ampl. displ. in. $\times 10^{-3}$	13.4	24.8	38.8	51.2	56.0
	mode shape	.15	.28	.43	.57	.62
11 1st mode 2330 lbs 2.51 cps	single ampl. accel. $g \times 10^{-3}$	4.97	9.32	14.7	19.15	21.6
	single ampl. displ. in. $\times 10^{-3}$	7.70	14.5	22.8	29.7	33.5
	mode shape	.15	.28	.43	.56	.63

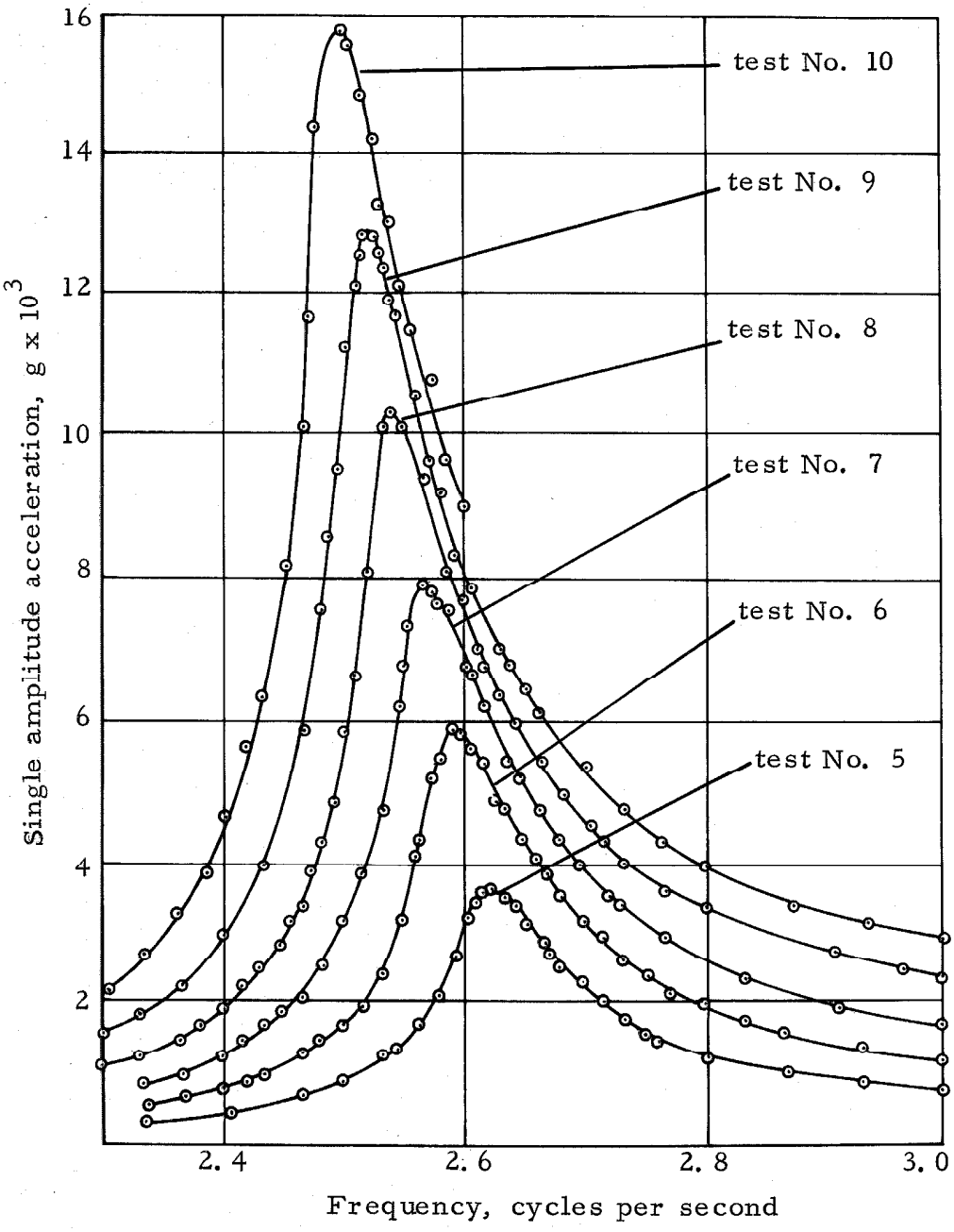

Fig. 3-13 3rd FLOOR RESPONSE, LOWEST TRANSLATIONAL MODE (E-W)

structure. This non-linear effect will be discussed further in the end of this chapter in the section on non-linearities of the response.

Figure 3-13 shows the acceleration response of the 3rd floor as the structure is excited in the lowest translational mode at different force levels. Again in this case the decrease in natural frequency as the structure experiences higher stress levels is typically that of a "softening spring". The decrease in resonant frequency from the lowest to the highest stress level is about 5%. The corresponding change in stiffness of the structure is thus about 10%.

Determination of the Structural Properties from the Experimental Results

Even though each of the columns of the building is symmetrical having the same moment of inertia with respect to an axis through the centroid of the column; regardless of whether this axis be parallel to the short side or the long side of the building the stiffness of each column differs widely in the two directions. In the long north-south direction the deep girders not only restrain the columns against joint rotation but also decrease the effective story heights. In the short east-west direction the floor slabs afford almost no restraint against joint rotation and the effective story height is approximately equal to the 12'-6" distance from center of floor slab to center of floor slab.

It is evident that almost all of the stiffness in the short east-west direction stems from the two end walls and the columns cast integrally with the end walls. The height to width ratio of the end walls is about 2.5 indicating that the end walls will vibrate partly as

bending beams and partly as shear beams. The mode shape for the lowest translational mode in the east-west direction is shown in Fig. 3-16a, It can be seen that the deflected shape of the structure varies almost linearly from the ground indicating neither the mode shape typical of a uniform shear beam nor that of a uniform bending beam.

In investigating the relative influence of different types of distortion on the natural periods of uniform cantilever beams Jacobsen[50] showed that the Dunkerley's empirical formula:

$$T_{sf} = \sqrt{T_s^2 + T_f^2}$$

gave excellent results for the resultant period T_{sf} when the "isolated component" periods T_s and T_f were determined using shear alone and bending alone, respectively. Assuming that half the total mass of the building is distributed uniformly along the total height of one end wall the natural period of vibration considering shear deformation only is:

$$T_s = .288 \sqrt{\frac{1.11\, wL^2}{2AG}}$$

and the natural period of vibration considering bending deformation only is:

$$T_f = .258 \sqrt{\frac{wL^4}{8EI}}$$

The end walls are cast integrally with the end columns. This type of shear wall has been extensively tested and analyzed by Benjamin and Williams.[51] In their tests static shear forces were applied in the plane of the wall and the effect of panel and column proportions and reinforcing was investigated. The results of interest

for the present investigation are:

1) The reinforcing is only effective after cracking begins and not before.

2) In calculating the area of the wall cross section reinforcing steel and columns should be neglected.

3) In calculating the moment of inertia of the entire cross section the columns should be included but the reinforcing steel should be neglected.

The static tests were performed on concrete for which the compressive strength varied between 2×10^3 psi and 4×10^3 psi. E was found to vary between 2.0×10^6 psi and 2.6×10^6 psi.

The shear walls are 10 inches thick and the total distance from the ground to the top of the walls is 65 feet. Distributing half the total weight of the building uniformly along one end wall the following values can be found:

$$wL = 1905 \text{ kips}$$

$$A = 2760 \text{ in}^2$$

$$I = 43.4 \times 10^6 \text{ in}$$

$$L = 65 \text{ feet.}$$

Using $G = .4E$, the following results are obtained for the natural period T_f when taking only bending into account and the natural period T_s when taking only shear into account:

$$T_s = .288 \sqrt{\frac{1.11wL^2}{2AG}} = .288 \sqrt{\frac{7.5 \times 10^5}{E}}$$

$$T_f = .258 \sqrt{\frac{wL^4}{8EI}} = .258 \sqrt{\frac{2.6 \times 10^6}{E}}$$

The natural frequency as determined from the vibration tests varied between 2.49 cps and 2.62 cps according to force level used in exciting the natural mode. This corresponds to a natural period of approximately .39 sec. By use of the Dunkerly formula the experimental result can be related to the expected results; again in this case the value of E is regarded as unknown:

$$T_{exp} = .39 = \sqrt{T_s^2 + T_f^2} = \sqrt{\frac{23.5 \times 10^4}{E}}$$

or

$$E = 1.55 \times 10^6 \text{ psi}$$

This value of E is consistent with the values determined from the vibration tests in the long north-south direction when using an effective story height equal to the "free" height between floors. Again in this case the E-value is lower than expected but no definite conclusions can be made and interesting future research is certainly indicated.

Determination of Damping

The values of damping as determined from the response at resonance are listed in Table III-7. In this table the acceleration amplitude ratios, the displacement amplitude ratios and the force ratios are shown as well. These values follow directly from Table III-6. The values of damping show a consistent increase with increasing force levels. This is also evident from the fact that the amplitude at resonance increases less rapidly than the exciting force. It is of interest to note that the displacement amplitude increases more rapidly than the acceleration amplitude. This of course

is due to the decrease in resonant frequency as the force level is increased.

TABLE III-7

Damping of different force levels

Test No.	5	6	7	8	9	10	11
Damping %	2.1	2.3	2.4	2.4	2.5	2.7	2.6
Force ratios	1	1.8	2.5	3.3	4.2	5.6	3.2
Acceleration amplitude ratios	1	1.7	2.3	2.9	3.7	4.6	2.7
Displacement amplitude ratios	1	1.7	2.4	3.1	4.0	5.1	2.9

It is evident that the damping is not purely viscous since the resonant amplitude increases less rapidly than the exciting force. However, as noted before, the damping is quite low making the concept of "equivalent viscous damping" a reasonable one to use. Again in this case the values of damping as determined from the width of the response curve are found to give lower values than those determined from the response at resonance. Determining the values of damping from the width of the response curves shown in Fig. 3-13 a value of about 1.8 percent of critical damping is found regardless of which one of the response curves is used. Only a slight indication of an increase in damping as the force level increases can be found.

Torsional Motion

With the same location of the vibration exciters as previously

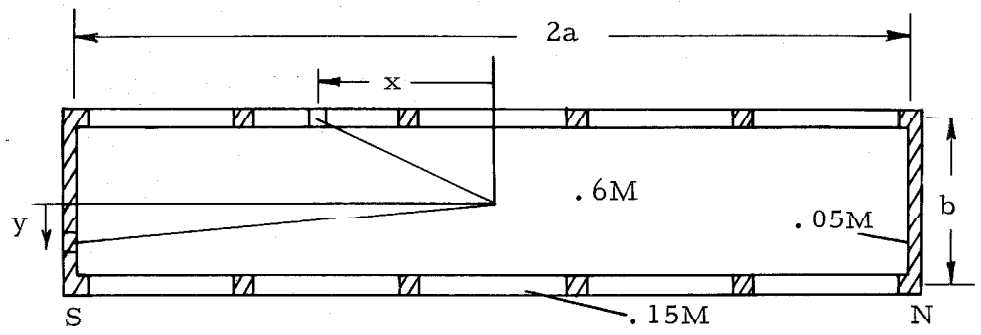

Fig. 3-14a DETERMINATION OF POLAR MOMENT OF INERTIA

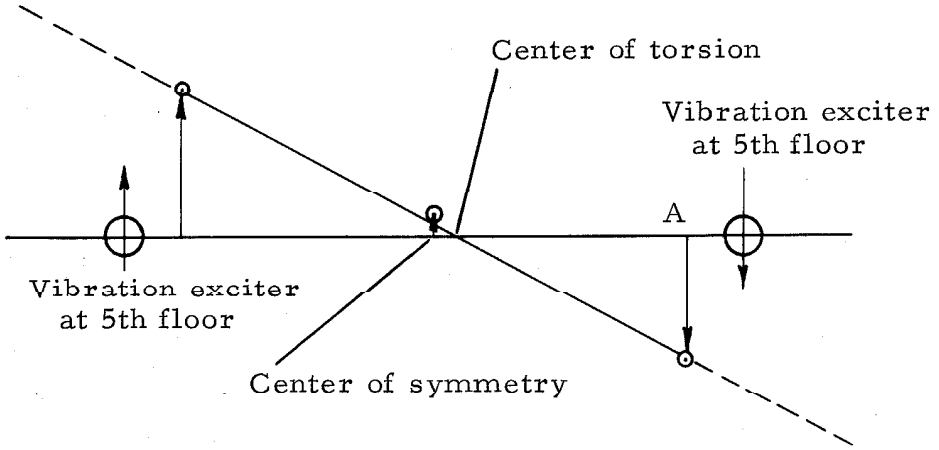

Fig. 3-14b ACCELERATION OF 2nd FLOOR, LOWEST TORSIONAL MODE, RESPONSE CURVE FOR POINT A SHOWN IN FIG. 3-15.

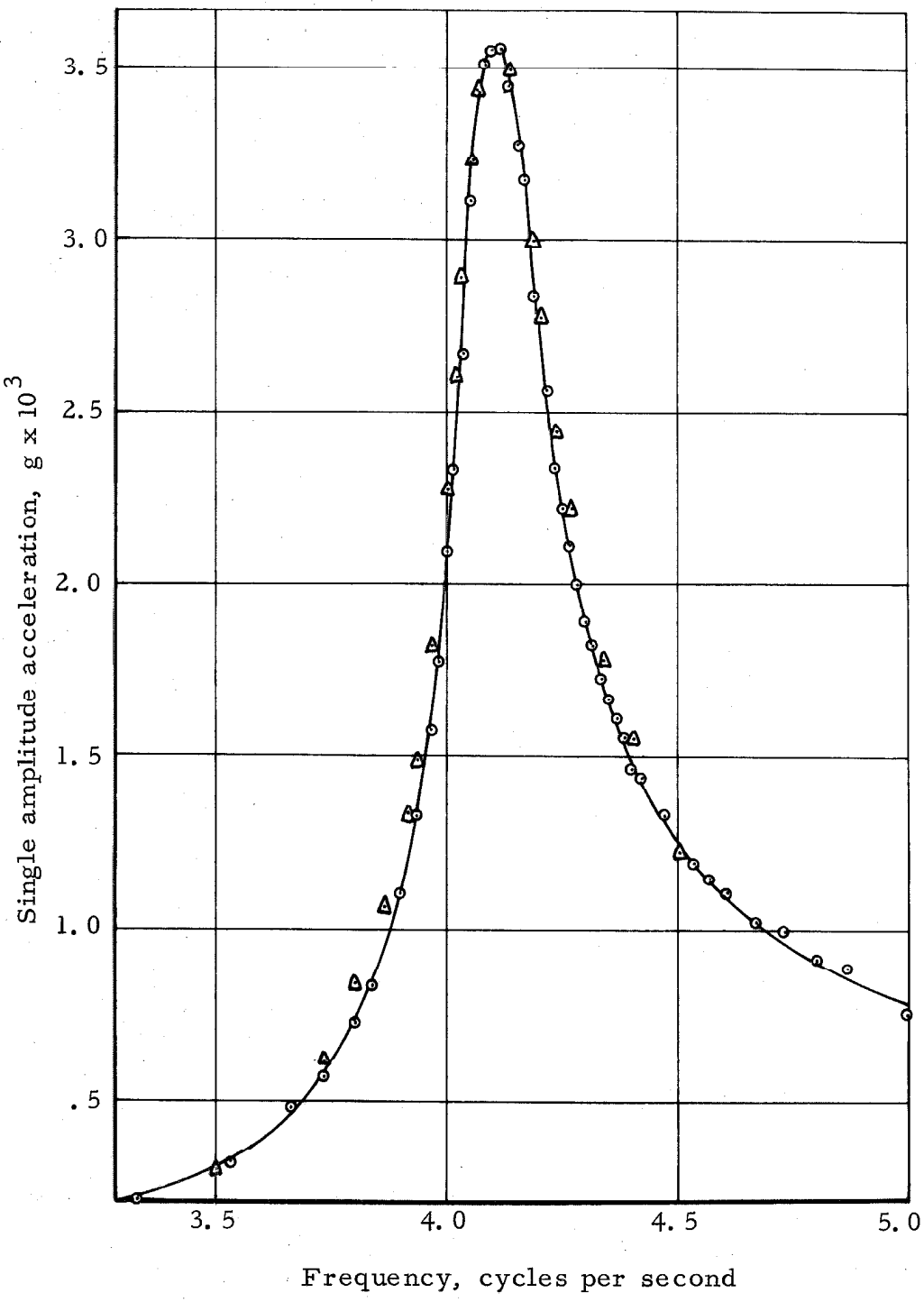

Fig. 3-15 2nd FLOOR RESPONSE, LOWEST TORSIONAL MODE (POINT A IN FIG. 3-14b)

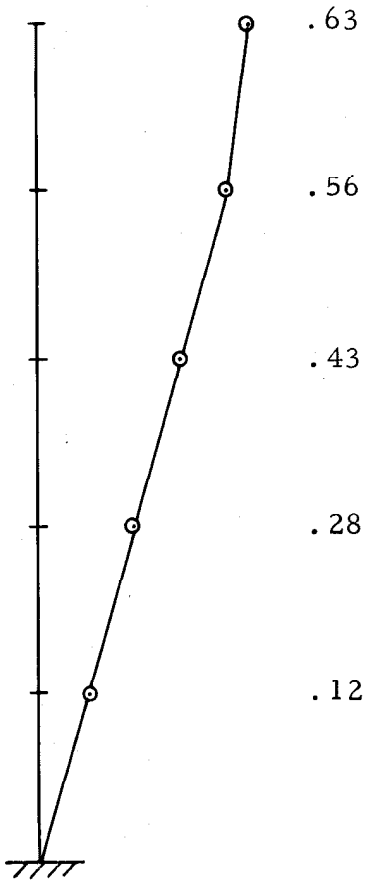

ω = 2.49 - 2.62 cps

β = 2.1 - 2.7%

Fig. 3-16a

LOWEST TRANSLATIONAL MODE (E-W)

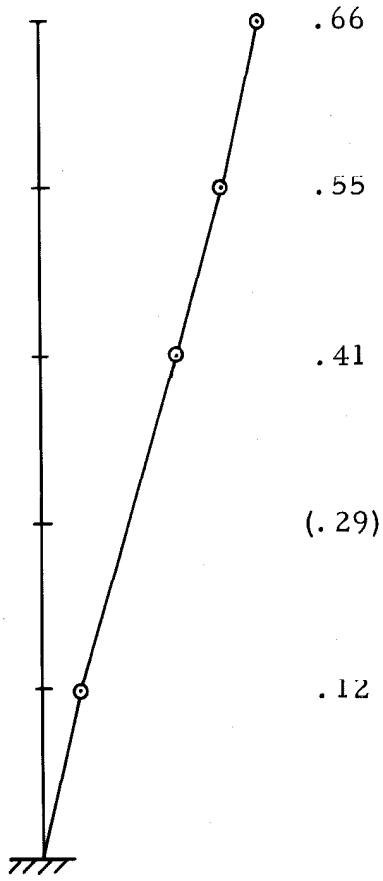

ω = 4.10 cps

β = 2.3%

Fig. 3-16b

LOWEST TORSIONAL MODE

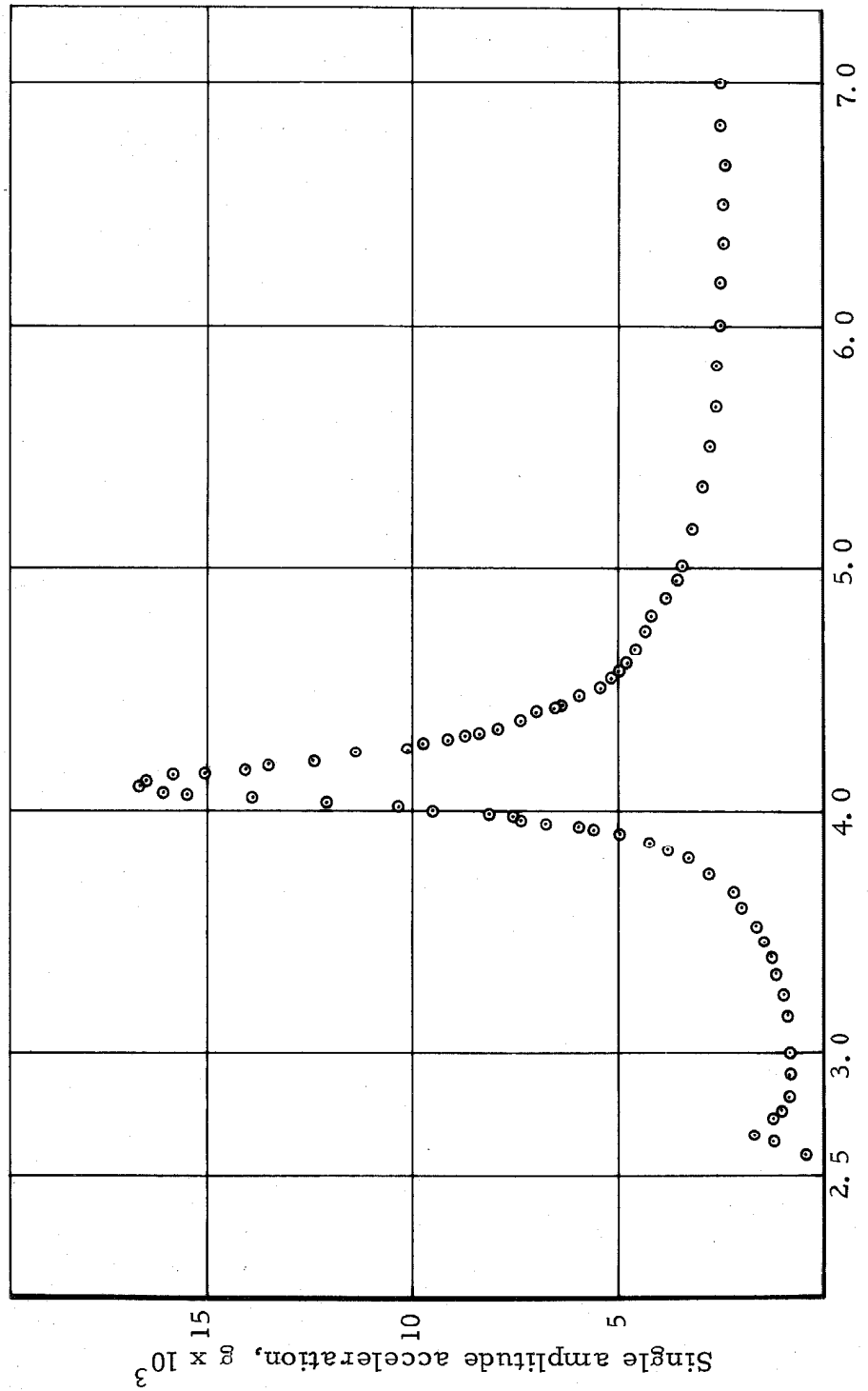

Fig. 3-17 5th FLOOR RESPONSE, TORSION (25 FEET FROM NORTH END)

described, the building was excited in torsion by running the two vibration exciters synchronously but with a phase angle of 180° between them. Figure 3-17 shows the acceleration response of a point on the longitudinal axis of the fifth floor located 25 feet from the north end of the building. The lowest torsional mode is purely excited at a frequency of 4.10 cps. Figure 3-15 shows the acceleration response of a point on the longitudinal axis of the second floor at a distance of 25 feet from the north end of the building. The location of this point is shown as point A on Fig. 3-14b. During the preliminary tests three accelerometers were located as shown in Fig. 3-14b at points A, B and C. Simultaneous readings of acceleration were taken as the building was excited in its lowest torsional mode. The peak response values are shown in Fig. 3-14b. It is evident that the floor vibrates in pure torsion and that the center of torsion is located very close to the center of symmetry of the floor.

In order to determine the mode shape for the lowest torsional mode, accelerometers were located on all floors at a distance of 25 feet from the north end of the building. Again the locations correspond to point A of Fig. 3-14b. The mode shape as determined from the simultaneous measurements of all floors is shown in Fig. 3-16b. During the test a malfunction developed in the channel recording the 3rd floor response. The value shown for the 3rd floor modal component in Fig. 3-16b was obtained by a linear interpolation between the 2nd floor and the 4th floor response values. The deflected shape of the structure varies almost linearly from the ground, and the

mode shape for the lowest torsional mode is very close in appearance to that of the lowest translational mode shown in Fig. 3-16a.

A simple relationship exists relating the frequency of the lowest torsional mode to the frequency of the lowest translational mode. Let the equivalent spring factor from each of the end walls be k, then the lowest translational frequency can be found from the equation:

$$M\ddot{x} + 2kx = 0 \quad ; \quad \omega_1^2 = \frac{2k}{M}$$

The lowest torsional frequency can be found from the equation:

$$J\ddot{\varphi} + 2ka^2\varphi = 0 \quad ; \quad \omega_2^2 = \frac{2ka^2}{J}$$

or

$$\frac{\omega_2^2}{\omega_1^2} = \frac{Ma^2}{J}$$

J is the polar moment of inertia of the masses of the structure with respect to an axis through the centroid of the floor system. The dimensions of interest are shown in Fig. 3-14a. For each floor of the building the floor slab contributes 60% of the total floor mass, girders and columns contribute 30%, and the end walls contribute 10% of the total floor mass. Referring to Fig. 3-14a, the polar moment of inertia is:

$$J = \frac{1}{12}(.6M)(4a^2+b^2) + 4\int_0^a \frac{.15M}{2a}\left(\left(\frac{b}{2}\right)^2 + x^2\right)dx + 4\int_0^{\frac{b}{2}} \frac{.05M}{b}(a^2+y^2)dy$$

$$= .4Ma^2 + .14Mb^2$$

The predicted ratio of the frequency of the lowest torsional mode and the frequency of the lowest translational mode can now be found, noting

that 2a = 125 feet and b = 25 feet:

$$\frac{\omega_2}{\omega_1} = \sqrt{\frac{Ma^2}{J}} = \sqrt{\frac{Ma^2}{.4Ma^2 + .14Mb^2}} = 1.54$$

From the forced vibration tests the resonant frequency of the lowest torsional mode was found to be 4.1 cps and the resonant frequency of the lowest translational mode was found to be 2.6 cps. Thus the ratio of the experimentally determined values becomes

$$\frac{\omega_2}{\omega_1} = \frac{4.1}{2.6} = 1.58$$

The theoretically predicted ratio and the experimentally determined ratio are seen to be in close agreement.

The percentage of critical damping in the lowest torsional mode was determined from the width of the response curve at $\sqrt{2}/2$ times the resonance amplitude. Using the response curve shown in Fig. 3-15 a value of 2.3% was obtained. Again in this case it can be seen from Fig. 3-15 that the points determined from the steady-state tests using decreasing frequencies tend to give a slightly broader response curve than the points determined from the steady-state tests using increasing frequencies.

The force amplitude applied by each of the two vibration exciters at resonance for the lowest torsional mode is equal to 892 lbs. The distance between the two vibration exciters on the 5th floor is 93 feet, so the amplitude of the moment applied at resonance is 892 x 92 = 82,000 ft-lbs.

The torsional vibration tests provide an interesting verification of how well the two vibration exciters act synchronously in applying a pure moment to a structure. Returning to Fig. 3-17 it can be seen that a small resonance is excited at 2.6 cps which is the natural frequency of the translational mode. If each of two vibration exciters applied exactly the same force and the phase angle between them were exactly 180° a pure moment would be applied to the structure and the translational mode would not be excited at all. The small response at 2.6 cps is thus an indication of the magnitude of imperfections in the forcing system when two vibration exciters are acting synchronously with a phase angle of 180° between them. It is quite evident that this inperfection is of negligible magnitude. Figure 3-17 shows clearly that the small response at 2.6 cps in no way interferes with the response of the torsional mode.

Motion of Foundation

In the preceding analysis it has been assumed that the structure was fixed at the ground floor, i.e., that the ground floor did not experience any translation or any rotation. However, in all the tests attempts were made to measure the translational motion as well as the rotational motion of the ground floor. Only at the highest level of excitation in the short east-west direction (test No. 10) was the rotation of the ground floor of sufficient magnitude to be measurable. To measure the rotation one accelerometer was placed on the north side of the ground floor and one accelerometer was placed at the

south side of the ground floor. The distance between the two accelerometers was 31 feet with both accelerometers oriented such that vertical accelerations were measured. It was necessary to use the most sensitive setting of the Brush Amplifiers. At this setting the noise in the instrumentation system becomes noticeable. It is felt that the results of the vertical acceleration measurements are not precise enough to warrant an analysis as to the rotational characteristics of the ground floor. However, the results are indicative of the very small effect the translation and the rotation of the ground floor has on the total response. Assuming that the translational motion of the ground floor represents a translational motion of the entire structure and also assuming that the measured vertical accelerations of the ground floor represent a rigid body rotation of the entire structure, the effect of the ground floor motion can be evaluated in terms of the total response of the different floors of the structure, as shown in Table III-8.

TABLE III-8

Response of ground floor compared to total response; Test No. 10; lowest translational mode E-W; single amplitude acceleration.

	1st	2nd	3rd	4th	5th	Roof
Translation of ground floor $g \times 10^{-3}$	.8	.8	.8	.8	.8	.8
Rotation of ground floor $g \times 10^{-3}$	0	.24	.48	.72	.96	1.2
Total response $g \times 10^{-3}$	.8	8.5	15.8	24.6	32.5	35.5

It is evident from Table III-8 that the motion of the base accounts for a very small portion of the total response. It is of interest to compare the results with those found by Japanese investigators. Kawasumi and Kanai[13] report that in small amplitude vibration tests of a seven-story reinforced concrete building having plan dimensions of 90 feet by 72 feet the translation of the base accounted for 40 per cent of the total response of the roof, while rotation of the base accounted for about 20 per cent of the total response of the roof. In the present tests, as can be seen from Table III-8, the rigid body translation of the building as found from the response of the ground floor accounts for only 2 per cent of the total response of the roof, while the rigid body rotation of the ground floor accounts for about 3 per cent of the total response of the roof. The large differences in test results can be attributed to two sources. First, the Japanese building was a very rigid building; this would tend to facilitate the rigid body translation and rotation to a higher degree than would be the case for a more flexible building. Second, the Japanese building is probably supported on softer soil than that encountered for the building described in this chapter.

Non-Linearities of the Response

In exciting the lowest translational mode in the north-south direction as well as in the east-west direction, the steady-state resonance curves were obtained for a number of force levels. Figures 3-4 and 3-13 show clearly how the resonant frequency decreases as

the force level increases. The shift in frequency being typically that of a "softening spring". It is of interest to compare the response curves of Figs. 3-4 and 3-13 to those shown in Fig. 3-20. The general shape of the resonance curves of Fig. 3-20 and their shift in natural frequency bears a close resemblance to the experimentally determined resonance curves of Figs. 3-4 and 3-13. The resonance curves shown in Fig. 3-20 were obtained by Jennings[52] in a theoretical study of the steady-state response of a yielding one degree-of-freedom structure subjected to a sinusoidal force excitation. It is not possible to make a quantitative comparison between Jennings' theoretical results and the experimentally determined results. As Jennings points out, it would be necessary to extend his theory by including non-integer values of the parameters used in the description of the hysteretic relations. It would also be necessary to include a viscous damping coefficient in addition to the pure hysteretic type damping in order to account for the observed energy dissipation at low amplitude levels.

In exciting the lowest translational mode in the east-west direction, test No. 5 corresponds to the lowest level of excitation while test No. 10 corresponds to the highest level of excitation. It was decided that after performing these tests it would be valuable to duplicate one of the intermediate tests to investigate whether the excitation at the higher force levels had changed the dynamic characteristics of the structure to a measurable degree. Test No. 11 was then carried out with the same set of weights in the vibration

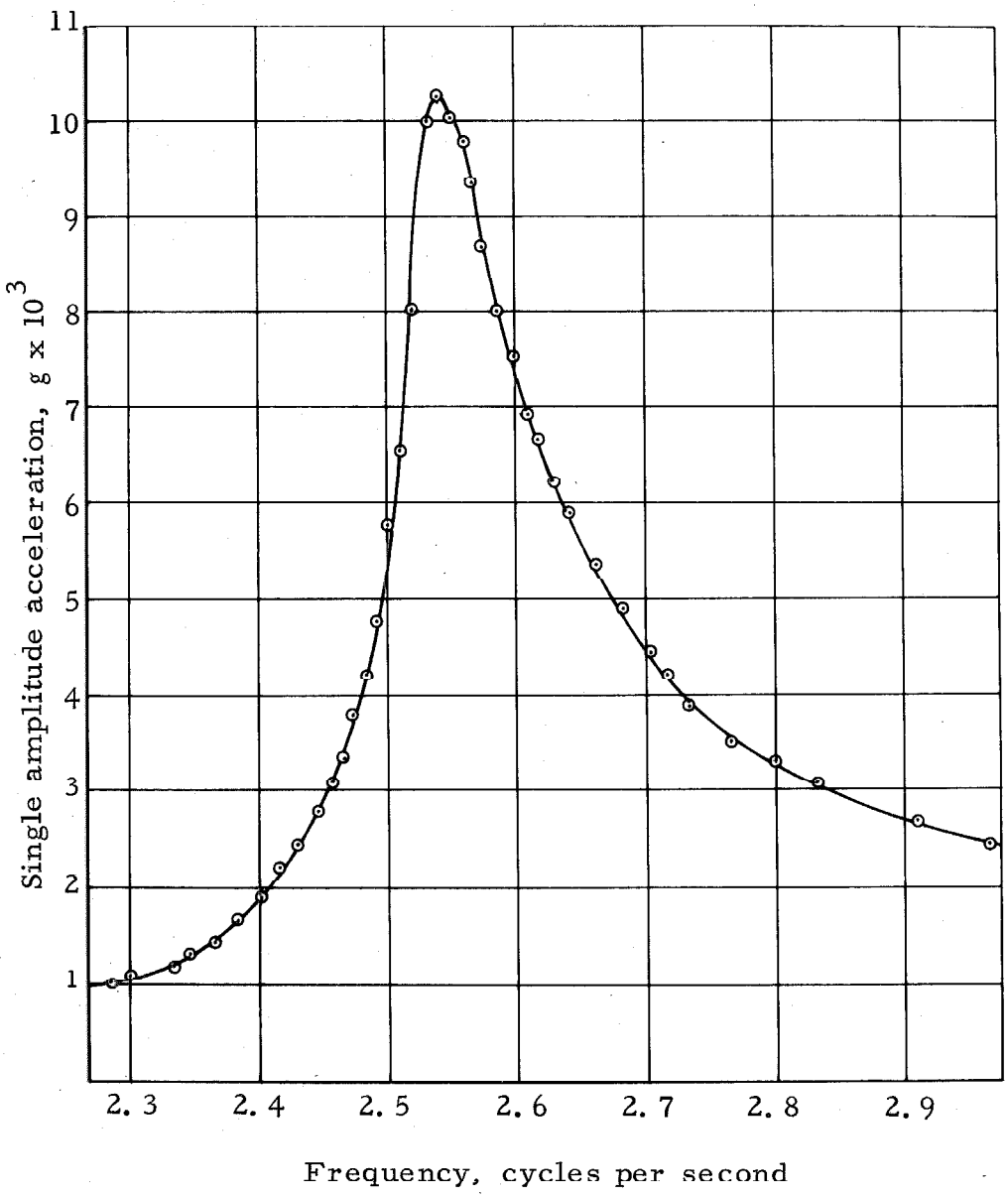

Fig. 3-18 3rd FLOOR RESPONSE, LOWEST TRANSLATIONAL MODE (E-W), TEST NO. 8

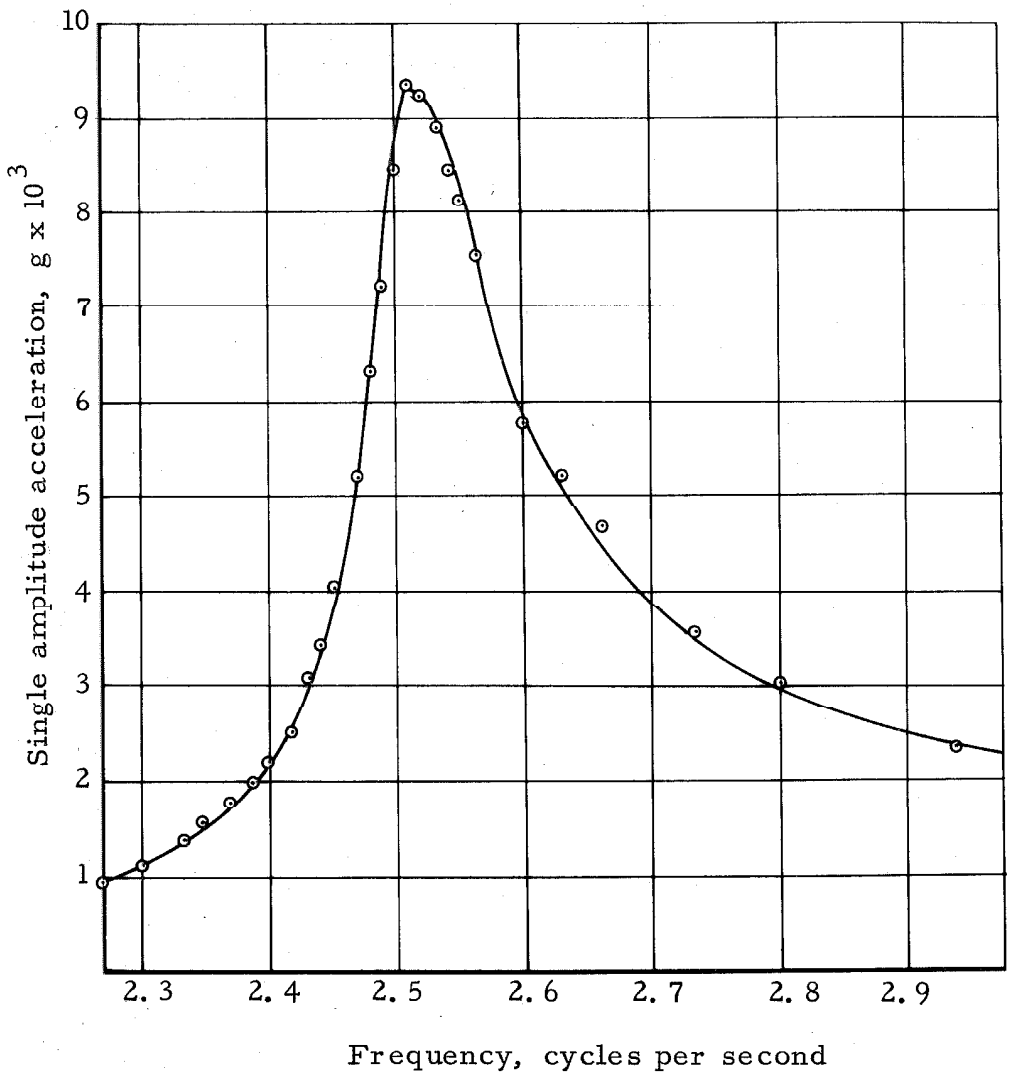

Fig. 3-19 3rd FLOOR RESPONSE, LOWEST TRANSLATIONAL MODE (E-W), TEST No. 11

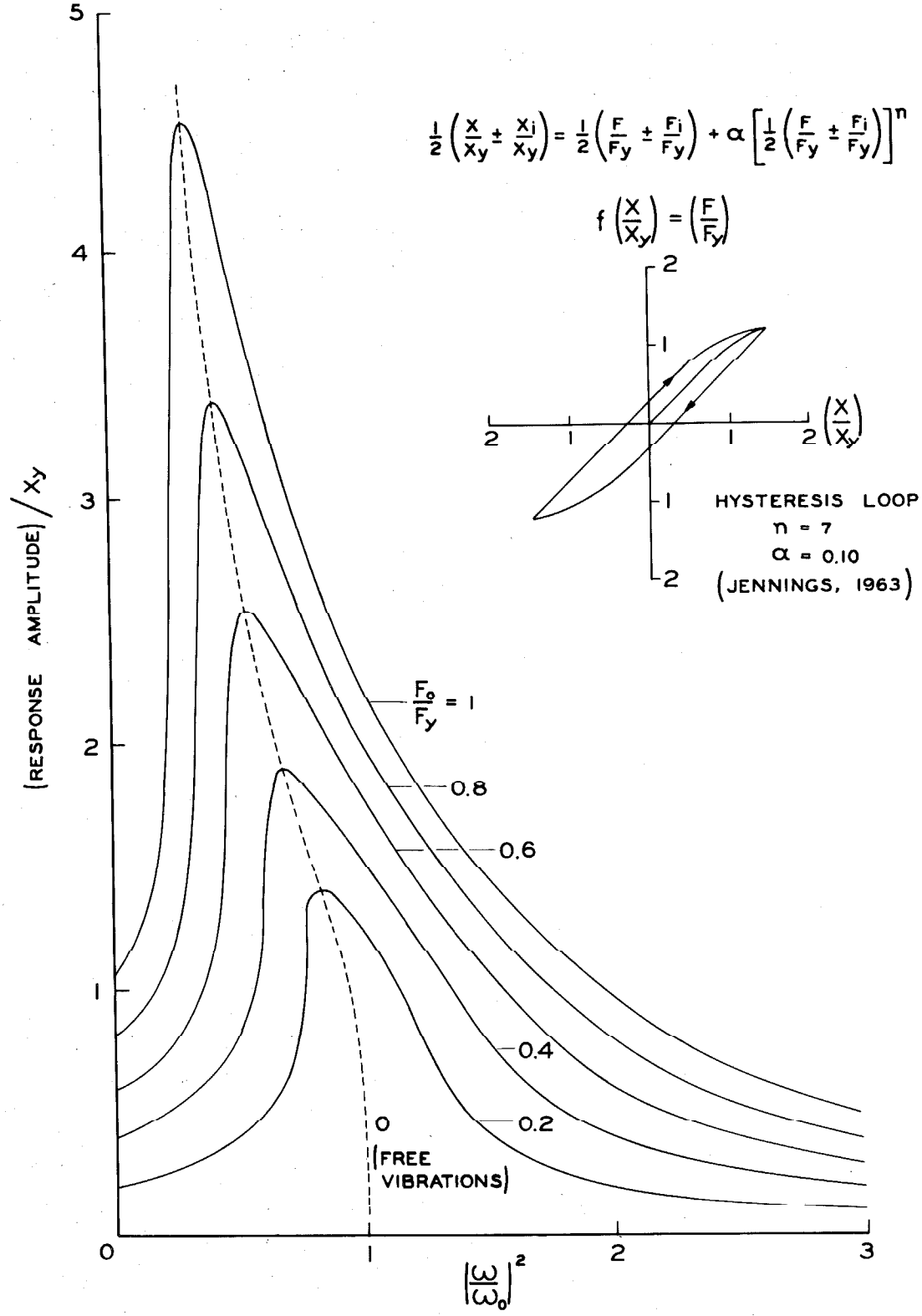

FIG.3-20 HYSTERESIS TYPE RESONANCE CURVES

exciters as had been used during test No. 8. The 3rd floor response of test No. 8 is shown in Fig. 3-18, while Fig. 3-19 shows the 3rd floor response of test No. 11. Several differences in the response from the two tests are noteworthy. First, the resonant frequency found from test No. 11 is 2.51 cps while that of test No. 8 is 2.54 cps. So by experiencing higher levels of excitation the structure has "softened" as indicated by the 1% lowering of the resonant frequency. This change in frequency changes the force at resonance from 2380 lbs in test No. 8 to 2330 lbs in test No. 11. The two tests are in other words not exactly alike as to level of force excitation but the difference is only about 2%. A significant change in peak response value occurs. As can be seen from Table III-6 the mode shape found from test No. 8 is identical to that found from test No. 11. However, it is evident from Table III-6 that the peak response values for all the floors as found from test No. 11 are about 10% lower than those found from test No. 8. The excitation of the structure at the higher force levels has increased the damping value by about 10%. This is also evident from the width of the two response curves in Figs. 3-18 and 3-19. The percentage of critical damping as determined from the width of the response curve in Fig. 3-19 (test No. 11) is equal to 2.0% while that of Fig. 3-18 (test No. 8) is equal to 1.8%. Again it is found that the damping determined from the width of the response curves is lower than the damping as determined from the peak response; the latter values as shown in Table III-7 were 2.6% for test No. 11 and 2.4% for test No. 8.

The above mentioned changes in response are of a small magnitude but they point towards some interesting possibilities. Since the small amplitude vibration tests were capable of producing a measurable increase in damping value, it would seem possible that small vibrations caused by traffic, small tremors, use of machinery in the building, etc., over a period of time would also tend to increase the value of damping. These effects might be cumulative or the value of damping might approach a limiting value. More research is certainly indicated to explore these questions.

Level of Excitation in Terms of Base Shear

The lateral force requirements of most building codes are based on the concept of a total lateral force to be distributed roughly linearly over the height of the building from the base of the building. It is of interest to express the levels of excitation of the steady-state resonance tests in terms of the base shear. Considering the lowest translational mode it is possible to express the forces acting on the structure as it is deflected in its extreme position at resonance. The forces acting on the building in this position can be found by the use of d'Alembert's principle by considering the inertia force $-m_i\ddot{x}_i$ acting at the i^{th} floor, m_i is the mass of the i^{th} floor and $\ddot{x}_i$ is the single amplitude acceleration of the i^{th} floor at resonance. The total base shear is then equal to the sum of the inertia forces. This sum expressed as a percentage of the total gravity load is shown in Tables III-9 and III-10.

TABLE III-9

Lowest translational mode (N-S)

Base Shear

Test No.	1	2	3	4
Base Shear, %g	.4	1.0	2.1	1.6

TABLE III-10

Lowest translational mode (E-W)

Base Shear

Test No.	5	6	7	8	9	10	11
Base Shear, %g	.5	.9	1.2	1.5	1.9	2.3	1.4

The values for the base shear developed during the dynamic tests can be compared to the design value for the building which according to the Los Angeles Building Code would be approximately 7% g for both principal directions of the building.

CHAPTER IV

VIBRATION TESTS OF A NINE-STORY STEEL FRAME BUILDING

A modern nine-story steel frame building in the southern California area has been subjected to extensive dynamic testing. The vibration tests ranged in complexity from "man-excited" vibration tests as described in detail in Chapter VI to steady-state resonance tests employing several synchronized vibration exciters. A total of eleven normal modes were determined from the steady-state resonance tests; four of these were translational modes in the long direction of the building, three were translational modes in the short direction, three were torsional modes and one mode was excited in which the floor slabs vibrated in the horizontal plane as free-free beams. Run-down tests were performed as well in order to explore the differences in the response as compared to the response of steady-state tests. The results of these comparison tests are given in detail in Chapter V.

Description of Building

The building is a symmetrical nine-story steel frame building with plan dimensions 220 feet by 40 feet. Overall dimensions of the building and some of the pertinent construction details are shown in Fig. 4-1. Further details are shown in Figs. A-5 through A-14 in the Appendix. The floor slabs were 5-inch reinforced lightweight concrete slabs. The 10th floor contained rooms for heavy equipment. At the time when most of the steady-state vibration tests were performed, the

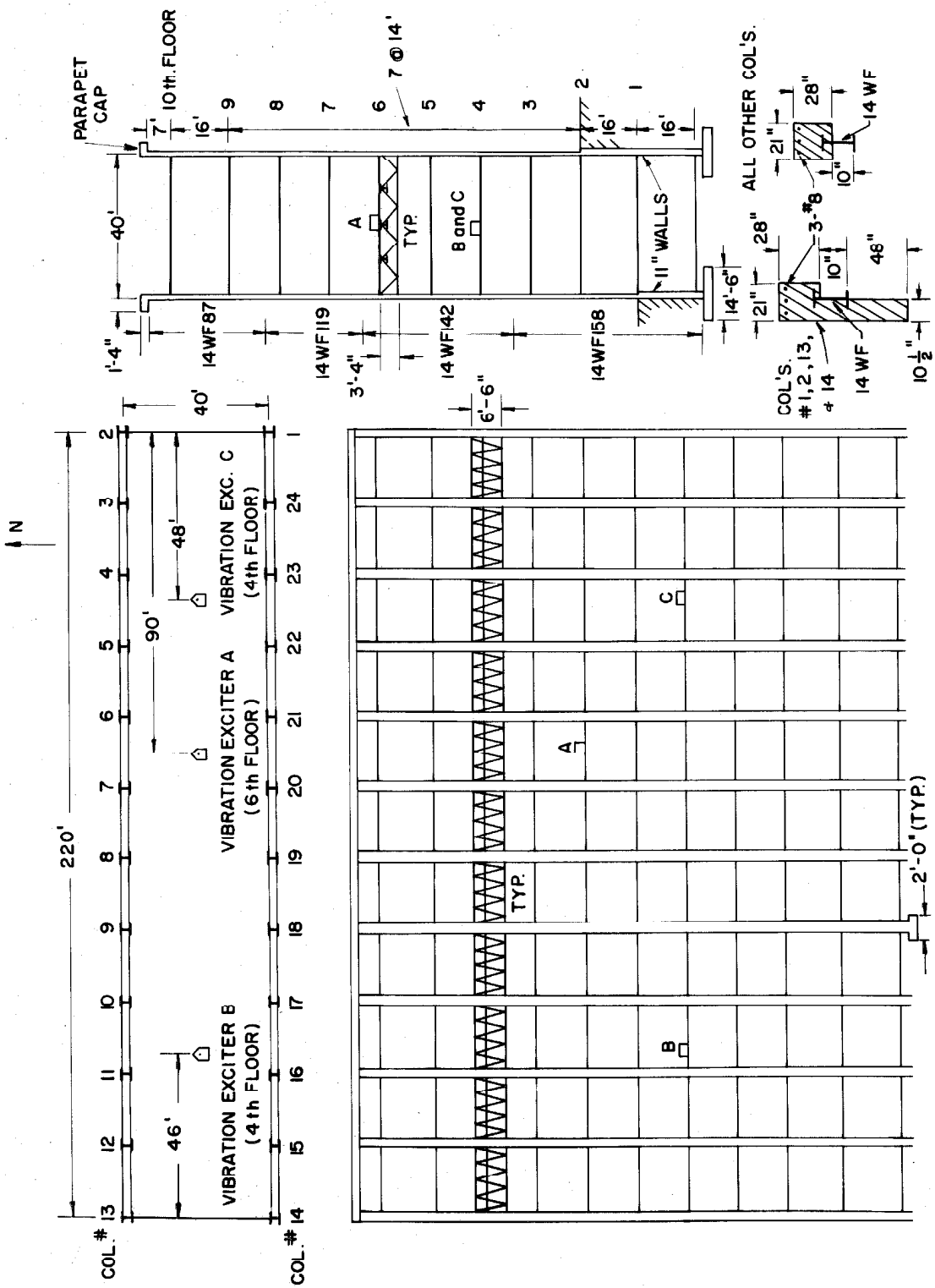

FIG. 4 - 1 STEEL FRAME BUILDING

weight of each of the floors above the 2nd floor was estimated from construction drawings to be approximately 920 kips, except for the 10th floor which was estimated to have a weight of 1640 kips.

The steel frame was designed to carry all loads. Details of the column construction are shown in Fig. 4-1. At the final stage of construction wire mesh and plaster was used on the inside of the columns to complete the fireproofing of the steel columns. Details of the column construction are also shown in Figs. A-11 through A-14.

The building is characterized by the very rigid girders in the long East-West direction. Details are shown in Fig. 4-1, Fig. A-9 and Figs. A-11 through A-14. The welded girders are attached to the columns by high-strength bolts. The girders have a depth of 6'-6", typical top and bottom chords are 8-inch channels. The welded trusses in the short North-South direction are attached to the columns by high-strength bolts. The typical truss has a depth of 3'-4", top chords consist of two 5" by 3" angles while bottom chords consist of two 6" by 3-1/2" angles. The beams in the long East-West direction are 12WF 27.

Staircases are located at the ends of the building as can be seen in Fig. A-7. The staircase sections are attached to the building by expansion joints and will add no appreciable stiffness to the building. The floor slabs had cuts to accommodate air conditioning ducts and elevators; these cuts can be assumed to have a negligible effect on the vibrational characteristics of the building.

Soil borings showed that the soil at basement level consisted of

very dense well-graded sandy gravel. Allowable soil pressure is 6,000 psf, dead load plus live load.

Measurements of Periods During Construction

Measurements of the natural periods of vibration at different stages of construction of a building can yield important information about the relative effect on the dynamic characteristics of the building of the various elements as they are added to the building. Blume and Binder[53] measured the natural periods of vibration of a fifteen-story steel frame building at twenty stages of its construction. The measurements were made of wind-induced vibrations. As pointed out in Chapter VI, the method of "man-excited" vibrations has several important advantages over wind-excited vibrations. One of the main advantages is that by manually exciting a building at well-chosen points in the building, it is possible to isolate the periods of interest.

Table IV-1 shows the results of period measurements made during the construction of the nine-story steel frame building described above. The results obtained from steady-state resonance tests are listed as well as those obtained from "man-excited" vibrations. It is interesting to note how well the results from the rather simple "man-excited" tests compare with those obtained from the much more complex steady state tests. Table IV-1 shows in considerable detail the changes in periods as building elements are added to the structure. The data could be subjected to an extensive analysis; in the following only the major points of interest will be considered.

Test No. 2, when compared to Test No. 1, shows a decrease in

TABLE IV-1

Period measurements during construction, "man excited" and steady-state tests.

* denotes steady-state tests

Date	Test No.	Additions to building	Translation E-W		Translation N-S		Torsion	
			ω_1 cps	ω_2 cps	ω_1 cps	ω_2 cps	ω_1 cps	ω_2 cps
Jan. 30, 63	1	Steel frame only, 9th & 10th floors not yet in, soil to 1st floor on north side	1.17		.93			
Feb. 15	2	add 9th and 10th floor	1.04		.85		1.02	
March 7	3	Add concrete on columns No. 1 through No. 12 up to 7th floor	1.05	2.86	.86	2.50	1.07	
March 12	4	Add concrete on columns No. 1 through No. 12 up to 9th floor	1.05	2.92	.86	2.50	1.08	
March 16	5	Add concrete on columns No. 1 through No. 12 up to 10th floor	1.03		.87	2.70	1.08	3.54
March 16,17 Vibration exciter A	6*				.86	2.71	1.08	3.52
March 23	7	Add concrete on columns No. 13 through No. 24 up to 3rd floor	1.03	3.01	.87	2.74	1.07	3.50
March 25	8	Add concrete on columns No. 13 through No. 24 up to 4th floor	1.04	3.01	.89	2.77	1.07	3.54
March 28	9	Add concrete on columns No. 13 through No. 24 up to 5th floor	1.04	3.00	.92	2.78	1.09	3.50

TABLE IV-1 CONTINUED

Date	Test No.	Additions to building	Translation E-W		Translation N-S		Torsion	
			ω_1 cps	ω_2 cps	ω_1 cps	ω_2 cps	ω_1 cps	ω_2 cps
April 2	10	Add concrete on columns No. 13 through No. 24 up to 6th floor	1.05	2.90	.94	2.78	1.10	3.50
April 8	11	Add concrete on columns No. 13 through No. 24 up to 8th floor	1.04	2.90	.94	2.80	1.10	3.54
April 18	12	Add concrete on columns No. 13 through No. 24 up to 10th floor. Soil filled in up to 2nd floor on North side, all concrete finished on 10th floor.	1.03	3.02	.95	3.17	1.10	3.80
April 20, 21 Vibration exciter A	13*	Airconditioning ducts in			.97	3.21	1.10	3.72
April 27, 28 Vibration exciter A	14*		1.02	3.00	.96	3.19	1.10	3.76
May 10, 11 Vibration exciters B & C	15*	Fire-proofing material sprayed on all girders and trusses			1.01	3.24	1.09	3.72
May 17, 18 Vibration exciters B & C	16*		1.04	2.95		3.23		3.68
June 21	17	all windows in North side in	1.03	3.02	1.02	3.22	1.07	
Nov 2, 63	18	building ready for occupancy, all partitions, curtain walls, windows in, floors finished. Wire mesh and plaster on inside of all columns.	1.10	3.4	1.14	3.5	1.37	3.8

natural frequency of approximately 10% for the translational motion in the East-West direction as well as in the North-South direction. Since the stiffnesses in the building have not been changed between the two tests, the change in frequency is solely a function of the added masses. The natural frequency is inversely proportional to the square root of the mass of the structure. The 10% decrease in frequency corresponds then to approximately a 20% increase in mass which is in close agreement with the amount of mass which was added in the period between the two tests.

The changes in frequencies occurring between test No. 2 and test No. 12 will give information about how the column concrete affects the effective stiffnesses of the columns. The total mass of the structure was increased by a factor of about 1.45 between the two tests. The natural frequency of translational vibration in the long East-West direction has hardly changed during this interval. Since the natural frequency is proportional to the square root of the ratio of the stiffness of the structure and the mass of the structure, the stiffness must also have been increased by a factor of 1.45. The natural frequency of vibration in the short North-South direction has increased by a factor of 1.1, the addition of column concrete has then caused an increase in effective stiffness of $(1.1)^2 \times 1.45 = 1.75$. It should be noted that this factor cannot be directly attributed to an increase in the moment of inertia of the columns. The trusses connecting the columns in the North-South direction are not of sufficient rigidity so that joint rotation can be neglected. The addition of column concrete will change the relative

rigidities of columns and trusses so the effect of joint rotation will be stronger for test No. 12 than for test No. 2.

A comparison of the results of tests No. 17 and 18 are interesting since the additions to the building in this time interval have consisted essentially of the "non-structural" elements such as partitions, false ceilings, etc. These additions have caused an increase in stiffness represented by the 10% increase in natural frequency of vibration for the North-South direction as well as for the East-West direction. The increase in the torsional frequencies are of considerably larger magnitude, this increase being close to 30%. This can be explained by the fact that the partitions around the staircase sections probably stiffen up the connection between the building and the two staircase sections. For small amplitude vibrations the staircase sections will then add stiffness to the building; this added stiffness will increase the natural frequency of vibration of the translational modes as well as the torsional mode. The torsional frequency will, however, be much more affected on account of the large distance between the staircase sections.

Testing Procedure and Results of the Preliminary Tests

In the initial tests one vibration exciter was installed on the 6th floor. The location is shown in Fig. 4-1. The exciter was located away from the center of the floor so that both translational and torsional modes could be excited. It was known from the "man-excited" tests as described in Chapter VI and also from an approximate analysis of the structure that the 6th floor would be quite close to a nodal point

for the third lowest translational and torsional modes. It was felt, however, that at the relatively high frequencies for these modes the vibration exciter would create enough force output to overcome the difficulties in exciting the modes close to a nodal point. This proved to be a fallacy; it was not possible to excite accurately the third lowest translational mode in the North-South direction nor the third lowest torsional mode. The mode shapes for these two modes, as they were later determined by installing two vibration exciters on the 4th floor are shown in Figs. 4-12 and 4-16. It can be seen that the nodal points are extremely close to the 6th floor.

The main problems in gaining the most information from forced vibration tests are (1) to locate the vibration exciters far enough away from nodal points of the desired modes, (2) to locate the vibration exciters such that interference between the response of modes that have frequencies close together is eliminated. Figure 4-2 shows the frequencies of all the modes excited and the close spacing of some of the modes. There is a close connection between the points mentioned above. With the location of the vibration exciter at the 6th floor, the third lowest translational mode in the North-South direction and the third lowest torsional mode could not be cleanly excited; the response records indicated that not only was the response very small due to the closeness of the exciter to the nodal point, but also that mode interference took place. There was possibly even some interference from the mode in which the floor slabs vibrated as free-free beams. (3) The problems in positioning the response pick-ups correctly so that a clear indication is gained about the type of mode that is being excited. The

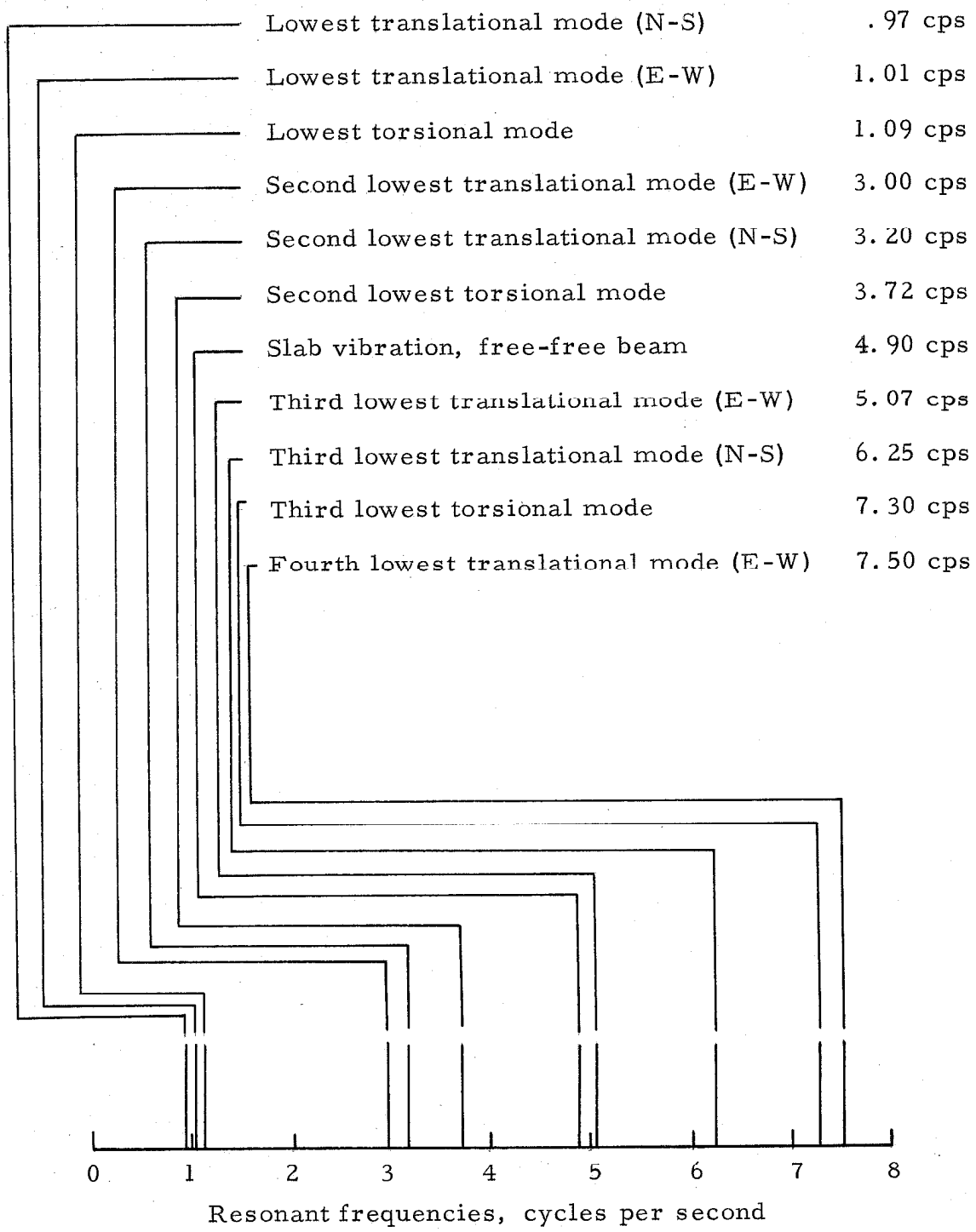

Fig. 4-2 DISTRIBUTION OF RESONANT FREQUENCIES

preliminary tests proved to be an excellent example of the care that should be taken in vibration tests.

In order to locate approximately the frequencies of the modes that could be excited, two accelerometers were placed on one of the floors, one at each end of the building. In exciting the building in the North-South direction it was felt that by noting the phase angle between the two responses, it would be evident from the records at which frequencies the translational modes were excited and at which frequencies the torsional modes were excited. The second lowest translational mode occurred at about 3.2 cps, the responses of the two accelerometers being in phase and equal in magnitude. The second lowest torsional mode occurred at about 3.7 cps, the responses being equal in magnitude with a phase angle of 180° between them. At about 4.9 cps a mode was cleanly excited, the responses of the two accelerometers being in phase and of equal magnitude. At the time this was erroneously considered to be the third translational mode. As the tests progressed and the responses of all the floors were recorded, it became evident that the mode excited at 4.9 cps could not possibly be the third translational mode, since the responses of all floors were in phase. It was then decided to locate all four accelerometers connected to the Sanborn equipment on the 6th floor to explore in more detail the response at the frequency of 4.9 cps. The results are shown in Fig. 4-3c; it is obvious that the floor slab vibrates as a free-free beam. As pointed out later, calculations of the period of vibration of the floor slabs vibrating as free-free beams are in close agreement

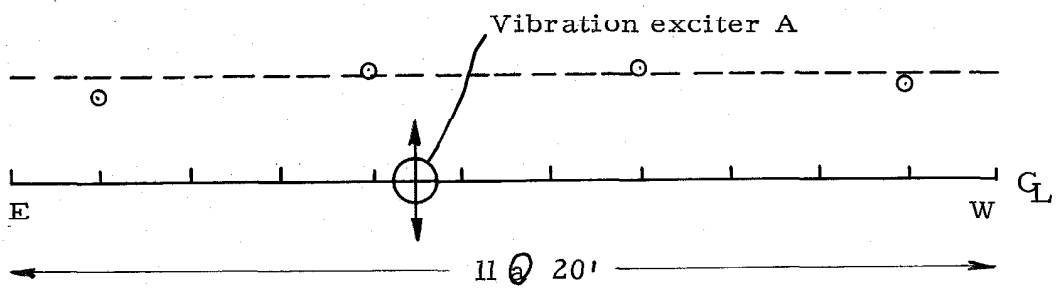

a) Second lowest translational mode (N-S), resonant frequency 3.2 cps

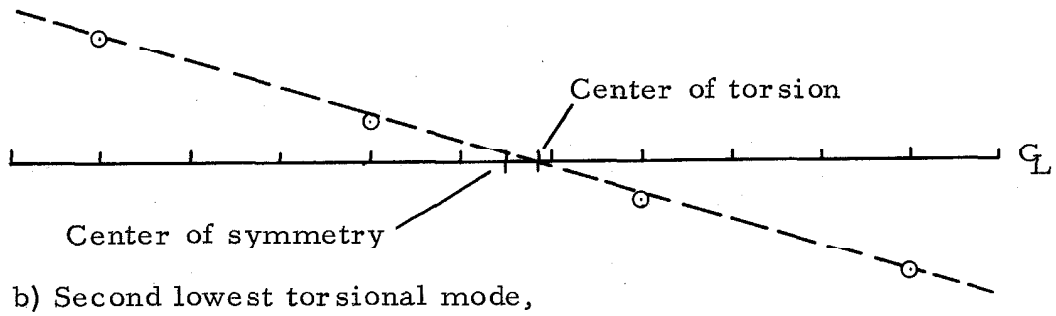

b) Second lowest torsional mode, resonant frequency 3.7 cps

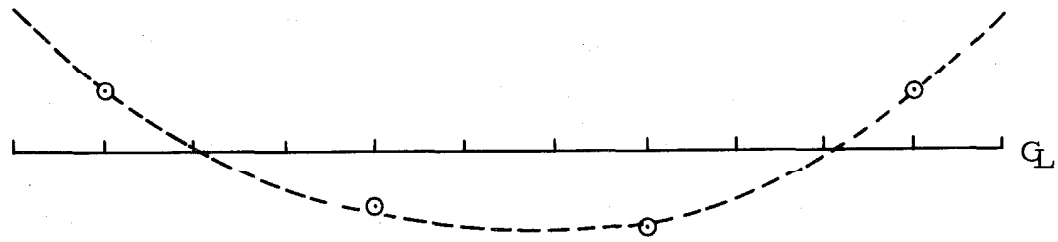

c) Floor slab vibrating as free-free beam, resonant frequency 4.9 cps

Fig. 4-3 MOTION OF 6th FLOOR, VIBRATION EXCITER A

with the experimental results, so this mode of vibration should have been anticipated.

Figure 4-3 shows also the recorded motion of the 6th floor as the translational and torsional modes are being excited at resonance. It is of interest to note that the center of torsion falls very close to the center of symmetry of the building.

Permission was later given to install two additional vibration exciters. The results of the preliminary tests were used in locating the vibration exciters so that the missing modes could be excited. Vibration exciters B and C were located as shown in Fig. 4-1 on the 4th floor. The 4th floor location was dictated by the fact that the component of the 4th floor of the mode shapes for the third lowest translational and torsional modes would be relatively large. In order to eliminate any possible interference from the mode in which the floor slabs vibrate as free-free beams, the vibration exciters B and C were located as close as practically possible to the nodes of this motion. It is clear from Fig. 4-3c that each of the vibration exciters should be positioned at a distance of close to 40 feet from the end of the building. With these positions of the vibration exciters it was possible to excite cleanly the third lowest translational and torsional modes.

The instrumentation systems used were the same as those described in Chapter III. Since only six simultaneous records of acceleration could be obtained, it was necessary in order to determine mode shapes to repeat each of the tests. In all the tests one accelerometer was kept in the same position for the two tests required to determine the complete mode shape. This was done for two reasons.

First, it would give information about the repeatability of the two tests; it would also give information whether the tests in any way affected the dynamic characteristics of the building. As shown in Chapter III this indeed was the case for the five-story reinforced concrete building. In the tests of the nine-story steel frame building as reported in this Chapter, the response stayed quite constant from one test to the next test conducted at the same force level even in cases where the building had been excited at higher force levels in between the two similar tests.

Translational Motion in the Long East-West Direction of the Building

In this direction four modes were excited. The natural frequencies are ω_1=1.01 cps; ω_2=3.00 cps; ω_3=5.07 cps and ω_4=7.50 cps. It can be seen that the ratios of frequencies are very close to the 1 : 3 : 5 : 7 theoretical ratios for the vibration of a uniform shear beam. The mode shapes for the four experimentally determined modes are shown in Fig. 4-8. Most of the modes were excited at a number of force levels. It was found that all mode shapes stayed constant regardless of level of force excitation. Similarly it was found that for all of the four modes all the floors experienced their maximum response at the same frequency. For each of the modes excited it was also evident that the shape of the response curve close to the resonant frequency was the same regardless of which floor response was used in plotting the response curve.

Figure 4-4 shows the response of the 5th floor as the structure is being excited at and close to the natural frequency. It is evident

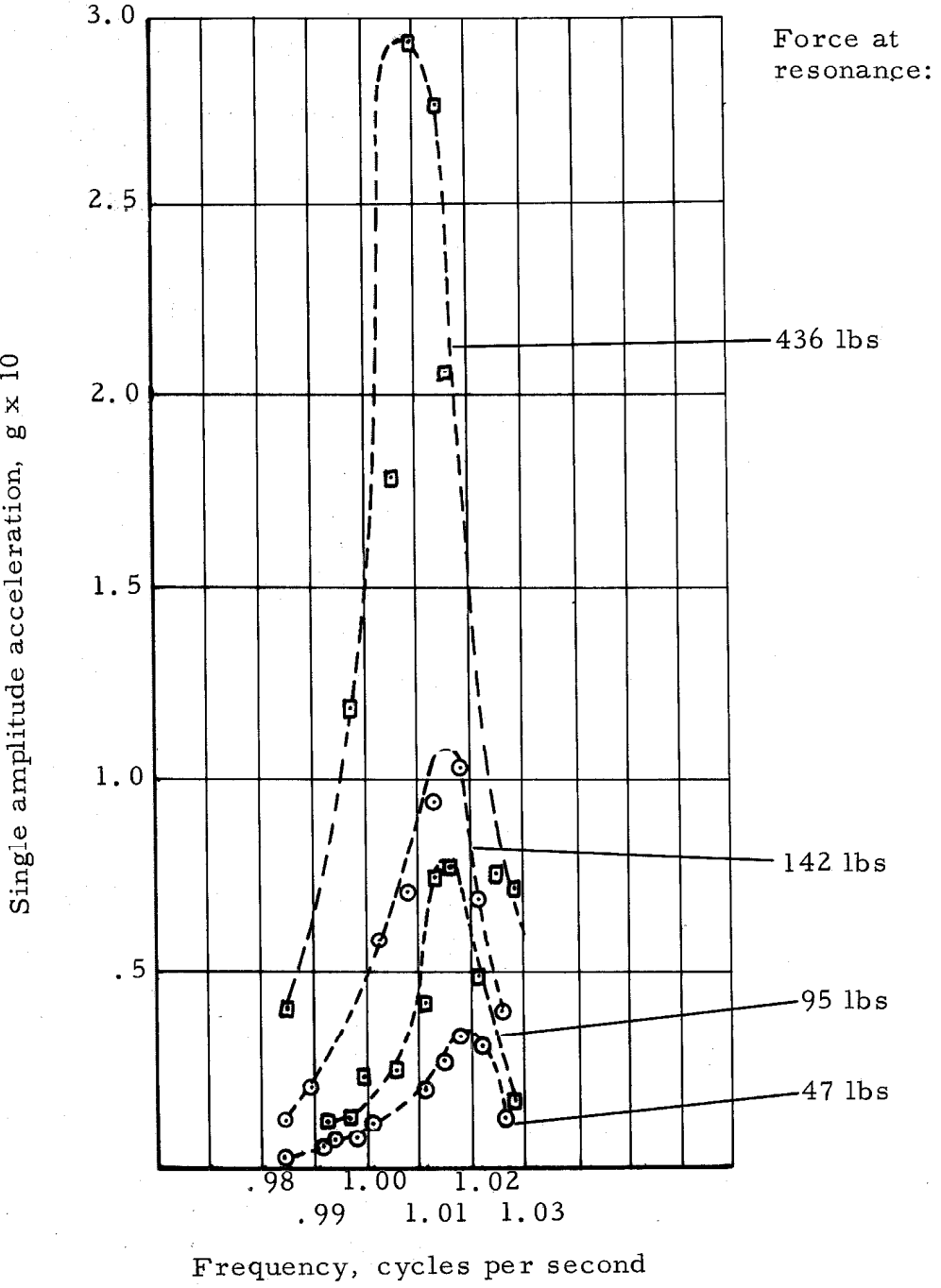

Fig. 4-4 5th FLOOR RESPONSE, LOWEST TRANSLATIONAL MODE (E-W), VIBRATION EXCITER A.

that the damping is very small; all the measurable responses are contained within a range of only about 0.04 cps. The response curves clearly indicate the extreme accuracy of the speed control necessary to precisely define the response curve. Figure 4-4 shows a slight tendency of a decrease in natural frequency as the force level is increased, except for the test in which the force at resonance is 142 lbs. The response curve from this test could well be inaccurately determined for the following reason. It was found that on account of the very low amount of damping in this mode that extraordinary care had to be taken in recording the response. It was necessary to wait for several minutes before taking records after the exciters were set at a specific frequency. As pointed out in Chapter V, the transient vibrations from the prior excitation took that long to damp and leave only the true steady-state response from the presently excited frequency. By running the recorders for a sufficiently long time at each frequency of excitation, it was possible to detect this interference, since the records showed clearly a typical series of "beats". Also, by running recorders for a sufficiently long period of time it was possible to detect whether the true steady-state response was obtained as indicated by the absence of "beats" on the records. The mode shape for the lowest mode is shown in Fig. 4-8; it is very close in appearance to that of a uniform shear beam.

Figure 4-5 shows the response of the second lowest mode. Again in this case a small non-linear effect is noticeable since the resonant frequency decreases slightly as the force level is increased.

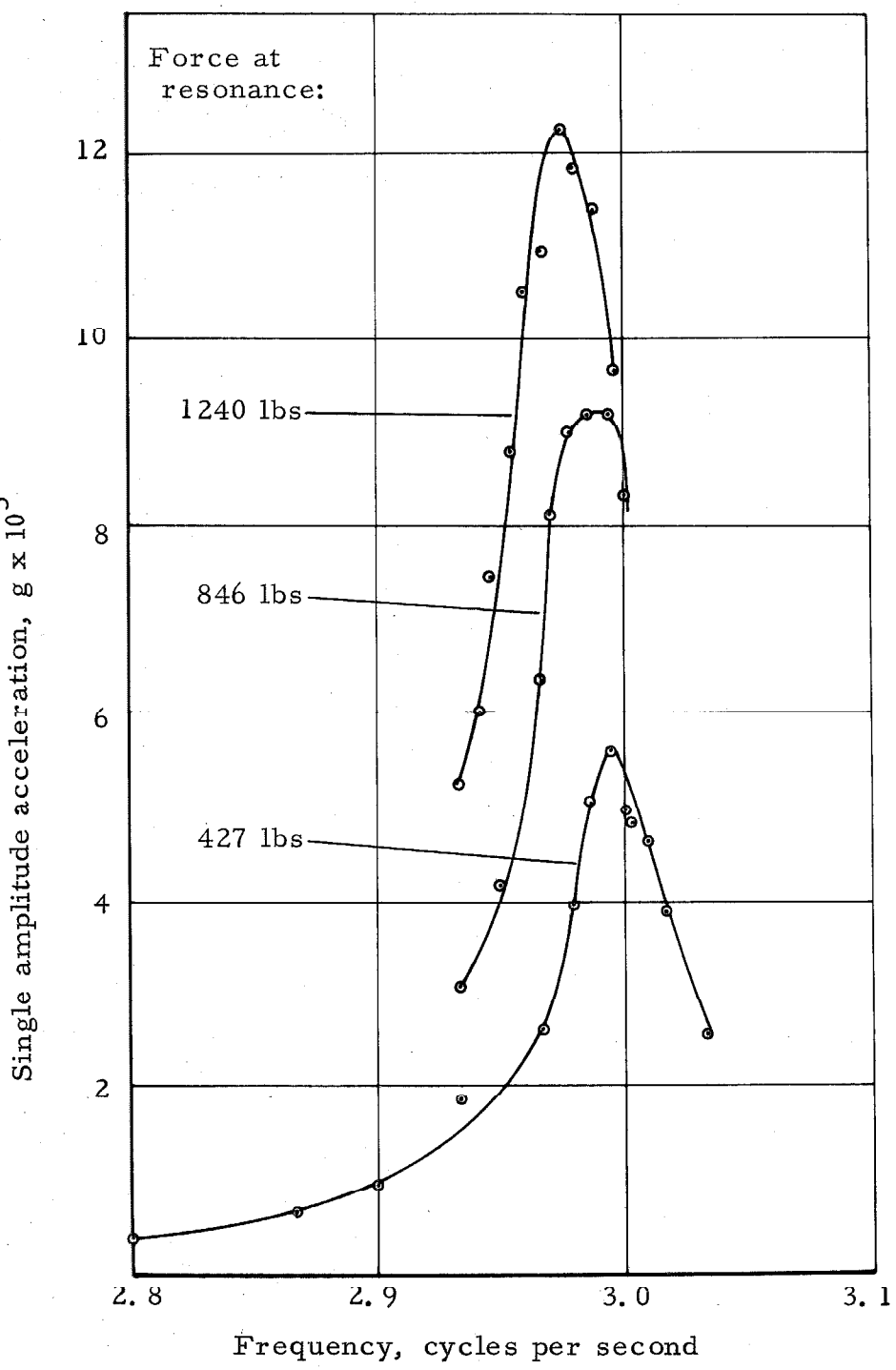

Fig. 4-5 5th FLOOR RESPONSE, SECOND LOWEST TRANSLATIONAL MODE (E-W), VIBRATION EXCITER A.

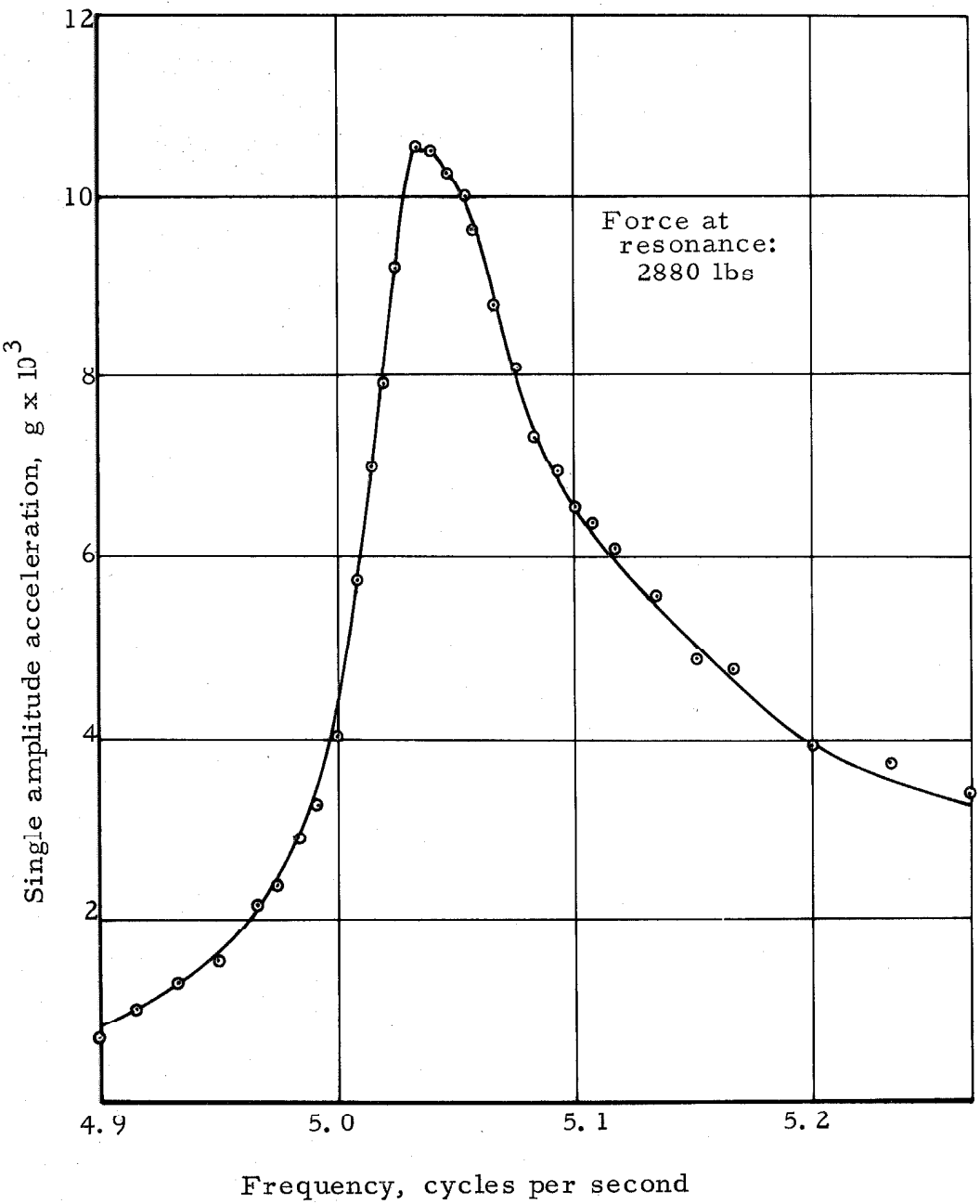

Fig. 4-6 3^{rd} FLOOR RESPONSE, THIRD LOWEST TRANSLATIONAL MODE (E-W), VIBRATION EXCITERS B AND C.

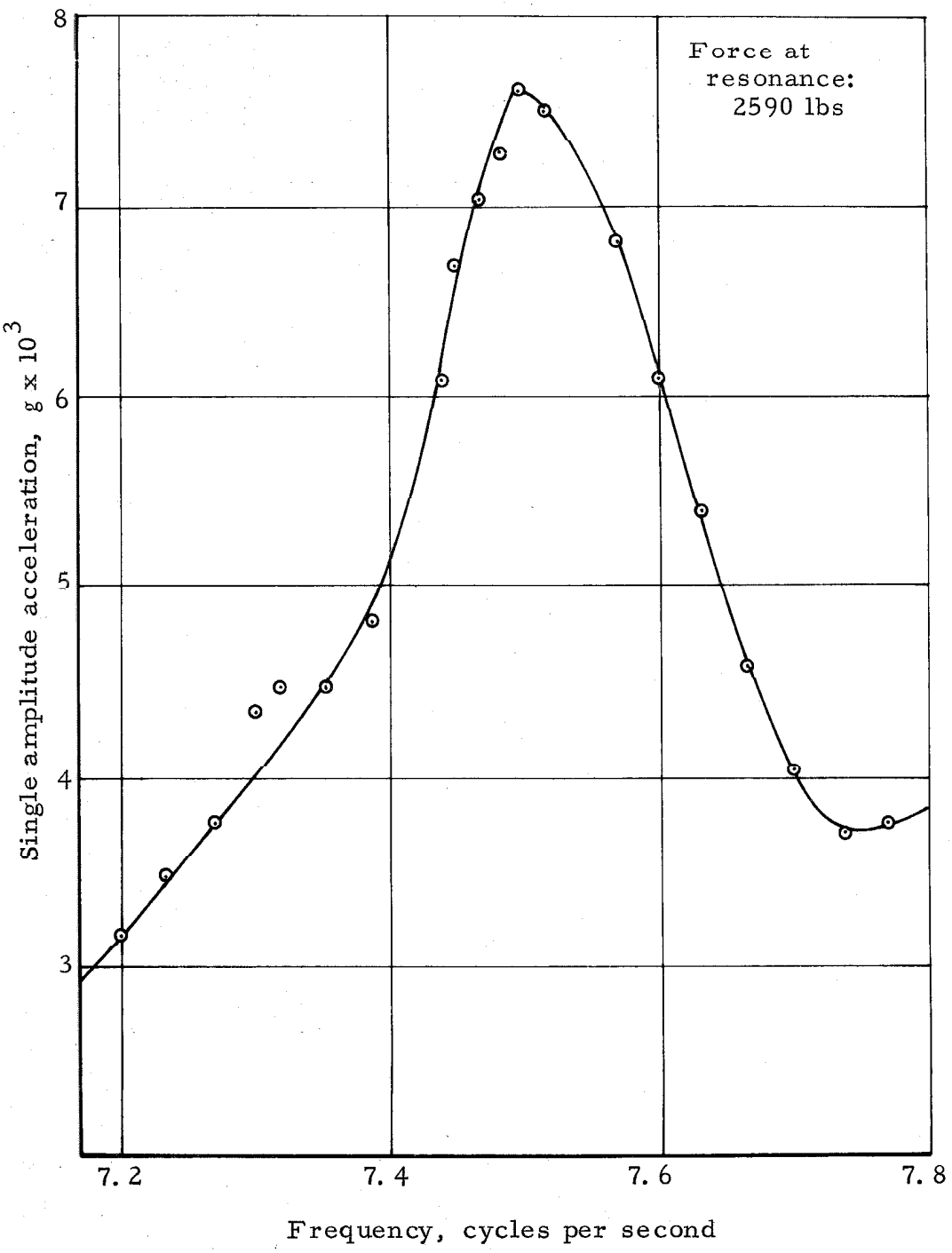

Fig. 4-7 3rd FLOOR RESPONSE, FOURTH LOWEST TRANSLATIONAL MODE (E-W), VIBRATION EXCITER A.

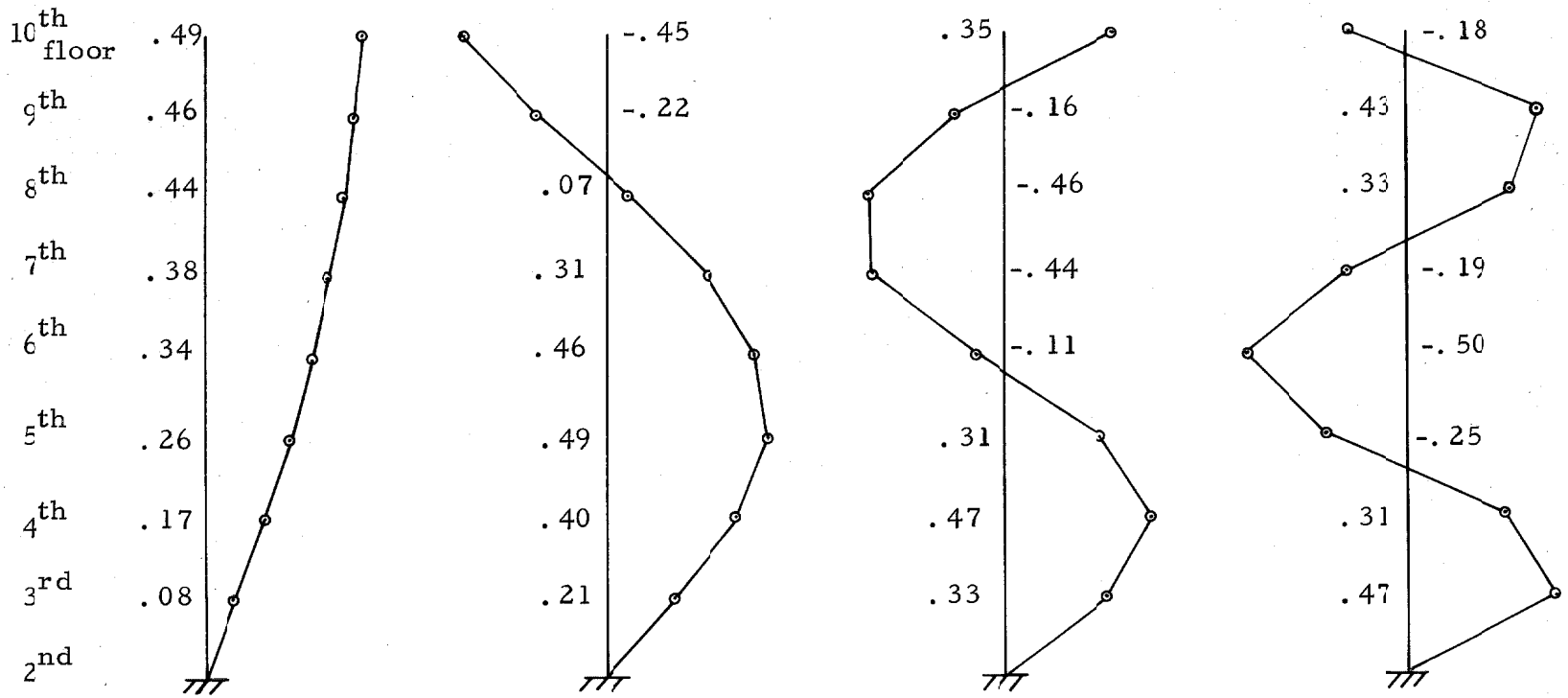

ω_1 = 1.01 cps
β_1 = .55%

ω_2 = 3.00 cps
β_2 = .85%

ω_3 = 5.07 cps
β_3 = 2.0%

ω_4 = 7.50 cps
β_4 = 3.6%

Fig. 4-8 MODE SHAPES, TRANSLATION (E-W).

The behavior is typically that of a "softening" spring.

The response curves for the third lowest and the fourth lowest mode are shown in Figs. 4-6 and 4-7. The mode shapes are shown in Fig. 4-8. It should be noted that all the response curves show single amplitude acceleration versus frequency, and the exciting force is proportional to the frequency squared.

Determination of the Stiffness Matrix

The mode shapes and the natural frequencies of the four experimentally determined modes of translational vibrations in the long East-West direction are shown in Fig. 4-8. As shown in Chapter II, the stiffness matrix can be determined from

$$[K]\{\psi^{(r)}\} = [M]\{\psi^{(r)}\}\omega_r^2 \qquad (2.67)$$

For each of the experimentally determined modes one equation of this form is available while Eq. 2.67 expresses as many equations as the system has degrees of freedom. In the present case four modes were experimentally determined in an eight degree of freedom system, so a total of 32 equations are available to determine the elements of the stiffness matrix. The girders in the long East-West direction of the building are sufficiently rigid to make the effect of joint rotation negligible. The mathematical model of the building can then be represented by a simply coupled system, i.e., a system in which the stiffness matrix $[K]$ is tridiagonal, the elements of each row (or column) being interrelated. The stiffness matrix would contain

8 unknown elements, namely the spring factors connecting each mass to the adjacent masses. The stiffness matrix could also be looked upon as representing a close coupled system, i. e., tridiagonal with no assumed interrelation between the elements of each row (or column). It is in this case of interest to see from the results of the calculations whether the elements of each row (or column) are in fact interrelated.

As shown in Chapter II the above Eq. 2.67 can be written in the following form:

$$\frac{1}{\omega_r^2}\left[A^{(r)}\right]\{k\} = \left[M\right]\{\psi^{(r)}\} \qquad (r=1, 2, 3, 4) \qquad (2.101)$$

In this equation $\left[A^{(r)}\right]$ contains elements from the known mode shapes and $\{k\}$ represents the unknown elements of the tridiagonal stiffness matrix. Since symmetry of the stiffness matrix is assumed, $\{k\}$ will in the present case contain 15 elements. The equations are in the form

$$\left[A\right]\{y\} = \{b\} \qquad (2.72)$$

There are 32 equations and 15 unknowns to determine. Performing the least squares fit by premultiplying Eq. 2.72 by $\left[A\right]^T$ and after solving the resulting system of equations, the results expressed in the form of $\left[K\right]$ are

$$[K] = \begin{bmatrix} 7488 & -3483 & 0 & 0 & 0 & 0 & 0 & 0 \\ -3483 & 7233 & -3606 & 0 & 0 & 0 & 0 & 0 \\ 0 & -3606 & 7016 & -3493 & 0 & 0 & 0 & 0 \\ 0 & 0 & -3493 & 7137 & -3914 & 0 & 0 & 0 \\ 0 & 0 & 0 & -3914 & 7494 & -3373 & 0 & 0 \\ 0 & 0 & 0 & 0 & -3373 & 6188 & -3045 & 0 \\ 0 & 0 & 0 & 0 & 0 & -3045 & 6101 & -2909 \\ 0 & 0 & 0 & 0 & 0 & 0 & -2909 & 2896 \end{bmatrix} \frac{\text{kips}}{\text{in}} \qquad (4.1)$$

No assumption was made concerning any interrelation between the elements of each row (or column). Still, it is evident that for each of the rows (or columns) the sum of the absolute values of the off-diagonal terms is quite close to the value of the diagonal term. In the "pure shear" building with no joint rotation these sums would be exactly equal. The small differences in the stiffness matrix expressed in Eq. 4.1 probably stem from inaccuracies in the data.

The stiffness matrix of Eq. 4.1 was determined from 32 equations containing 15 unknown elements. There will be both random and systematic errors in the original data rendering inconsistencies in the equations. Some idea about the magnitudes of these inconsistencies can be obtained by substituting the values of $\{k\}$ back into the original Eq. 2.72. The results are

$$[A]\{y\} = \begin{Bmatrix} .19 \\ .36 \\ .63 \\ .63 \\ .90 \\ 1.06 \\ 1.09 \\ 2.03 \\ .51 \\ 1.12 \\ 1.10 \\ 1.02 \\ .81 \\ .16 \\ -.70 \\ 1.86 \\ .83 \\ 1.12 \\ .86 \\ -.15 \\ -1.30 \\ -.87 \\ -.59 \\ 1.46 \\ 1.09 \\ .67 \\ -.50 \\ -.87 \\ -.26 \\ .61 \\ .96 \\ -.79 \end{Bmatrix} \qquad \{b\} = \begin{Bmatrix} .19 \\ .41 \\ .62 \\ .81 \\ .91 \\ 1.05 \\ 1.10 \\ 2.03 \\ .50 \\ .95 \\ 1.17 \\ 1.10 \\ .74 \\ .17 \\ -.52 \\ 1.87 \\ .79 \\ 1.12 \\ .74 \\ -.26 \\ -1.05 \\ -1.10 \\ -.38 \\ 1.45 \\ 1.12 \\ .74 \\ -.60 \\ -1.19 \\ -.45 \\ .79 \\ 1.03 \\ -.75 \end{Bmatrix}$$

Considering that the solutions stem from 32 equations in only 15 unknowns, the errors are reasonably small. It is possible to gain a better physical picture of the errors involved. The stiffness matrix expressed in Eq. 4.1 represents a model of the structure determined from a knowledge of some of the experimentally determined modal properties of the structure. Knowing the mass matrix and using the stiffness matrix of Eq. 4.1, the natural frequencies and mode shapes can be determined as explained in Chapter II. The frequencies and mode shapes can then be compared to the experimentally determined frequencies and mode shapes that were used in the determination of the stiffness matrix. The comparison will give a good indication of how well the determined model represents the actual structure. The results are listed in Table IV-1.

TABLE IV-1

Frequencies and Mode Shapes
Translation (E-W)

	Experimentally determined				Determined from $[K]$ of Eq. 4.1			
Frequency cps	1.01	3.00	5.07	7.50	.99	3.02	5.12	7.00
Mode	1	2	3	4	1	2	3	4
10^{th} floor	.49	-.45	.35	-.18	.49	-.47	.32	-.23
9	.46	-.22	-.16	.43	.46	-.22	-.15	.40
8	.44	.07	-.46	.33	.44	.06	-.49	.42
7	.38	.31	-.44	-.19	.38	.30	-.40	-.17
6	.34	.46	-.11	-.50	.34	.46	-.09	-.48
5	.26	.49	.31	-.25	.26	.48	.32	-.16
4	.17	.40	.47	.31	.17	.38	.50	.36
3	.08	.21	.33	.47	.08	.20	.35	.44

Table IV-1 shows a reasonably close agreement between the natural frequencies and mode shapes of the model and those determined experimentally.

The stiffness matrix expressed in Eq. 4.1 is a "best" determination in the sense that all the available data was used. It is of some interest to see how well the stiffness matrix would be determined if only part of the available data was used in the determination of $[K]$. For instance, in the preliminary tests it was not possible to obtain any information about the third lowest mode, so it would be of interest to see how well the stiffness matrix determined by using modes 1, 2 and 4 would compare with the "best" stiffness matrix obtained by using modes 1, 2, 3 and 4. The results for a number of combinations of modes are shown in Table IV-2.

In Table IV-2 the individual story stiffnesses can be read off as follows; k_{12} is the stiffness between the 2nd and the 3rd floor, k_{23} is the stiffness between the 3rd floor and the 4th floor, etc. In general it can be seen that in all the cases where three of the experimentally determined modes are used the stiffnesses are rather close to the "best" determined stiffnesses. In the cases where only two experimentally determined modes are used in the calculations, some rather large discrepancies start showing up. For example, in using modes 1 and 2 k_{23} is almost 20% lower than the "best" value of k_{23}. In using modes 1 and 4 k_{45} and k_{67} are much higher than the corresponding values as determined from modes 1, 2, 3 and 4.

TABLE IV-2

Non-zero elements of stiffness matrix, kips/in

Translation East-West

Experimentally determined modes	k_{11}	k_{12}	k_{22}	k_{23}	k_{33}	k_{34}	k_{44}	k_{45}	k_{55}	k_{56}	k_{66}	k_{67}	k_{77}	k_{78}	k_{88}
1, 2, 3, 4	7486	-3483	7233	-3606	7016	-3493	7137	-3914	7494	-3373	6188	-3045	6101	-2909	2896
1, 2, 3	7084	-3291	6760	-3351	6609	-3307	6748	-3693	7063	-3169	5904	-2941	5936	-2847	2838
1, 2, 4	7627	-3549	7270	-3609	7295	-3706	7687	-4262	7980	-3521	6329	-3058	6263	-3049	3026
1, 3, 4	7577	-3527	7536	-3787	7098	-3468	6757	-3593	7954	-4019	7525	-3794	6824	-2917	2902
1, 2	7260	-3373	6329	-3040	6452	-3344	7030	-3920	7366	-3254	5948	-2931	6041	-2969	2953
1, 4	7724	-3595	7721	-3887	6904	-3270	9076	-5809	11300	-5201	12892	-7961	10492	-2624	2627
1, 3	7109	-3304	7057	-3540	6623	-3227	6134	-3200	5615	-2299	5886	-3645	6637	-2874	2862

Experimentally Determined Stiffnesses Compared With Calculated Stiffnesses

The stiffnesses determined by the use of all four experimentally determined modes can be seen in Table IV-2. The stiffnesses decrease in magnitude from the top of the building down, except for k_{45} which has a larger value than the stiffness k_{34}. Theoretically, k_{45} and k_{34} should be equal. The stiffness between the 5th floor and the 6th floor is represented by k_{45} and k_{34} represents the stiffness between the 4th and the 5th floor. The column size stays constant between the 4th floor and the 6th floor so there is no apparent reason why k_{45} should be larger than k_{34}.

The forces transmitted from the floors to the columns do not act through the centroids of the column sections since the column concrete is so heavily concentrated towards the outside of the steel columns. As the floors vibrate the columns will be acted upon by a twisting moment as well as a translational force. The increase in stiffnesses of the steel columns by the addition of the concrete to the columns was earlier shown to be approximately 45%. Let the known moment of inertia of the steel columns be increased by 45% and the stiffness of any story can be expressed as

$$k = \sum \frac{12E\, I_{st} \times 1.45}{L^3}$$

where the summation extends over all the columns. The calculated results show a reasonable agreement with the experimentally determined stiffnesses. For example, consider the stiffness between the 7th floor

and the 8th floor. From Table IV-2 this stiffness is found to be 3373 kips/in. The moment of inertia of the steel column is 473 in^4, Let $E_{steel} = 30 \times 10^3$ ksi and let the effective story height L be considered unknown. Extending the summation over the 24 columns the above equation takes the form

$$3374 = 24 \frac{12 \times 30 \times 10^3 \times 473 \times 1.45}{L^3}$$

or L, the effective story height, is found to be 10 feet. The distance between the floors is equal to 14 feet, while the "free" height from top of girder to bottom of the girder above is equal to 7-1/2 feet. The effective story height is seen to be closer to the "free" height between stories than to the distance between floor slabs.

Determination of Damping Values

As shown in Chapter II the values of damping can be found from the acceleration response at resonance. The values of damping for the lowest translational mode are shown in Table IV-3. In this table the acceleration amplitude ratios and the force ratios are shown as well. All of these values follow directly from Fig. 4-4.

TABLE IV-3

Damping at different force levels, lowest translational mode (E-W)

Damping %	.5	.5	.5	.6
Force ratios	1	1.98	2.98	9.15
Response ratios	1	2.25	2.9	8.4

It can be seen that there is only a slight indication of an increase in damping as the force level increases. A determination of the damping from the width of the response curves in Fig. 4-4 yields almost identical results.

Table IV-4 shows the damping values obtained from the response at resonance for the second lowest translational mode. The values listed follow from Fig. 4-5.

TABLE IV-4

Damping at different force levels,
Second lowest translational mode (E-W)

Damping %	.8	1.0	1.1
Force ratios	1	1.98	2.9
Response ratios	1	1.65	2.2

The values in Table IV-4 seem to indicate a definite increase in damping as the force level is increased.

The value of damping for the third lowest translational mode was found to be 2.0% and the damping in the fourth lowest translational mode was found to be 3.6%. These values were determined from the peak response values. It is of interest to note that by using the width of the response curve in determining the value of damping in the fourth lowest translational mode, a damping value of only 1.5% is found. The response curve shown in Fig. 4-7 gives an indication of the reason for the large difference in results. At frequencies higher than the resonant frequency the response is clearly affected by the next higher

mode. This interference will affect the peak response value less than it will the responses at the higher frequencies leading to a much less accurate determination of the damping value from the width of the response curve.

Determination of the Damping Matrix $[C]$

As shown in Chapter II, the damping matrix can be determined from the following equation

$$[C]\{\psi^{(r)}\} = [M]\{\psi^{(r)}\}\ 2\beta_r\ \omega_r \qquad (2.68$$

$$(r=1, 2, 3, 4)$$

The mode shapes and the values of damping to be used in the determination of $[C]$ are listed in Fig. 4-8. Assuming a close coupled system, i.e., a tridiagonal matrix with no interrelation between the elements of each row (or column) a total of 32 equations are available to determine the 15 unknown elements of $[C]$. After performing the least squares fit and solving the resulting set of equations, the results in the form of $[C]$ are:

$$[C] = \begin{bmatrix} 9.48 & -4.42 & 0 & 0 & 0 & 0 & \\ -4.42 & 8.49 & -4.13 & 0 & 0 & 0 & 0 \\ 0 & -4.13 & 7.79 & -3.78 & 0 & 0 & 0 \\ 0 & 0 & -3.78 & 7.57 & -4.04 & 0 & 0 \\ 0 & 0 & 0 & -4.04 & 7.60 & -3.30 & 0 \\ 0 & 0 & 0 & 0 & -3.30 & 6.09 & -2.94 \\ 0 & 0 & 0 & 0 & 0 & -2.94 & 6.13 \\ 0 & 0 & 0 & 0 & 0 & 0 & -2.96 \end{bmatrix} \begin{matrix} \\ \\ \\ \\ \\ \\ -2.96 \\ 3.06 \end{matrix} \quad \frac{\text{kips-sec}}{\text{in}}$$

It is of interest to note that no assumption was made as to any interrelation between the elements of each row (or column). Nevertheless, it can be seen that for each row the sum of the absolute values of the off diagonal terms is very close to the value of the diagonal term. This is an interesting point since this interrelation was not evident in the damping matrix determined in Chapter III for the five-story reinforced concrete building. For that building the conclusion was that the model of the structure should be represented as having "absolute dashpots" as well as "relative dashpots". In the present case the conclusion is that the model of the structure should have only inter-floor dashpots.

This difference in results obtained from the tests of the five-story reinforced concrete building and those obtained from the nine-story steel frame building is also evident from the fact that in the tests of the five-story reinforced concrete building the damping values of the lowest and the second lowest translational mode were almost identical. Figure 4-8 shows clearly how the damping values found for the nine-story steel frame building increase almost linearly with increasing frequencies.

The damping matrix shown above is a "best" determination since all the available data was used in its determination. Again here, as it was done in the case of the stiffness matrix, the damping matrix has been calculated using a number of combinations of the experimentally determined modes. The results are shown in Table IV-5. Again in this case it is evident that by using any three of the

TABLE IV-5

Non-zero elements of damping matrix, kips-sec/in

Translation East-West

Experimentally determined modes	c_{11}	c_{12}	c_{22}	c_{23}	c_{33}	c_{34}	c_{44}	c_{45}	c_{55}	c_{56}	c_{66}	c_{67}	c_{77}	c_{78}	c_{88}
1, 2, 3, 4	9.47	-4.42	8.49	-4.13	7.79	-3.78	7.57	-4.04	7.60	-3.30	6.09	-2.94	6.13	-2.96	3.06
1, 2, 3	7.65	-3.53	7.03	-3.43	6.78	-3.35	6.77	-3.62	6.82	-2.95	5.54	-2.70	5.65	-2.73	2.84
1, 2, 4	9.69	-4.52	8.14	-3.86	7.28	-3.51	7.19	-3.88	7.27	-3.14	5.72	-2.72	5.74	-2.79	2.90
1, 3, 4	10.50	-4.87	10.18	-5.06	9.29	-4.45	8.67	-4.57	10.83	-5.68	10.23	-4.93	8.96	-3.82	3.88
1, 2	5.85	-2.67	5.11	-2.41	5.21	-2.65	5.67	-3.11	5.94	-2.58	4.81	-2.31	4.89	-2.36	2.50
1, 4	11.75	-5.45	11.75	-5.90	10.56	-5.00	13.79	-8.77	17.10	-7.85	19.32	-11.84	15.74	-3.99	4.04
1, 3	8.85	-4.09	8.78	-4.38	8.25	-3.99	7.64	-3.96	7.02	-2.86	7.35	-4.51	8.27	-3.55	3.63

experimentally determined modes the elements of the resulting damping matrix will be reasonably close in value to the "best" determined elements.

Translational Motion in the Short North-South Direction

In the short North-South direction, the trusses give very little rigidity to the floor system. The joints are only restrained against joint rotation to a very small degree. It was shown in Chapter II that far coupling resulted when the girders were not of sufficient rigidity to prevent joint rotation. For an n-degree of freedom system, the matrix would contain $n(n+1)/2$ unknown elements. If s modes are determined experimentally sn equations are available to determine the unknowns. In case the number of unknowns exceeds the number of equations, no unique solution exists.

In the short North-South direction it was only possible to excite the three lowest translational modes due to the frequency limitations of the vibration exciters. A total of $3 \times 8 = 24$ equations are then available to determine the $8 \times \frac{9}{2} = 36$ unknowns and no unique solution exists. It is obvious from physical considerations that the elements farthest away from the diagonal elements will be of the smallest absolute value. It was felt that by treating the stiffness matrix as a five diagonal matrix, it would be possible to get a somewhat reasonable approximation to the complete matrix. This proved not to be the case. By assuming the stiffness matrix to be five diagonal, the matrix will contain 21 unknown elements; since 24 equations are available from the three modes determined, it is possible to solve the resulting set of equations by

using the least squares procedure previously described. The resulting stiffness matrix did not make physical sense. For instance, some of the off-diagonal terms were larger in magnitude than the corresponding diagonal terms. This of course cannot occur in a passive system with positive stiffnesses. The best approach to the problem of finding the stiffness matrix and the damping matrix in such cases where the number of unknowns exceeds the number of equations would probably be a trial and error procedure. Starting with a stiffness matrix calculated from a knowledge of the structure, without much regard to the experimentally determined frequencies and mode shapes, it might be possible by making successive changes in the assumed stiffnesses to approximate reasonably well the experimentally determined frequencies and mode shapes. These problems could well deserve some future attention.

The resonant frequencies of the three lowest translational modes were found from steady-state tests to be ω_1=0.97 cps; ω_2=3.20 cps and ω_3=6.25 cps. The ratios are approximately 1 : 3.2 : 6.25. It is interesting to compare the ratios to those found from the three lowest translational modes in the long East-West direction. These were 1 : 3.0 : 5.1 or very close to those of a uniform shear beam.

Figure 4-9 shows the 9th floor response of the lowest translational mode as the structure is being excited at a number of force levels. The values of damping as determined from the peak responses are shown in Table IV-6.

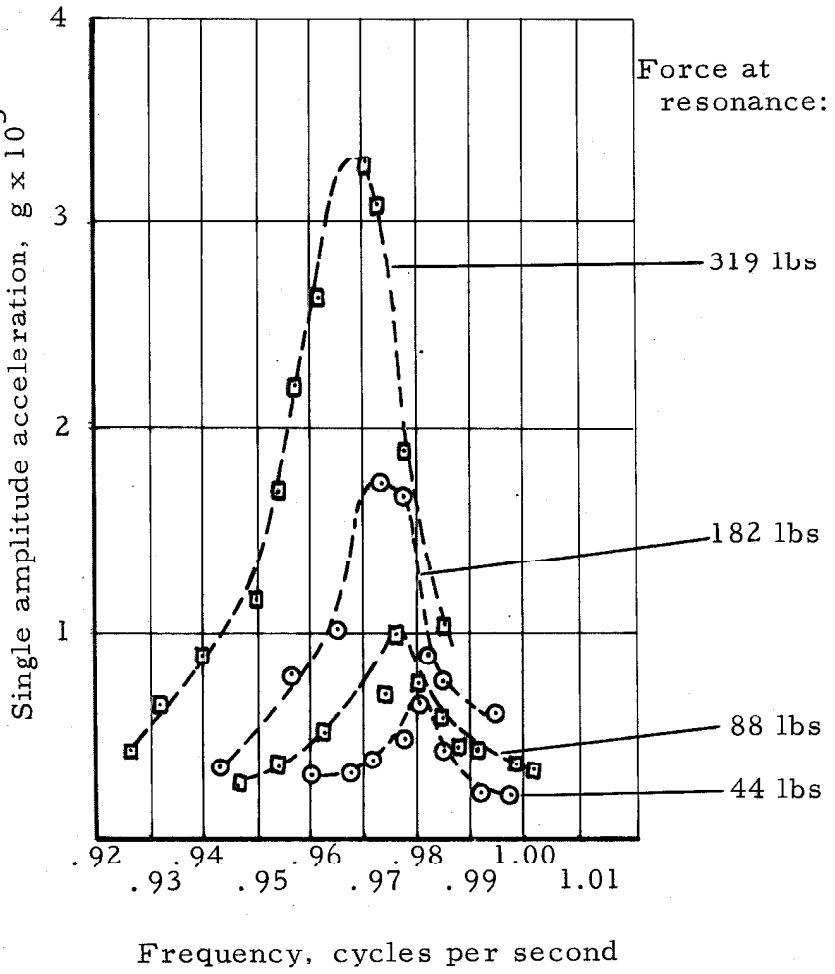

Fig. 4-9 9^{th} FLOOR RESPONSE, LOWEST TRANSLATIONAL MODE (N-S), VIBRATION EXCITER A.

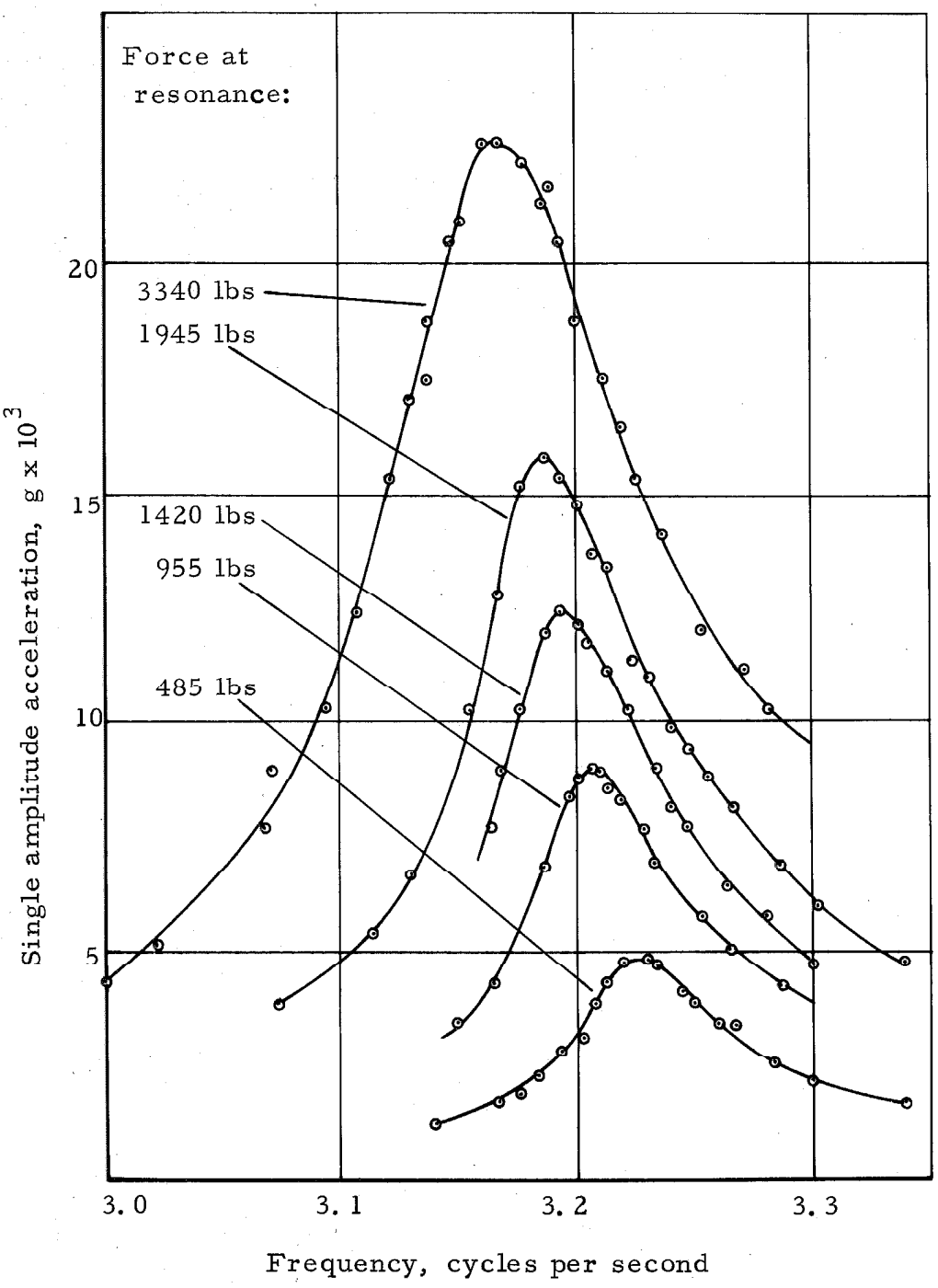

Fig. 4-10 6^{th} FLOOR RESPONSE, SECOND LOWEST TRANSLATIONAL MODE (N-S), VIBRATION EXCITER A.

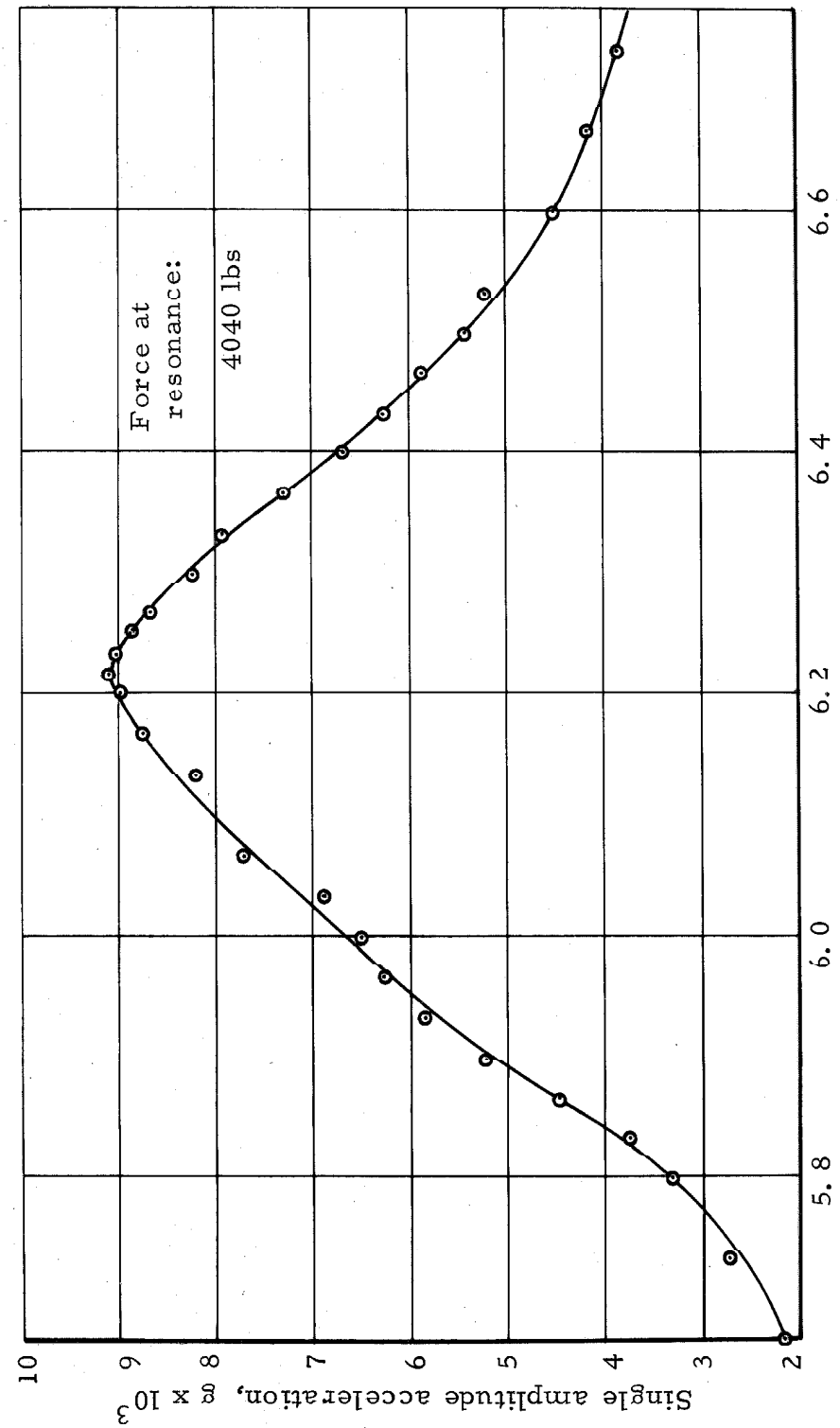

Fig. 4-11 3^{rd} FLOOR RESPONSE, THIRD LOWEST TRANSLATIONAL MODE (N-S), VIBRATION EXCITERS B AND C.

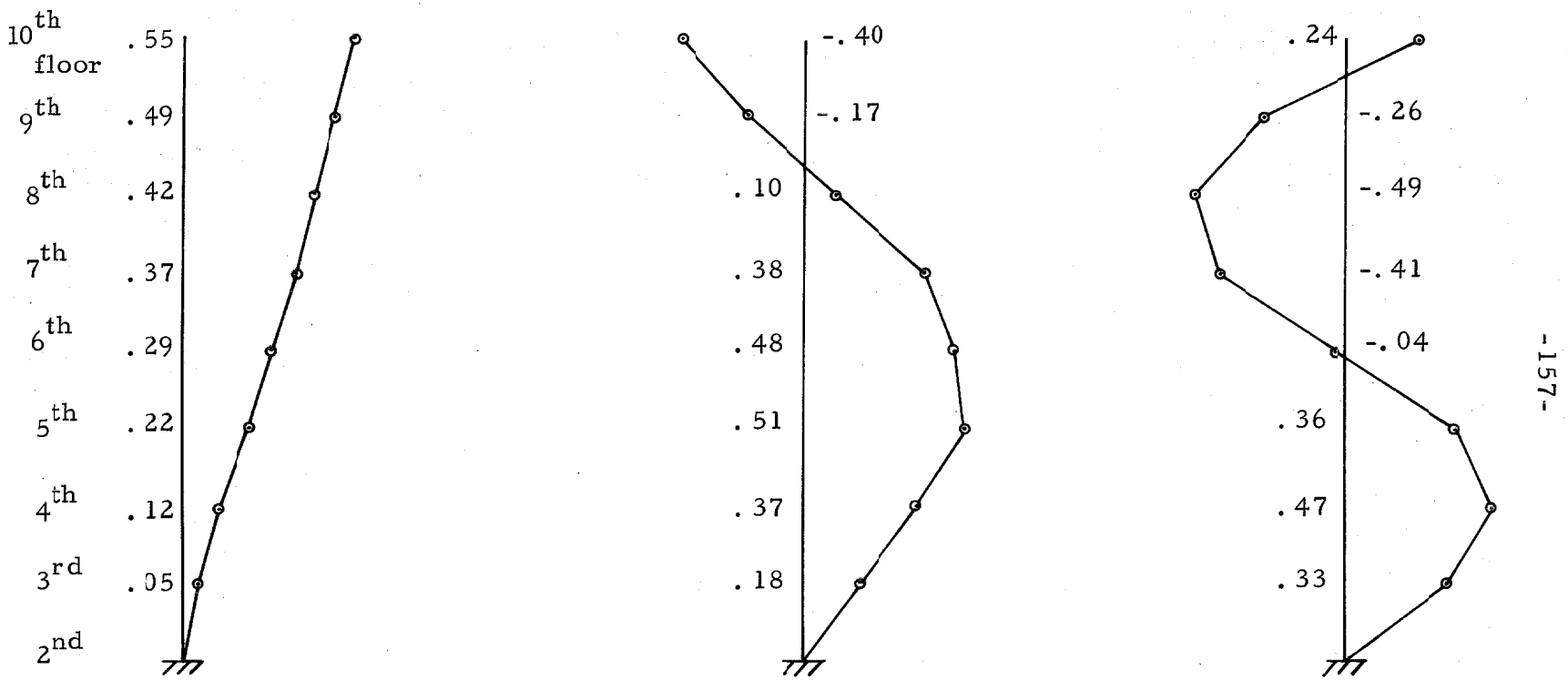

ω_1 = . 97 cps
β_1 = . 6%

ω_2 = 3. 20 cps
β_2 = 1. 3%

ω_3 = 6. 25 cps
β_3 = 3. 7%

Fig. 4-12 MODE SHAPES, TRANSLATION (N-S).

TABLE IV-6
Damping at different force levels,
lowest translational mode (N-S)

Damping %	.4	.5	.6	.6
Force ratios	1	2	4.13	7.25
Response ratios	1	1.53	2.66	5.1

A slight increase in damping as the force level is increased is seen from Table IV-6.

Figure 4-10 shows the 6th floor response as the structure is being excited at various force levels in its second lowest translational mode. The response curves show a well-defined shift in resonant frequency as the force level is increased. This shift in frequency is typically that of a softening spring. The shift in resonant frequency from the lowest to the highest level of force excitation is approximately 2%; this would then correspond to a 4% change in stiffness between these two levels of excitation. The values of damping as determined from the peak responses are shown in Table IV-7. A slight but very systematic trend for the damping values to increase as the force level increases can be seen from Table IV-7.

The 3rd floor response of the third lowest translational mode is shown in Fig. 4-11. All the mode shapes, frequencies and damping values are listed in Fig. 4-12. It can be seen that the value of damping increases almost linearly with the increase in frequency.

TABLE IV-7

Damping at different force levels,

Second lowest translational mode (N-S)

Damping %	1.13	1.18	1.28	1.37	1.64
Force ratios	1	1.97	2.92	4.00	6.8
Response ratios	1	1.88	2.59	3.30	4.74

Torsional Motion

With the two vibration exciters located at the 4th floor it was possible to excite the torsional modes of vibration by running the two exciters synchronized with a phase angle of 180^{o} between them. Figure 4-13 shows the 10th floor response as the structure is being excited at and close to its lowest torsional resonant frequency. From the width of the response curve, the damping was estimated to be 0.8%. The response was not of sufficient magnitude to make possible a determination of the mode shape.

Figure 4-14 shows the response curve for the motion of the 3rd floor as the second lowest torsional mode is being excited. The value of damping as measured from the width of the response curve is estimated to be 1.3%. The mode shape is shown in Fig. 4-16.

Figure 4-15 shows the 3rd floor response as the third lowest torsional mode is being excited. The value as determined from the width of the response curve is equal to 3.1%. The mode shape is shown in Fig. 4-16.

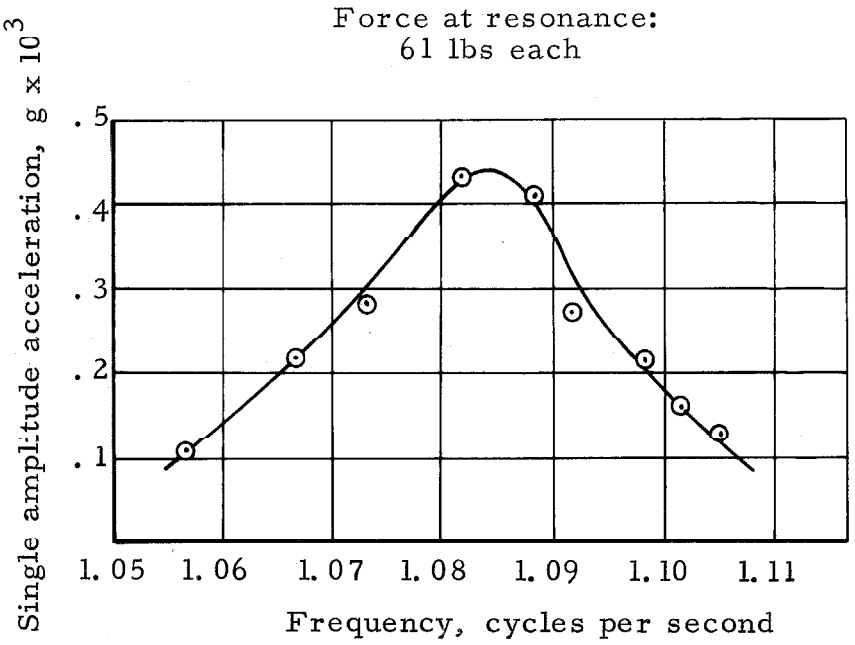

Fig. 4-13 10^{th} FLOOR RESPONSE, LOWEST TORSIONAL MODE, MEASURED 20 FEET FROM EAST END OF BUILDING, VIBRATION EXCITERS B AND C.

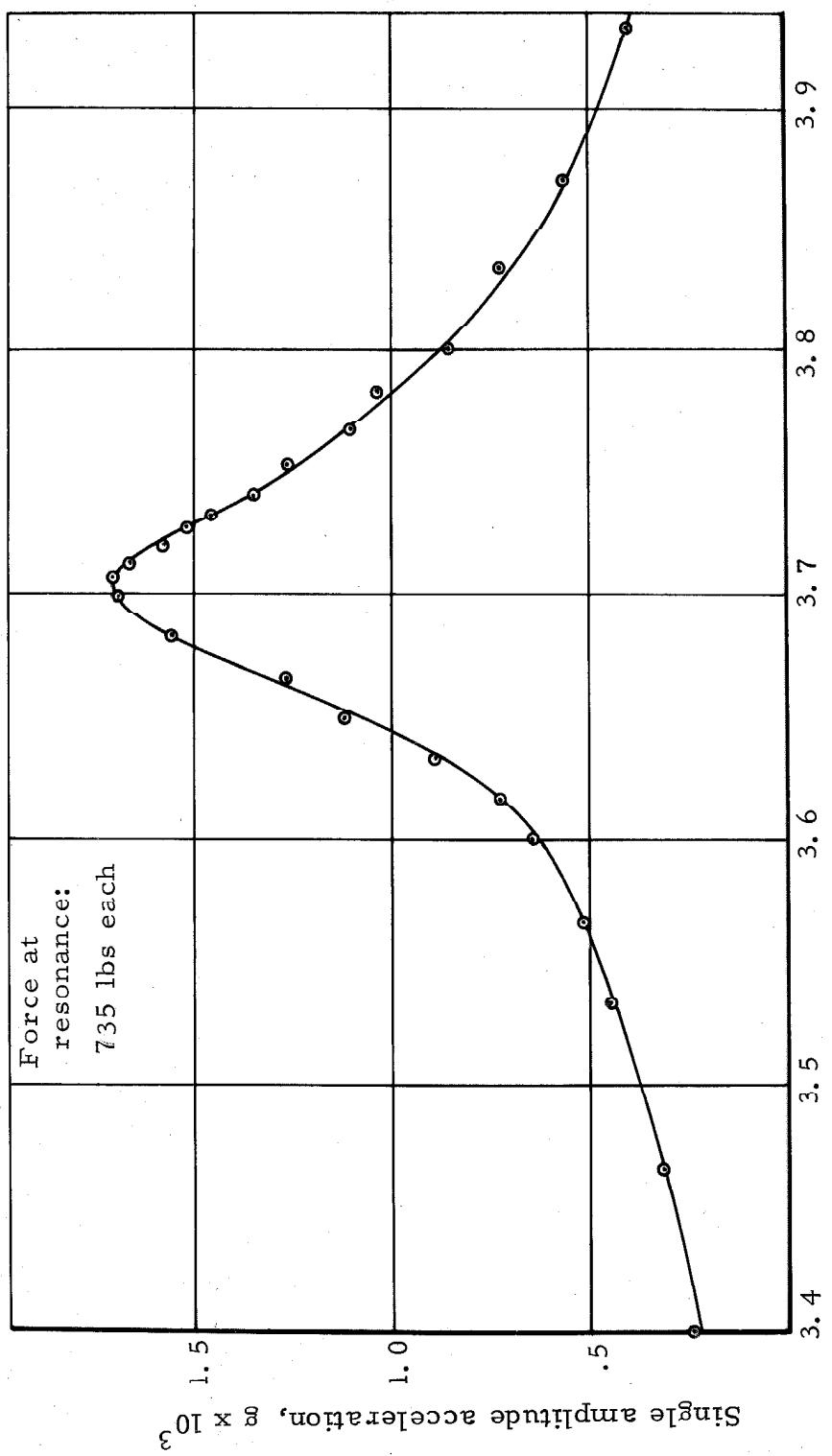

Fig. 4-14 3rd FLOOR RESPONSE, SECOND LOWEST TORSIONAL MODE, MEASURED 60 FEET FROM EAST END OF BUILDING, VIBRATION EXCITERS B AND C.

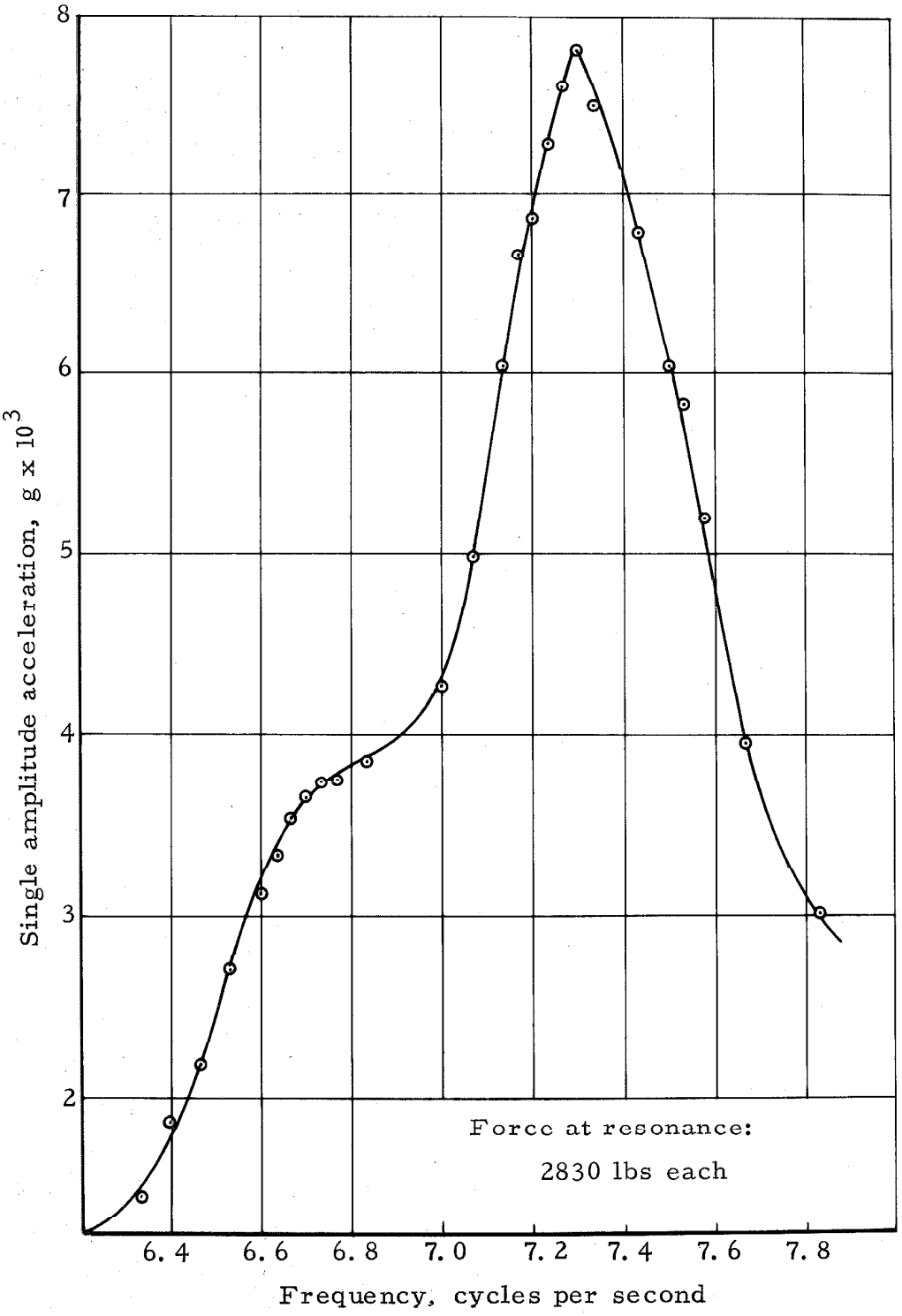

Fig. 4-15 3rd FLOOR RESPONSE, THIRD LOWEST TORSIONAL MODE, MEASURED 60 FEET FROM EAST END OF BUILDING, VIBRATION EXCITERS B AND C.

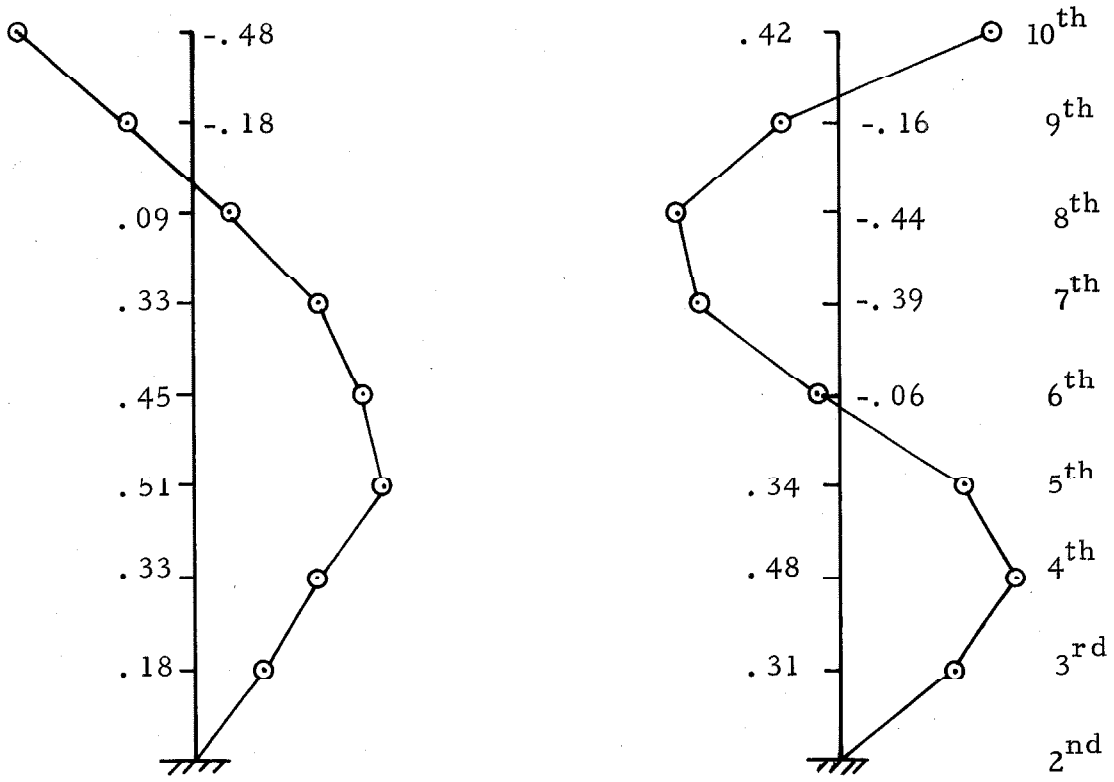

ω_2 = 3. 72 cps
β_2 = 1. 3%

ω_3 = 7. 30 cps
β_3 = 3%

ω_1 = 1. 08 cps; β_1 = . 8%

Fig. 4-16 MODE SHAPES, TORSION

Slab Vibration, Free-Free Beams

It has already been mentioned that a mode was excited in which the floor slabs vibrated as free-free beams. Figure 4-17 shows the configuration of the 6th floor as the resonant frequency for this mode is being excited. The mode shape is also shown in Fig. 4-17. In determining this mode shape, accelerometers were located at point A on all the floors. It is of interest to note that the building moves with essentially no relative displacements between adjacent floors. This means that in this mode of vibration no stresses are developed in the columns.

The response curve for point A in Fig. 4-17 is shown in Fig. 4-18. The value of damping as determined from the width of the response curve is found to be close to 2% of critical damping. It is interesting to note that the vibration tests of the five-story reinforced concrete building as described in Chapter III generally showed damping values close to 2% of critical damping.

The natural frequency of a beam vibrating as a free-free beam can be found from the following expression

$$f_n = 3.56 \sqrt{\frac{EI}{mL^4}}$$

Since the floor slabs are made of light weight concrete, the modulus of elasticity for concrete is estimated to be 2×10^6 psi; the typical floor weight is 920 kips. Distributing the masses uniformly over the slab gives a value of m equal to .9 lbs-sec^2/in^2. The moment of inertia

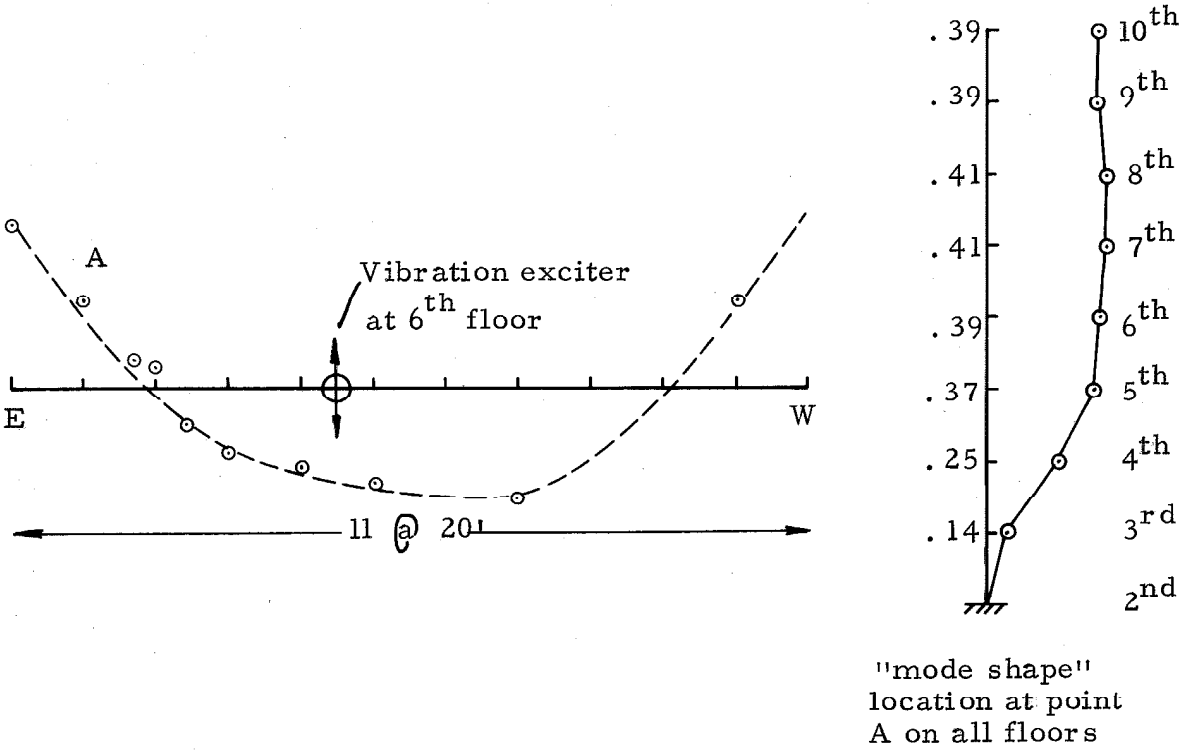

Fig. 4-17 6^{th} FLOOR RESPONSE, FLOORS VIBRATING AS FREE-FREE BEAMS, RESPONSE CURVE FOR POINT A SHOWN IN FIG. 4-18.

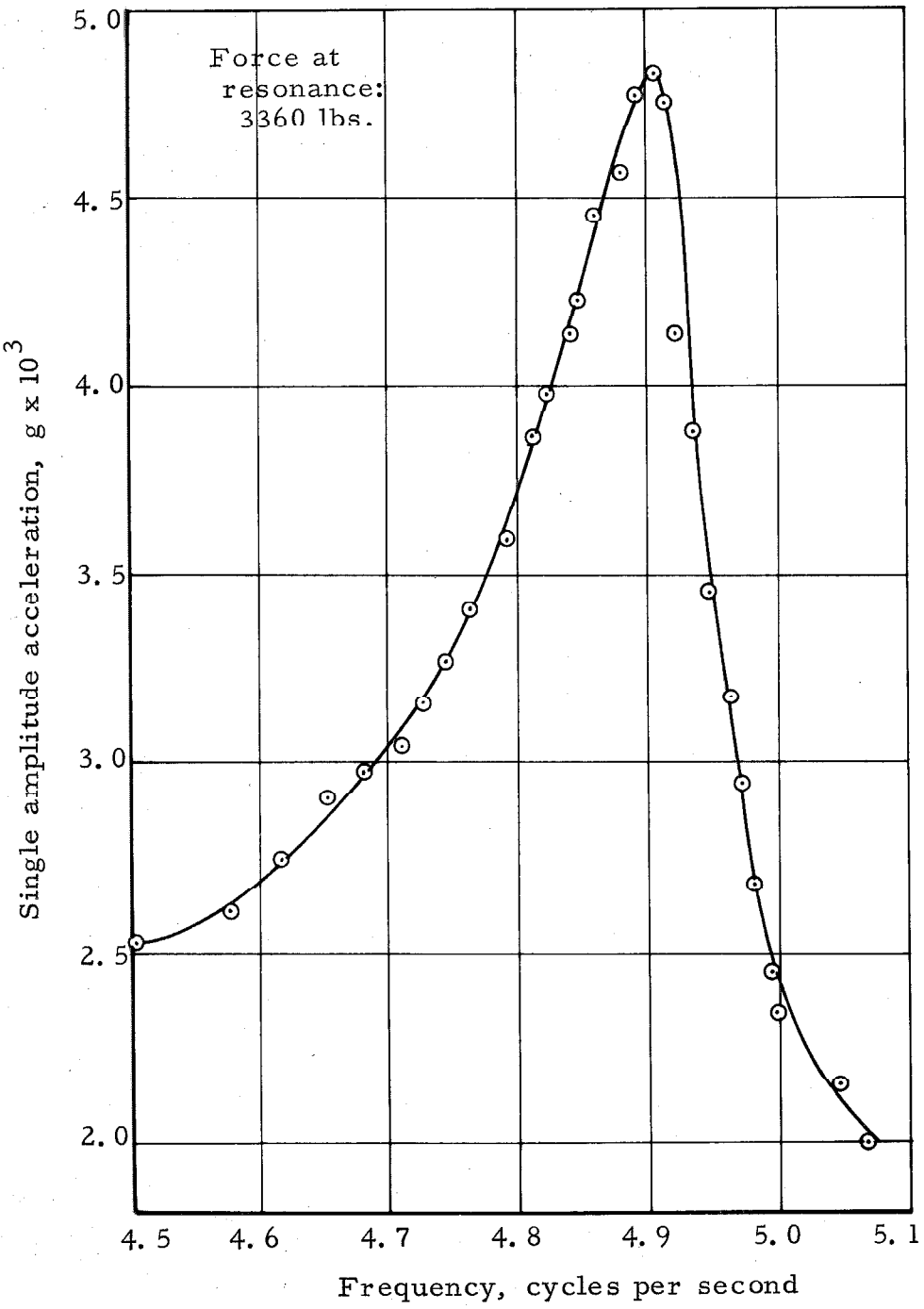

Fig. 4-18 6^{th} FLOOR RESPONSE OF POINT A IN FIG. 4-17. FLOORS VIBRATING AS FREE-FREE BEAMS.

is calculated using the total cross-section of the slab but excluding reinforcing bars. The result of the frequency determination is

$$f_n = 3.56\sqrt{\frac{2 \times 10^6 \times 5 \times (40)^3 (12)^3}{12 \times .9 \times (220)^4 (12)^4}} = 5.1 \text{ cps}$$

The resonant frequency excited during the vibration tests was equal to 4.9 cps; the two values are in close agreement.

CHAPTER V

STEADY-STATE VERSUS RUN-DOWN TESTS OF STRUCTURES

The vibration tests described in Chapters III and IV were steady-state resonance tests. In these tests the speed of the vibration exciters can be controlled to an accuracy of about 0.1%, i.e., after running the exciter at a specific frequency, and recording the building response, it is possible to change the frequency to a new value that only differs 0.1% from the previous value. Dynamic tests of buildings and other civil engineering structures have in the past often been in the form of run-down tests, in which a sinusoidal vibration exciter is allowed to decelerate through resonance under friction forces. In this case the response curve, the natural frequency, the damping, etc., are determined from the recorded run-down motion of the structure. The speed control on the earlier exciters was not very precise so run-down tests were the most feasible method of performing structural dynamic tests on full-scale structures. Since the present vibration exciters can be used to subject a building to forced vibration run-down tests as well as forced vibration steady-state tests, the two methods of testing were used on the two buildings described in Chapters III and IV. The response curves obtained from the two types of tests were then analyzed and the results were compared.

In a run-down test it is not possible to use multiple vibration exciters since the electrical synchronization system is not energized while the units coast to rest with the power off. The comparison tests

were therefore run using only one exciter on one of the upper floors without changing the instrumentation for the response pick-up between tests. The comparison vibration tests on the five story reinforced concrete frame building were part of the preliminary tests performed three weeks prior to the tests reported in Chapter III. In this three week period several non-structural elements were added to the building such as windows, false ceilings, air conditioning ducts and facing bricks. These additions had no significant effect on the vibrational characteristics of the building; the tendency was to lower slightly the natural periods of vibration and to increase slightly the amount of damping in the various modes of vibration.

In Fig. 5-6a the acceleration response of the 4th floor of the 9-story steel-frame building of Chapter III is shown; the mode excited is the second torsional mode. It is clear from this record that a very slight change in frequency can give a significant change in the response amplitude; the record shows clearly that with a less accurate control of the frequency, a significant part of the response would have been lost. Actually, the steady-state acceleration response reproduced in Fig. 5-6a corresponds to discrete changes in frequency from 3.680 cps to 3.713 cps or less than a 1% total change in frequency. If it had only been possible to change the frequency in steps of about 1%, all the record between 3.680 cps and 3.713 cps could have been lost. Since the acceleration at 3.700 cps is about 20% more than at 3.680 cps, the peak amplitude would thus have been found as only 80% of the true value. While this would have had only a very minor effect upon

the determination of the natural frequency, it would affect the determination of the damping significantly.

It is interesting to note that in performing the steady-state dynamic tests as described in Chapters II and III, it was necessary in some cases to wait for several minutes before taking records after the exciters were set at a specific frequency. The transient vibrations from the prior excitation took that long to damp out and leave only the true steady-state response from the presently excited frequency. Especially at frequencies slightly higher than a natural frequency this interference between the natural frequency of the system and the frequency of excitation appeared on the records of acceleration as a typical series of "beats!" The fact that many cycles of excitation were needed for the structure to obtain its true steady-state response led to the questions explored in this chapter. Since a run-down test employs not discrete changes in frequency, but rather a sweep through the frequencies of interest, it was felt that run-down tests might not give a good representation of a steady-state response but rather an obscure mixture of transient and steady-state responses.

Run-Down Tests

In a run-down test the forces are applied to the structure in the same way as for the steady-state tests, but instead of exciting the structure with discrete changes in the frequency, a continuous sweep of the frequencies is made. The vibrator is speeded up to a frequency that is higher than the natural frequency of interest; the power to the

vibrator is then cut off or the belt connecting the motor to the rotating weights is removed, and the system is permitted to decelerate under action of friction forces. As the vibrator coasts down to rest, continuous measurements of the response are taken. The record will directly show how the response varies with the frequency. By measuring the amplitude of the response and the corresponding frequency at several points on the record it is possible to plot the response in the form of a response curve. In the past this response curve has been analyzed in the same way as the response curve from a steady-state test to find the natural frequency of the system and the damping in the particular mode. The implication of this procedure is that the response found from a run-down test is the same as that found from a steady-state test. Indeed this would be true if the vibrator were to coast down to rest slowly enough so that at any exciting frequency the structure has time enough to build up to its steady-state response.

If the vibrator coasts down too fast, the response at any frequency will consist of both transient vibrations and steady-state vibrations. Furthermore, at frequencies close to the natural frequency of the system, the amplitude might not have time enough to build up to its steady-state value during the time the system is being vibrated near its natural frequency. The reason why so many structural dynamic tests on full-scale structures in the past have used run-down tests is that it appeared to be the most feasible method. The speed control on the earlier exciters were not very precise and thus it was difficult to trace out a response curve by means of discrete changes in frequency. Also another difficulty appearing in some drive systems is that close to a

resonant condition the speed control could not keep the exciter running at a constant frequency. While it is obvious that the rate of sweep of the frequencies in a run-down test will affect the response of the structure, this is not the only factor that determines how well the response would compare with the true steady-state values of the response. As will be shown later on, the response is also affected by the natural period of the structure and to a very high degree by the amount of damping in the mode investigated.

The problem of how well the response found from a run-down test compares with that found from a steady-state test has been treated theoretically in connection with mechanical engineering problems involving the acceleration of unbalanced rotating machinery through critical speeds. While the problem has been looked at from a somewhat different viewpoint from that used in the present discussion, the results are still useful. Lewis[55] analyzed the response of a one degree of freedom system acted upon by a sinusoidal force whose amplitude is constant but whose frequency either increased or decreased at a uniform rate. The main conclusions to be drawn from Lewis' work are the following: (1) The natural frequency of the system found by letting the applied force sweep through resonance with a uniform decrease in frequency is less than that found from a steady-state test, the higher the rate of sweep and the lower the damping in the structure the greater the shift in frequency. (2) The peak amplitude found from a run-down test will be less than the peak value found from a steady-state test; the faster the rate of run-down and the lower the damping the greater the

change in peak value. (3) For low values of damping the amplitude of motion in a run-down test will decay in a series of beats which can be regarded as an interference between the free and the forced motion of the system.

As Lewis points out, it was not possible to find an analytical expression relating the above mentioned shifts in frequency and peak value to the rate of sweep and the damping in the structure. Attempts at finding general empirical relationships which would express approximately the changes in frequency and peak value as a function of run-down rate and damping in the structure have not been successful. However, it was possible to solve the problem for a number of given sweep rates and for different values of damping. Parker[56] later treated the same problem by use of an analog computer, extending Lewis' work by considering a wider range of damping values.

References (55) and (56) show clearly that for values of damping and rates of sweep that would be typical for a run-down test on full-scale structures the shift in frequency is of little importance. This shift in frequency would at the most be of the order of 10%. On the other hand, it is quite evident from references (55) and (56) that the peak response value as found from a run-down test could be quite different from the steady-state response. The peak response values found by sweeping through the natural frequency of a linear single-mass system are shown in Table V-1. The numerical values given in Table V-1 are the ratios of the peak response from a sweep of frequencies with an infinitely slow sweep rate (i.e., a steady-state test)

Table V-1
(From References (55) and (56))

$q = \frac{N^2}{h}$	β =	.5%	1.0%	1.67%	2.5%	5%
-385		2.17	1.49	1.17	1.04	1.02
-131				1.46	1.24	1.10
-42					1.47	1.23

divided by the peak response found from a sweep of frequencies at a finite constant sweep rate. In this table β is the percentage of critical damping qhile q is a factor expressing the natural frequency and the rate of change of frequency during the sweep. The factor q is equal to the square of the system's natural frequency in cycles per second divided by the rate of change of frequency in cycles per second per second, i.e.,

$$q = \frac{N^2}{h}$$

Table V-1 can be regarded as the correction factor that should be applied to the peak value as found from a test using a sweep through the natural frequency in order to obtain the steady-state response. However, as will be shown later on, the damping is not sufficiently well known from a sweep test to make this a practical way of finding the steady-state peak response value. It is clear from the table that this correction factor depends strongly on the damping in the structure.

Experimental Results

Figure 5-1 shows how the speed of the vibration exciter changes

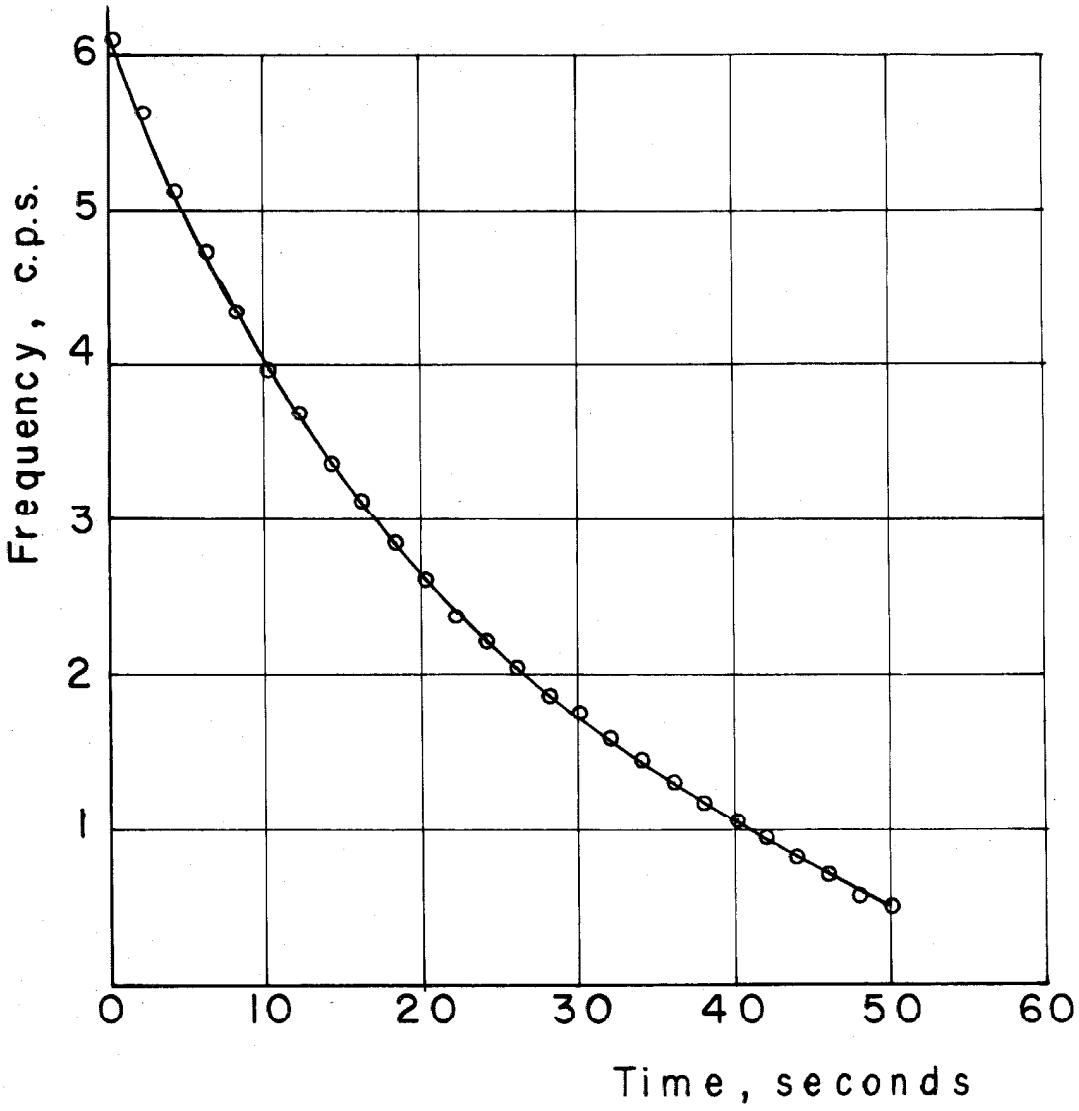

FIG. 5-1 FREQUENCY CHANGE DURING RUN-DOWN

with time as the vibrator coasts down to rest. The speed of the vibration exciter was read from a digital electronic counter which was triggered by a tachometer mounted on the drive motor shaft. The counter contains its own frequency standard accurate to 0.01%. The record is typical in the sense that there seems to be no significant changes in the rate of change of speed during run-down, regardless of the type of structure the vibrator is attached to. The mechanical condition of the vibrator, however, could be an important factor as the rate of change of speed during run-down could be affected by such factors as tightness of the drive chains and the lubrication of the bearings. It was found that the curve shown in Fig. 5-1 could be well represented by the following expression:

$$f = 6.1\, e^{-.04t} \tag{5.1}$$

where f is the speed of the vibrator in cycles per sec and t denotes time in seconds. The rate of change of speed at any frequency then becomes

$$h = \frac{df}{dt} = -.04f = -\frac{1}{25} f \tag{5.2}$$

It is of interest to note that the rate of change of speed of the exciter during run-down is proportional to the speed. This is perhaps fortuitous as the friction causing the vibrator to slow down comes from several sources. The air resistance against the rotating buckets that carry the weights would be approximately proportional to the frequency squared while other friction effects in chains and bearings probably would be more or less independent of speed.

The sweep expressed by Eqs. 5.1 and 5.2 is known as a logarithmic sweep. It will be shown later that less than half of a cycle per second is needed to fully define the response curve. Within this short range of frequencies the rate of change of speed would be nearly constant and can be expressed as

$$h = -\frac{1}{25} f = -\frac{1}{25} N \tag{5.3}$$

where N is the system's natural frequency in cycles per second. By means of Eq. 5.3 the factor q used by Lewis and Parker can be expressed as

$$q = \frac{N^2}{h} = \frac{N^2}{-\frac{1}{25} N} = -25N \tag{5.4}$$

The range of frequencies of excitation that can be obtained by using the vibration exciter is 1 to 9 cps so from Eq. 5.4 it follows that the applicable values for q fall in the range $-225 < q < -25$. This range is covered approximately by the values of q in Table V-1.

One of the buildings tested was the five-story reinforced concrete frame building of Chapter III. The vibration exciter was attached to the fifth floor of the building close to the longitudinal axis of symmetry at a distance of 16 ft from one end. Accelerometers were located on all floors on the longitudinal axis of symmetry at a distance of 50 ft from one end. With this location of the exciter and the accelerometers it was possible to excite and record both translational and torsional modes of vibration.

Figure 5-2a shows the acceleration measured at the fourth and fifth floors from a steady-state vibration test as the structure is

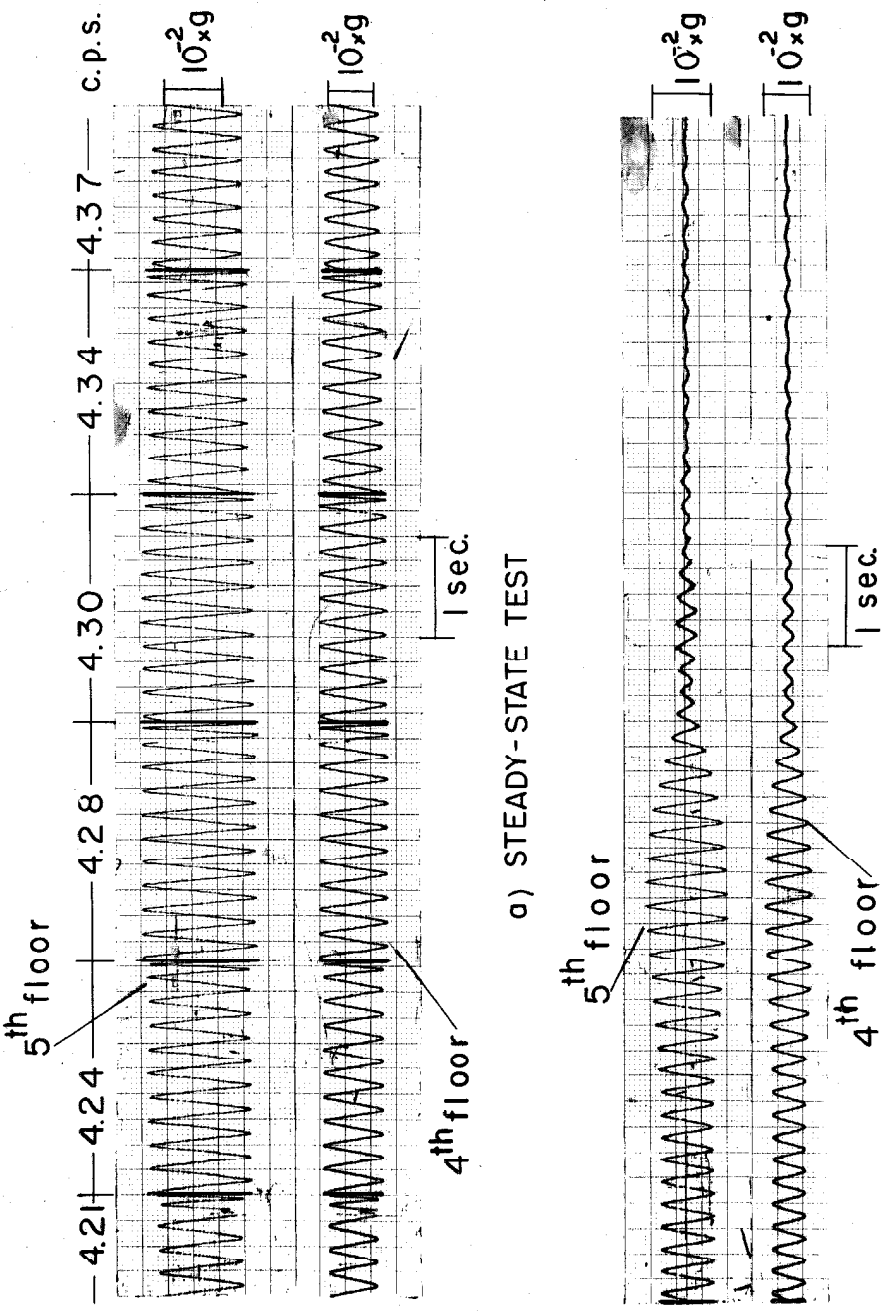

FIG. 5-2 ACCELERATION RESPONSE, LOWEST TORSIONAL MODE OF 5-STORY REINFORCED CONCRETE BUILDING

excited into its lowest torsional mode with discrete changes in frequency. Figure 5-2b shows the same recorded response but from a run-down test as the vibrator sweeps through the resonance for this mode. It is evident from Figs. 5-2a and 5-2b that the peak accelerations obtained from the steady-state test are considerably greater than those obtained from the run-down test.

In Fig. 5-3 the responses of the fifth floor have been plotted as a function of frequency. The response has been reduced to single amplitude displacement at constant force. With the steady-state response plotted in this fashion it is common practice to evaluate the damping from the width of the response curve measured at an amplitude of $\sqrt{2}/2$ times the resonant amplitude. The same procedure has been commonly used on the response curves of run-down tests. A summary of the quantities determined from Fig. 5-3 is shown in Table V-2.

It is seen in Table V-2 that the resonant frequency as found from the run-down test is slightly smaller than the value found from the steady-state test, the difference in frequency being about 3%. However, the damping deduced from the run-down test is almost twice as large as the value determined from the steady-state test. The peak response values obtained from the two types of tests are also significantly different.

The ratio of the maximum steady-state acceleration divided by the maximum run-down acceleration is 1.45 for both the fourth and fifth floor measurements. This factor can be compared to the theoretically deduced factors given in Table V-1. Using the value of

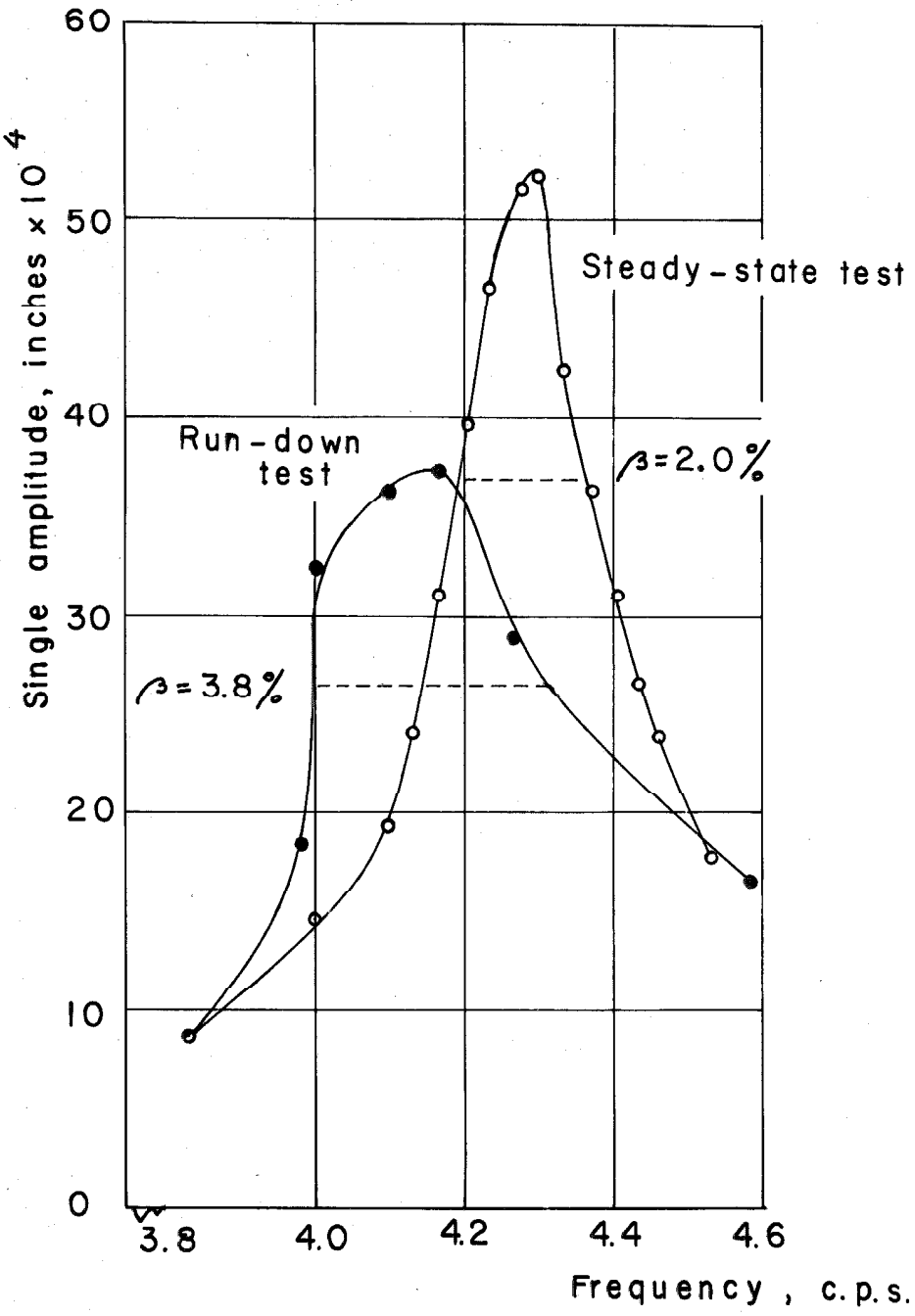

FIG. 5-3 RESONANCE CURVES, LOWEST TORSIONAL MODE OF 5-STORY REINFORCED CONCRETE BUILDING

Table V-2

5-Story R. C. Building, Lowest Torsional Mode

	Run-down Test		Steady-State Test	
Resonant frequency, cps	4. 16		4. 28	
Damping % critical	3. 8		2. 0	
	4th Floor	5th Floor	4th Floor	5th Floor
Peak acceleration single amplitude 10^{-3} g	5. 05	6. 70	7. 30	9. 80
Peak displacement single amplitude 10^{-3} inches	2. 84	3. 75	3. 90	5. 25

β = 2% and from Eq. 5. 4 the value of q = -25N = -25 x 4. 28 = -107 it is seen that the experimental factor 1. 45 is consistent with the values in Table V-1. It is only possible to make an approximate comparison of the experimental value and the theoretical values of Table V-1 as the experimentally determined values for β and q fall slightly outside the range of values in Table V-1. However, enough of a trend can be established to conclude that the theoretical work done by Lewis and Parker on a one degree of freedom system is well supported by the experimental results obtained from actual tests of multi-degree of freedom systems. The mode being tested was sufficiently well separated from other modes so that in the short range of frequencies needed to define the response curve there was no interference of

other modes. The theoretical results were found assuming the force amplitude to be constant and a linear sweep of frequencies during run-down. In the actual tests the force varied as the frequency squared and the sweep of frequencies was a logarithmic sweep rather than a linear sweep. However, as can be seen from Fig. 5-3 the resonance curve spans only a very narrow range of frequencies, less than half a cycle per second is needed to fully define the resonance curve. Within this short range of frequencies the force applied would be almost constant. Similarly, it is evident from Fig. 5-1 that even though the rate of change of speed is not constant for the full range of frequencies, the rate of change of speed would be nearly constant for a range of frequencies spanning only about half a cycle per second.

With the same location of the vibration exciter and the accelerometers, the first translational mode in the short direction of the building was also investigated. The acceleration measurements are shown from the steady-state test in Fig. 5-4a and from the run-down test in Fig. 5-4b. Again, it is evident that the peak accelerations found from the steady-state test are considerably greater than for the run-down test. Figure 5-5 shows the resonance curves for the fifth floor as found from the two tests, the response being reduced to single amplitude displacement at constant force.

Table V-3 gives a summary of the results. In this table the peak acceleration values are also given for the other floors of the building so that differences in mode shapes, if any, can be seen. The resonant frequency determined from the run-down test is about 3% lower than

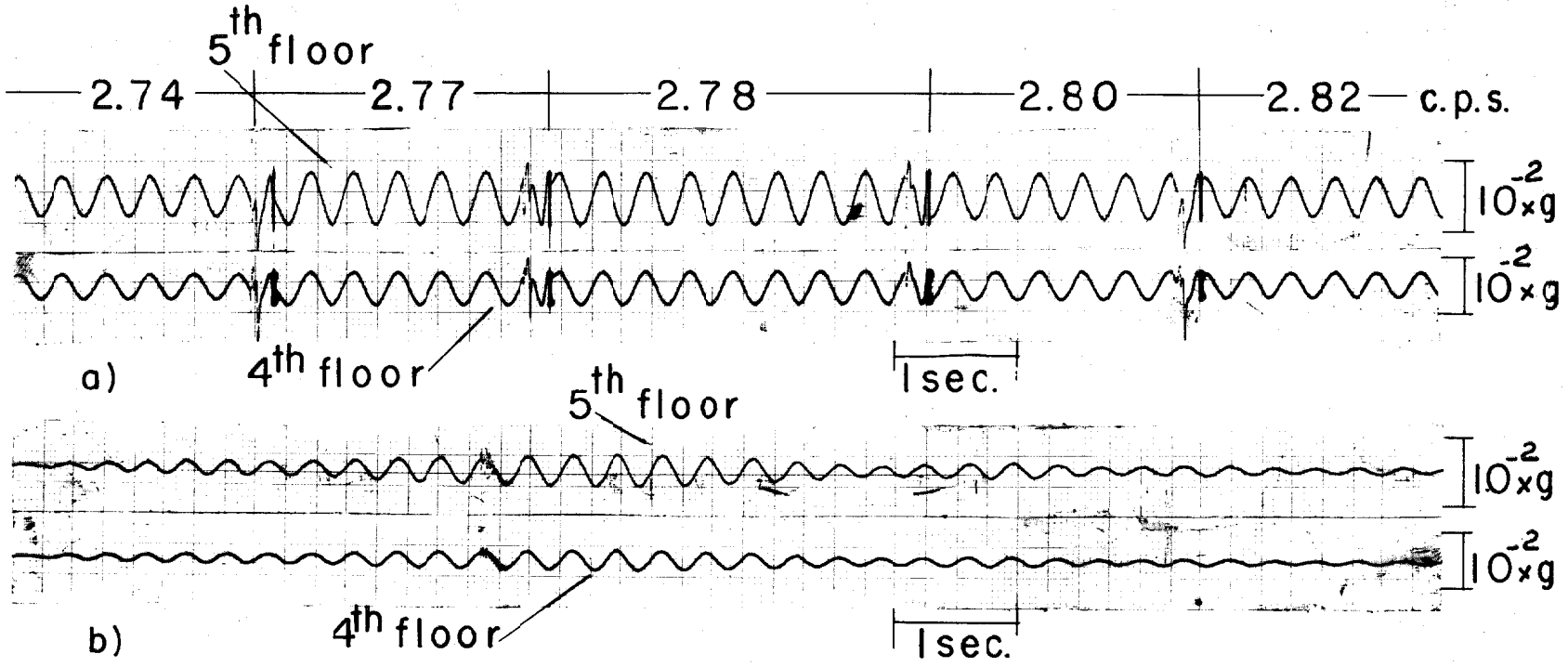

FIG. 5-4 ACCELERATION RESPONSE, LOWEST TRANSLATIONAL MODE OF 5-STORY REINFORCED CONCRETE BUILDING

a) STEADY-STATE TEST

b) RUN-DOWN TEST

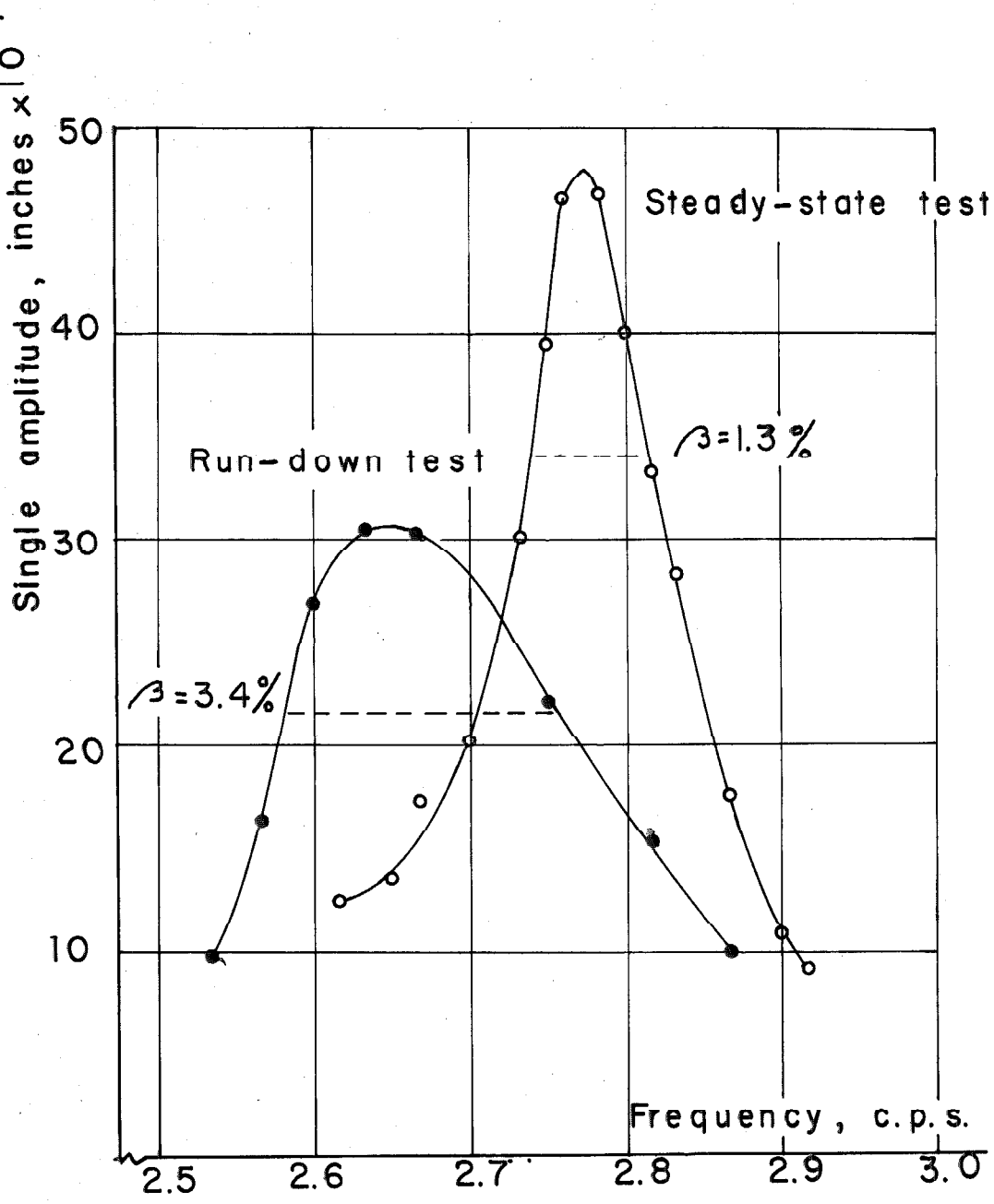

FIG. 5-5 RESONANCE CURVES, LOWEST TRANSLATIONAL MODE OF 5-STORY REINFORCED CONCRETE BUILDING

Table V-3

5-Story R. C. Building - Lowest Translational Mode

	Run-down Test					Steady-state Test				
Natural frequency cps	2.64					2.77				
Damping % critical	3.4					1.3				
	2nd floor	3rd floor	4th floor	5th floor	Roof	2nd floor	3rd floor	4th floor	5th floor	Roof
Peak acceleration single amplitude 10^{-3} g	.63	1.15	1.72	2.18	2.77	1.08	2.06	2.94	3.87	4.72
Peak displacement single amplitude 10^{-3} in.	.88	1.61	2.42	3.05	3.90	1.38	2.62	3.74	4.92	6.00
Mode shape normalized	.15	.28	.42	.53	.67	.15	.29	.41	.54	.66

the resonant frequency determined from the steady-state test. It is significant that damping determined from the run-down test is about 2. 5 times as large as the damping determined from the steady-state test. By dividing the peak acceleration found from the steady-state test with that obtained from the run-down test, a factor of 1. 75 is found from measurements at all floors.. Using the value of β = 1. 3% and from Eq. 5. 4 q = -25N = -25 x 2. 77 = -70 it is possible to compare the experimental value of 1. 75 to the theoretical values listed in Table V-1. Again in this case it is found that the experimentally determined value is consistent with the values in Table V-1.

It is of interest to note in comparing the results of the run-down test with those of the steady-state test that the values of damping differ much more than the peak response values. This is also evident from Fig. 5-5 where it can be seen that not only is the peak response lower in the run-down test, but the response curve found from the run-down test is much broader. It is evident from Table V-3 and Fig. 5-5 that the response curve, as plotted from a run-down test, cannot be analyzed as if it were a steady-state response curve.

Table V-3 shows also the normalized mode shapes as obtained from the two types of tests. The results are almost identical, as would be expected, since it is clear from the acceleration records that the structure is excited in a normal mode as the vibration exciter sweeps through the natural frequency of the structure during the run-down test.

Steady-state tests and run-down tests were also carried out on

the 9-story steel frame building of Chapter IV. A vibration exciter was attached to the fourth floor away from the shear center so both translational and torsional modes could be excited. Figure 5-6a shows the recorded acceleration response of the fourth floor as the structure was excited near its second lowest torsional frequency by discrete changes in frequency. Figure 5-6b shows the same recorded response but from the run-down test. It is seen that the peak acceleration during the steady-state test is much larger than during the run-down test. It is seen in Fig. 5-6b that after the structure has been excited into resonance the acceleration response decays in a series of "beats". The physical explanation is that the motion at frequencies slightly lower than the resonant frequency is partly a free motion and partly a forced motion. The "beating" phenomena can thus be regarded as an interference between the free and the forced motion.

The "beats" in the run-down record make it impossible to construct the resonance curve and calculate the damping from the run-down test. The steady-state test determined the damping in this mode to be 1.1%. The peak single amplitude accelerations during the steady-state test and during the run-down test are equal to 6.1×10^{-3}g and 3.4×10^{-3}g, respectively. The ratio of the two measurements is 1.8. Using the value of $\beta = 1.1\%$ and from Eq. 5.4 $q = -25N = -25 \times 3.7 = -92$ it is seen that the experimental value 1.8 is consistent with the range of theoretical values in Table V-1. It is evident that the ratio of maximum steady-state acceleration divided by the maximum run-down acceleration depends strongly upon the damping in the structure.

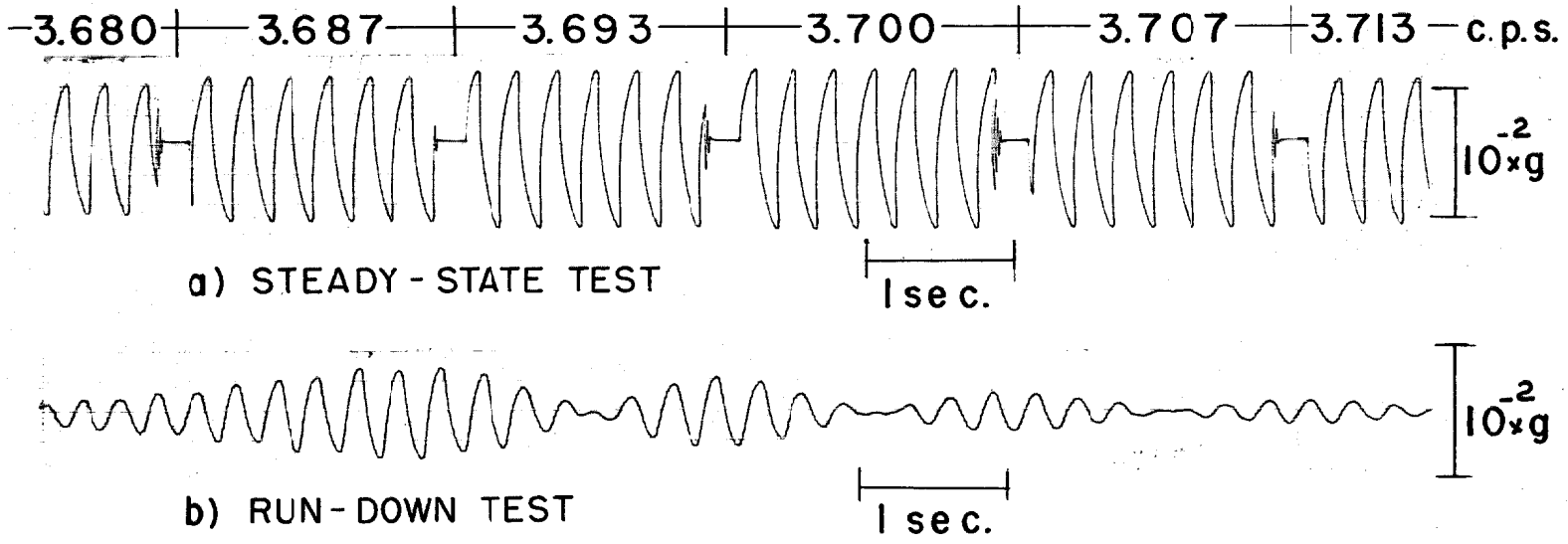

FIG. 5-6 ACCELERATION RESPONSE, SECOND LOWEST TORSIONAL MODE OF 9-STORY STEEL FRAME BUILDING

The value of q in the example above is equal to -92, but even if the run-down rate were more than four times as slow, say q = -385, then the values given in Table V-1 would predict that for a structure with 0.5% damping the ratio of peak acceleration responses would be 2.17 and if the damping was 1.0% the predicted ratio would be 1.49.

Conclusions

Steady-state and run-down tests have been made on two modern multistory buildings. The response curves obtained from the two types of tests have been analyzed and the results compared.

The natural frequency as determined from a run-down test is a few per cent lower than the natural frequency determined from a steady-state test. The mode shapes, as determined from the two types of tests, are identical. The peak response value determined from a run-down test is as much as 50% lower than the steady-state response value. Damping determined from a run-down test is up to 2.5 times as large as the damping determined from a steady-state test. It is concluded that a run-down test is not, in general, a suitable experimental method for dynamic testing of structures. It is also concluded that data from past run-down tests are of questionable accuracy.

CHAPTER VI

A NEW METHOD FOR THE MEASUREMENT OF THE NATURAL PERIODS OF BUILDINGS*

The natural periods of vibration of a structure are perhaps the most significant dynamic parameters involved in response analysis. Not only are the numerical values needed for computations, but a comparison between experimentally determined values and calculated values is an important check on the validity of the simplified mathematical models which must of necessity be used in the analysis.[58]

The importance of the fundamental natural period as an indication of the dynamic behavior of structures is emphasized by the introduction of this parameter into some modern earthquake-resistant building codes. The "Recommended Lateral Force Requirements" of the Structural Engineers Association of California,[59] for example, fixes the basic lateral force coefficient to be used in design by a formula involving the fundamental natural period.

An additional reason for an interest in these natural periods is the belief that concealed structural damage such as might occur during a strong earthquake might significantly alter the fundamental period, and hence period measurements before and after an earthquake might reveal such hidden damage. Although there is some evidence from

---

* This chapter has been published with minor modifications in the Bulletin of The Seismological Society of America.[57]

past measurements that significant period shifts have been caused by earthquakes, the presently available data are not sufficient to arrive at any definite conclusion. It is important that period measurements be made on existing structures so that, should an earthquake occur, the basic data will be available for comparison. At present, accurate period data is at hand for only a very few buildings.

Experimental Methods

The experimental methods that have been used for period measurements of full-scale structures are: (1) resonance testing, using a variable frequency sinusoidal vibration generator; (2) free vibration decay tests, excited by initial displacements or velocities; (3) wind-excited forced vibration tests, using the very small amplitudes set up by natural gusts.

The first two types of tests require relatively elaborate equipment, and in practice it is seldom possible to secure permission to make such tests in buildings. The wind-excited tests can be quickly carried out without the installation of any equipment in the building, it being only required to temporarily place a portable seismograph in an upper story position.

The difficulties with the wind excited tests are: (1) suitable natural gusts may not always be available; (2) very low amplitude levels are set up, and thus some structural elements may not be brought into action in a typical way; (3) since the form of the exciting force is not known, no information on structural damping can be

deduced from the record; and (4) usually only the fundamental mode of vibration will have an appreciable motion, and thus no information on the higher modes is obtained. In spite of these defects, the simplicity of the test, and the fact that it is the only possibility for most buildings, has given it an important place in structural dynamic investigations. A considerable amount of such data was collected in the early 1930's by the United States Coast and Geodetic Survey and reported in the publication "Earthquake Investigations in California."[60] At the present time the United States Coast and Geodetic Survey is reactivating and enlarging this period measuring program with improved instrumentation.

As an example of the results that can be obtained with such wind-excited tests, Fig. 6-1 shows measurements made on a 100 ft high concrete intake tower of a dam.[61] This test was unusual in that a second mode of vibration was also clearly excited during part of the record, and hence the first two periods of vibration could be determined. The records of Fig. 6-1 were obtained on a photographically recording portable seismograph having a natural period of about 2 seconds and a magnification of approximately 400.

There is a possibility that some information on structural damping could be extracted from a wind-excited vibration record such as Fig. 6-1 if some data on the input force could be obtained. If, for example, the exciting force power spectrum could be simultaneously measured, something might then be deduced about the damping. This does not seem to be feasible in practice, however, because of the

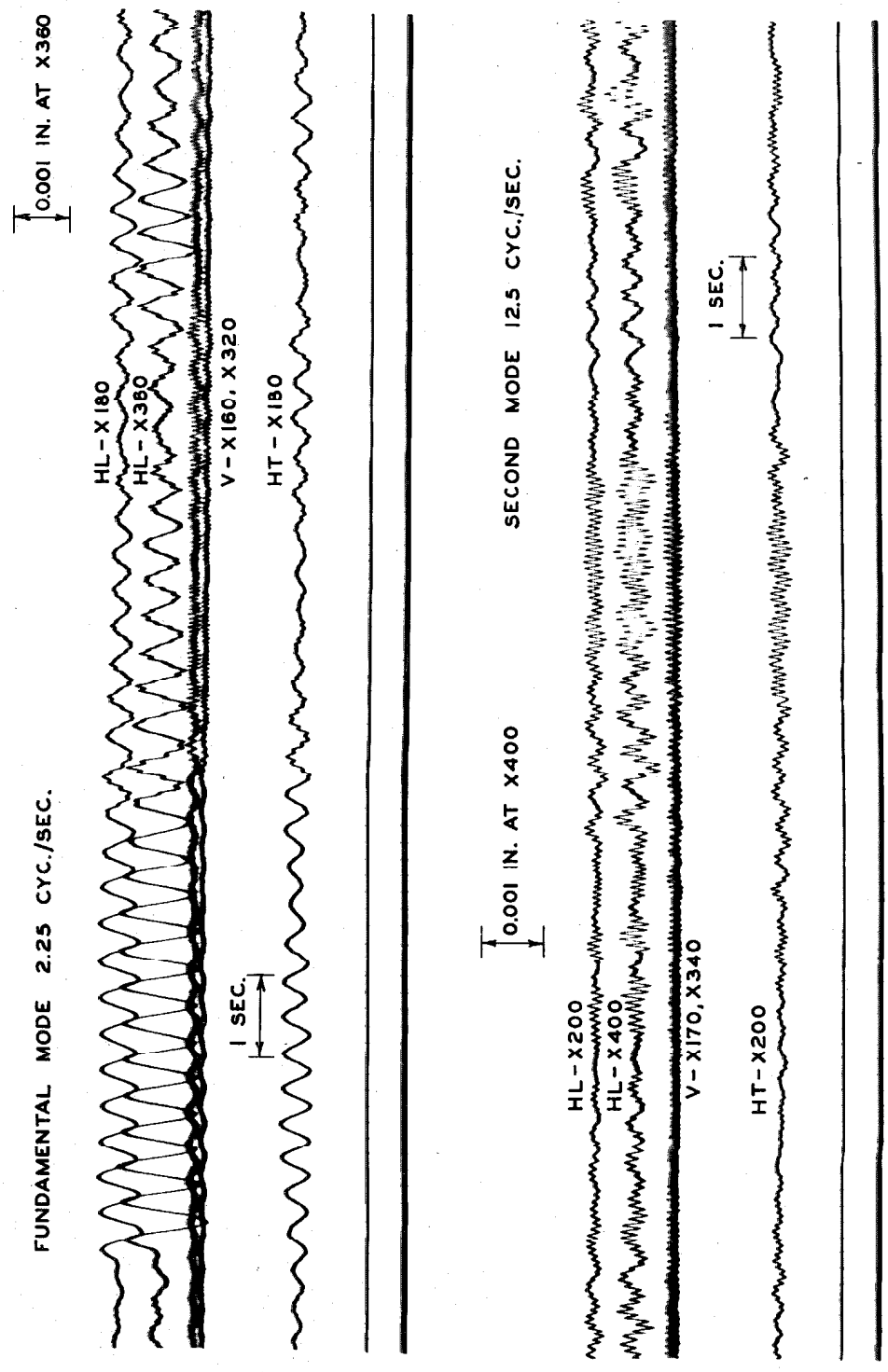

FIG. 6-1 SAMPLE RECORDS OF WIND-EXCITED TOWER VIBRATIONS

large size of the structures involved, which would require that the input wind forces be simultaneously measured at a number of points to arrive at the integrated exciting force.

A New Method of Excitation

During some wind-excited tests of a 150 ft high concrete intake tower, it was noted that a considerable deflection of the seismograph recorder could be set up by the operator jumping laterally at the top of the tower. This suggested that the small inertia force generated by the operator himself, if it were properly synchronized with the natural period of the tower, might be sufficient to build up a measurable resonant vibration. With a little practice it was found that this was indeed the case. By keeping one eye on the seismograph recorder to observe the way the vibrations were building up, an operator with an ordinary sense of rhythm could by periodic motions of his body produce considerably larger amplitudes of motion at the fundamental period than had been produced by the wind. Figure 6-2 shows the record obtained in this way on the 150 ft high concrete intake tower using the same seismograph that was used for Fig. 6-1.

It was immediately evident that this method of excitation had three important advantages over the wind-excited force: (1) larger amplitudes of motion could be built up at a definite period; (2) the test could be carried out at any time, in the presence or absence of wind; and (3) in the absence of wind, by stopping the exciting force after an appreciable motion had been built up, the decay of free

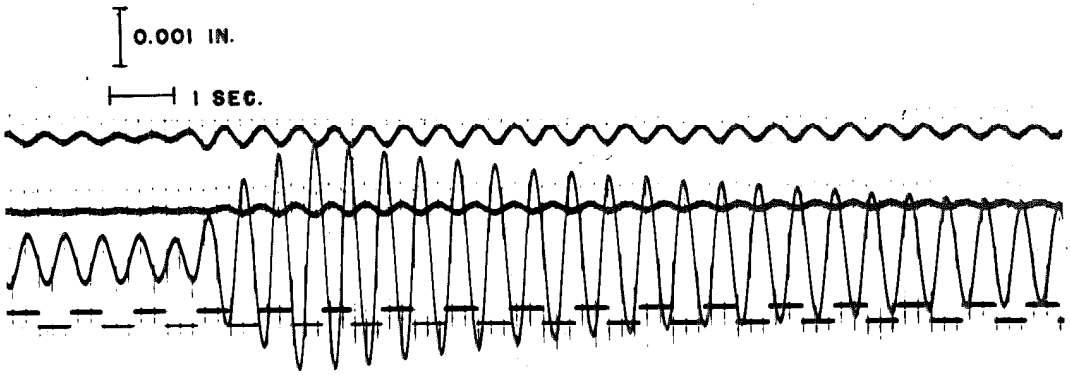

FIG. 6-2 "MAN-EXCITED" VIBRATIONS OF 150 FT. HIGH CONCRETE INTAKE TOWER OF DAM

vibrations could be recorded, and hence damping could be measured.

A vibration of the above kind is in one sense a "self-excited" vibration. Since this phrase, "self-excited", is already used in mechanics for a rather different phenomenon in which the forces sustaining the motion are derived from the motion itself, it might be better to refer to this particular type of forced vibration as a "man-excited" motion. This method of excitation naturally recalls the old stories often mentioned in mechanics lectures of bridges destroyed by marching armies, and the supposedly common rule that soldiers should break step when crossing a bridge.

At first thought it seemed unlikely that a sufficient exciting force could be obtained in this very simple way to be useful for large structures such as multistory buildings. However, it turns out that it is just for such large structures with their relatively low natural frequencies that the method is most useful. As will be shown by some specific examples, it is often possible in multistory buildings to achieve an amplitude far exceeding that obtained from the wind.

The essential feature in producing a significant "man-excited" vibration is to insure that the center of mass of the body moves with as large as possible an amplitude at a reasonably constant frequency. One effective technique is to stand facing perpendicular to the direction of excitation and then to sway the body sideways, shifting the weight from one leg to the other. Another technique is to hold a column or door-jamb, and then move the body backward and forward, transmitting the force to the structure through the arms and legs.

Other interesting possibilities, perhaps involving the synchronized efforts of several people, will suggest themselves.

An idea as to the magnitude of the force generated in this way can be gained by supposing that the center of mass of a 150 lb man is moved sinusoidally through a double amplitude of 6 in. at a frequency of 1 cps. This would produce an inertia force magnitude of 46 lb. Considering that a structure having 1% of critical damping has a dynamic amplification factor at resonance of 50, such force magnitudes can easily produce measurable displacements.

Returning to Fig. 6-2, it is of interest to note how quickly the vibration amplitudes build up at resonance. Only four cycles of motion were required to bring the amplitude to a large value, from which a clear free vibration decay record was obtained. From this decay curve, the damping can be calculated to be less than 1% of critical. The values of period and damping obtained in this way were subsequently found to be in good agreement with those calculated from resonance curves determined with a sinusoidal vibration generator installed at the top of the tower.

At this stage in the investigations, a new portable seismograph became available which proved to be particularly well suited to such tests. Through the courtesy of the Seismological Laboratory of the California Institute of Technology, an experimental model of the "lunar seismometer",[62] along with a compact recording drum and pen recorder system, was borrowed for a number of building period tests. This lunar seismometer is a permanent magnet-moving coil

type adjusted to a natural period of about 1 second. By means of a simple transistor amplifier, a 5 in. ink-recording pen can be driven at a maximum magnification of about 10,000 at 4 cps and about 1000 at 1 cps. A small recording drum of 3-3/4 in. diameter is operated at a recording speed of 1 cm/sec. The combination of large output, high gain variable over a large range, compactness, and ruggedness, makes this instrument very suitable for building period tests. Another important advantage is the pen-recorder, which not only gives an immediately visible record, but which has a relatively large mechanical moving element to watch, which assists in synchronizing the applied inertia force and the resonant vibrations.

Tests on Building Frames

The first tests with the lunar seismograph were made during construction of the five-story reinforced concrete building described in Chapter III. Figure 6-3 shows typical records from which both the fundamental natural period and the damping can be obtained as given. These values are in good agreement with the resonance curve calculations from the steady state sinusoidal vibration generator tests.

A second test of the method was made at various stages of construction of the steel-frame building described in Chapter IV. In this case it was possible to clearly distinguish between 8 different modes of vibration, as shown in Figs. 6-5, 6-6 and 6-7. Figure 6-4 shows the general configuration of the building, and indicates the locations of the points of excitation. These points of excitation should be

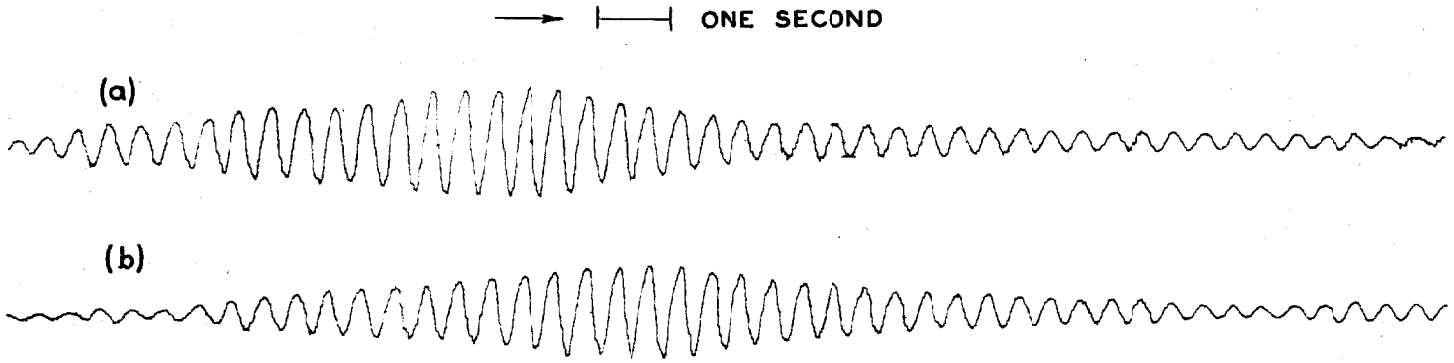

FIG. 6-3 "MAN-EXCITED" VIBRATION OF FIVE-STORY REINFORCED CONCRETE FRAME BUILDING. FUNDAMENTAL MODE - 2.36 CPS DAMPING ≈ 1.8 % CRITICAL

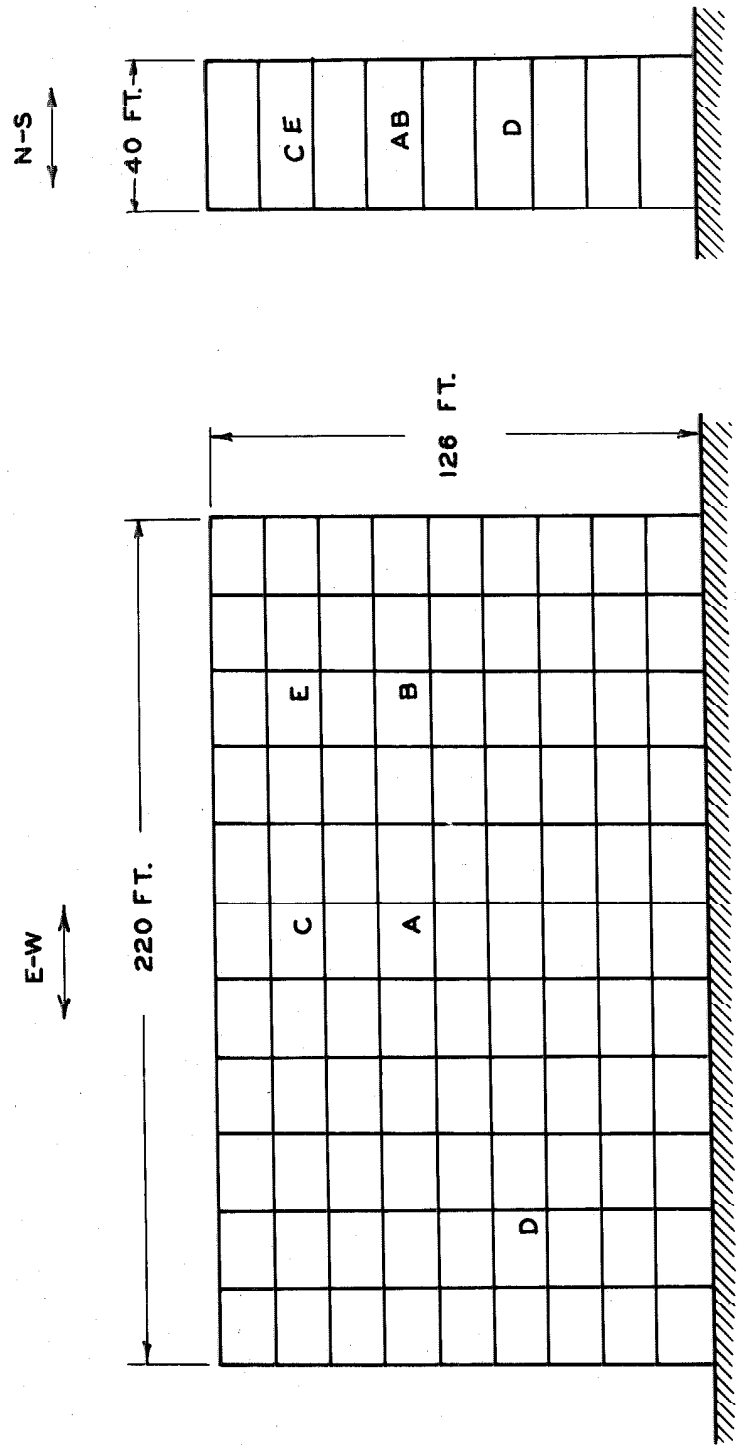

FIG. 6-4 NINE-STORY STEEL-FRAME BUILDING USED FOR "MAN-EXCITED" VIBRATION TESTS. LETTERS MARK POINTS OF EXCITATION AND MEASUREMENT.

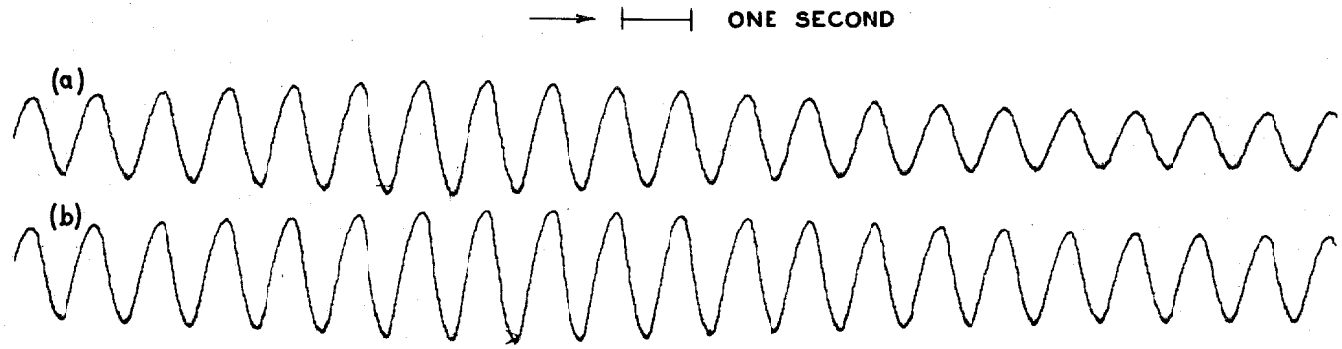

FUNDAMENTAL E-W TRANSLATION, 1.04 CPS
(POINT A IN FIG. 6-4)

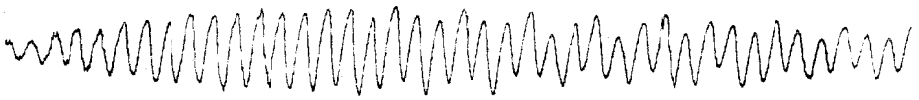

SECOND MODE E-W TRANSLATION, 3.0 CPS
(POINT A IN FIG. 6-4)

FIG. 6-5 "MAN-EXCITED" VIBRATIONS OF NINE-STORY STEEL-FRAME BUILDING. E-W LATERAL TRANSLATION MODES.

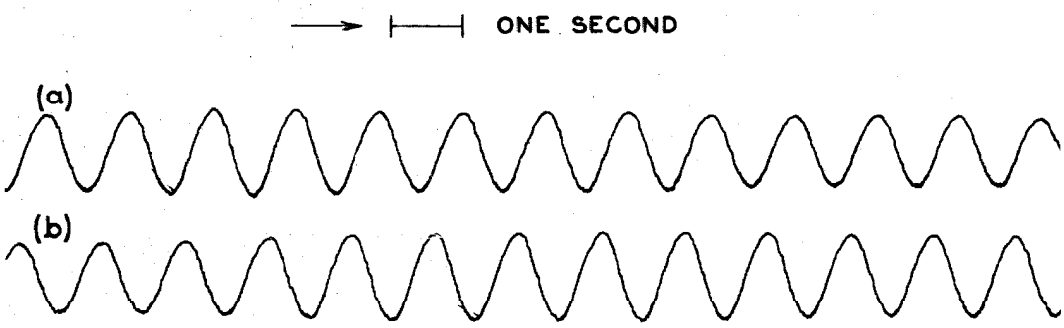

FUNDAMENTAL N-S TRANSLATION, 0.86 CPS
(POINT A IN FIG. 6-4)

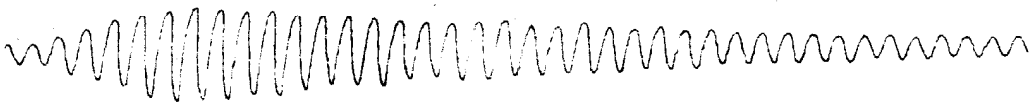

SECOND MODE N-S TRANSLATION, 2.8 CPS
(POINT A IN FIG. 6-4)

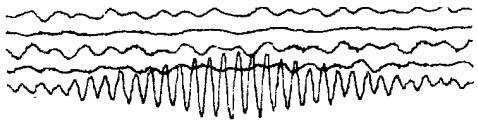

THIRD MODE N-S TRANSLATION, 5.0 CPS
(POINT D IN FIG. 6-4)

FIG. 6-6 "MAN-EXCITED" VIBRATIONS OF NINE-STORY STEEL-FRAME BUILDING. N-S LATERAL TRANSLATION MODES.

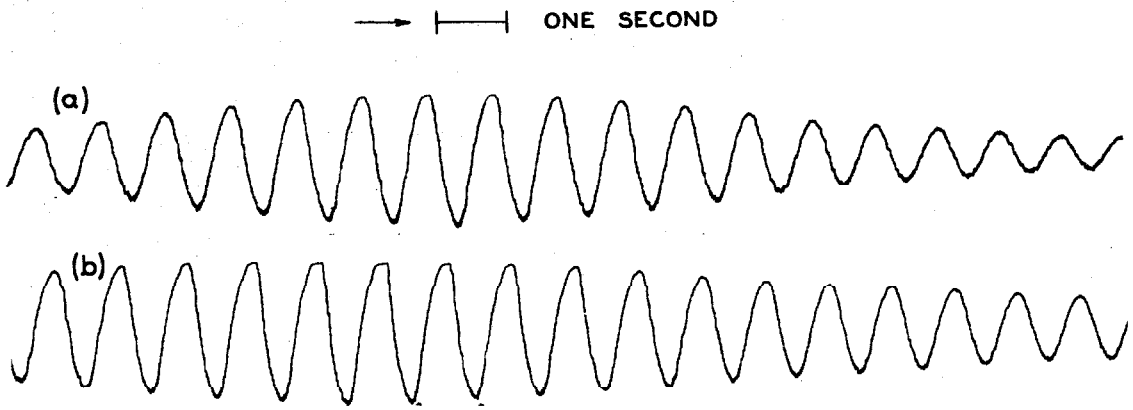

FUNDAMENTAL TORSION MODE, 1.08 CPS
(POINT B IN FIG.6-4)

SECOND TORSION MODE, 3.5 CPS
(POINT B IN FIG. 6-4)

THIRD TORSION MODE, 7.2 CPS
(POINT E IN FIG. 6-4)

FIG. 6-7 "MAN EXCITED" VIBRATIONS OF NINE STORY STEEL-FRAME BUILDING. TORSIONAL MODES.

selected to emphasize the mode desired, and to suppress other modes. For example, by applying the exciting force at a node for the 2nd mode of vibration, the 3rd mode can be more easily recognized. Although these mode shapes will, of course, not be accurately known for actual structures, it will be possible to make a sufficiently accurate estimate from the general configuration of the structure.

Figure 6-5 shows two lateral translational modes in the long E-W direction of the building. The damping in the fundamental mode is about 1% of critical, definitely less than that of the reinforced concrete frame of Fig. 6-3.

Figure 6-3 shows three lateral translation modes in the short N-S direction of the building. The damping of the fundamental mode is considerably less than in the other direction; in fact, the decrease in the successive amplitudes is so small as to be scarcely measurable. In this case an approximate value of damping of the second mode could also be obtained.

Figure 6-7 shows three torsional modes excited by transverse inertia forces at the end of the building. The damping of the fundamental mode in torsion is appreciably greater than the lateral modes, and is about 2% critical. The value of the fundamental torsional frequency, 1.08 cps, is very close to the lateral E-W frequency of 1.04 cps. It should be noted, however, that the direction of the exciting force for the torsional mode is perpendicular to that which would excite this E-W frequency, and hence the two modes can be separated even though their frequencies are so close together.

As an additional means of studying the dynamic properties of structures, period tests with the lunar seismograph were made at intervals during construction of the nine-story building. By noting the way in which the periods change as various structural elements are added, considerable detail concerning the dynamic action of these structural elements can be obtained. These results are described in detail in Chapter IV.

Earthquake Response of a Steel Frame Building

In the course of the period measurements on the nine-story steel-frame building, an extra premium was obtained in the form of a natural earthquake which excited a building motion considerably greater than had been involved in the period tests.

During adjustment of the lunar seismograph prior to a period test, a large signal appeared which was at first believed to be an instrument malfunction. Fortunately the recorder was kept running for a time, for the cause of the motion turned out to be a magnitude 5.0 earthquake with an epicenter about 70 miles from the building. (28 February 1963; 4:25:58 PST; 34°56'N, 118°59'W). Figure 6-8 shows the N-S lateral response of the building to this earthquake. The strong motion begins at P and continues for several widths of the record as indicated. During the short time interval Q-R the recorder was turned off while the gain was reduced for the remainder of the record. The initial strong motion of the building quickly passes into an almost pure 3rd mode of lateral translation, which then gradually passes into a

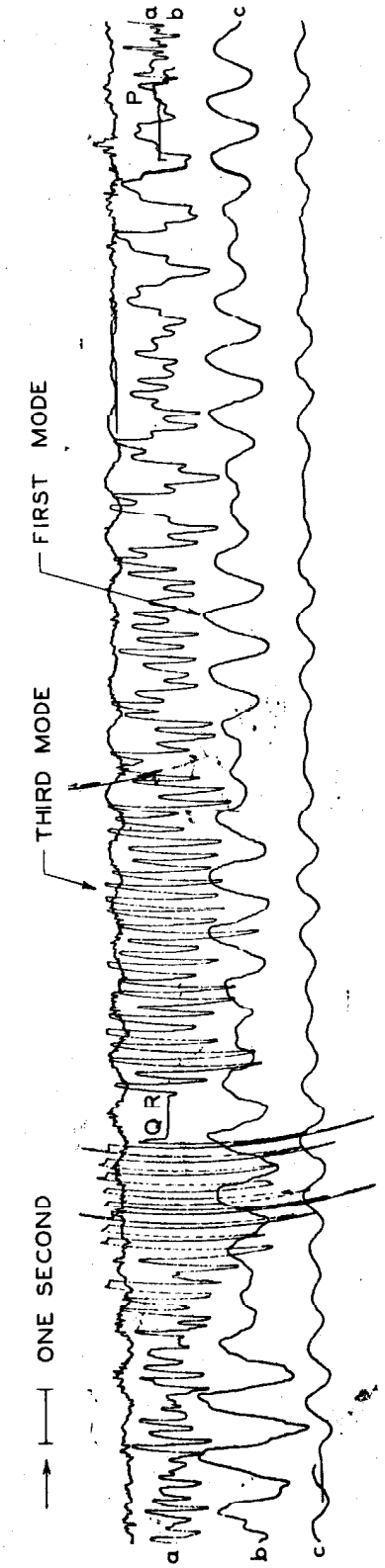

FIG. 6-8 EARTHQUAKE RESPONSE RECORDED BY LUNAR SEISMOGRAPH IN NINE-STORY STEEL-FRAME BUILDING N-S

motion which is almost entirely the fundamental mode. The 3rd mode frequency is very close to 5 times the fundamental frequency, which would be the exact ratio for a uniform shear type structure. The 2nd mode of lateral translation is not prominent on the record because the seismograph was located on the 8th floor, near a node for the 2nd mode of vibration. The frequencies excited by the earthquake of Fig. 6-8 cannot be compared numerically with the "man-excited" frequencies of Fig. 6-6 because the structure of the building frame was altered between the two tests by the addition of fire-proofing material to the columns.

Records of actual earthquake induced motions in multistory buildings are, of course, very rare, and the above extremely fortuitous record gives important direct information on the way in which the higher modes of vibration are set up in such structures.

Conclusions

It is believed that the simple means of building excitation described above will make it possible to considerably improve the data hitherto obtained from many buildings by wind-excited tests. Although the amplitude levels of such tests are very small, the data may be useful for design purposes. Several instances have already occurred in which wide differences between building periods as measured by the above means and calculations based on the design model have led to a re-evaluation of the design procedures, and a clarification of the way in which the structural members were behaving.

Since tests of the above type may be the only feasible way of acquiring data on most actual buildings, possibilities of improvements in instruments and techniques should be carefully studied.

CHAPTER VII

SUMMARY AND CONCLUSIONS

Chapter II treated the theory of structural testing; the major points of interest are:

1. In order to force excite a pure normal mode in a complicated dynamic system an iterative process that converges on the excitation of the desired mode is needed. In most multistory buildings the natural frequencies are sufficiently well separated and the damping is sufficiently low so that the iterative process is not needed in its full generality. However, the underlying principles of the iterative process are of value in positioning the vibration exciters so that the modes of interest are purely excited and the undesired modes are subdued or eliminated entirely.

2. The equations from which the stiffness and damping matrices can be determined from the experimentally determined modal properties have been developed. The equations were developed for the model representing a "shear building" with infinitely rigid girders, i.e., each mass is connected by springs and dashpots to adjacent masses only; also, for the close coupled system in which each mass is connected by springs and dashpots to adjacent masses as well as to the base; finally the equations were developed for the far coupled system, representing the model of the structure in which the girders are not sufficiently rigid to prevent joint rotation, i.e., each mass is connected by springs and dashpots to every other mass. For each case the least number of experimentally determined modes required for a

solution of the system of equations has been established.

3. In the case of the "shear building" with no joint rotation the stiffnesses and damping elements can be determined from an experimental determination of only one mode. However, some of the equations can be very ill-conditioned leading to large errors in the determination of some of the stiffnesses and damping elements.

4. It has been shown that several methods are available to determine the amount of "equivalent viscous damping" from an experimentally determined steady-state response curve.

Chapter III describes the results obtained from an extensive series of steady-state vibration tests of a modern five-story reinforced concrete building having plan dimensions 25 feet by 125 feet. The major results are:

1. In the long direction of the building two translational modes were excited. The ratio of the two resonant frequencies is 1 : 3.1. The mode shape determined for the lowest translational mode was close in appearance to that of a uniform shear beam.

2. Damping in the lowest translational mode was found to vary between 1.8% and 2.2% showing a slight tendency of a decrease in damping with increasing force levels. Damping in the second lowest translational mode was found to be 2.1%.

3. In determining the damping matrix it was found that the best representation of the model of the structure required "absolute" dashpots as well as "relative" dashpots. While "absolute" dashpots are needed to best describe the mathematical model of the structure,

they do not seem compatible with a physical description of how the energy is absorbed. This points to the question of how well the damping mechanism in a structure can be represented by the simple model employing dashpots representing the energy absorbing elements of the structure.

4. In the short direction of the building only one mode could be excited due to the frequency limitations of the vibration exciters. The response curves were determined for a number of different force levels. The value of damping was found to vary between 2.1% and 2.7%, showing a consistent increase with increasing force levels.

5. The response curves show a well-defined nonlinearity typically that of a "softening spring". This nonlinearity can be well explained from the hysteretic material properties of the structure.

6. After exciting the building at increasing force levels one of the intermediate tests was duplicated in order to investigate whether any measurable changes in response could be detected. The changes in response characteristics were of a small but measurable magnitude. The most pronounced change was an increase in damping from 2.4% to 2.6%. Since the change is measurable even at these very low force levels, the possibility exists that vibrations caused by nearby traffic, small tremors, use of machinery in the building, etc., over a period of time would also tend to increase the value of damping.

7. The lowest torsional mode was excited at a frequency very close to the theoretically predicted resonant frequency. The value of damping was found to be approximately 2.3%.

8. In all the dynamic tests attempts were made to measure the motion of the ground floor. Only at the highest force level of excitation in the short direction of the building was such motion measurable. It was found that the translational as well as the rotational motion of the ground floor constituted a negligible portion of the total response of the building.

Chapter IV describes the results of the vibration tests of a modern nine-story steel frame building having plan dimensions of 40 feet by 220 feet. The major results are:

1. "Man-excited" vibration tests were carried out during a 10-month period of construction. The changes in natural periods of vibration give detailed information on how the various elements of the building affect the dynamic characteristics of the structure.

2. Steady-state vibration tests revealed that with the initial location of one vibration exciter it was not possible to excite cleanly some of the desired modes. This was partly due to the fact that the vibration exciter was located too close to one of the nodal points of the desired mode and partly due to interference from other modes. The problems were solved by installing two vibration exciters at the nodal points of the undesired modes and at the same time at points for which the mode shape components of the desired modes were relatively large.

3. In the long direction of the building it was possible to excite the four lowest translational modes. The ratios of the resonant frequencies were 1 : 3.0 : 5.0 : 7.5. Damping in the lowest trans-

lational mode is found to be 0. 5% with only a slight indication of an increase in damping as the force level is increased. The second lowest translational mode had damping ranging from 0. 8% to 1. 1% increasing with an increase in force level. The value of damping for the third lowest translational mode was found to be 2. 0% and the damping in the fourth lowest translational mode was found to be 3. 6%.

4. It was found that in the long direction of the building the vibrational behavior was that of a "shear-building" with infinitely rigid girders. Assuming the stiffness and damping matrices to be tri-diagonal with no interrelation between the elements of each row (or column), the 15 unknowns could be determined from the 32 equations stemming from the four experimentally determined modes. It was found that the damping mechanism in this case, contrary to the damping mechanism found necessary for the case of the reinforced concrete building, was well described by "relative" dashpots only.

5. More modes were determined than necessary for the solution of the equations from which the stiffness and damping elements could be found. The stiffness and damping matrices were then determined using only some of the experimentally determined modes. It was found that by using any three of the modes, stiffness and damping matrices quite close to those found by using all of the four modes were determined.

6. In the short direction of the building the vibrational behavior was very much different from that of the long direction of the building. The rigidities of the floor systems are such that the joints are very little restrained against rotation. The three lowest translational

modes were determined from the steady-state vibration tests. The ratios of the resonant frequencies were 1 : 3. 2 : 6. 25. Damping in the lowest translational mode was found to be 0. 5% with only a slight indication of an increase in damping as the force level is increased. The second lowest translational mode had damping ranging from 1. 1% to 1. 6% increasing with an increase in force level. The third lowest translational mode had a damping value of 3. 7%. It is of interest to note that the damping in each mode is close to being proportional to the resonant frequency.

7. In the short direction of the building a sufficient number of modes could not be determined experimentally so that the stiffness and damping matrices could be calculated. As pointed out in Chapter IV, each of the matrices contained 36 unknown elements while only 24 equations were available for the determination of the unknown elements.

8. Three torsional modes of vibration were also excited. The resonant frequencies were ω_1=1. 08 cps; ω_2=3. 72 cps and ω_3=7. 30 cps. The values of damping in the three modes were β_1= . 8%; β_2= 1.3% and β_3= 3%.

9. A mode in which the floor slabs vibrated in the horizontal plane was excited at a resonant frequency of 4. 90 cps; the value of damping being approximately 2%.

In Chapter V the results of steady-state vibration tests are compared to the results obtained from run-down tests; the main conclusions to be drawn from the comparison tests are:

1. The natural frequency as determined from a run-down test

is a few per cent lower than the natural frequency determined from a steady-state test.

2. The mode shapes, as determined from the two types of tests, are identical.

3. The peak response value determined from a run-down test is as much as 50% lower than the steady-state response value.

4. Damping determined from a run-down test is up to 2.5 times as large as the damping determined from a steady-state test.

5. It is concluded that a run-down test is not, in general, a suitable experimental method for dynamic testing of structures. It is also concluded that data from past run-down tests are of questionable accuracy.

In Chapter VI a new method for the measurement of the natural periods of buildings is proposed. The principle of "man-excited" vibrations is basically that an operator by periodic motions of his body can excite one of the natural periods of a structure, by keeping the frequency of the periodic motions close to the natural frequency of interest. The method has several advantages over wind-excited vibrations which have been used extensively in the past to measure the natural periods of buildings. The main advantages are:

1. Larger amplitudes of motion can be attained.

2. The test can be carried out at any time, in the presence or absence of wind.

3. In the absence of wind, by stopping the exciting force after an appreciable motion has been built up, the decay of free vibrations

can be recorded and hence damping can be estimated.

4. By performing the "man-excited" vibrations at well chosen locations in a building it is possible to excite a large number of modes. For example, torsional modes can be excited by performing "man-excited" vibrations at one of the ends of a long building.

5. By performing "man-excited" vibrations at a nodal point for a mode, it is possible to eliminate the effect of that mode in order to more cleanly excite another mode.

REFERENCES

1. Kobayashi, H., "Dynamic Properties of Buildings Decided by Measurements of Vibration During Earthquake", Proceedings of the Second World Conference on Earthquake Engineering, Tokyo, Japan, (July, 1960), pp. 1121-1136.

2. Hudson, D. E., "A Comparison of Theoretical and Experimental Determinations of Building Response to Earthquakes", Proceedings of the Second World Conference on Earthquake Engineering, Tokyo, Japan (July, 1960), pp. 1105-1120.

3. Blume, J. A., "Structural Dynamics in Earthquake-Resistant Design", Paper No. 1645, Proceedings of the American Society of Civil Engineers, (July, 1958).

4. Hudson, D. E. and Housner, G. W., "Structural Vibrations Produced by Ground Motion", Transactions of the American Society of Civil Engineers, Vol. 122 (1957).

5. Earthquake Investigations in California, 1934-1935, Special Publication No. 201, Coast and Geodetic Survey, U. S. Dept. of Commerce, Washington, D. C. (1936).

6. Hudson, D. E., "Dynamic Tests of Buildings and Special Structures", Experimental Techniques in Shock and Vibration, American Society of Mechanical Engineers (Nov. 1962), pp. 81-91.

7. Wilbur, J. B. and Hansen, R. J., "Behavior of Structural Elements Under Impulsive Loads, I and II". Report submitted to New England Division, Corps of Engineers. M. I. T. (Nov., 1950).

8. Penzien, J., "Damping Characteristics of Prestressed Concrete", Report to U. S. Naval Civil Engineering Laboratory, Port Hueneme, California. University of California, Berkeley (Jan., 1962).

9. Pian, T. H. H., Hallowell, F. C. and Bisplinghoff, R. L., "Investigations of Structural Damping in Simple Built Up Beams", Contract Report on ONR Project NR-035-259 at M. I. T.

10. Lycan, D. L. and Newmark, N. M., "Effect of Structure and Foundation Interaction, Journal of the Engineering Mechanics Division, Proceedings of the ASCE, (Oct. 1961).

11. Merritt, R. G. and Housner, G. W., "Effect of Foundation Compliance on Earthquake Stresses in Multistory Buildings", Bulletin of the Seismological Society of America, (Oct., 1954).

12. Housner, G. W., "Interaction of Building and Ground During an Earthquake", Bulletin of the Seismological Society of America, (July, 1957).

13. Kawasumi, H. and Kanai, K., "Small Amplitude Vibrations of Actual Buildings", Proceedings of the World Conference on Earthquake Engineering, Berkeley, California, (June 1956), pp. 7_I-1 to 7_I-14.

14. Hisada, T and Nakagawa, K., "Vibration Tests on Various Types of Building Structures up to Failure", Proceedings of the World Conference on Earthquake Engineering, Berkeley, California, (June 1956), pp. 7_{II}-1 to 7_{II}-10.

15. Penzien, J., "Dynamic Response of Elasto-Plastic Frames", Journal of the Structural Division, Proceedings of the ASCE, (July 1960).

16. Veletsos, A.S. and Newmark, N. M., "Effect of Inelastic Behavior on the Response of Simple Systems to Earthquake Motions", Proceedings of the Second World Conference on Earthquake Engineering, Tokyo, Japan (July, 1960), pp. 895-913.

17. Berg, G. V., "The Analysis of Structural Response to Earthquake Forces", Ph. D. Thesis, University of Michigan, (1958).

18. Thomaides, S. S., "Effect of Inelastic Action on the Behavior of Structures During Earthquakes", Ph. D. Thesis, University of Michigan, (1961).

18a. Sekaran, A. R.C., "Effect of Joint Rotation on the Dynamics of Multistoreyed Frames", Second Symposium on Earthquake Engineering, School of Research and Training in Earthquake Engineering, University of Roorkee, (1962).

19. Rubinstein, M. F. and Hurdy, W. C., "Effect of Joint Rotation on Dynamics of Structures", Journal of the Engineering Mechanics Division, Proceedings of the ASCE, (Dec., 1961).

20. Rubinstein, M. F., "Effect of Axial Deformation on the Periods of a Tall Building", Bulletin of the Seismological Society of America, (Feg., 1964).

21. Kimball, A. L., "Friction and Damping in Vibrations", Journal of Applied Mechanics, (March, 1941), pp. A-37 to A-41.

22. White, M. P., "Friction in Buildings: its Magnitude and its Importance in Limiting Earthquake Stresses", Bulletin of the Seismological Society of America, (April, 1941).

23. Den Hartog, J. P., "Forced Vibrations with Combined Coulomb and Viscous Friction", Transactions of the ASME, APM-53-9, (1931).

24. Jacobsen, L. S., "Steady Forced Vibration as Influenced by Damping", Transactions of the ASME, APM 52 15, (1930).

25. Kanai, K. and Yoshizawa, S., "On the Period and the Damping of Vibration in Actual Buildings", Bulletin of the Earthquake Research Institute (Japan) (1961), pp. 477-489.

26. Dockstader, E. A., Swiger, W. F., and Ireland, E., "Resonant Vibration of Steel Stacks", Transactions of the ASCE, Vol. 121, (1956), pp. 1088-1112.

27. Bleich, F. and Teller, L. W., "Structural Damping in Suspension Bridges", Proceedings of the ASCE, Structural Division, Vol. 77, (March, 1951).

28. Jacobsen, L. S., "Frictional Effects in Composite Structures Subjected to Earthquake Vibrations", Dept. of Mech. Eng. Stanford University, Stanford, California, (March, 1959).

29. Berg, G. V., "Finding System Properties from Experimentally Observed Modes of Vibration", Primeras Jornadas Argentinas de Ingenieria Antisismica, (April 1962).

30. Kanai, K., "A Method of Determining the Stiffness of Each Story of a n-Storied Building", Earthquake Research Institute (Japan), (1950), pp. 161-163.

31. Hudson, D. E., "Synchronized Vibration Generators for Dynamic Tests of Full-Scale Structures", Earthquake Engineering Research Laboratory, California Institute of Technology, Pasadena, California, (Nov., 1962).

32. Keightley, W. O., "Vibration Tests of Structures", Earthquake Engineering Research Laboratory, California Institute of Technology, Pasadena, California, (July, 1963).

33. Perlis, S., Theory of Matrices, Addison-Wesley Publishing Company, Inc., (1958).

34. Hildebrand, F. G., Methods of Applied Mathematics, Prentice-Hall (1952).

35. Strutt, J. W., Baron Rayleigh, The Theory of Sound, Dover Publications (1945).

36. Caughey, T. K., "Classical Normal Modes in Damped Linear Dynamic Systems", Journal of Applied Mechanics, 59-A-62, (1959).

37. Caughey, T. K. and O'Kelly, M. E. J., "General Theory of Vibration of Damped Linear Dynamic Systems, Dynamics Laboratory, California Institute of Technology, Pasadena, California (June, 1963).

38. O'Kelly, M. E. J., "Normal Modes in Damped Systems", Dynamics Laboratory, California Institute of Technology, Pasadena, California (1961).

39. Foss, K. A., "Co-ordinates which Uncouple the Equations of Motion of Damped Linear Dynamic Systems", Journal of Applied Mechanics, 57-A-86 (1957).

40. Caughey, T. K. and O'Kelly, M. E. J., "Effect of Damping on the Natural Frequencies of Linear Dynamic Systems", The Journal of the Acoustical Society of America (Nov., 1961).

41. Lewis, R. D. and Wrisley, D. L., "A System for the Excitation of Pure Natural Modes of Complex Structure", Journal of the Aeronautical Sciences, (Nov., 1950).

42. Zehlen, M., "Linear Estimation and Related Topics", A Survey of Numerical Analysis, J. Todd, editor, McGraw-Hill Book Co., Inc., (1962).

43. Newman, M., "Matrix Computation", A Survey of Numerical Analysis, J. Todd, editor, McGraw-Hill Book Co., Inc., (1962).

44. Iwan, W. D., "The Dynamic Response of Bilinear Hysteretic Systems", Earthquake Engineering Research Laboratory, California Institute of Technology, Pasadena, California (July, 1961).

45. Hudson, D. E., "A New Vibration Exciter for Dynamic Testsof Full-Scale Structures", Earthquake Engineering Research Laboratory, California Institute of Technology, Pasadena, California, (Sept. 1961).

46. Timoshenko, S., and Goodier, J. N., "Theory of Elasticity," McGraw-Hill Book Co., Inc. (1951).

47. Pauw, A., "Static Modulus of Concrete as Affected by Density," Proceedings, American Concrete Institute, Vol. 57 (Dec. 1960), pp. 679-687.

48. Caughey, T. K. - Private communications.

49. Merchant, H. C., "Mode Superposition Methods Applied to Linear Mechanical Systems under Earthquake Type Excitation," Earthquake Engineering Research Laboratory, California Institute of Technology, Pasadena, California (March 1961).

50. Jacobsen, L. S., "Natural Periods of Uniform Cantilever Beams," Proceedings of the ASCE, (March 1938).

51. Benjamin, J. R. and Williams, H. A., "Behavior of Reinforced Concrete Shear Walls," Proceedings of the ASCE, Structural Division, (May, 1957).

52. Jennings, P. C., "Response of Simple Yielding Structures to Earthquake Excitation," Earthquake Engineering Research Laboratory, California Institute of Technology, Pasadena, California, June, 1963.

53. Blume, J. A. and Binder, R. W., "Periods of a Modern Multi-Story Office Building During Construction," Proceedings of the Second World Conference on Earthquake Engineering, Tokyo, Japan, (July, 1960), pp. 1195-1206.

54. (Deleted)

55. Lewis, F. M., "Vibration During Acceleration Through a Critical Speed," Transactions of the ASME, (1932), pp. 253-261.

56. Parker, A. V., "The Response of a Vibrating System to Several Time Dependent Frequency Excitations," Thesis, Iowa State University of Science and Technology, Ames, Iowa (1962).

57. Hudson, D.E., Keightley, W.O. and Nielsen, N.N., "A New Method for the Measurement of the Natural Periods of Buildings," Bulletin of the Seismological Society of America, (Feb. 1964).

58. Housner, G.W., "The Significance of the Natural Periods of Vibration of Structures," Primeras Journadas Argentinas Antisismica (1962).

59. Structural Engineers Association of California, "Recommended Lateral Force Requirements and Commentary," San Francisco.

60. Earthquake Investigations in California, 1934-1935, Special Publication No. 201, Coast and Geodetic Survey, U.S.Dept. of Commerce, Washington, D.C. (1936).

61. Keightley, W.O., Housner, G.W. and Hudson, D.E., "Vibration Tests of the Encino Dam Intake Tower," Earthquake Engineering Research Laboratory, California Institute of Technology, Pasadena, California (1961).

62. Lehner, F.E., Witt, E.O., Miller, W.F. and Gurney, R.D., "A Seismometer for Ranger Lunar Landing," Seismological Laboratory, California Institute of Technology, Pasadena, California (1962).

APPENDIX

FIGS. A-1 to A-4:

DETAILS OF FIVE-STORY REINFORCED CONCRETE BUILDING, CHAPTER III.

FIGS. A-5 to A-14:

DETAILS OF NINE-STORY STEEL FRAME BUILDING, CHAPTER IV.

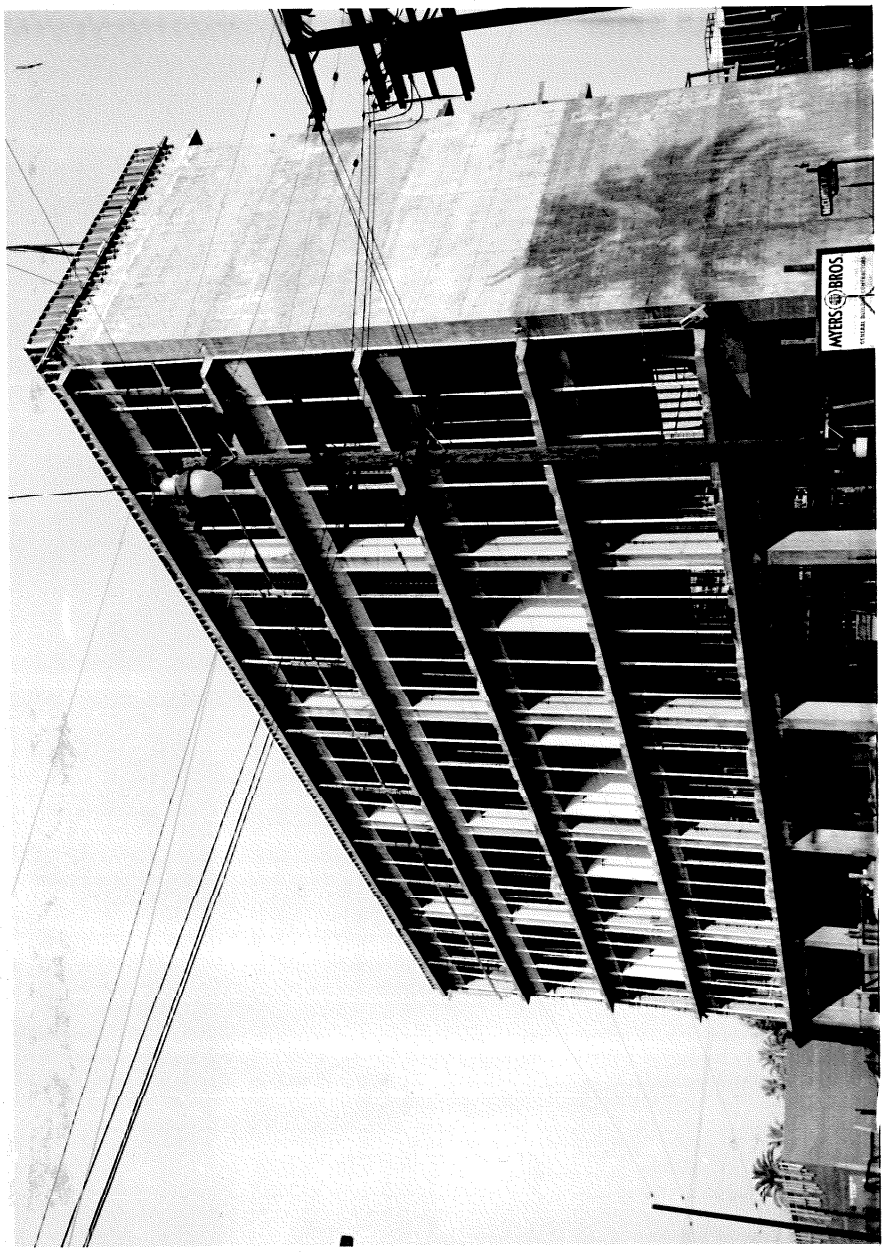

Fig. A-1 GENERAL VIEW, LOOKING NORTHEAST.

Fig. A-2 GENERAL VIEW, LOOKING NORTHEAST.

Fig. A-3 VIBRATION EXCITER INSTALLED ON 5th FLOOR.

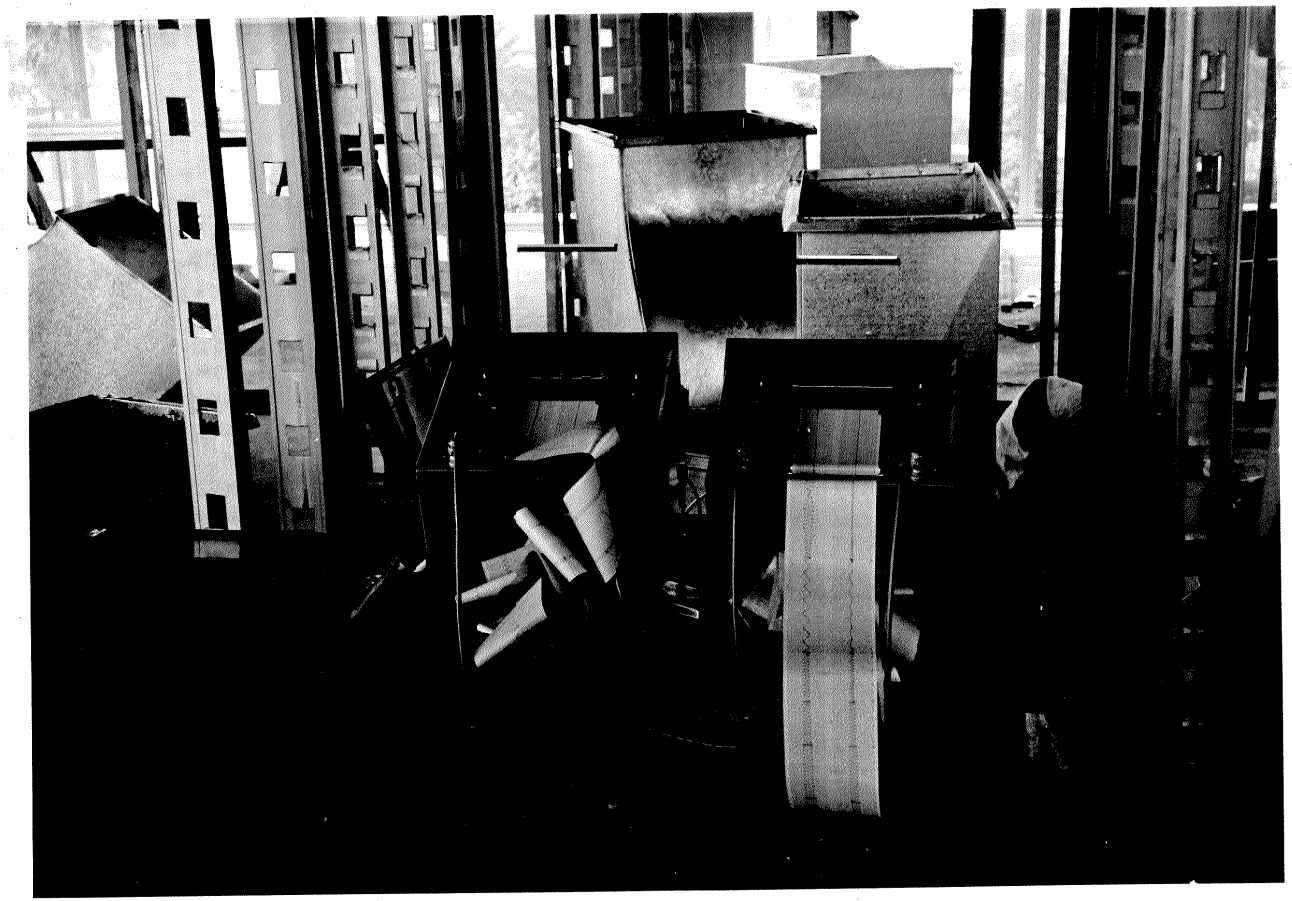

Fig. A-4 RECORDING INSTRUMENTS, BRUSH AMPLIFIERS AND RECORDERS AT LEFT, SANBORN RECORDERS AT CENTER.

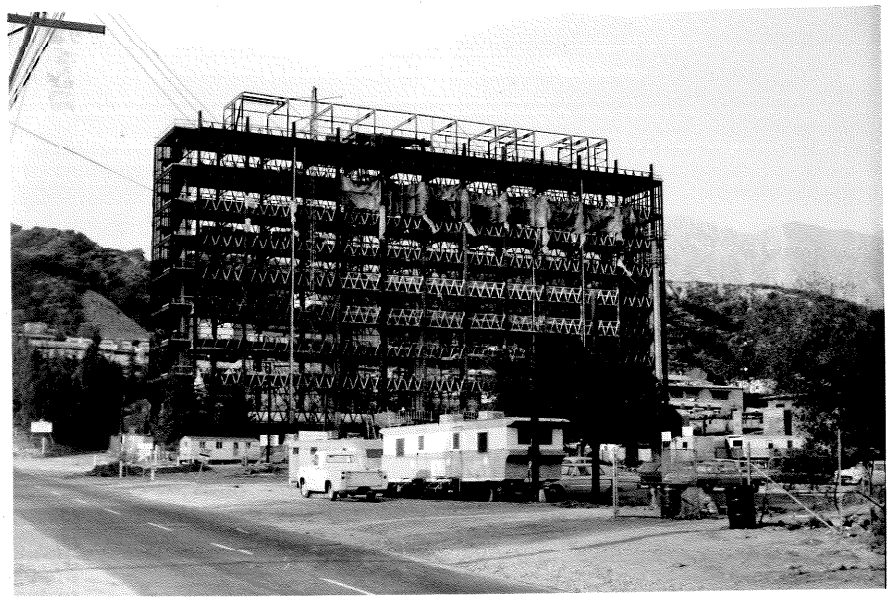

Fig. A-5 GENERAL VIEW, LOOKING NORTH.

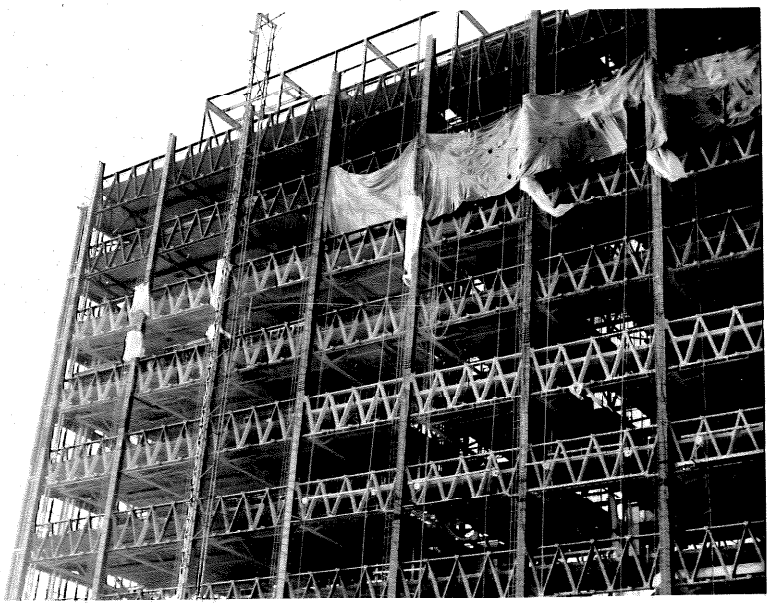

Fig. A-6 EXTERIOR VIEW, LOOKING NORTHWEST.

Fig. A-7 INTERIOR VIEW, LOOKING EAST.

Fig. A-8 INTERIOR VIEW, LOOKING SOUTHEAST.

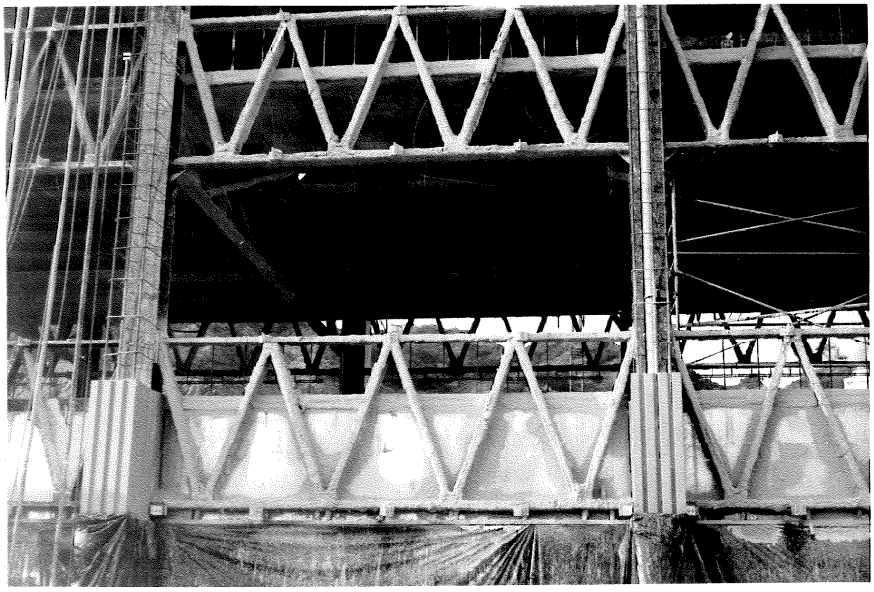

Fig. A-9 EXTERIOR VIEW, SOUTH SIDE.

Fig. A-10 EXTERIOR VIEW, NORTH SIDE, SOIL UP TO 1st FLOOR LEVEL.

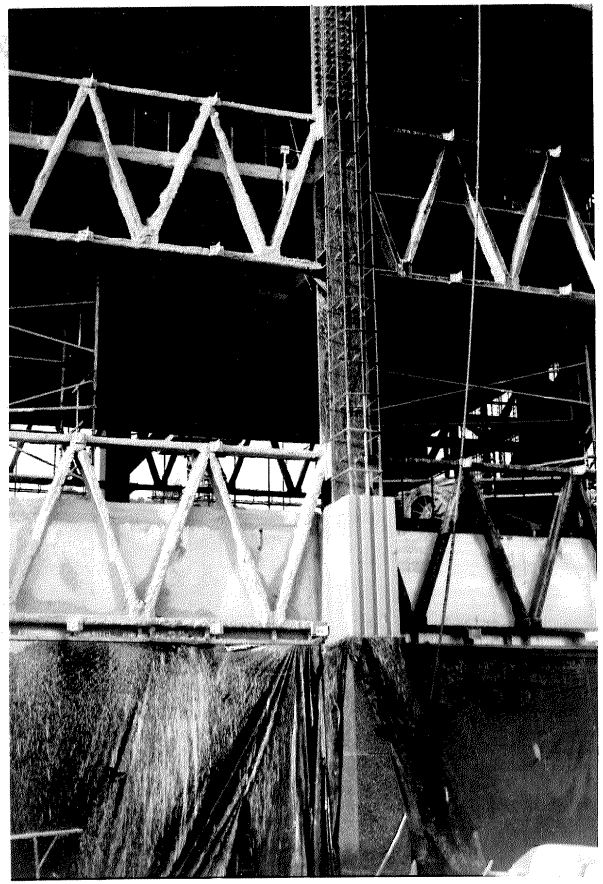

Fig. A-11 GIRDER AND COLUMN DETAIL, SOUTH SIDE.

Fig. A-12 GIRDER AND COLUMN DETAIL, SOUTH SIDE.

Fig. A-14 COLUMN DETAIL.

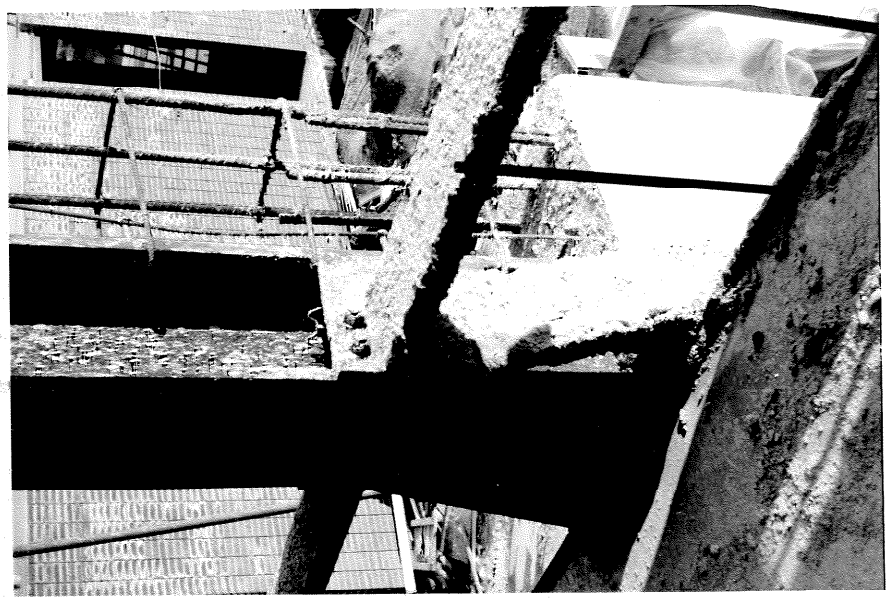

Fig. A-13 COLUMN DETAIL.